UNIVERSITY OF SOUTHERN QUEENSLAND

FACULTY OF ENGINEERING AND SURVEYING

A Yield Mapping System For Sugar Cane Chopper Harvesters

A dissertation by

GRAEME J COX

in fulfilment of the requirements of degree of Doctor of Philosophy

Submitted: December, 2002

Abstract

Yield maps provide essential information for the spatial analysis and evaluation of crop production management at a within field level. Technology has been developed to conduct yield mapping in various crops including grain, potatoes and forage, but as yet no technology exists for yield mapping sugar cane. The chopper harvester is the most common form of mechanical harvester for sugar cane. Therefore, the goal of this research is to develop a yield mapping system for the chopper type sugar cane harvester.

After a review, it is proposed that a suitable accuracy goal for the sugar cane mass flow sensor would be 'less than 5% cumulative measurement error, 95% of the time (2 standard deviations), measured over a 100m^2 harvest area'.

Existing mass flow sensors for other crops are reviewed. Based on this review four potential techniques are proposed to measure the mass flow rate of sugar cane. These were defined as the chopper power, elevator power and feed roller separation and weigh pad. These were tested simultaneously by placing various sensors on a single harvester and comparing the sensor outputs with the mass flow rate as measured by a weigh truck. In this trial, all techniques offered potential but none produced results close to the accuracy goal. A weighing technique, known as the 'weigh pad', offered the most potential for improvement and potential to accurately measure the mass flow rate with a single calibration under all conditions. The weigh pad technique suffered from very small load cell sensitivity to flow rate, drift in baseline readings and susceptibility to mechanical noise/acceleration dynamics.

An opportunity arose to install a complete yield mapping system on a harvester within a commercial operation. This opportunity was accepted to assess the potential for applying yield maps to the agronomic management of sugar cane. Because the weigh pad sensor required further development at this stage, chopper and elevator power were used as a measure of mass flow rate. A full yield mapping system was developed. Yield mapping, directed soil sampling and variable rate gypsum application was conducted on a case study field. Economic analysis shows a clear economic benefit when compared with standard management.

Analysis is conducted on the weigh pad sensor examining its susceptibility to mechanical noise/acceleration dynamics. Theory is developed to mathematically model the effects of acceleration dynamics on the accuracy of weigh pad sensor. Laboratory bench testing

supported the mathematical model. From the theoretical and experimental analysis a number of conclusions are drawn:

- The weigh pad should be made as light as possible to minimise the error due to dynamic conditions.
- Electronic analogue filters should be used to reduce the noise due to external acceleration.
- The weigh pad should be as rigid as possible to maximise its natural frequency.

A new weigh pad sensor was designed based on these conclusions. Field trials indicated the effects of external accelerations dynamics were significantly reduced. Baseline drift was then found as the next major factor limiting accuracy. The baseline drift was principally caused by the secondary extractor fan of the harvester inducing a negative pressure on the weigh pad. A rubber curtain placed between the weigh pad and the secondary extractor fan reduced the negative force on the weigh pad due to the secondary extractor fan by 74% (from 17 N to 4.4 N). Therefore it is recommended the curtain be used to minimise the impact of the secondary extractor fan on the baseline drift of the weigh pad.

A yield mapping system has been developed for the sugar cane chopper harvester incorporating the weigh pad sensor, a ground speed sensor, a DGPS receiver, a yield display/monitor and data logger. Three identical systems have been constructed and installed on three harvesters for the 1998 cane harvest season. The results show sugar cane could be yield mapped using standard yield mapping principles.

The level of accuracy being achieved by the yield mapping system is less than 16% error, with 95% confidence, over a measurement area of approximately 1400 m^2. Although the accuracy achieved is not to the desired research goal, yield maps were produced with satisfactory detail to make agronomic management decisions. The reliability of the sugar cane yield mapping system under field condition in a commercial operation was satisfactory. However, two techniques are proposed ("auto-zeroing" and "batch weighing" techniques) to improve the accuracy and reliability of the weigh pad readings during wet or adverse harvesting conditions.

After note: At the time of writing the NCEA along with Case Austoft (CNH) were continuing to conduct research and development on the system and are intending to make the yield mapping system available as a standard item on new harvesters and a retrofit unit on existing harvesters in the near future (C. Barret, per. comm. 2001). The proposed "auto-zeroing" and "batch weighing" techniques are being tested.

Acknowledgments

Dedicated to Flora Cox (Mum).

Thanks for doing the best you could.

I would firstly like to show appreciation to my supervisors, Assoc Prof Harry Harris, Dr Randoph Pax and Dr Nigel Hancock. Their continual support and advice throughout the project gave me what was required to keep the job going.
I gratefully acknowledge the support and contribution made by:

- Australian Sugar Research and Development Corporation (SRDC) for a postgraduate scholarship.
- Les Perkins, Don Pollock and other Pivot Agriculture staff in their financial support of this research,
- Dave Cox and for providing a trial site and the purchase field equipment,
- Robert Dick for ongoing advice and support and proof reading of thesis,
- Neil Havermale from Red Hen systems for providing GPS and data logging hardware,
- Alan Green and Burdekin Agriculture College for providing a trial site and harvester,
- Mal Baker and other Case Austoft staff for assistance and providing harvesters for trials,
- Bundaberg Sugar staff from Fairymead Sugar Mill who providing a trials site,
- Pat Brosnan and other Davco Farming staff for their assistance,
- Incitec staff who assisted with the soil analysis,
- BSES for a weigh truck.

I must thank my friends for their help and good times.

Special thanks go to my wife, Helen, who has been a great support and motivator.

Certification Of Dissertation

I certify that the ideas, experimental work, results, analyses, software and conclusions reported in this report are entirely my own effort, except where due acknowledgment has been given. I also certify that the work is original and has not been previously submitted for assessment in any other course.

G J Cox
Signature of Candidate

30/9/02
Date

Q92108105
Student Number

ENDORSEMENT:

Supervisors:

H D HARRIS
Name

Dr. N.H. HANCOCK
Name

ASSOC PROF
Position

Assoc Prof
Position

H. Harris
Signature

N H Hancock
Signature

2/9/02
Date

7 Oct 2002
Date

Table of Contents

List of Figures

List of Tables

Chapter 1 - Introduction

'Precision agriculture', 'precision farming' or 'site specific crop management' are the terms used to describe a new concept in agriculture. The concept involves the management of crop production at spatial scales smaller than the usual field scale. This has the potential to offer significant environmental and economic benefits through more precise management. A starting point in the adoption of this new concept is typically the process of mapping crop yield, known as yield mapping.

A yield map is a plan of a field, usually colour coded (Figure 1-1) or contoured to represent the changes in crop yield. The data required to produce these maps are generally collected during harvesting of the crop. Sensors are mounted on the harvesting machine to continuously measure crop yield in real time. Global Positioning System (GPS) technology is used to calculate the position of the harvester in the field and this position, along with the corresponding yield, is recorded on computer hardware. At the completion of the harvest the information is downloaded to a PC for the production of yield maps. These maps provide a layer of spatial information required for the implementation of precision agriculture.

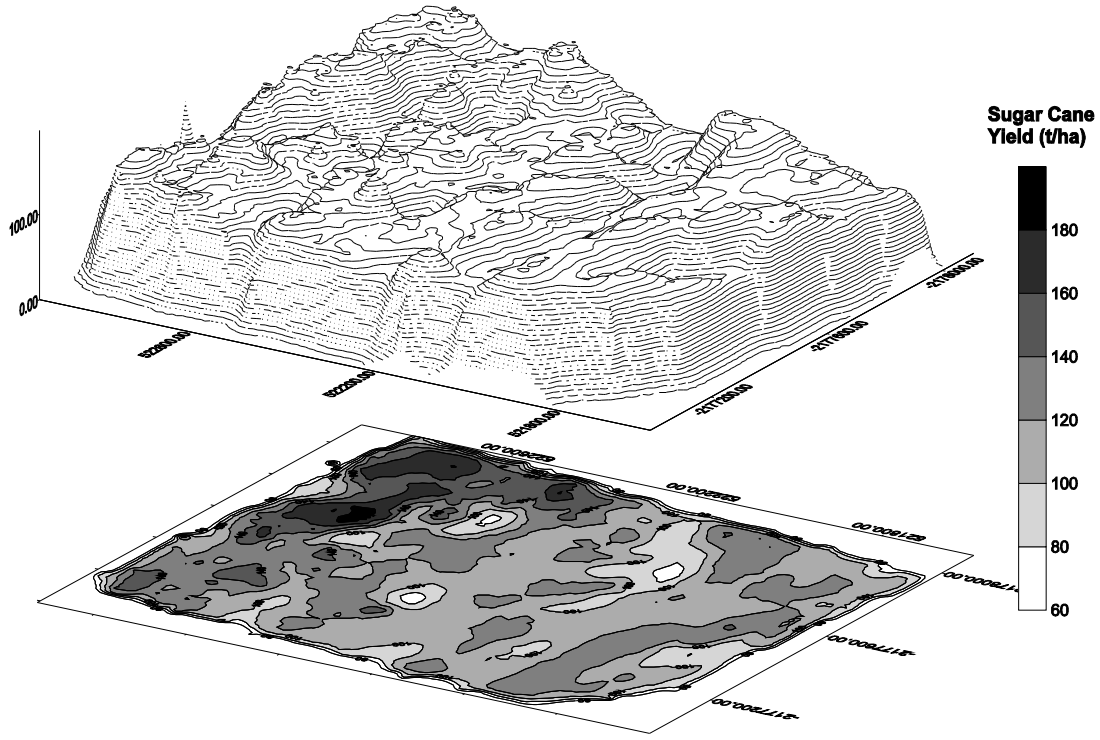

Figure 1-1. Sugar cane yield map derived from the outcomes of this research.

Technology has been developed (as reviewed later) to conduct yield mapping in various crops including grain, potatoes and forage, but as yet no technology exists for yield mapping sugar cane. The goal of this research was to achieve yield mapping in sugar cane. The unique component required for yield mapping sugar cane (or any other crop) is a reliable technique for measuring the mass flow rate of crop through a harvester. The chopper harvester is the most common form of mechanical harvester for sugar cane. Therefore the objectives of this research are stated in Section 1.1 below.

1.1 Objectives

The broad objective of the research was to develop a yield mapping system for the chopper type sugar cane harvester.

The specific objectives were:

(1) To develop a reliable and accurate means for measuring mass flow rate through

a chopper sugar cane harvester.

(2) To combine this measurement with GPS information to derive yield mapping data.

(3) Using GIS techniques, to develop sugar cane yield maps.

1.2 Publications From This Research

This research was successful in achieving the objectives stated above. As a result a number of papers were written and published. These were:

COX, G., HARRIS, H., & COX, D, 2000, 'Application of precision agriculture to sugar cane', Sugar 2000 Conference, Cairns, 2000

COX, G., HARRIS, H., & COX, D, 1998, 'Application of precision agriculture to sugar cane', Proc. 4th Intn. Conf. on Precision Agriculture. Minnesota, US, In Print.

HARRIS, H., & **COX, G**., 1997, 'Yield mapping- current capabilities in yield mapping for sugar cane, are these limiting to the introduction of precision agriculture to the sugar industry?', Proceedings of the workshop on "Precision Agriculture: What can it offer the Australian sugar industry" 1997, Townsville Aust.

COX, G., HARRIS, H., & PAX, R., 1997, 'The potential of precision agriculture for the Australian sugar industry', Proc. Aust. Soc. Sugar Cane Technol. 1996 Conference

COX, G., HARRIS, H., & PAX, R., 1997, 'Development and testing of a prototype yield mapping system', Proc. Aust. Soc. Sugar Cane Technol. 1996 Conference

A patent was also grant based on this research:

"Mass Flow Rate Sensor for Sugar Cane Harvesters", Australian Patent No. 744047 The specific details of the sensor design were published by the Australian patent office on November 4, 1999.

1.3 Definition of Terms

Billets: short lengths of sugar cane (generally 150 to 300 mm long) made by chopping full sugar cane stalks into smaller sections.

Baseline: the sensor reading when there is no cane flow (0 kg/s). An important parameter in the calibration function of a mass flow sensor. It could also be termed the "zero", tare value or free running.

Baseline drift: the change in the baseline value over time. This can be a gradual or abrupt change.

Chopper harvester: A mechanical harvester designed for sugar cane which cuts the sugar cane at ground level, then 'chops' the full stalks of cane into short lengths (billets).

Mass flow rate (kg/s): is defined as the quantity of material (measured in kilograms) passing a point in unit time (1 second). In this case it is the rate at which harvested material passes a sensing point in the harvester.

Yield mapping system: composed of a yield monitor along with the necessary DGPS and data logging equipment to record data for the production of yield maps.

Yield monitor: a device that measures the yield of a crop in real time, as it is harvested, by measuring the flow rate of crop material through the harvester and measurements of the area covered such as ground speed.

1.4 The Dissertation

The dissertation is divided into ten chapters after the introduction. These are:

- *Chapter 2 The Potential of Precision Agriculture for the Australian Sugar Industry:* examines how precision agriculture could provide benefits to the Australian sugar industry.
- *Chapter 3 Yield Mapping Review:* reviews the concept of yield mapping including the need, theory, processes, state of the art, mass flow measurement and the nature

of errors.

- *Chapter 4 Mass Flow Rate Sensing of Sugar Cane:* examines the requirements of a mass flow rate sensor for sugar cane and proposes four techniques that offer a potential solution.
- *Chapter 5 Preliminary Field Trials of Potential Sensors:* explains the initial field trials that were carried out on each of these techniques to assess their limitations, problems and potential.
- *Chapter 6 Development of Preliminary Sugar Cane Yield Maps And Their Agronomic Application:* Yield maps were developed for a single field to shows how yield maps and other precision agriculture practices such as soils sampling and variable rate application can be used to improve management and production of sugar cane.
- *Chapter 7 Dynamic Response of Weigh Pad:* The preliminary field trials showed one of the sensing techniques known as the weigh pad was vulnerable to the dynamic environment of the harvester. This problem was examined by developing a theoretical model of the system and then conducting laboratory trials to support the theory. Based on the results changes were made to the weigh pad sensor and field trials conducted on the new design.
- *Chapter 8 Effect of the Secondary Extractor Fan Suction on the Weigh Pad:* the secondary extractor fan of the harvester affected the accuracy of the weigh pad sensor. This problem was examined to determine the extent of the problem and solutions proposed.
- *Chapter 9 Weigh Pad Sensor Final Design:* gives recommended final design details for the weigh pad sensor based on the results of the prior research.
- *Chapter 10 Prototype Yield Mapping System:* details a yield mapping system developed incorporating the weigh pad sensor and tested on three harvesters.
- *Chapter 11 Conclusion:* summarises the research and provides recommendations for further research.

1.5 Background

1.5.1 Sugar Cane

Sugar cane (Figure 1-2) belongs to the Family *Gramineae* and is classified in the Genus

Saccharum.. This also places it in the vast family of grasses which contains some 5,000 species including other economic crops such as barley, wheat, oats, maize, rice and sorghum.

Sugar cane has the ability to trap the sun's energy and convert that energy into sucrose (sugar) more effectively than most other crops. Sugar is made in the leaves of the sugar cane plant by the natural process of photosynthesis and stored as a juice in its fibrous stalks.

The biomass production of sugar cane is very large when compared to other commercial crops. In ideal conditions yields of up to 300t/ha can be reached although the average production in Australia for the 10 year period between 1977-86 was 80t/ha, delivered to the mills. The approximate proportions of these constituents were 16% sucrose, 19% leaves, 15% bagasse (fibre), 5% other solids and 45% water (Reid, 1990).

Sugar cane is grown commercially in various countries around the world, and it is largely confined to the tropics where the growth of the crop is not limited by frost incidence.

Figure 1-2. A 12 month old sugar cane crop ready for harvest, which yielded 120t/ha.

1.5.2 Sugar Cane Harvesting

Sugar cane usually grows for 10 to 18 months before being harvested. Mature sugar cane stands two to four metres high and is usually harvested when the sugar content is at its

highest. In Australia this is between June and December.

All sugar cane grown in Australia is harvested mechanically by self-propelled harvesting machines. Elsewhere in the world however a significant proportion is still cut by hand but there is a trend towards mechanical harvesting. Australia pioneered mechanical cane harvesters and achieved 100 percent conversion to mechanical harvesting in 1976. Today, Australia is a world leader in the manufacture and export of mechanical cane harvesters.

The most common mechanical harvester is known as the 'chopper harvester'. During harvesting it moves along the rows of sugar cane (Figure 1-3) removing the leafy tops of the cane stalks, cutting the stalks off at ground level and chopping the cane into short lengths called billets. The billets are then loaded into self-propelled 'haul out' vehicles that travel alongside the harvester. The 'haul out' vehicles then take the cane to railway sidings or road haulage delivery points for transport to a sugar mill.

Sugar cane is harvested in either a green or burnt condition. Burnt cane harvesting involves burning the crop before harvest to remove leaves, weeds and other matter that can impede harvesting and milling operations. Green cane harvesting involves cutting the cane green (unburnt). The leafy matter on the cane stalks is extracted during harvesting and directed onto the ground.

Figure 1-3. A sugar cane crop being harvested 'green', with a 'Haul-out' truck along side.

Figure 1-4 gives a detailed view of the components and operation of the chopper type cane harvester. The operation begins with the "topper" chopping off the leafy matter at the top of the cane stalk. The cane is then knocked over slightly by the "knockdown" and "fin rollers" and cut at ground level by the "base cutters". The "feed rollers" then pull the whole stalks of cane up into the "choppers" which cut the cane into "billets" 200-300 mm long. At this point the "primary extractor fan" removes extraneous matter such as leaf and dirt, present amongst the billets. The billets then fall into the "elevator", and are lifted to a height suitable for delivery into the "haul out" vehicle. A "secondary extractor fan" removes some additional extraneous matter. For yield mapping purposes the flow rate must be measured somewhere within this system.

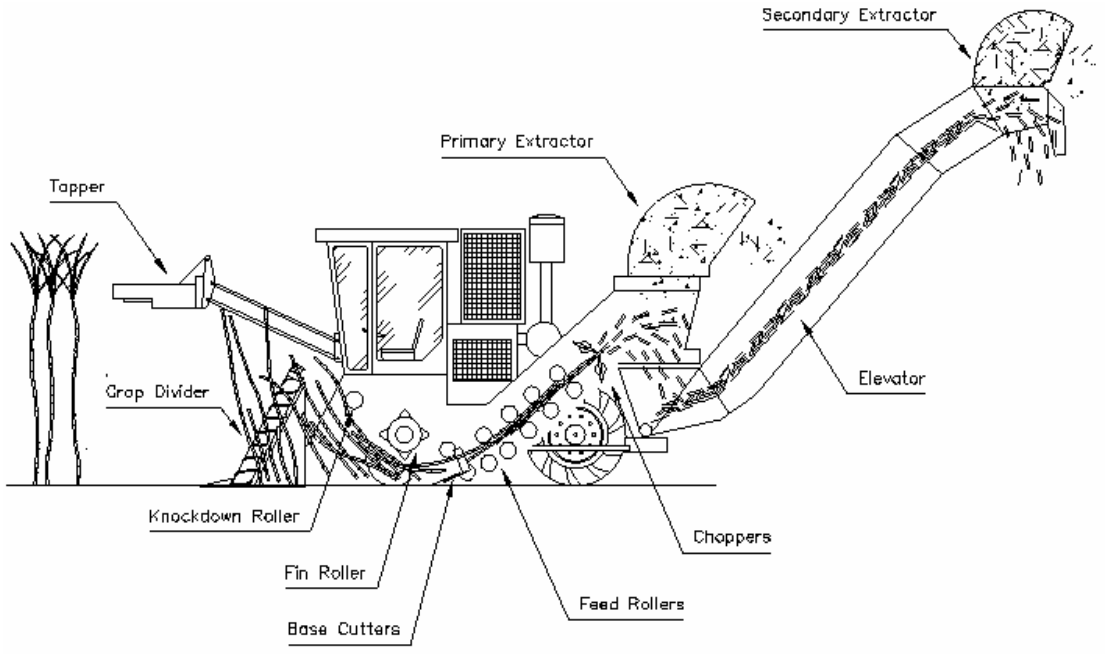

Figure 1-4. A side view of the chopper sugar cane harvester. (picture courtesy of S.Kroes)

1.5.3 Precision Agriculture (PA)

Ever since man began to farm there has been spatial variation in crop yields. When small areas were farmed by hand the variations were not so great and management could easily be adjusted to minimise this variation. For example, poorer areas would receive a little more manure or water than the better areas. However, as agriculture became mechanised the area

farmed by a single person grew dramatically, along with the size of the management units, until today where large fields are cropped with no change in treatment over their entirety. Although these fields are uniformly managed, the variation in production is large (Vansichen & de Baerdemaker, 1993). As shown in Figure 1.1, the crop yield can vary over 300% from minimum yield to maximum yield. In many industries this variation in production of 300% would not be acceptable. Agricultural industries are now taking note of this variation and looking at better ways to manage their farming systems to maximise production.

The extent of the spatial variation has led to the development of a concept known as Precision Agriculture (PA). This term refers to:

> "... an information and technology based agricultural management system to identify, analyse, and manage the spatial and temporal variability of soil and plants for optimum profitability, sustainability, and protection of the environment." (Anon., 1994)

Information and technology is used to more accurately manage the extensive temporal and spatial variation in crop production. As Clark, Schrock, and Young (1987) wrote, 'Modern information technologies will be used to improve the efficiency and cost effectiveness of today's resources'. Schumacher and Froehlich (1989) were some of the first to use these new technologies to achieve more efficient and cost effective chemical application. Schueller and Wang (1994) were also early researchers who examined variable rate fertilizer and pesticide application.

Figure 1-5 is an excellent illustration of the concepts and technologies involved in PA. The inner circle illustrates the management process of how results from one crop provide information to make decisions in the next crop. The outer circle depicts the flow of information between the various technologies such as the yield monitor, computer assessment and variable rate equipment. The concept of PA relies on these techniques.

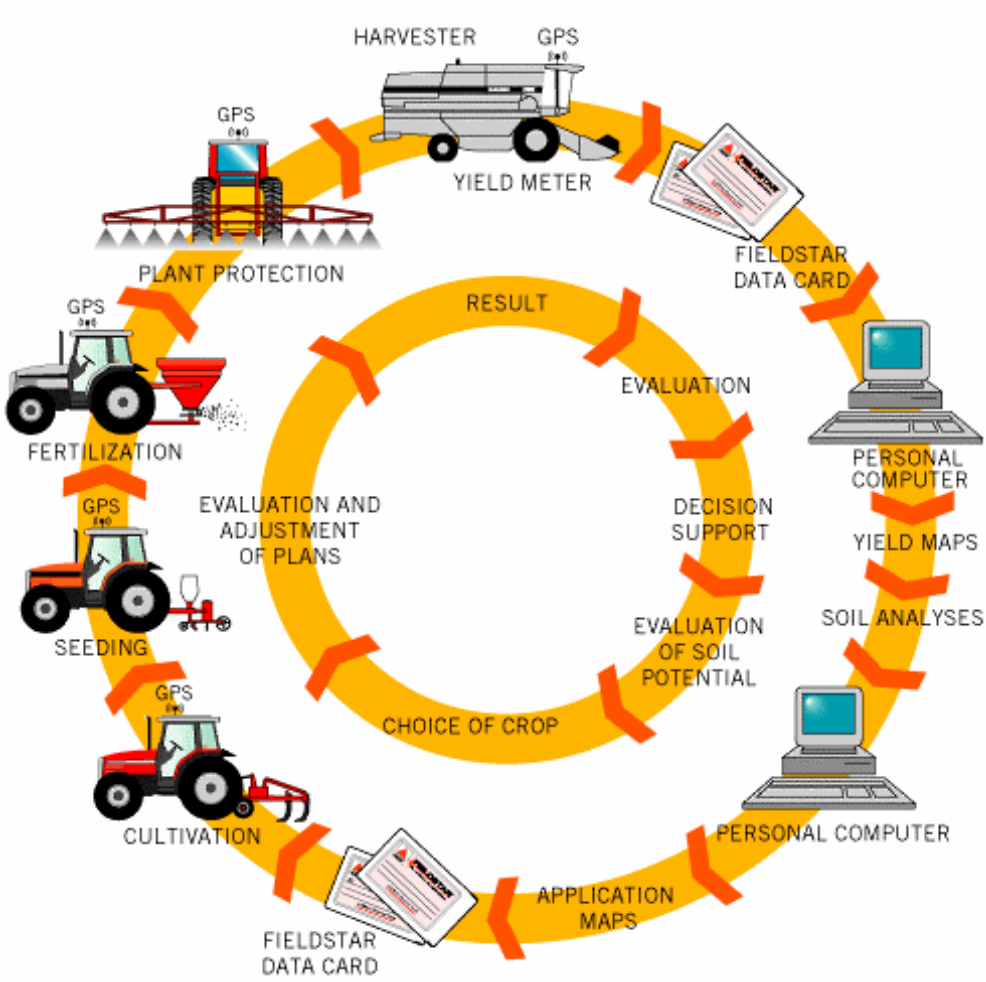

Figure 1-5. The concept of Precision Agriculture as seen by AGCO (Agco, 1998).

The rapid development of a few technologies over the last ten years has made PA possible. The most important of these technologies is the Global Positioning System. Also, powerful and high capacity computers have allowed the collection and analysis of the vast amount of data collected for PA. Finally, sensors have been developed for measuring a wide range of data, from crop yield to soil characteristics (Liu & Upadhyaya, 1996) to weed infestation (Benlloch *et al.*, 1996). These technologies all combine to provide a host of new tools that can improve the efficiency of farming.

1.5.4 Global Positioning System (GPS)

As the application of PA, along with yield mapping, hinges on GPS technology, the following overview is provided. GPS technology has been used extensively for agricultural

location and positioning applications by earlier researchers including Borgelt and Sudduth (1992), Colvin *et al*. (1991), Larsen *et al*. (1991) and others.

The Navstar Global Positioning System (GPS) is a satellite based radio navigation system developed and operated by the U.S. Department of Defence. GPS enables land, sea, and airborne users to determine their three dimensional position, velocity and time anywhere in the world with unprecedented accuracy. User's longitude, latitude and altitude are calculated by measuring the time taken for a radio signal once transmitted from GPS satellites to reach a receiver.

The accuracy of GPS depends on the mode of operation. There are two modes of operation, standard GPS (GPS) and Differential GPS (DGPS). Standard GPS requires the use of only one receiver which is known as a "stand-alone" GPS unit. The accuracy depends on "dilution" of precision by the US military (known as Selective Availability (SA)), the position of the satellites and the number of satellites in view. The error of standard GPS varies from ±several metres with SA off to over 100 metres with SA on (Harrison *et al,* 1992). Standard GPS is sufficiently accurate for many navigation tasks for marine, aviation or ground vehicle purposes, but insufficiently accurate enough for measurements such as surveying.

DGPS is designed to improve the accuracy of standard GPS. A stationary receiver at a known location (the "base station") receives signals from the satellites, and calculates its own position. Since the actual position of the base station is known, the errors in the satellite signals are accurately calculated. In PA, this error information is usually transmitted in real time to the mobile receiver (the "rover") over a land based radio or satellite link. This technique improves the typical error to less than 5m, 95% of the time, but depends on the distance between base station and rover (Shropshire *et al*, 1993). For agricultural purposes, a base station within 700 hundred kilometres provides sufficient accuracy of 5 to 7 metres (Higgins *et al,* 1992).

Chapter 2 - The Potential of Precision Agriculture for the Australian Sugar Industry

Before researching the concept of yield mapping sugar cane it was decided to examine the potential benefits of Precision Agriculture to set the context of the research. The review given here explores the direct benefits that the Australian sugar industry can gain from the concept of PA. The benefits were divided into the environmental benefits and economic benefits. Each of these areas is separately discussed.

2.1 Environmental Benefits

There is increasing pressure on farmers to minimise the environmental impact of their enterprises and develop sustainable practices. PA is seen by farmers and other interested parties as a potential major step in this direction. Environmental benefits will arise from better matching of inputs to the crop's requirements, resulting in the saving of inputs and in minimising the potential for off-site impact of agricultural chemicals. This positive approach is currently unsubstantiated, as there is no tangible evidence to support these claims. To quantify environmental factors, research is needed to put definite values on the off-site impact of on-farm chemical inputs and how PA may reduce these.

Considerable research is currently being carried out on the nutrient loading of various river systems in the sugar growing areas of Queensland (Mitchell et al, 1996). Initial results have shown significant concentrations of N, P and K. In one of these reports however Bramley and Johnson (1996) concluded 'the concentration of nutrient in stream water is generally below levels that have been deemed acceptable' and also 'the extent to which nutrient export impacts on ecosystems downstream has not been quantified'. Until these issues have been

resolved and substantiate a definable negative impact of sugar cane farming, then the potential environmental benefits obtainable from PA can not be claimed as a major reason for adoption in this industry.

Some other research that has implications for PA includes considerations of nitrogen leaching. Verburg *et al.* (1996) simulated a relationship between fertiliser application rate, crop yield and amount of leached nitrogen (Figure 2-1). The results show that as the yield response levels off, the amount of leached nitrogen rises dramatically. This type of research can help quantify the effect of over-application of nitrogen and therefore determine the environmental benefits of more precise farming. Nitrogen leaching is a major factor driving PA research in Europe, where the addition of nitrates to the ground water is of major concern.

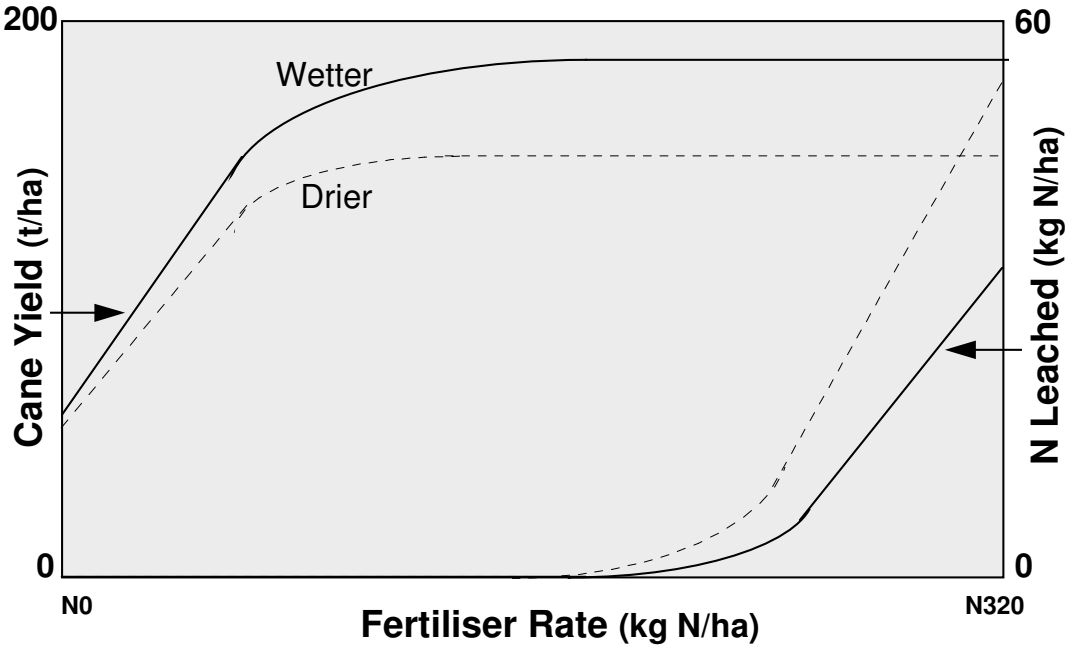

Figure 2-1. Effect of Nitrogen application rate on sugar cane yield and nitrogen leaching. (Adapted from Verburg *et al*., 1996)

In summary, PA has the potential to offer environmental benefits for the Australian sugar industry however at present these are difficult to define and are intangible. Until more research is carried out in this area, the environmental benefits should not be used as major driving factor.

2.2 Economic Benefits

Economic benefits have previously had the greatest impact on the adoption of new farming techniques and technology, and is likely to be the main factor determining the adoption of the PA concepts. There are two separate areas where PA can provide economic advantages over conventional practices, being input savings and production gains. These two areas are examined in sections 2.2.1 and 2.2.2 respectively.

2.2.1 Input Savings

In contrast with the concerns about nitrate leaching in Europe, the major focus of the development of PA in the United States has been on saving fertiliser inputs to grain crops. In these cropping systems the fertiliser contribution is a major portion of the total inputs. Initial research has shown up to a $50/ha saving on site specific application versus blanket (or uniform) application (Wollenhaupt and Buchholz, 1993). The same concept and technology could be applied to sugar cane production but it is unlikely that a typical grower would be interested in a $50/ha saving, particularly when there is a downside risk of lost production. This can occur in wetter than average years when higher than normal leaching and volatilisation losses can occur. (Les Chapman pers. comm. 1996). However depending on the type of input and the extent of the variability, there are potentially larger savings to be made. The levels of saving possible will be examined using a simple model.

This model uses some simple assumptions to determine the possible savings using site specific application as compared to blanket application. The model uses a hypothetical field with variable soil types and different input requirements. Although shown on a hypothetical field, the principle can be applied to any cane field. Some principles presented here have been adapted from Forcella (1993).

It is assumed there is a hypothetical field with two soil types, defined as Soil A and Soil B. Each soil type has different physical characteristics and therefore different yield potentials. Assuming these yield potentials are fixed and cannot be improved, then ideally the inputs should be applied differently depending on the yield potential of the soil type. Under these conditions the possible savings derived from site specific application depend on two

variables. These are, a) the extent of the soil variability and b) the *Differential Requirement Cost*. In the model the extent of the soil variability is measured by the ratio of the area of Soil A to the area of Soil B. The Differential Requirement Cost is calculated by the input cost ($/kg) multiplied by the difference in input required between the soil types (kg/ha). For example the input may be bulk fertiliser at $0.46/kg and the difference in input requirements between the soil types may be 27%. On a farm which applies 800 kg/ha to the crop this would result in a 217 kg/ha difference and therefore a $100/ha Differential Requirement Cost.

The model is shown graphically in Figure 2-2. Across the X axis is the ratio of the area of soil type A to soil type B in the field. The possible values for a field range between 100% Soil A to 100% Soil B. The Over-application Cost on the Y axis is the cost in dollars per hectare due to applying too much input to Soil B. This cost is calculated using the assumptions that Soil A has the higher yield potential and that when applying blanket rates the farmer would base them on Soil A's requirement so as not to limit its yield.

To complete the model a line is drawn from the origin to the Differential Requirement Cost on the right Y axis. These two points represent no over-application cost when the field is 100% Soil A and the full over-application cost when the field is 100% soil B. The slope of this line increases directly along with the Differential Requirement Cost. Three different lines are drawn which could represent the inputs of Gypsum, some herbicides and say, fertiliser. A single horizontal line is drawn indicating the fixed cost of Site Specific per hectare Management (Fixed SSM Cost/ha in Figure 2-2). This value has been estimated to be comparable with the quoted figures of approximately $30/ha, including yield mapping (Lowenberg-DeBoer and Swinton, 1995).

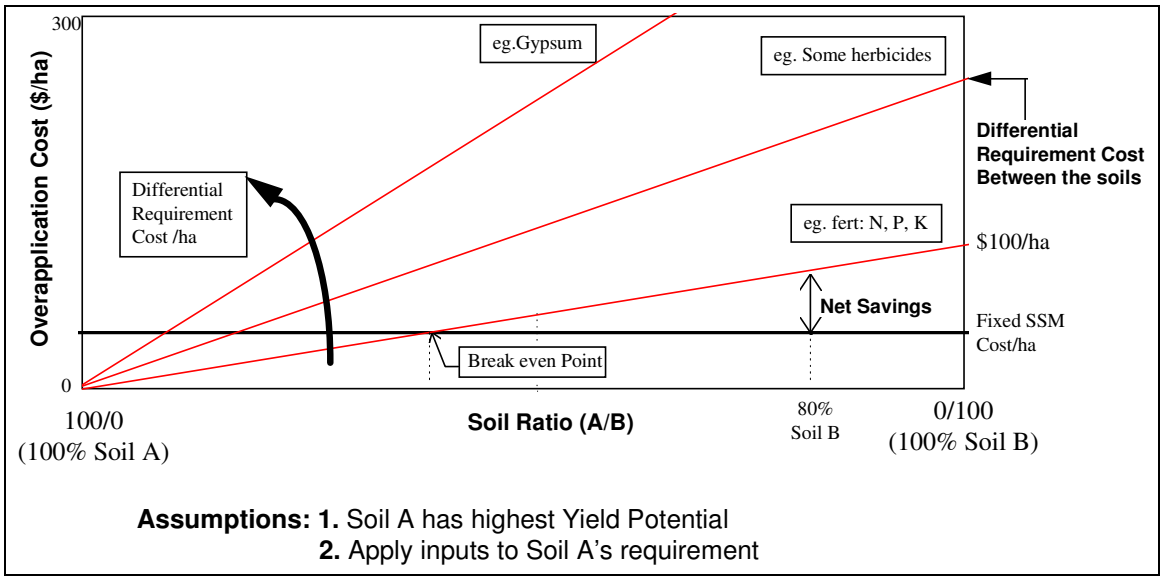

Figure 2-2. Model to determine the potential financial savings of site specific application of inputs versus blanket application, on a hypothetical field.

The net saving for a particular field depends on the soil ratio and is the difference between the fixed cost of the site specific management and the drawn line. An example is given on Figure 2-2 showing a soil ratio of 80% Soil B, giving a net saving of $50/ha for fertiliser inputs. However if there was 80% of Soil B then maybe the farmer should fertilise to Soil B's requirements. In this case there would be a yield sacrifices of the Soil A area. In the same way the yield loss could be estimated and used in the decision.

Figure 2-2 shows that the higher the differential requirement cost for a certain input, the larger the economic benefit possible from the use of PA. It also shows the high cost inputs per hectare ($/ha) such as gypsum have the highest cost/benefit ratio from the use of PA. It will be these inputs that will promote the early adoption of this technology in the Australian Sugar Industry.

Although this model shows the possible savings that can be made with site specific management it does not take into account the higher risks that are taken. The risk involved results from the potential to lose production due to under-fertilising the crop. Keating et al. (1994) clearly showed that in sugar cane there is economical advantage to err on the high side of fertilisation rates. Through site specific management, the risk of erring on the low side of fertilisation rates is increased. This is an important issue that should not be overlooked when examining site specific management for the sugar industry.

Another limitation of the model is that does not take into account the affect climate variability can play. As the climate changes from year to year crops on a particular soil type will respond differently. The model is still useful however in explaining the interaction of certain important variables.

2.2.2 Productivity Gains

The other major area where PA can provide an economic benefit is through productivity gains. These gains can be realised through the use of the PA concept to improve the information and practices that lead to increased sugar yield.

In the sugar cane crop there are two ways productivity gains can be achieved. These are through (i) increased crop yield and (ii) increased sugar content (commercial cane sugar, (CCS)). PA has the potential to boost both these measures in a number of ways.

Gains can be obtained from improved knowledge of the crop yield and field availability. Improved management will be possible, using more precise information available from sources such as yield monitors, remote sensing and soil and crop sensors. This increased management information will assist in determining the factors that are limiting yield and selecting a means for reducing their effect. Growers will be able to pinpoint problem areas and rectify them. Examples include detecting and fixing water/drainage problems (soil moisture & stresses), insect/weed problems (grubs and nematodes, etc), soil compaction and better selection of varieties/cultivars. With sugar cane being a relatively high value crop per hectare, this is likely to be where the greatest economic gains are to be made.

Another possibility for increasing production would be for site specific application of nitrogen to maximise sugar yield rather than cane yield. Growers perceive, and research shows, that excessive nitrogen application reduces CCS and therefore reduces their profit. For example, work by Wood (1990) reported that sucrose concentration in fresh cane decreases by 0.3-0.4% for each additional 50 kgN/ha applied above an appropriate level. Although this is confirmed, it is undecided whether sugar yield actually decreases. Keating *et al.* (1994) summarised various studies where, although CCS declined with nitrogen application, the increase in yield more than compensated for this loss and the actual sugar yield overall increased. More research is needed in this area to determine the effect of nitrogen on actual sugar yield. Crop modelling such as that discussed by Hammer (1993)

would be useful. If a clear optimum is found then this is strong support for the use of more precise application of nitrogen to maximise sugar production.

The potential for productivity gains is the major factor that will decide PA's adoption rate in the Australian sugar industry. If growers perceive clear productivity gains, then adoption will be rapid. This is precisely what has happened in the US sugar beet industry where "...there's a stampede to site-specific production practices. Research has shown increases in net profit in sugar beet up to $US352 per hectare (Reichenberger, 1995). This is a result of higher production through higher yields and higher-quality premiums. Precise nitrogen management affects both of these factors in sugar beet production. Excess nitrogen is detrimental to beet quality because sugar content is reduced and impurities result in more sugar being lost to molasses. It is possible that a similar development could occur in the Australian sugar cane industry.

2.3 Conclusion

There is real potential for PA to benefit the Australian sugar industry. At this stage the concept is still very young and to predict the exact impact is difficult.

Economically there is potential for input savings using site specific application practices. The possible production gains obtained through increased management information are where the greatest gains can be made. This will be the major factor that will determine the adoption of PA in the Australian sugar industry.

The environmental impact of existing farming practices must be determined before the environmental value of PA can be assessed.

Males and Clive (1996) in their paper 'Maintaining the international competitiveness of the Australian Sugar Industry' stated, 'Australia is at the forefront of technological innovation in the world sugar industry...'. For this reason PA should be viewed openly and with optimism that the concept will provide another technological advantage to keep the Australian sugar industry internationally competitive.

A yield monitor is a critical component of PA. Therefore this research is an important initial step in realising the potential gains PA has to offer.

Chapter 3 - Yield Mapping Review

3.1 Introduction

This chapter reviews the concept of yield mapping. The need for yield mapping in agriculture is examined and associated theory and processes are outlined. Previous developments in the field of yield mapping are reviewed to define the state of the art. The final section thoroughly examines the concept of mass flow measurement by reviewing the existing mass flow sensors developed for yield mapping and analysing the nature of their error.

3.2 The Need

A yield map shows the variation in crop density between fields, or within individual fields. Figure 1.1 is a yield map constructed using data collected from a sugar cane crop. This map shows that the variation in crop yield is significant across the block with definite trends. The figure also shows how evenly spread inputs do not produce even outputs. Yield maps provide essential information for spatial analysis and evaluation of crop production management within a field. This information can be an input to decision making for field operations during the next growing season (Vansichen & De Baerdemaeker, 1993). The crop yield is a function of many variables, but the effects are integrated in the final result at harvest. This culminating variable is the best and most practical method of assessing management techniques for site-specific farming practices. By studying several years of yield maps, areas of different yield potential can be identified. Seed, fertiliser and chemical application plans can then be designed around the yield potential of individual parts of each field (Massey Ferguson Group Limited, 1993). This site-specific management would result in a highly efficient crop production system. Russnogle (1991) believes yield maps of grain

crops, combined with soil maps to determine the site specific application rates, can result in an estimated 5% reduction in fertiliser application rates over rates determined by soil maps alone.

Yield maps can also greatly improve the information available for making management decisions. As well as use in site-specific farming purposes, a yield map can also highlight problems with drainage, disease or weed infestation (Clark, Schrock, and Young, 1987). With accurate yield maps, a farm manager can investigate the many possible reasons for yield variations, as they have a clear indication of good and poor areas of the field. Some reasons for yield variations are relatively easy to rectify, for example, by subsoiling compacted areas. Other reasons can be established by soil analysis, where the yield map allows this task to be performed more selectively than with traditional 'random sample' methods (Massey Ferguson Group Limited, 1993).

3.3 Yield Mapping Theory

During harvesting the local yield of a crop can be expressed as a function of the material flow rate into the harvester, the forward travel speed and the cutting width as shown in Equation 3.1.

$$Y(t) = \frac{F(t)}{S(t).W} \qquad \textbf{(Equation 3.1)}$$

where Y, is crop yield [kg/m^2];
F, is material flow rate [kg/s];
S, is driving speed of the harvester [m/s];
W, is actual cutting width [m]; and
t, time [s].

With sugar cane being a row crop and generally only harvested a single row at a time, the cutting width can be assumed constant. Although it may vary slightly between farms, it can easily be measured. Machine driving speed is a function of time, and for reliable yield maps it must be accurately measured. Driving speed can be measured in many ways and methods previously used during yield mapping operations include Radar Doppler measurement (Vansichen and De Baerdemaeker, 1993), direct wheel measurements (Lemne, 1992) and

even differentiation of GPS location data (Stott *et al*., 1993). This leaves the material flow rate into the machine as the final variable required to measure crop yield. This variable is also the most difficult to measure.

Note, the ultimate measure of sugar cane yield is the mass of sugar per area. This is related to the mass of sugar cane by the sugar content expressed as a percentage. The sugar content is typically in the range of 10 to 18%, and is generally measured at the sugar mill for payment purposes. A sensor for measuring sugar content in real time during harvest would improve the yield mapping process but as a first step, this thesis will focus on mass measurement.

3.4 Yield Mapping Technology

The main components of a automated yield mapping system are a DGPS receiver, mass flow sensor, ground speed sensor, yield monitor/display and a data logger. The relationship of these components is shown in Figure 3-1.

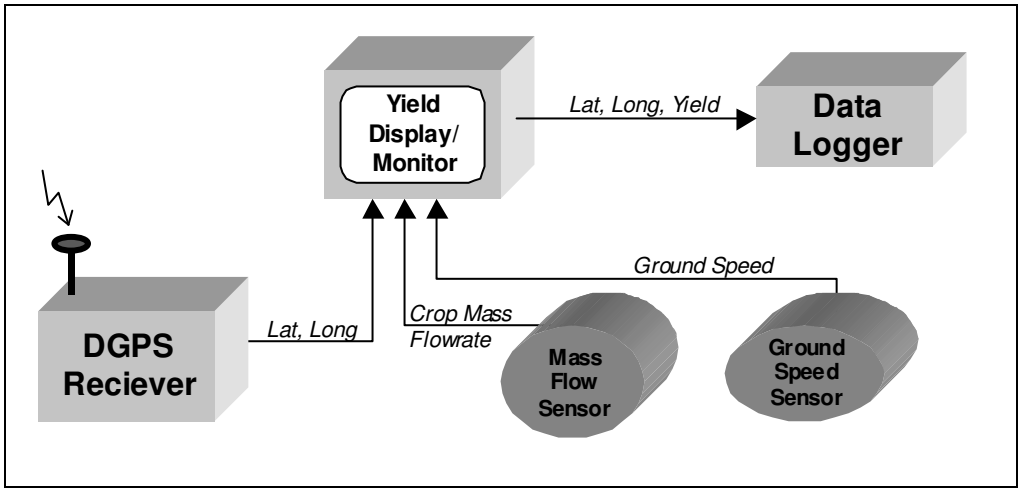

Figure 3-1. Yield Mapping Hardware

The process of yield mapping begins with the position (Longitude and Latitude) of the harvester being calculated each second by the DGPS receiver. These data, along with the sensor information, are relayed to the monitor/display, where the crop yield is calculated using equation 3.1 and displayed. All data are then integrated and stored at equal time intervals (usually each second) in the Data Logger. The standard medium for the storage of

yield data is PCMCIA SRAM memory cards. These cards are inserted into the data logger and when full (usual capacity of 10 to 30 hours of harvesting) are removed and the information is down loaded to a personal computer for the production of yield maps.

The process of producing yield maps from the raw yield data is shown in Figure 3-2. This process takes place on a personal computer. The data are firstly imported from the SRAM card into specialised yield mapping software. This software is typically a simple geographic information system specifically designed for PA use. Examples include AgLink by Agris, SSToolbox by SST Development Group, Farmstar by Fairport Technologies Pty Ltd and Farmsite by Farmworks. This software can display the individual data points as a yield map, but usually the data are smoothed to produce a map that is more readily analysed. The smoothing typically utilises an algorithm that interpolates from the raw data points to produce a grid as the output. This grid can also be contoured to enhance the output format. When this is completed a digital copy of the yield map is archived to hard disk and a hard copy map can be printed.

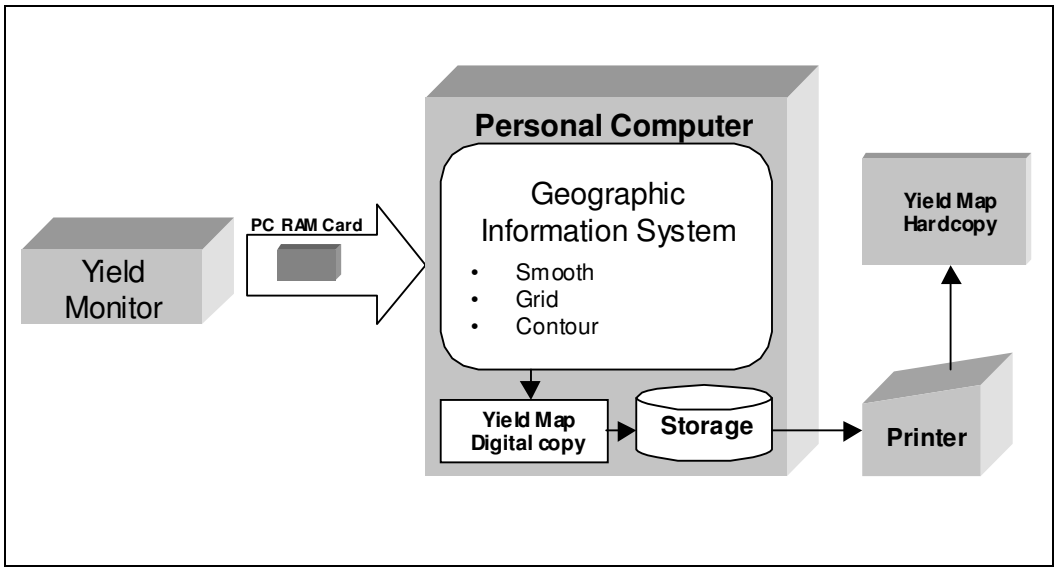

Figure 3-2. Process for yield map production.

This section has outlined the current technologies and processes of yield mapping. These technologies and processes have evolved to this state over almost two decades. The next section reviews this evolution, beginning with some of the initial yield mapping research.

3.5 Previous Developments

It should be noted that for this dissertation yield mapping is defined as the measurement of yield on the harvester in real time during harvest. Yield could always be mapped coarsely using a weigh wagon and an area measurement. However, this is not yield mapping as defined in the modern context. With this in mind it is difficult to state exactly when the development of yield mapping systems began.

One of the earliest researchers, John Schueller, stumbled across the idea in the early 1980s. Schueller (1997, pers. comm., 28 January) was conducting research in 1984 examining the real time control of the ground speed of grain harvesters. By measuring the amount of crop material entering the harvester, the ground speed could be adjusted to optimise the grain threshing operation and operational efficiency. As a spin-off from this work, the measurement of the material entering the harvester allowed the calculation of yield in real time when combined with the ground speed measurement. The variation in the yield Schueller measured on a seemingly uniform field was quite astonishing and proved more interesting than the initial control problem. From this point he began to examine the options for collecting this yield information during harvest, with the aim of improving agricultural production.

Although the technique of yield mapping may have been conceptualised, there was a vital ingredient missing. A positioning system was required to georeference the yield measurements to their positions within the field. In 1986, Schueller (1997, pers. comm., 28 January) attempted to use a positioning system developed for use in the petroleum industry, but this system proved unreliable and inaccurate. Around this time a location system was being developed by the US Department of Defence, known as the Global Positioning System (GPS). This system consisted primarily of a set of satellites placed in orbit and GPS receivers on mobile vehicles (Shropshire, Peterson, & Fisher, 1993). The GPS receivers monitored signals from the satellites and calculated their three-dimensional position, velocity and time anywhere in the world with unprecedented precision. This was the exact requirement for the automated georeferencing of yield data, and proved to be the catalyst for PA developments in general.

Although GPS made it possible for a whole range of new tools to be produced to improve agricultural production, it was perceived that yield mapping was of the highest priority. Yield maps provided information to direct site-specific practices and also a means to

evaluate these practices. The interest from producers and agricultural researchers produced a race to develop a reliable yield mapping system. Initially all research was undertaken for application to grain combines, which had the greatest worldwide market for this type of system.

In 1991, Massey Ferguson (Massey Ferguson Group Limited, 1993) was the first combine manufacturer to offer a yield mapping system for sale with their machines. Today there are twelve different yield mapping systems on the market for use in grain harvesters (@g/INNOVATOR Online, 1996). Their adoption has been rapid with the first units sold in 1993 and by the end of 1997, 25,000 units (@g/INNOVATOR Online, 1996) were sold. Milby (1997) stated that within a decade 50% of the combines within the US will incorporate these systems.

Recently research has been conducted in other crops. Walter *et al*. (1996) reported a yield mapping system developed for sugar beet and Campbell, Rawlins and Han (1994) reported a system developed for potatoes. Auernhammer *et al*. (1994) and also Vansichen and De Baerdemaeker (1993) reported a yield mapping systems developed for use in forage crops. The sensor details of these systems and the grain systems is discussed in the next section that reviews the concept of mass flow measurement.

3.6 Existing Mass Flow Rate Measurement

As previously stated, mass flow rate measurement is a vital component of any yield mapping system. Mass flow rate is defined as the mass of material (kg) passing a point in unit time (s). The SI unit for this quantity is kilograms per second (kg/s). Mass flow rate measurement has many applications outside agriculture, however for the purpose of yield mapping there are unique requirements that necessitate specialised solutions. For this reason mass flow rate sensors from other industries or applications cannot be easily transferred for use in yield mapping. This has led to the development of a number of different mass flow rate sensors for yield mapping various crops. The methods used to measure this variable are mixed, ranging from direct mass measurements to indirect measurements of the power required to process the material. This section reviews these sensors with the aim of establishing the state of the art and also examining their potential application to sugar cane.

3.6.1 Grain Sensors

Borgelt and Sudduth (1992) summarised thirteen different grain flow measurement devices developed by various parties. These devices all measured the clean grain flow prior to delivery to the storage tank on the harvester. Four of these techniques are explained below to give the reader an understanding of the concept of grain mass flow rate measurement:

- Gamma ray absorption

  This system consists of three units - a gamma ray emitter, a detector, and a display unit. The emitter is mounted under the crop material flow, with the detector mounted directly above the emitter. As the material passes through the measuring gap between the emitter and detector, it reduces the intensity of the gamma radiation registered by the detector. This reduction is proportional to the grain mass flow rate.

- Impact plate

  This sensor uses the change in momentum of moving crop matter, impacting against a curved plate, as an indicator of flow. The force exerted on this plate is proportional to the mass flow rate.

- Pivoted auger

  For the measurement of grain flow, an auger is mounted with one end pivoted and the opposite end supported by a load cell. As the grain is fed through the auger the load cell reading is a measure of mass flow.

- Elevator photodiodes.

  A light source and photodiodes can be mounted on an elevator to measure the depth of crop material on individual flights. The light that is received at the photo diodes gives an indication of the volume of material on each flight, and therefore an indirect measurement of mass flow.

Howard *et al.* (1993) described the development and testing of a grain flow sensor based on

a triangular paddle elevator. Grain yield measurements were accurate to within 5% full scale of the actual yields. Stott, Borgelt and Sudduth (1993) conducted research on a 'Claydon Yieldometer', which relies on a paddle wheel arrangement to measure grain volume. The research found the sensor operated with an overall accuracy of +/-1%. Birrell, Sudduth and Borgelt (1996) compared the various sensors and techniques for crop yield mapping.

To date, the most commercially successful sensors have been based on the impact plate technique, discussed by Borgelt and Sudduth (1992). However this method does suffer from inherent problems relating to the effect of friction, which are discussed in Strubbe, Missotten and De Baerdemaeker (1996), who proposed a configuration that minimised these effects.

3.6.2 Sugar beet and Potatoes Sensors

Walter *et al.* (1996) reported on a yield mapping system developed for sugar beet. Campbell, Rawlins and Han (1994) and Rawlins *et al.*(1995) reported a system developed for potatoes. Each of these systems incorporated a weighing type sensor for the measurement of mass flow rate. Rawlins *et al.*(1995) used a 'load cell suspension system' that relied on a conveyor being suspended at one end by a load cell. Campbell, Rawlins and Han (1994) improved this system to use a conveyor supported by 'idler wheel load cells'. Walter *et al.* (1996) laboratory tested the 'idler wheel load cell' along with a 'slide bar weight sensing assembly'. The research found that the slide bar configuration was the most accurate method. Field testing produced errors of up to 6.95% (average 2.28%) over areas of approximately 3000m^2.

3.6.3 Forage Sensors

The research carried out on the yield mapping of forage crops relied on two entirely different mass flow rate sensors. Auernhammer *et al.* (1994) detailed a system where 'different types of strain gauges located at different places in the vehicles (self loading trailers and round balers) were tested for their suitability as a weighing technique'. Vansichen and De Baerdemaeker (1993) developed a system that relied on the power or torque recordings of the base unit or the blower of a 2100 New Holland forage harvester.

The research of Auernhammer *et al.* (1994), using the weighing technique, provided an

extensive amount of information about the quality of the mass flow measurement. The accuracy of the measurement was better than +/-10%, 95% of the time, over an area of 250m^2. This type of sensor could have application in the sugar cane harvester and this possibility is discussed later.

The power measurements of Vansichen and De Baerdemaeker (1993) are an indirect method of measuring mass flow rate. It is based on the assumption that higher feed rates involve proportionally higher power to process the material. This technique achieved a linear calibration with an R^2 of 0.995, using limited data. This technique of using processing power to indirectly measure mass flow rate also has potential for application to sugar cane harvesters. This application is discussed further in the next chapter.

3.6.4 Nature of Measurement Errors

As previously stated the focus of this research will be the development of a mass flow rate sensor for sugar cane. The basis of this development will involve testing potential sensors. The primary measure of performance for any sensor is accuracy. Sydenham, Hancock and Thorn, (1989) put it another way; '*The design of measurement systems is primarily concerned with keeping errors under control*'. To examine the nature of the error inherent in current mass flow rate sensors used for yield mapping is important, as this will allow the potential sugar cane sensors to be properly evaluated. Also important to highlight is that the information presented here is largely based on results from grain yield mapping systems, as these systems are the most prevalent and best developed and reported. The nature of the measurement errors of these systems is expected to be typical of yield mapping systems of other crops. From these results, information can be derived and applied to the development of a sugar cane sensor.

Calibration Process

As with most sensors, two variables are required to define a linear calibration line (see Figure 3-3). One is the baseline that is also referred to as the tare, zero or null. The other is the gradient of the calibration line that is referred to as the sensitivity or calibration factor. In existing yield monitors the baseline can be reset manually or automatically. Drift in the baseline can be the cause of significant errors as displayed by early model John Deere Green

Star yield monitors (Doerge, 1999), however normally the baseline is relatively easily measured and adjusted. The more difficult and important parameter to measure is the sensitivity.

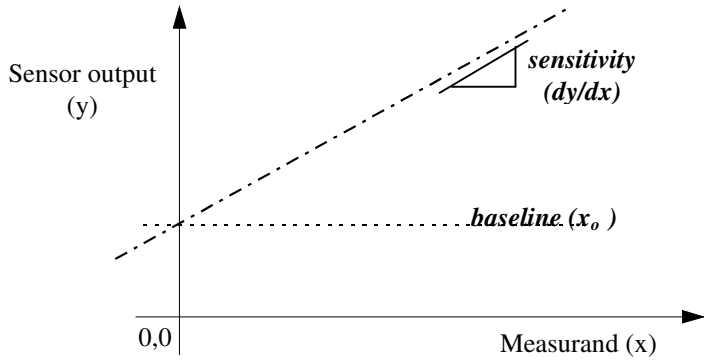

Figure 3-3. Linear calibration characteristics.

For current yield monitors the sensitivity or calibration factor is measured by harvesting a load of crop into a simple weighing device. The weight as measured by the weighing device is used to adjust the calibration factor of the yield monitor. Some yield monitors such as the Ag Leader unit utilise multiple calibrations factors to take into account any nonlinearly in the sensor output, but the principle is the same. Regular execution of this process is recommended by yield monitor manufactures to maintain accuracy. The result of this calibration process is the continual removal of the bias in the sensor measurement. The bias is defined here as the long-term error of the sensor calculated using infinite number of samples. Although with this calibration technique, a bias error can still exist or develop over time, it is generally kept within reasonable levels. Once the bias is removed the majority of the remaining error can be classed as random. The cause of this random error is any number of factors including vibrations, changes in the crop properties and more. This discussion will not define the exact cause of the random errors but will examine how its characteristics gives rise to the overall nature of the error in current yield mapping systems.

Random Error

The resulting random error of yield monitors results in some characteristics that are important when trying to define the nature of the error. The first characteristic is that the random error is likely to have a Gaussian or normal probability distribution function. This

distribution is centred around the bias, which we have previously stated as being roughly zero (Figure 3-4). This distribution of error makes it difficult to specify yield monitor accuracy with a simple percent error (i.e. less than 3%). To take into account this distribution, the percent error must also be given with the confidence level of this specification. A typical confidence level would be “1 sigma” (1 standard deviation) or “2 sigma” (2 standard deviation), representing 68% and 95% confidence levels respectively. An example would be 3% at 1 sigma, indicating 68% of the error measurements lie within the ±3%. This characteristic is somewhat acknowledged by Ag Leader (1997) who states that their yield monitors can be expected to be accurate "within 2% of the true value most of the time, and within 4% virtually all of the time." It could be assumed that “most of the time” represents one sigma and “virtually all of the time” represents two sigma. This detail of specification is not typical, with most yield monitor manufactures keeping the specification as a single number (e.g. 5%). The confidence level will be defined when specifying the accuracy of the sugar cane mass flow rate sensors studied in this research.

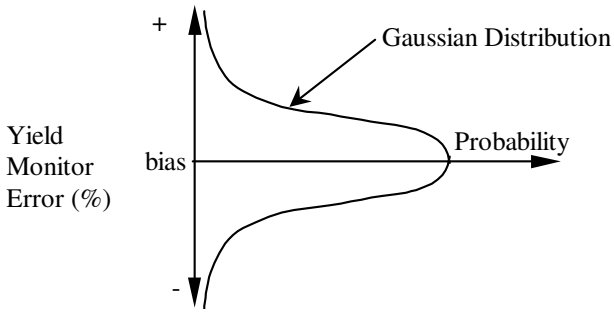

Figure 3-4. Probability distribution of yield monitor errors.

Another important characteristic of the yield monitor random error is the fact that the error reduces as larger loads or areas are harvested. That is, error will be proportionately higher for small harvested areas and lower for large areas. To put it more precisely, the distribution or spread of the error reduces as the sample size increases. This relationship is due to a basic statistical relationship that states the larger the sample size the greater the tendency for the mean of these samples to cluster around the population mean. In statistics this relationship is used to define the error of trying to measure a population mean from only a subsample of the population. In the context of yield mapping it can be used to explain the inverse relationship between yield monitor error and sample size. Any elementary statistic text such as Weiss and Hassett (1986) will show that the mathematical relationship between the standard deviation of the sample mean, $\sigma_{x,}$ the population standard deviation σ and the sample size, n, is given

by:

$$\sigma_x = \frac{\sigma}{\sqrt{n}} \qquad \textbf{(Equation 3.2)}$$

A graphical representation of this relationship is shown in Figure 3-5. The 3D solid shapes shown in the figure represent the error distribution for various sample sizes. The sample size can also be thought of as being proportional to the harvested area or load size. At the lowest sample sizes the spread of the error distribution is large. As the sample size increases the spread reduces. The figure also shows the two sigma confidence limit for the distributions. This value also reduces at the rate of square root of the sample size.

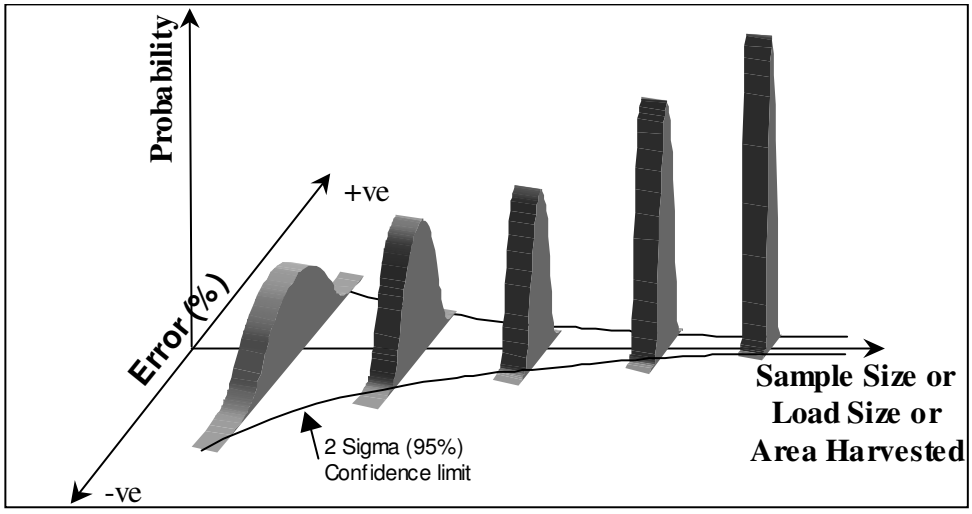

Figure 3-5. Relationship between yield monitor error and sample size.

These characteristics of the yield monitor error are supported by work by Doerge (1997) who measured the accuracy of 16 different yield monitoring units in the USA. These monitors represented the three grain yield monitor brands of AgLeader, Case AFS, and John Deere's GreenStar systems, which account for the majority of systems used throughout the world. One hundred and ninety-four measurements were taken at different load sizes to produce the results as shown in Figure 3-6. From this figure can be seen the random nature of the data scatter around the bias of close to 0% error. The bias for all the samples appears slightly positive and was actually 1.23% for loads greater than 4000 lb. This indicates the bias has been largely removed by the calibration process to leave only the random component of the

error. The next interesting point is the Gaussian distribution of the data around the bias. This is particularly evident around the 4000 lb mark where most of the points are clustered closely around the bias, and the number of points is reduced as the distance from the centre line increases. The last obvious point is that the distribution of the error reduces as the load size increases. The standard deviation of all loads greater than 4000 lb was 3.69%, however it is obvious that at the lower load sizes this standard deviation would be greater than 10%, and at higher load sizes it is smaller.

Similar results have also been found by Wilcox (1998) who conducted similar trials. The outcome of this work is shown in Figure 3-7. This figure displays more clearly the reduction in error as load sizes increases.

Figure 3-6. Result of trials by Doerge (1997) showing the nature of yield monitor error.

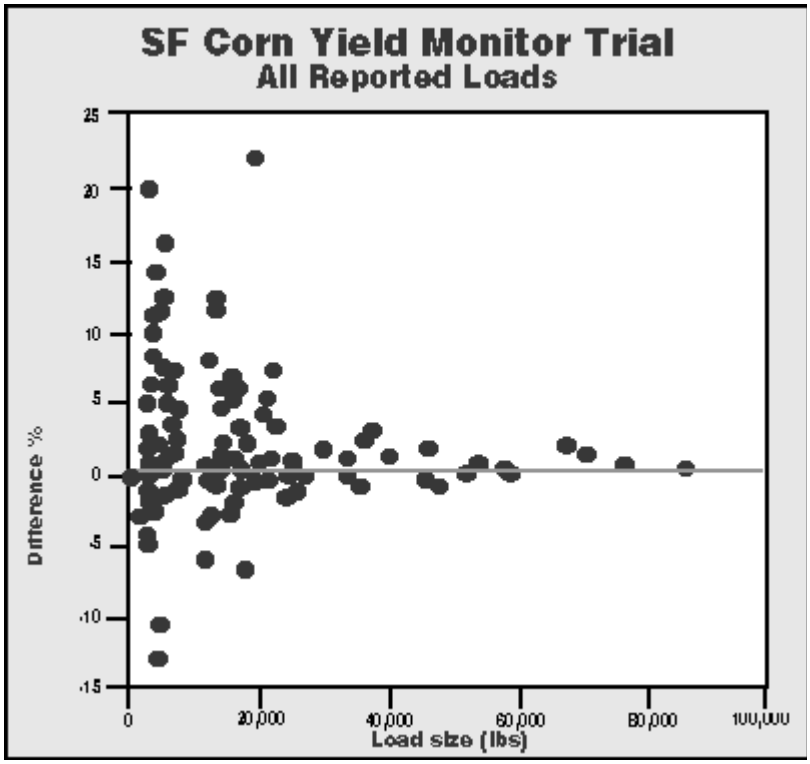

Figure 3-7. Result of trials by Wilcox (1998) showing the nature of yield monitor error.

These results are also supported by Auernhammer *et al*. (1994) who conducted research on the accuracy of three grain flow sensors. The results showed that the errors of the sensors was less than 1% over a total area of 40 ha, less than 11% over one full grain tank (approximately 1 ha) and on 15.2m long segments (approx. $100m^2$) the error went up to less than 25%.

Error Model

From these findings a mathematical model can be proposed to characterise the nature of yield monitor error, being:

$$M_e = \frac{R(b,\sigma)}{\sqrt{a}} \qquad \textbf{(Equation 3.3)}$$

where M_e is the yield monitor mass measurement error [%];

$R(b,\sigma)$ is a random number with a standard deviation of σ and a mean of b;

b is the bias error [%];

σ is the standard deviation of the error measured over 1 ha; and

a is the area over which the measurement is taken [ha].

To define the error in terms of a two sigma or a 95% confidence level, $M_{e95\%}$, then Equation 3.3 can be simplified to Equation 3.4.

$$M_{e95\%} = b + \frac{2.\sigma}{\sqrt{a}} \qquad \textbf{(Equation 3.4)}$$

The model shown in equation 3.3 has been used to simulate the error characteristics of a yield monitor with a bias of 0% and a standard error of 5% at an area of one hectare. The results of this simulation using a random number generator are shown in Figure 3-8. On this figure the two sigma confidence limit is also shown as calculated using equation 3.4.

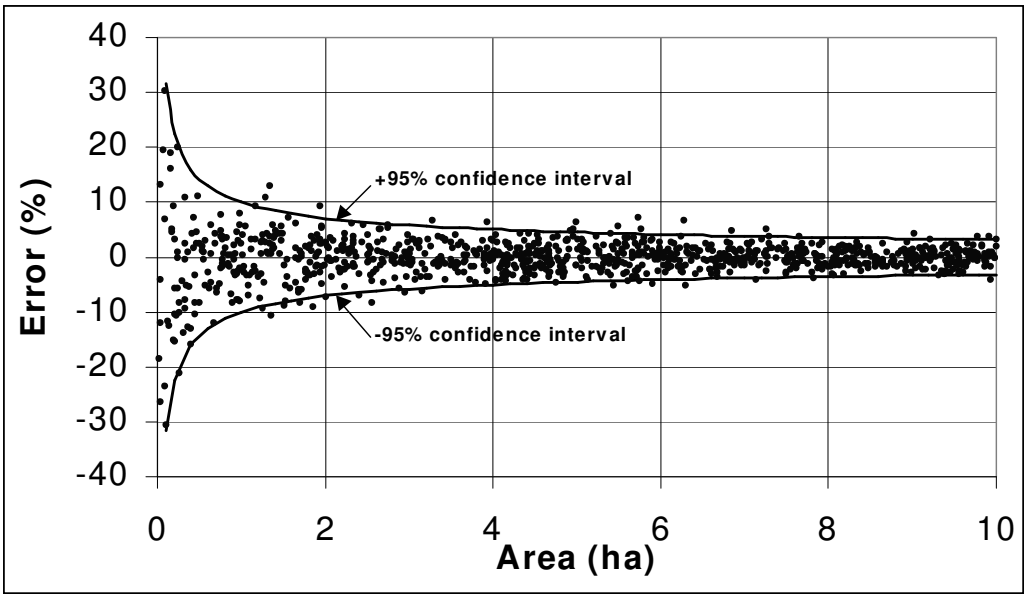

Figure 3-8. Yield monitor error modeled with a bias of 0% and standard deviation of 5% at 1ha.

Defining Yield Monitor Accuracy

From these findings it is obvious that stating the accuracy of a yield monitor mass flow rate sensor using only the average error can be misleading. To correctly state the accuracy it needs to be defined by three factors:

1. Percentage error of measurement
2. Confidence limit of this value (e.g. 95% of the time).
3. Area over which the measurement is made.

The area over which the measurement is made should be in line with the minimum area of interest that will be used for agronomic purposes. This means that if the yield map is used to base site specific decisions at a resolution of 1 ha then this is the area used for the specifications. If it is used to vary application rates of an input over a 20 x 20m grid then the area should be $400m^2$. When the yield data are analysed to produce a yield map then the map should be smoothed to the same scale. This will result in yield maps accurate to the specifications given.

Based on these definitions of accuracy, the results from Doerge (1997) and Wilcox (1998) can be used to define the level of accuracy for current grain yield monitors. The extensive study of Doerge (1997) found the standard deviation of 3.69% for all loads greater than 1.8t (4000 lb). Assume this figure represents the standard deviation at this load size. Assuming an average yield of 9 t/ha (8000 lb/acre) then the specification of $M_{e95\%}$ would be 7.38% over an area of 0.2 ha. Put more simply, the yield monitor error is less than 7.38%, 95% of the time, over an area of 0.2 ha (0.5 acre).

The Asgrow Seed Company (1997) found similar results. They conducted yield monitor accuracy trails over small areas of approximately 0.04 ha (0.1 acre). They found a standard deviation of 6.4% over this area. Using equation 3.4 to extrapolate to an area of 0.2 ha, these findings would produce a specification of $M_{e95\%} = 5.72\%$.

Other Sources of Error

The mass flow measurement is however not the only source of error for yield calculation. The other variables in Equation 3.1 of ground speed and cutting width can also introduce errors.

Ground speed is relatively simple to measure and also does not introduce significant error into the yield calculation. Speed error has been measured by Missotten *et al.* (1996) at 2.5%, while Trimble Inc (1998) specifies their Ag132 GPS system as having an error of 0.16 km/h. At an average harvest speed of 6 km/h this equates to 2.6% error. This would result in a

random error that has the advantage of becoming less significant over larger sample sizes as with the mass flow measurement error.

Width measurement can also introduce an error to the yield calculation. Missotten *et al.* (1996) measured this in a grain combine as 5%. When harvesting row crops the potential for error in the width measurement is minimised. Changes in row spacing can vary between fields, and within fields however it has not been identified as an important source of error.

It should also be noted that the errors from these other sources do not sum to give the total error in the yield measurement. Due to the fact that they are random errors the total error is given by:

$$Y_e = \sqrt{M_e^2 + S_e^2 + W_e^2} \qquad \textbf{(Equation 3.5)}$$

where Y_e is the yield measurement error [%];
M_e is the mass flow rate measurement error [%];
S_e is the ground speed measurement error [%]; and
W_e is the width measurement error [%].

The benefit of the ground speed and width errors being random is the fact that the error will reduce as more measurements are taken, just like the mass flow errors. This characteristic can be used to advantage during the processing of the data for yield map production. Although each measurement, which represents 4.5 m^2 at normal operating conditions (row width x ground speed x sample interval: 1.5 m x 3 m/s x 1 s) may involve a significant error, when these errors are averaged over an area of 100 m^2 to produce a yield map with a pixel size of 10 x 10 m then this error would be considerably reduced. As shown before, the error reduces with the square root of the sample size. Therefore if the initial sample size was 4.5 m^2, and it is then averaged to 100 m^2, then the error would reduce $((100/4.5)^{0.5})$ by a factor of 4.7. This result relies heavily on the fact that the error in each consecutive measurement is not related to the previous error and is therefore purely random. It could be debatable if this is true all the time. For example width measurement error may change on a greater spatial scale than every 4.5 m^2. Putting this aside however, it is still reasonable to assume that error reduces with sample size.

Although these two other sources of error occur in the yield measurement, it is believed the major source of error is the mass flow rate sensor. Therefore to limit the scope of this

research mass flow measurement errors will be the major focus.

3.7 Literature Review Update

Previous literature review was carried out in 1996 prior to the majority of the research being conducted. An updated review was required to check the state of the art at the time of submission of this thesis. This is given below.

3.7.1 Sugar Cane Yield Monitor Developments

A number of researchers around the world have recently conducted research into yield mapping in sugar cane similar to the work presented in this thesis. This other research was conducted after the research presented in this thesis. This is supported by the dates of publication of papers and patent in Section 1.2. The other research is reviewed below.

Benjamin *et al.* (2001) developed a sugar cane yield monitoring system very similar to the system presented in this thesis. It consisted of a scale, a data acquisition system, and a differential global positioning system. The scale consisted of a weigh plate fully supported by load cells (not hinged). It was mounted in the floor of the elevator to directly record instantaneous measurements of the mass flow rate of sugar cane. Experiments were run with different levels of cane maturity, variety, row/section length, and flow rate. The scale readings were totaled and compared to the actual yield, which was measured by a weigh wagon. The yield sensor predicted the sugar cane yield with a slope of 0.900, R-squared of 0.966 and average percent error of 11.05 percent. The different cane varieties had an effect on the scale readings, but the maturity of the cane, section length, and the flow rate did not have a significant effect.

Pagnano *et al.* (2001) also developed a very similar yield sensor to that researched in this thesis. The weight sensor was mounted in the upper section of the harvester's elevator and consisted of a plate fully supported by load cells (not hinged). A Butterworth low-pass filter was used to filter out higher frequencies. Their data showed percent errors for measuring sugar cane yield ranging from 8.74 to -26.65%.

Wendte et al. (2001) has a patent for a sugar cane yield monitor that uses a pressure sensor on a deflection plate positioned at the end of the elevator to measure the mass flow rate of harvested sugar cane. They also use a low pass filter to smooth the peaks in the pressure

signal. No measures of accuracy are given.

Cora and Marques (2000) claimed to apply precision agriculture to sugar cane in Brazil with an attempt to understand spatial variability of soil properties, improve production and reduce the undesirable effects of agriculture on the environmental quality. They began with a directed soil-sampling regime based on soil-related maps and landscape. Resultant soil tests indicated a strong variability of soil chemical properties in classes of soils. A yield mapping system was then developed (it is assumed to be the same one developed by Pagnano et al. (2001) above). They produced yield maps which displayed yield variations from 70 t/ha to 200 t/ha. They concluded that precision agriculture was viable for Brazilian sugar cane agriculture. Note this paper is very similar in method to that presented by Cox, Harris and Cox two years earlier in 1998 (see Section 1.2).

Saraiva *et al.* developed a weight measurement system for sugar cane grab loaders. It was based on a mechanical device that contains a load cell adapted to the grab loaders. A mathematical model was developed to assess the effect of critical parameters on the dynamics of the load and on the measured weight. An experimental measurement system was assembled and used in field tests. The results showed that the model was able to describe the machine behavior within the limits considered. Mean errors of ±2% or less were obtained for each load if the sampling period was adequately chosen.

3.7.2 Some Yield Monitor Developments In Other Crops

Durrence *et al.* (1999) developed a prototype peanut yield monitoring system based on load cell transducers. Noise characteristics under simulated field conditions were examined and the effect of mixing within the peanut combine during harvest was also investigated. Evaluation results showed that the system has potential for providing limited quality site-specific yield measurements for yield mapping applications because of errors associated with mechanical noise and convolution effects.

Ehlert (2000) developed a novel technique of measuring the mass flow of potatoes by a bounce plate. Using the theory that the integral force on the bounce plate is proportional to mass flow if a constant velocity difference of falling potatoes can be achieved. This can be produced when potatoes hit a plate on which the potatoes bounce almost vertically.

Laboratory trials found a rubber coated plate with a force measuring instrument showed a clear linear relationship between mass flow and force. Results showed a correlation with a R^2 of 0. 99 and, in some cases, standard error was less than 0.083 kg/s.

Algerbo and Ehlert (2000) reported on measuring the mass flow of potatoes using an optical sensor system based on a digital camera. The optical sensor unit consisted of a digital camera illuminated with infrared light. The cross-sectional area of a passing object was determined and with a correlating equation the weight of the object was calculated. Field tests showed a difference in weight between load-cell-weighing and calculated weight by the camera from 1% to 8%, depending on the varieties of the potatoes.

Arslan and Colvin (2002) examined the accuracy of yield measurements with an impact based mass flow sensor on a grain harvester. They found the yield measurements were more prone to errors as the harvest lengths decreased. Grain yield difference between the yield sensor and electronic scale ranged from 5% to 14%, 4% to 13%, 3% to 12%, and 2% to 11% for 15, 30, 60, and 300 m long segments. They also examined the effect on harvester ground speed variation on accuracy. They found constant ground speed provided more stable grain flow values than varying ground speed. The average error in yield estimate was 3.4% and 5.2% at constant ground speed and varying speed, respectively.

Reyns *et al.* (2002) comprehensively reviewed research on the evaluation of commercially available sensors for yield mapping on grain harvesters (e.g. for measuring grain yield and grain moisture content) as well as research on the development of new sensors (e.g., grain protein content and straw yield).

3.8 Conclusion

To measure crop yield during harvest, the critical variables are:

1. material flow rate through the harvester;
2. driving speed of the harvester; and
3. actual cutting width of the harvester.

The essential components of a yield mapping system are a mass flow sensor, ground speed sensor, yield monitor/display, DGPS receiver and a data logger. Data is recorded on the data logger from the sensors and georeferenced with positional data from the DGPS receiver.

Yield maps are produced from processing the raw data by specialised yield mapping software on a personal computer.

The development of yield mapping systems has occurred since at least 1984 when one of the earliest researchers, John Schueller, examined the application to grain harvesters. Since then research has been conducted in other crops including sugar beet, potatoes and forage crops. Today there are over twelve different yield mapping systems on the market for use in grain and other crops. Adoption is occurring quickly.

A number of different mass flow rate sensors have been developed for yield mapping various crops. The methods used are mixed, ranging from direct mass measurements to indirect measurements of the power required to process the crop material. Sensors used for yield mapping grain, sugar beet, potatoes and forage were reviewed.

The nature of the error from current grain yield monitors was reviewed. The application of typical calibration procedures produces a random error that decreases as measurement time or area increases. Due to this, three variables are required to correctly define the accuracy of a yield monitor and its mass flow rate sensor. These are:

1. Percentage error of measurement
2. Confidence limit of this value (e.g. 95% of the time).
3. Area over which the measurement is made.

It has been identified that a major focus of this research is the development of a mass flow rate sensor for sugar cane. The next chapter examines the functional and performance requirements of such a sensor, including an accuracy specification defined using the findings presented in this chapter. Then four sensing techniques that appear to offer a solution to the requirements are proposed and examined.

Chapter 4 - Mass Flow Rate Sensing of Sugar Cane

The previous chapters reviewed the literature related to precision agriculture and yield mapping. Part of this review showed that the basic technology is available for yield mapping of sugar cane except for the mass flow rate sensor. From this review it was identified that the major focus of this research was to be on the development of a mass flow rate sensor. This chapter begins to cover this development. The functional and performance requirements of a mass flow rate sensor for sugar cane are defined and four sensing techniques that appear to offer a solution to the requirements are proposed and examined.

Note focused on mass flow rate mesurement ultimately want to kn Ow sugar /hectare

4.1 Sensor Requirements

The first step in the research process of the sugar cane flow rate sensor is to define the functional and performance requirements.

4.1.1 Functional Requirements

De Baerdemaeker *et al.* (1985) formed a set of functional requirements for mass flow rate sensors developed for grain yield mapping. These requirements have been reviewed and from this the functional requirements of the sugar cane mass flow rate sensor have been developed. These requirements are:

1. The current maximum flow rate of sugar cane through a single row harvester is

approximately 75 kg/s. The flows in the harvester can fluctuate significantly, implying that the proposed accuracy should be maintained over the entire range of flows.

2. Crop conditions such as size, variety, moisture content, foreign material, etc, should not influence the obtained results; however if they do, it should be in a predictable manner.

3. Even when operating on slopes, the accuracy should be maintained.

4. Machine vibrations or shocks should not influence the readings.

5. The sensing device should under no circumstance impede the material flow in such a way that normal harvester operation is slowed down.

6. The fitting, installation and removal of the monitor should be possible without major rebuilding.

7. The cost should not exceed $3000.

8. Calibration checks must be easy and practical.

9. The sensing device and associated electronic circuitry must operate properly in rough, hot, dusty and moist conditions.

These functional requirements give the basic framework on which to develop and assess the potential sensing techniques.

4.1.2 Performance Requirements

By their definition, sensors are designed to measure physical quantities. The ultimate measure of their performance is the accuracy with which they measure the stimuli. The outcomes of this research will be primarily judged by the accuracy achieved by the ultimate sensor, hence the need to strive for a specific accuracy is important. De Baerdemaeker *et al.* (1985) believes it would be necessary to have accuracy within 2 %, if the grower desires a gross measurement for each field. In the previous chapter it was shown that the accuracy of mass flow rate sensor for yield mapping cannot be defined solely by a percentage error as

stated here. These figures are useful however when setting realistic goals. Previously it was shown the accuracy should be defined by:

- Percentage error of cumulative measurement ((sensor measured yield/actual yield*100)-100)
- Probability confidence limit of this value (eg. 95% of the time).
- Area over which the measurement is made.

Based on a review of the accuracy of grain mass flow sensors and assumptions concerning the measurement accuracy required for agronomic purposes in sugar cane, a desirable and achievable accuracy goal for the sugar cane mass flow sensor would be:

- less than 5% error ((sensor measured yield/actual yield*100)-100)
- 95% of the time (2 Sigma)
- over an 100 m^2 measurement area

The level of these parameters is based on a balance between what is technically possible and what is required for the agronomic purposes of precision agriculture. In terms of what is required for the agronomic purposes, lower accuracy yield maps could easily be used to make agronomic decisions. For example, yield maps with only three levels of productivity measure (e.g. low, medium and high yield) could be very effective for use in the calculation of variable rate application maps for various crop inputs and given that yield maps typically display yield variations of greater than 100%, then three levels of productivity could be measured with a mass flow sensor exhibiting errors much greater than 5%. But a yield map with errors similar to those given in the accuracy goal stated above would be more effective and tending towards the most desirable accuracy.

In terms of what is technically possible, the sensor will be required to operate in an environment with significant vibrations, foreign matter and other adverse conditions. The sugar cane sensor will operate in conditions worse than existing grain yield monitors, and the proposed accuracy targets are much more demanding than what is being achieved by these systems. For example some research conducted by Asgrow Seed Company (1997), titled *Comparison of Weigh Wagon and Yield Monitor Results* indicated that over a measurement area of 400 m^2 commercial grain yield monitors are only achieving an accuracy of less than 12.8% error at the 95% confidence level. When compared with these results the selected accuracy goal for the sugar cane mass flow sensor is a formidable target.

In terms of the agronomic requirements, these specifications would permit the production of relatively accurate yield maps. If the maps were smoothed to a pixel size of 10 x 10 m (100 m^2, or some rectangular shaped pixel), a user of these maps could be confident (95% confident) that the value of each pixel is within 5% of the actual yield. The measurement area of 100 m^2 was selected because it represents a minimum area that a manager may decide to manage. This level of detail is currently much finer than is being used for PA in other crops, but sugar cane is an intensively grown crop with smaller field sizes than most crops.

The level of success of this research is judged by this accuracy goal. Various sensing techniques are developed and tested and their results compared to this goal. The potential techniques are now discussed.

4.2 Potential Sensing Techniques

The previous chapter included a section that reviewed the existing techniques for measuring mass flow rate for various yield mapping purposes. From this review and by analysing the cane harvester operation, various techniques appear to offer a solution to the problem in sugar cane. These techniques are defined as:

1. Chopper Power Measurement,
2. Elevator Power Measurement,
3. Volumetric Measurement and,
4. Mass Measurement.

The locations of sensors for each of these techniques on the harvester are shown in Figure 4-1. In this section the basic operation and theory behind each technique is discussed, along with their respective advantages and disadvantages.

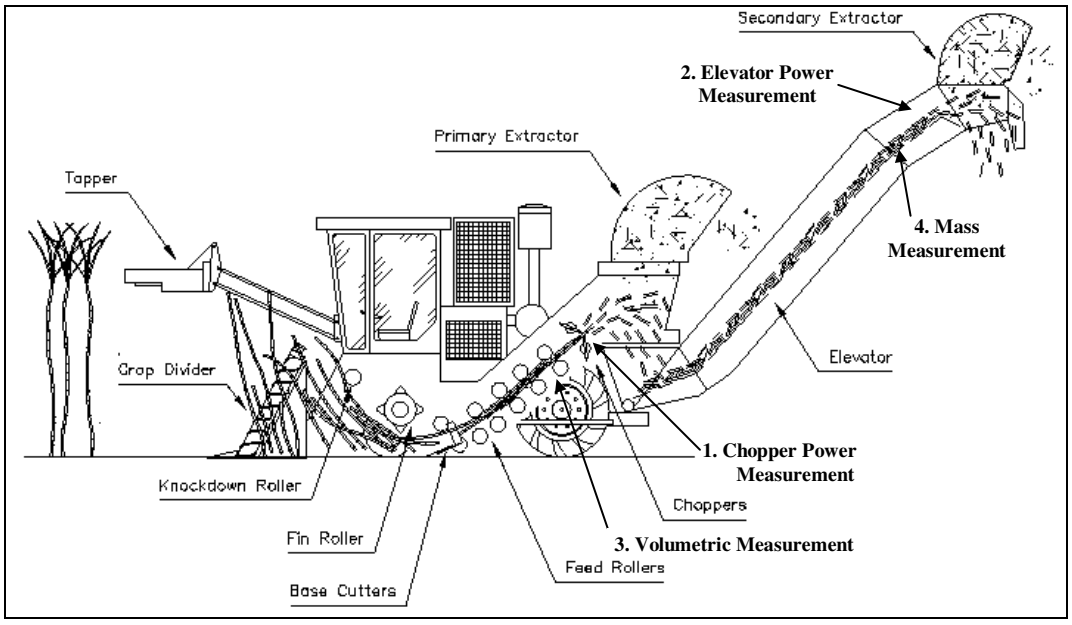

Figure 4-1. The location of the four mass flow sensing techniques throughout the sugar cane harvester (picture courtesy of S. Kroes).

4.2.1 Chopper Power Measurement

The chopper power technique for the measurement of mass flow relies on the assumption that the power required to chop the sugar cane into billets is proportional to the mass flow rate of sugar cane through the choppers. The chopper system of the cane harvester consists of two hydraulic motors driving the chopping cylinders that have blades running along their lengths (Figure 4-2). These blades chop the cane stalks into billets approximately 30 cm long and propel them back to the elevator.

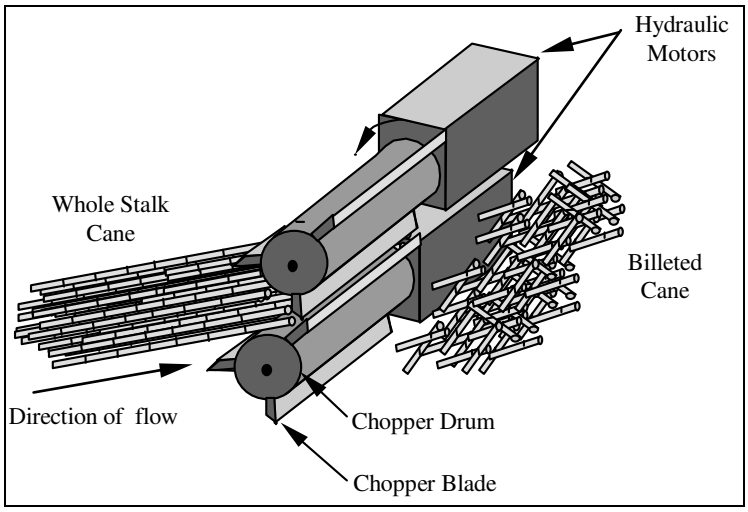

Figure 4-2. Chopper system of the sugar cane harvester.

Hydraulic power can be measured using pressure transducers positioned in the hydraulic circuit of the chopper motors and with magnetic sensors monitoring the hydraulic motor speed. Assuming that there is negligible leakage in the motors and therefore the angular speed is proportional to the oil flow rate, the hydraulic power is calculated from Equation 4.1.

$$P = psc \qquad \textbf{(Equation 4.1)}$$

where P is the chopper operating power [W];

p is the pressure to drive the chopper motors [Pa];

s is the angular velocity of the motors [revs/s]; and

c is the capacity of the motors [m^3/rev].

In practice, the calibration equation for this technique would be in the form of Equation 4.2.

$$m_f = \frac{(P - f)}{e} \qquad \textbf{(Equation 4.2)}$$

where m_f is the mass flow rate [kg/s];

e is the specific cutting energy [J/kg];

P is the chopper power measurement [W]; and

f is power required to operate the chopper system with no cane flow (free running power) or the x axis intercept [W].

Persson (1987) has reviewed the significant research that has been conducted in the area of cutting plant material. This research has shown that along with other factors the power requirement to cut plant material is proportional to the flow rate. As noted previously, Vansichen and De Baerdemaeker (1993) used a similar technique to measure the mass flow rate through a forage harvester and they also found a strong linear relationship. The uncertainty with this technique however is the effect of the other factors apart from the mass flow rate. Equation 4.2 is inferred using the assumption of a constant specific cutting energy (J/kg) but the magnitude of this quantity may vary due to a number of factors such as (Persson, 1987):

1. Material moisture. Sugar cane moisture is a naturally changing parameter in a range of 15-20% for a particular field.
2. Length of cutting.
3. Cutting cylinder revolution speed.
4. Clearance distance or space between blades leads to an additional cutting energy.
5. Knife sharpness.
6. Knife sharpening angle.

These factors suggest that one should not use the chopper power measurement to monitor mass flow rate. For this technique to work, all these variables would have to remain relatively constant and so retain a constant specific cutting energy. This is unlikely over a full harvesting season, but if these variables remain constant over a harvested field then this technique could be used to measure relative yield differences. These relative results can be used directly for crop management purposes. Actual yield variation could be determined by post calibrating the data with the known total yield of the field. So, although there are many variables that could affect the accuracy of the flow rate measurements of the chopper system, it could be successful in measuring relative yield differences, from which actual yield differences can later be determined.

Although this technique has a great deal of factors which can affect the accuracy of its operation, the benefit of this system is its simplicity, reliability and low cost which must be taken into account.

Advantages

- Simple sensor design.

- Sensor components can be purchased off the shelf.
- Reliable as no part is in contact with crop material.

Disadvantages

- Not a direct indication of mass flow rate.
- Measurement affected by changes in crop conditions such as burnt/green cane, moisture content and fibre content.
- Measurement affected by machine conditions such as blade sharpness.

4.2.2 Elevator Power Measurement

The elevator of a sugar cane harvester (Figure 4-3) has the task of delivering billeted sugar cane from the chopper system up and into the 'haulout' vehicles. This system is typically driven by two hydraulic motors, coupled at the top of the elevator. Billeted cane is lifted some 3 vertical metres over the length of the elevator. Energy is required to overcome gravity and friction on the elevator floor as the sugar cane is dragged up the elevator. From these two effects it would indicate that the mass flow rate of cane through the elevator would be proportional to the power required to move it.

Figure 4-3. Elevator of the chopper sugar cane harvester.

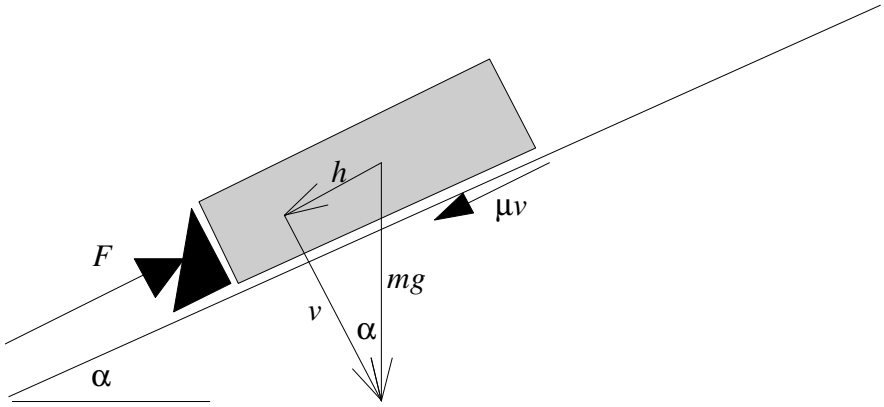

Figure 4-4. Simple model of the force, necessary to raise sugar cane billets up a harvester elevator.

Figure 4-4 shows the simple model to calculate the force, F, required to move a flight full of cane up the elevator. The force has a component due to gravity along with the component due to friction. This process can also be represented as Equation 4.3, 4.4 and 4.5.

$$F = h + \mu v \qquad \textbf{(Equation 4.3)}$$

$$= m g \sin\alpha + \mu m g \cos\alpha \qquad \textbf{(Equation 4.4)}$$

$$= m g \sin\alpha + \mu g \cos\alpha \qquad \textbf{(Equation 4.5)}$$

where F is the force required to shift the cane up the elevator [N];
h is the force component to shift the cane against gravity [N];
μ is the coefficient of friction [no units];
v is the normal force of the cane on the floor [N];
m is the mass of cane in the elevator [kg];
g is the acceleration due to gravity [m/s^2]; and
α is the angle of the elevator to the horizontal [degrees].

Equation 4.5 can be used to develop the relationship between elevator power, P [W], and mass flow rate, m_f [kg/s], as shown in Equations 4.6 through 4.10.

$$P = F s \qquad \textbf{(Equation 4.6)}$$

$$P = (m\,(g \sin\alpha + \mu\, g \cos\alpha))\, s \qquad \textbf{(Equation 4.7)}$$

$$ms = \frac{P}{g\sin\alpha + \mu\, g\cos\alpha} \qquad \textbf{(Equation 4.8)}$$

where s is the elevator speed [m/s].

Because the mass flow rate through the elevator is related to the elevator length, l [m], and speed of the elevator by Equation 4.9.

$$m_f = \frac{m}{l} s \qquad \textbf{(Equation 4.9)}$$

then Equation 4.8 can be substituted into Equation 4.9 to get:

$$mf = \frac{P}{[g\sin\alpha + \mu\, g\cos\alpha]\, l} \qquad \textbf{(Equation 4.10)}$$

In practice the calibration equation would become Equation 4.11 to account for the 'free running power', F [W], required to drive the elevator with no cane in it. Also the gravity and friction and elevator length terms could be combined into a calibration constant, defined as the specific elevating constant, e [J/kg].

$$m_f = \frac{P - F}{e} \qquad \textbf{(Equation 4.11)}$$

where $e = (g \sin\alpha + \mu\, g \cos\alpha).l$

For this technique the hydraulic power can be measured using the same method as the chopper power measurement described previously.

Equation 4.10 indicates the ability of the elevator power technique to accurately represent the mass flow rate is dependent on the variation of the elevator angle and the coefficient of friction. These parameters do change. For example a harvester operating on slopes will

change the relative horizontal angle of the elevator and the coefficient of friction may also vary due to crop properties or available water. The effect of these variables on the accuracy of the technique depends on the sensitivity of the power requirement to these variables, and the extent to which they vary. Some preliminary analysis has been carried out to determine the sensitivity of the power requirements of the elevator to its angle to the horizontal and coefficient of friction. The calculations are graphically represented in Figure 4-5. From the figure it appears that the power requirement is most sensitive to the coefficient of friction, with an approximated 30% increase in power over the given range. The variation in elevator angle also produces significant changes in the power requirement, with an approximated 20% increase in power over the 20 degree change. Although the coefficient of friction is unlikely to vary from 0.1 to 0.5 and the elevator angle from 40 degrees to 60 degrees, the graph does give an indication of the errors that may be involved. From this analysis it appears that the two parameters of elevator angle and coefficient of friction, could produce significant errors in the measurement of mass flow rate. The change in elevator angle could be compensated for with an inclinometer for added expense and complexity. The coefficient of friction is more difficult to determine, however one technique to minimise its effect would be to replace the current floor lining of steel with a plastic or some other material with a low coefficient of friction.

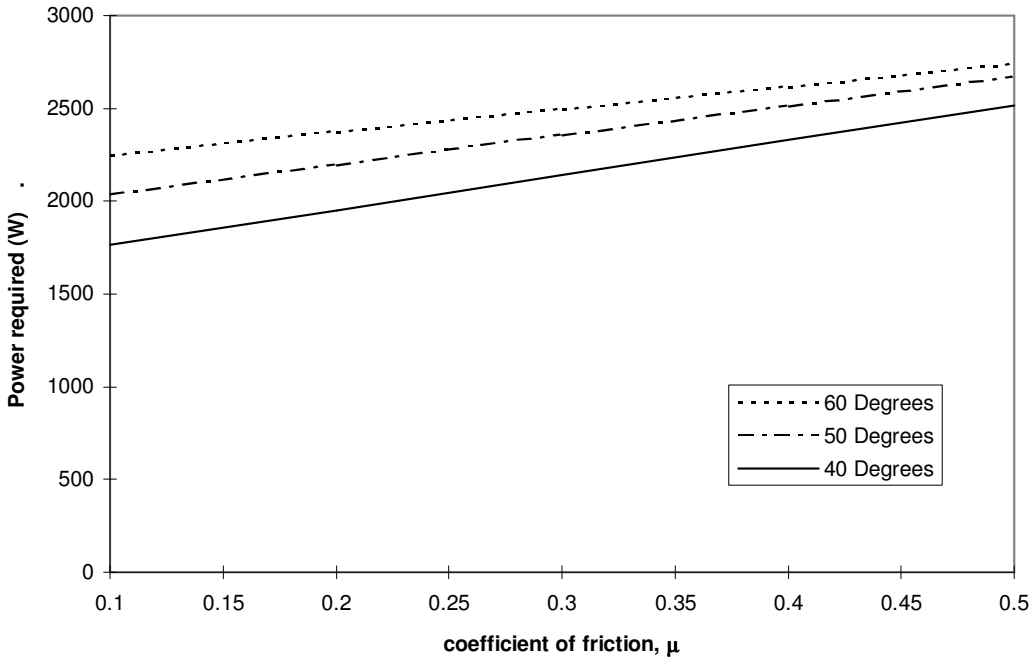

Figure 4-5. Theoretical elevator power requirement for varying coefficients of friction and elevator angles.

The other important consideration for this technique is that the increase in power required to elevate the cane, would be negligible to the total power required just to run the elevator system with no cane. If this was the case it would result in the measurement being masked by small changes in the free running power. This statement is refuted by Dick (1995, pers. comm.), who did some preliminary work looking at the pressure fluctuations in the elevator hydraulic system of a CAMECO cane harvester. He found that there was a significant difference between 'free running' (no load) hydraulic pressure of the elevator motors to the heavily loaded condition. The pressure readings increased from a 800 kPa at 'free running' to an operating pressure of 1400 kPa. This factor is examined later in the dissertation.

Like the Chopper Power technique, the Elevator Power technique has the advantages of its simplicity, reliability and low cost. However it also suffers from similar disadvantages of being affected by factors that can change during the harvesting process.

Advantages

- Simple sensor design
- Sensor components can be purchased off the shelf
- Reliable as no part is in contact with crop material
- A more direct technique of measuring mass flow than the chopper system

Disadvantages

- Requires correct operation of the elevator system. For example if the elevator begins to jam or the chain becomes loose the power requirement will change.
- Measurement affected by changes in friction of crop material over elevator floor. This could change with different harvesting conditions such as wet/dry field conditions and green/burnt cane.

4.2.3 Volume Measurement – Feed Roller Separation

A simplistic technique for measuring mass flow rate is to measure the volume of material passing a point and then apply a density factor to this measurement to achieve mass flow rate. Although this is not a direct measure of mass flow rate it can be a simple and effective

technique. There are various grain yield monitors that rely on this technique including RDS and the Clayton Yieldometer (Borgelt and Sudduth, 1992).

The cane harvester offers a potentially simple method of measuring the volume of material passing through it. This could be implemented on the harvester in the area known as the 'feed roller' system. The feed roller system on the sugar cane harvester consists of a series of cylinders that feed the cane stalks through the machine, from the base cutters to the choppers as shown in Figure 4-1. The feed rollers operate in pairs, one above the other with the cane fed through the middle. While the bottom rollers are fixed in position, the top rollers are mounted on swing arms which allows them to "float" and adjust to the different thickness of cane passing through (Figure 4-6). The separation between the bottom rollers and the top rollers could be used as a measure of the volume of cane flowing through the machine.

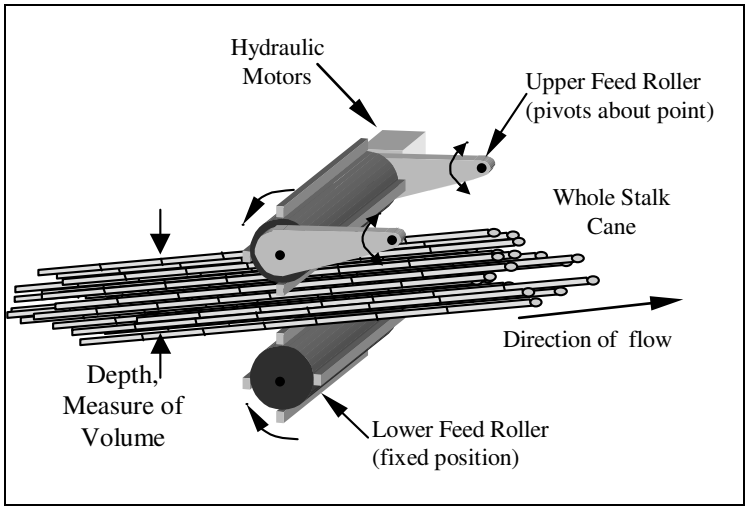

Figure 4-6. Volume measurement using the Feed roller operation

The volume flow rate , v_f [m^3/s], through the feed rollers can be calculated using Equation 4.12. Along with the feed roller separation, d [m], the additional variables w [m], the width of the cane mat, and v [m/s], the velocity of the cane through the feed rollers, are required. Fortunately these two variables are relatively constant, and it is not necessary to monitor them over time. This is particularly the case at the last set of feed rollers in the feed train. At this point, the cane mat has had time to spread out over the full width of the feed rollers to allow even processing by the chopper system. The velocity of the cane through the last set of feed rollers is also relatively constant due to the cutting action of the choppers that pulls the mat through at an even rate to achieve a consistent billet length.

$$v_f = v\ w\ s \qquad \textbf{(Equation 4.12)}$$

$$m_f = \rho\ v_f \qquad \textbf{(Equation 4.13)}$$

$$= \rho\ v\ w\ s \qquad \textbf{(Equation 4.14)}$$

where m_f is the mass flow rate [kg/s];
ρ is the density of the cane mat [kg/m^3];
v is the velocity of the cane through the feed rollers [m/s];
w is the width of the cane mat [m]; and
s is the feed roller separation distance [m].

This can be simplified to:

$$m_f = c.s \qquad \textbf{(Equation 4.15)}$$

where c is the calibration constant [(kg/s)/(m of separation)].

To calculate the mass flow rate from the volume flow rate measurement requires the assumption of a density as shown in Equation 4.14. This is difficult to measure and not as consistent as the width and velocity of the cane mat. Density of the cane mat can vary due to many factors including differences in extraneous matter level, whether the crop is harvested green or burnt and the age of the crop. Also the bulk density of the cane billets can vary with different moisture contents, different varieties and different aged crops. The variation in density could result in a significant source of error. Alone, the variation in extraneous matter between burnt and green cane harvested crop can be as high as 30% by weight (Ridge and Dick, 1988) and this would result in a difference in density of a similar magnitude.

In practice the density of the cane mat, the velocity of the cane through the feed rollers and the width of the cane mat would be assumed to be constant. These variables would be represented by the calibration constant, m [(kg/s)/(m of separation)] and Equation 4.15 would be used to calculate the mass flow rate. The separation could be measured by a Linear Variable Differential Transformer (LVDT) or an angle sensor measuring the angular rotation of the feed roller about the pivot point. Although this technique is not a direct measure of mass flow rate, it is a simple and robust sensing point.

Advantages

- Simple sensor design
- Robust and reliable as no part of the sensor is in contact with crop material
- Cheap to manufacture
- Measures mass flow rate before cane losses through the extractor fans. These losses can be significant and therefore this technique maybe more desirable to produce a yield map without these losses.

Disadvantages

- Not a direct indication of mass flow rate.
- Affected by variation in material density caused by changes such as green/burnt cane and varietal differences.
- Relies on the assumptions of constant velocity and constant width of the cane mat through the feed roller. These assumptions may not always be valid.
- Measures all extraneous matter. This technique measures flow rate before the cleaning of the crop of extraneous matter. Therefore all extraneous matter is included.

4.2.4 Mass Measurement – Weigh Pad

The final potential technique for measuring the sugar cane mass flow rate utilises a direct measurement of mass flow. That is, the weight of the mass is directly sensed and is not inferred by some indirect factor such as processing power. This technique was first conceptualised by Derek Bakker (CSR sugar research officer, Ayr, Queensland, Australia), who proposed the idea in 1996 to University of Southern Queensland (USQ) Professor Harry Harris. From this proposal an undergraduate project was initiated at the USQ by Professor Harry Harris. This project was taken up by USQ engineering undergraduate Simon Zillman who conducted the initial trials that are presented in Chapter 5. From this point the technique appeared to offer potential, but required further research to overcome its limitations.

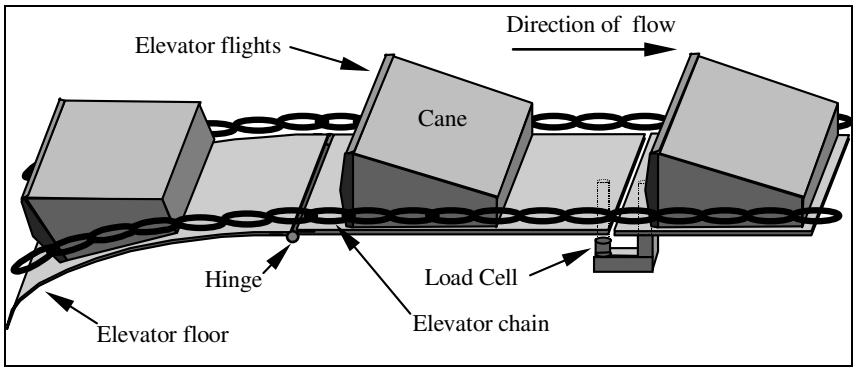

Figure 4-7. Conceptual design of elevator weigh pad.

The sensor developed using this mass measurement technique was defined as the 'weigh pad'. In its original design the weigh pad consisted of a plate mounted in the elevator floor, hinged at one end and supported with a load cell on the other end (Figure 4-7). This design was adopted to minimise cost and complexity by reducing the number of load cells required and maximise strength. The weigh pad is positioned in the upper section of the elevator as shown in Figure 4-1. The flights of the elevator push the billets of sugar cane over the plate to register the mass on the load cell. The theory behind the principle of the measurement of mass flow rate on a conveyor is shown in Equation 4.16.

$$m_f = m_l s \qquad \textbf{(Equation 4.16)}$$

where m_f is the mass flow rate [kg/s];
m_l is the mass of cane per unit length on the elevator [kg/m]; and
s is the speed of the elevator [m/s].

Equation 4.17 shows the variables required to calculate the flow rate of sugar cane for the hinged weigh pad. Due to the hinging action, the load cell only measures half of the mass of the cane passing over the pad. The speed of the elevator can easily be monitored using a magnetic pick-up device on a shaft driving the elevator. The cos(α) term takes into account the angle of the weigh pad surface to the horizontal as the elevator operates on approximately a 25 degree slope.

$$mf = \frac{2m}{l.\cos(\alpha)}.s \qquad \textbf{(Equation 4.17)}$$

where mf is the mass flow rate [kg/s];

m is the mass as measured by the load cell [kg];

l is the length of the weigh pad [m];

s is the speed of the elevator [m/s]; and

α is the angle of the weigh pad surface to the horizontal [degrees].

Figure 4-8 shows the theoretical measurement error of the weigh pad due to variation in operating slope. This figure shows that variation in operating slope can potentially be a significant source of error.

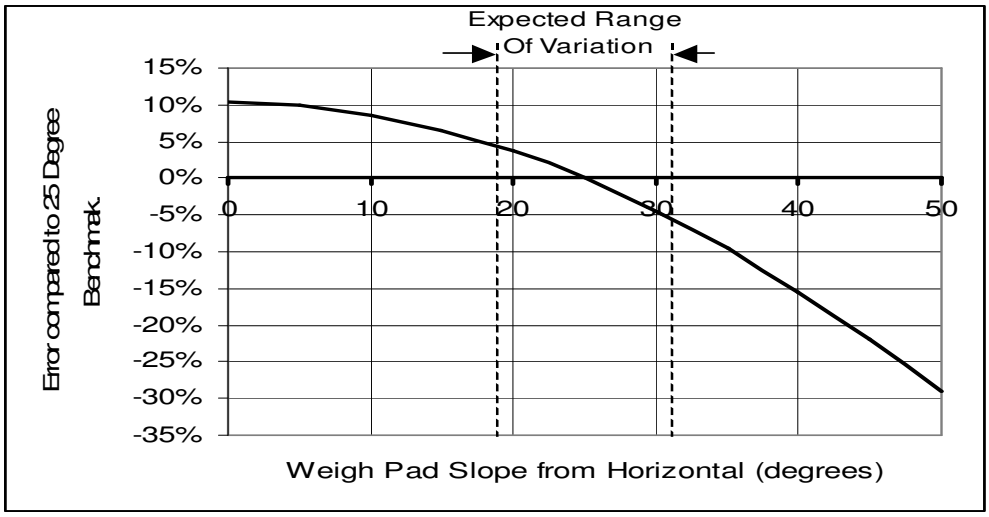

Figure 4-8. Theoretical error of weigh pad for varying operating slopes.

The force transferred to the weigh pad could also be affected by friction. That is, friction on the elevator flights and on the elevator walls would result in some load transferred to them, thereby reducing the force on the weigh pad. Assuming a coefficient of friction of 0.3 and that $1/6^{th}$ of the downward force (conservative) is transferred into horizontal forces onto the side walls and elevator flight, this would result in a 5% reduction in the force transferred to the weigh pad. This would not be a significant problem as long as this reduction did not vary greatly, however it should be taken into consideration.

The major advantage of this technique is the fact that it is a direct measurement of mass flow rate that should not be affected by crop conditions. The concern with the technique is its complexity and the reliability of the system that may be difficult to maintain in the harvesting environment.

Advantages

- A direct measurement of mass flow rate with a theoretical basis.

- Calibration that is not affected by crop conditions.
- Simple to calibrate using single weight.

Disadvantages

- Susceptible to mechanical noise.
- Relatively complex sensor design.
- Must have contact with the crop material which means it is susceptible to fouling by build-up of foreign matter.

4.3 Position of Mass Flow Measurement

There is a difference between the mass of material that passes the feed rollers and choppers compared to the elevator and weigh pad sensing techniques. This is due to the significant mass of material that is removed by the secondary extractor fan. Most of this is extraneous leaf matter (as per it's design purpose) but some is sugar cane billets (unintentionally removed). Therefore these sensing techniques are measuring slightly different mass flow rates (hence "yields") however any sensor technique will most likely be calibrated with post harvest mass measurements (e.g. weigh truck/wagon). Therefore the final yield map will be based on post harvest yields. This would be different to the pre-harvest yield, which would not be reduced by the harvester losses. This difference could cause increased difficulty/errors when trying to calibrate the feed roller separation and chopper power techniques.

4.4 Conclusion

The functional and performance requirements of a sugar cane mass flow sensor have been given. Based on a review of the accuracy of grain mass flow sensors and assumptions concerning the measurement accuracy required for agronomic purposes in sugar cane, a desirable and achievable accuracy goal for the sugar cane mass flow sensor was selected as:

- less than 5% error
- 95% of the time (2 Sigma)

- over an $100m^2$ measurement area

Four potential techniques have been proposed to measure the mass flow rate of sugar cane through the chopper harvester. These techniques are defined as:

1. Chopper Power Measurement,
2. Elevator Power Measurement,
3. Volumetric Measurement - Feed Roller Separation and,
4. Mass Measurement – Weigh Pad.

The theory, advantages and disadvantages of each technique have been discussed. The next chapter will determine if the theory of operation of these sensing techniques is useful in practice. To test these techniques field trials are conducted to see if the results agree with theory. An outcome of this research is calibration curves for each sensing technique and details on their accuracy. The next chapter deals with these field trials.

Chapter 5 - Preliminary Field Trials of Potential Sensors

5.1 Introduction

The previous chapter discussed the four potential techniques for measuring the mass flow rate through the chopper harvester. This chapter explains the initial field trials that were carried out on each of these techniques. The primary objective of the trials was to compare the performance of the four sensing techniques and to assess their limitations, problems and potential. The four techniques were tested simultaneously by placing various sensors on a single harvester and comparing the sensor outputs with the mass flow rate as measured by a weigh truck. The results presented in this chapter showed that each technique had potential, but also inherent problems and limitations.

5.2 Materials

5.2.1 Harvester and Weigh Truck

A 1995 model, Austoft 7000 sugar cane chopper harvester was the chosen test platform for these trials. The machine was set up with various sensors to represent the four mass flow rate sensing techniques discussed in the previous chapter. The sensors were interfaced to a digital data acquisition system, which recorded each sensor's output for later analysis. The four techniques and the data acquisition system will be explained in detail in the next section.

A weigh truck was used to measure the mass of cane harvested for mass flow rate calculations. It consisted of a body truck with a weighing bin positioned on the back. This

bin was supported by four load cells that measured the mass of cane via relevant electronics and reported the mass to the driver in the cab. The weighing capacity of the truck was 4 t and the truck had to be stationary to measure accurately. It had been recently calibrated and had a readout resolution of 1kg although accuracy was expected to be ±15kg. The bin also involved an elevating feature to empty the bin when the weighing was completed.

5.2.2 Sensor Designs

In the previous chapter the four potential sensing techniques for measuring the sugar cane mass flow rate through the harvester were discussed. In this chapter they will be referred to as 'Chopper Power', 'Elevator Power', 'Feed Roller Separation' (volume measurement) and 'Weigh Pad' (mass measurement). The specific details of the implementation of each of these techniques for this trial are outlined in this section.

Chopper Power

The Chopper Power was monitored using transducers to measure hydraulic pressure, and Hall effect sensors to measure motor speed. The pressure transducers were Druck PTX 1400 with a range of 0-100 bar, with an equivalent electrical output of 4-20 mA. Their non-linearity and hysteresis error was specified as ±0.25 % full-scale max. Two pressure transducers were positioned in the hydraulic circuit with one before and one after the chopper motors. As the chopper motors were hydraulically connected in parallel, the pressure transducer measured the pressure drop across both motors. The differential pressure measurement using the two transducers enabled the power consumption of the chopper system to be measured separately from any hydraulic motors driven by this system. In this case it was the feed roller system that was connected in series after the chopper system.

A Hall effect sensor was fitted at an appropriate position to measure the angular speed of the chopper system. These sensors produced a 5 to 0 V pulse when the magnet passed. A single magnet was glued to one of the chopper drums to produce a sensor pulse for every revolution, which resulted in approximately 4 pulses per second. The sensors were sourced from and constructed by Agridry-Rimik (Toowoomba, Australia).

From the pressure and speed measurements the hydraulic power was calculated as per

Equation 4.1. An assumption required for the correct measurement of power using this equation is that there is negligible leakage in the hydraulic motors. This means the angular speed, as measured by the Hall effect device, is directly related to the oil flow rate via the capacity of the motor. This is a valid assumption as the harvester was relatively new (12 months old) and the hydraulic motors were in good conditions. The variation in overall motor efficiency with flow and pressure has been ignored in these comparative measurements.

Elevator Power

The Elevator Power measurement was carried out in the same fashion as the chopper power measurement. The major difference was that only one pressure transducer was used to monitor the pressure drop across the hydraulic motors. This was possible as the outlet of the elevators motors feeds into the return tank and therefore the pressure in this line can be assumed to be zero ignoring the small friction loss in the return line. The pressure transducer used was the same model as for the chopper system and was positioned in front of the two hydraulic motors, which were connected in parallel.

A Hall effect device also monitored the speed of the elevator motors. The magnet was mounted on a shaft of the elevator system. This resulted in a pulse output from the sensor at a rate of approximately 4 Hz or one pulse per 50 cm of elevator travel.

Feed Roller Separation

A specially developed sensor measured the feed roller separation. The final set of feed rollers in the feed train (before the chopper box) were instrumented with this sensor. The sensor measured the angle of rotation of the upper feed roller about its pivot point as shown in Figure 5-1. From this angular measurement the perpendicular separation between the upper and lower roller was calibrated.

The sensor was based on a linear Hall effect sensor. The magnet was mounted in an external brass housing. Brass was selected for its non-magnetic properties. Within this housing a hollow brass rod was fitted to rotate and a Hall effect sensor was mounted within the rod. The swing arm attached to the feed roller rotated the brass rod. This rotation feed roller was detected by a voltage change in the Hall effect sensor. The resolution of this sensor was

0.5mm of separation. The design drawings and calibration data for this sensor are given in Appendix A.

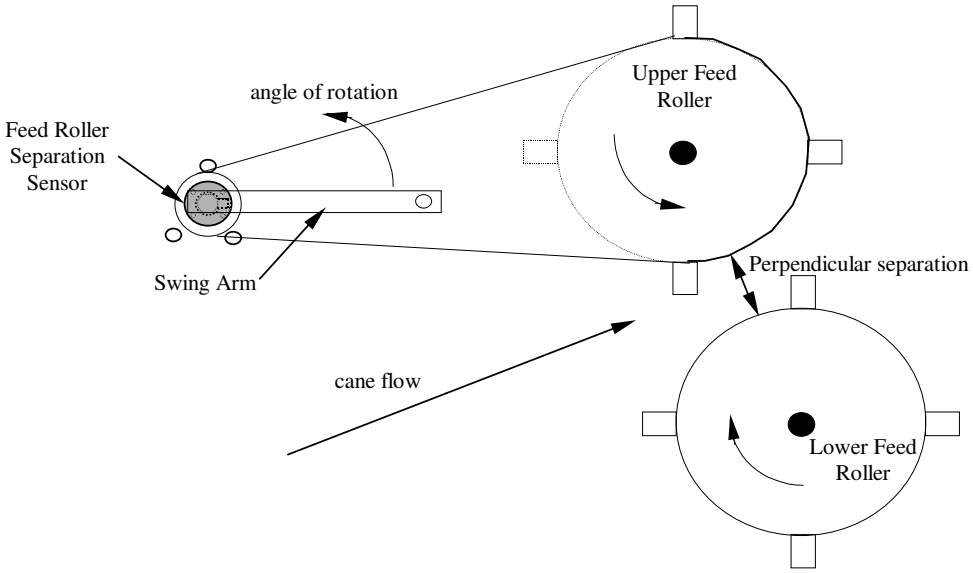

Figure 5-1. Feed roller separation sensor arrangement.

Weigh Pad

The weigh pad consisted of a plate mounted in the elevator floor, hinged at one end and supported with two load cells on the other end (Figure 5-2). An accelerometer was included to measure the dynamics of this system, with the potential to improve the mass flow rate measurements.

The trials conducted on the weigh pad system were the responsibility of student Simon Zillman as part of his final year undergraduate engineering project. A detailed description of the sensor design and field testing is given in the thesis (Zillman, 1996). After this initial testing the author took over the responsibilities of further research on the weigh pad technique. For completeness of the weigh pad development, this earlier work is reported here.

The weigh pad design was very basic. A section of the 3 mm mild steel floor was cut out and used as the weigh plate surface. The hinges were general-purpose door hinges welded between the weigh plate and the surrounding steel. The load cells were two single point load cells with capacities of 10 kg each. The dimensions of the weighing surface were 180 mm (in

the direction of the elevator flow) by 700 mm.

The elevator flights or chain did not come into contact with the weigh pad. Friction has very little effect on the load cell readings as the friction force is directed in line with the hinges and therefore they take the majority of the force and little is transferred to the load cells.

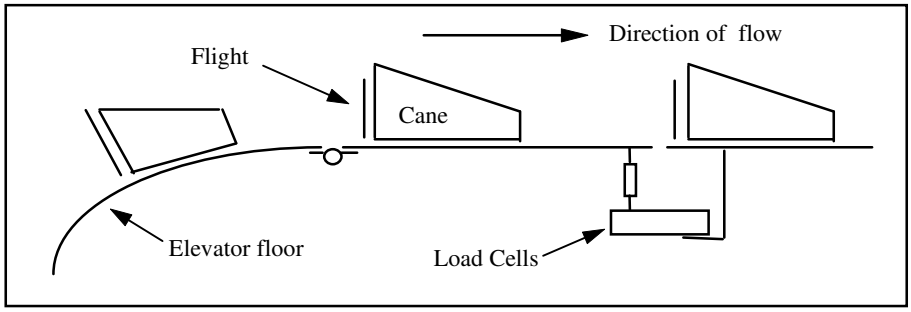

Figure 5-2. Elevator weigh pad arrangement.

5.2.3 Data Acquisition System

The data acquisition system consisted of a laptop computer with an external analogue to digital data acquisition card (see Figure 5-3). The 486DX 2-66Mhz laptop computer contained a 120 Mb hard drive, 4 Mb of RAM and operated on the Microsoft Windows 3.1 platform. The data acquisition card was a National Instruments AT-MIO-16E-2 that was capable of up to 500,000 samples per second of 8 differential analogue inputs, sampled at 12-bit resolution.

A software program was written in National Instrument's "Labview" specifically to control the data acquisition process. The program controlled the start and stop of the data acquisition card and wrote the data to a file on the hard drive every second. With this configuration of computer and data acquisition card, the maximum acquisition rate for the 8 analogue data channels was 100 Hz. The primary factor restricting the acquisition rate was the speed with which the data could be written to file. Using the Nyquist criterion, with an acquisition rate of 100 Hz, all signals with frequencies below 50 Hz will be acquired without aliasing. All sensors with perhaps the exception of the weigh pad sensors will produce signals under this limit. The weigh pad data along with the output from the other sensors were analysed for their frequency components and given in the results section.

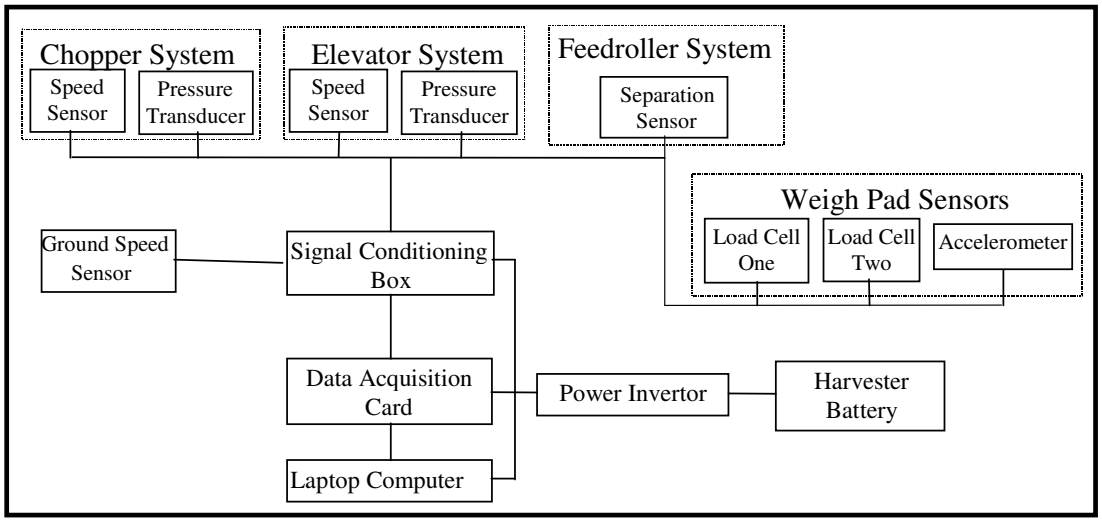

Figure 5-3. Block diagram of the instrumentation on the cane harvester.

Signal Conditioning

Appropriate signal conditioning was fabricated to power the various sensors and interface their signals to the ±5 V inputs for the data acquisition card. See Appendix B for a circuit diagram.

5.3 Method

5.3.1 Site

The trials occurred from the 10th to the 12th of July 1996, at the Burdekin Agriculture College. The college is situated in the Burdekin River Irrigation Area (BRIA), near the town of Clare in northern Queensland, Australia. The site was selected primarily for the availability of the harvester. The college donated their time and equipment for the duration of the trials.

5.3.2 Testing Procedure

The trials were divided into 'runs', with each run defined as the harvesting of a single row of cane (1.5 m wide), 100 m long, into the weigh truck. Each run was marked out in the field by

witches hats. The area of the field was selected for its higher than average yield and uniformity. This assisted with the aim of maintaining constant flow rates during each run. A typical field layout is shown in Figure 5-4. The row prior to each run was harvested normally and then the harvester was stopped. The weigh truck mass measurement was then tared and the data acquisition system set to record. After approximately 5 seconds the run was then harvested at a preselected ground speed. At the completion of the run the harvester's forward speed was stopped and it was allowed to empty out into the weigh truck. The data acquisition system was stopped approximately 5 seconds after the harvester had emptied. The harvested weight was recorded in the weigh truck and the process started again.

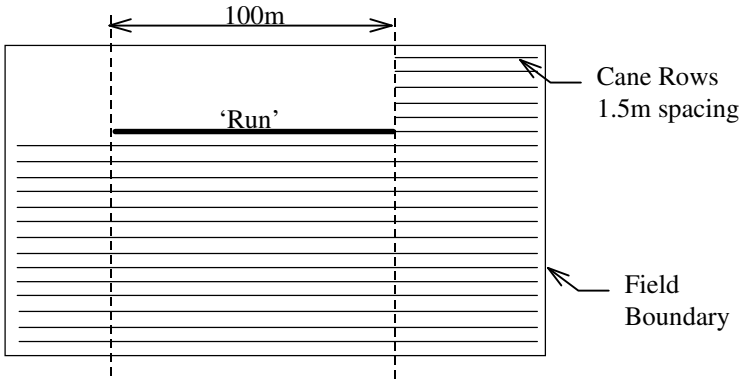

Figure 5-4. Field layout for the sensor trials.

One of the primary requirements of the trials was to test the sensors over the full range of possible flow rates. To achieve this, the harvester was driven at a different speed for each run. These speeds ranged between 3 km/hr and 9 km/hr and were selected randomly. During each run, the speed of the harvester was maintained as constant as possible to achieve an even flow rate.

To calculate the average mass flow rate for each run, the total mass harvested, as recorded from the weigh truck, was divided by the time to harvest each run as recorded by the data acquisition system. Overall, forty of these 'runs' were carried out over the three days, giving an adequate data set to compare the measurement techniques.

Throughout the trials various 'free running' runs were also conducted. These runs were defined as operating the harvester at but at full (normal) engine speed with all components running normally as if harvesting. Each of these measurements was carried out for approximately 60 s and measured the baseline value for each of the sensing techniques.

These runs were carried out at zero ground speed to minimise the impact of any additional errors from a moving harvester.

5.3.3 Field/Crop Conditions

Results were obtained in a variety of conditions to observe the effect of these conditions on the sensing techniques calibration. The conditions included burnt and green cane, different varieties of cane and a range of crop yields. The data in the calibration figures are derived from the three days the trials took place. On Day 1 the conditions were burnt cane in variety Q117 with relatively low yields of 65 t/ha. Day 2 was carried out in burnt cane of variety Q96 with an average yield of 80 t/ha. Day 3 was cut in variety Q117 with green cane cut in the morning and then burnt cane in the afternoon with an average yield of 120 t/ha. These conditions were largely not under the control of the trial as the commercial harvesting operation took priority.

Low crop yields and inexperienced drivers (college students) restricted the higher flow rates that could be achieved to less than 35 kg/s.

5.3.4 Data Processing

The data collected in the field were analysed on a personal computer. Another program was written in "Labview" to carry out this task. The function of this program was to select the appropriate data for each run and calculate the average reading for each sensor during the run. The appropriate data were selected by clipping each end of the data files to remove the data measured during no cane flow. The average was simply calculated by integrating the sensor readings over the length to the run and dividing this by the time for each run. The speed measurements required a small amount of additional processing to convert the pulses to a revolution per second reading. The output data from this process were then transferred to Microsoft Excel. In Microsoft Excel the average voltage and speed measurements were converted to pressure from the pressure transducer, oil flow rate for the hydraulic motor speed sensors, ground speed for the ground speed sensor and weigh pad readings were converted to mass measurements and accelerations. From pressure and oil flow rate measurements the power of the chopper and elevator were also calculated. The average mass flow rate was also calculated for each run by dividing the mass harvested by the time

duration of the run.

5.4 Results

The output of the data processing discussed in the previous section is given here. These results are presented separately for each sensing technique and include example data, a frequency spectrum of the signal and the calibration lines.

The example data is the first 37 seconds from a run in Day 2 of testing. The harvester was travelling at a particularly high speed to achieve a relatively high average flow rate of 31 kg/s. Figure 5-5 shows the harvester begins to move at the 4 second mark with the ground speed increasing quickly to approach the target of 10 km/hr at the 12 second mark. The square or blocky nature of the speed measurements is due to the fact that the speed measurements were calculated over one second intervals. The pressure, feed roller separation and weigh pad sensors begin to register increases after a lag of between three and five seconds after the harvester begins to move.

A frequency spectrum of the signals produced by the pressure, feed roller separation and weigh pad sensors is given after the example data from each. These figures were developed by conducting a Fast Fourier Transform on the data. The Y-axis is the magnitude of the power spectrum at the various frequencies along the X-axis.

The third set of graphs for each sensor shows the calibration results for each technique. In these graphs, each point represents a different 'run'. On the Y-axis the average reading of the respective measurement technique is plotted and on the X-axis, the average mass flow rate of cane. The calibration results of these figures are summarised in Table 5-1. The results for the elevator power and the feed roller separation do not contain measurements for Day 1 due to problems encountered with the elevator speed sensor and feed roller sensor on that day. Although this resulted in a smaller data set for these sensors, valid information was still derived. Each day of results for the weigh pad has been treated separately because of the obvious differences between them and this will be discussed further in the next section.

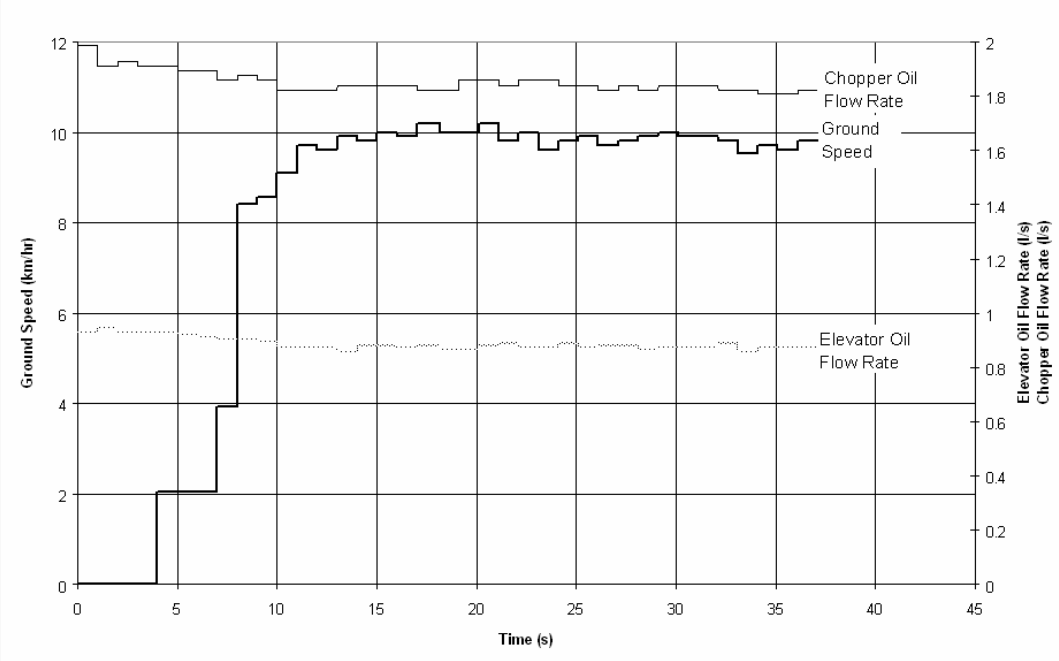

Figure 5-5. Typical data from the beginning of a run for the ground speed and oil flow rate measurements.

5.4.1 Chopper Power

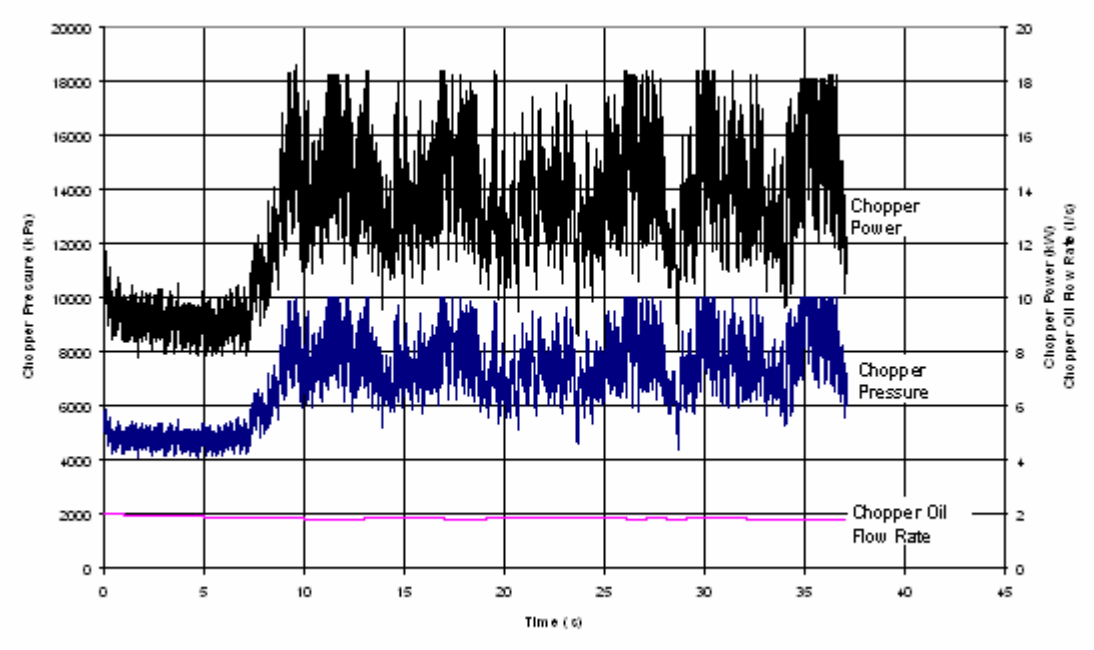

Figure 5-6. Typical data from the beginning of a run for the chopper power measurements.

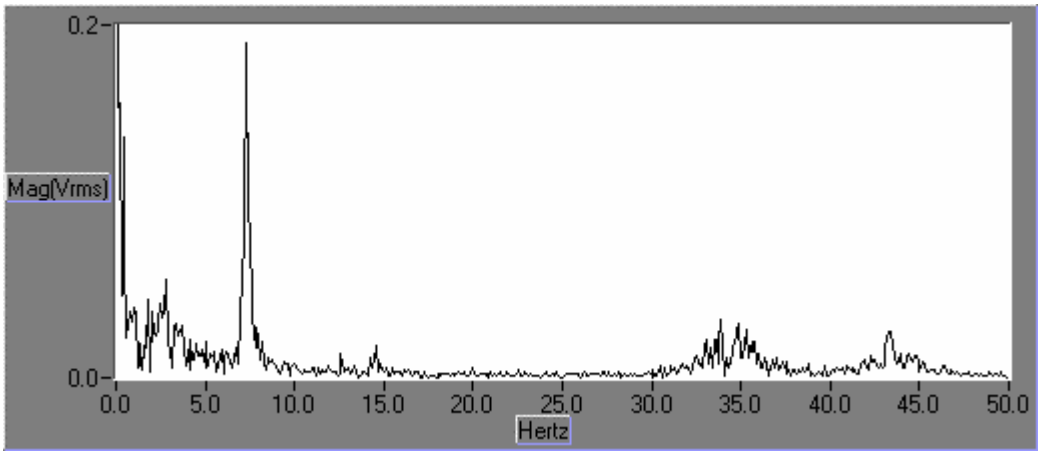

Figure 5-7. Frequency spectrum of the chopper pressure signal during normal cane flow conditions.

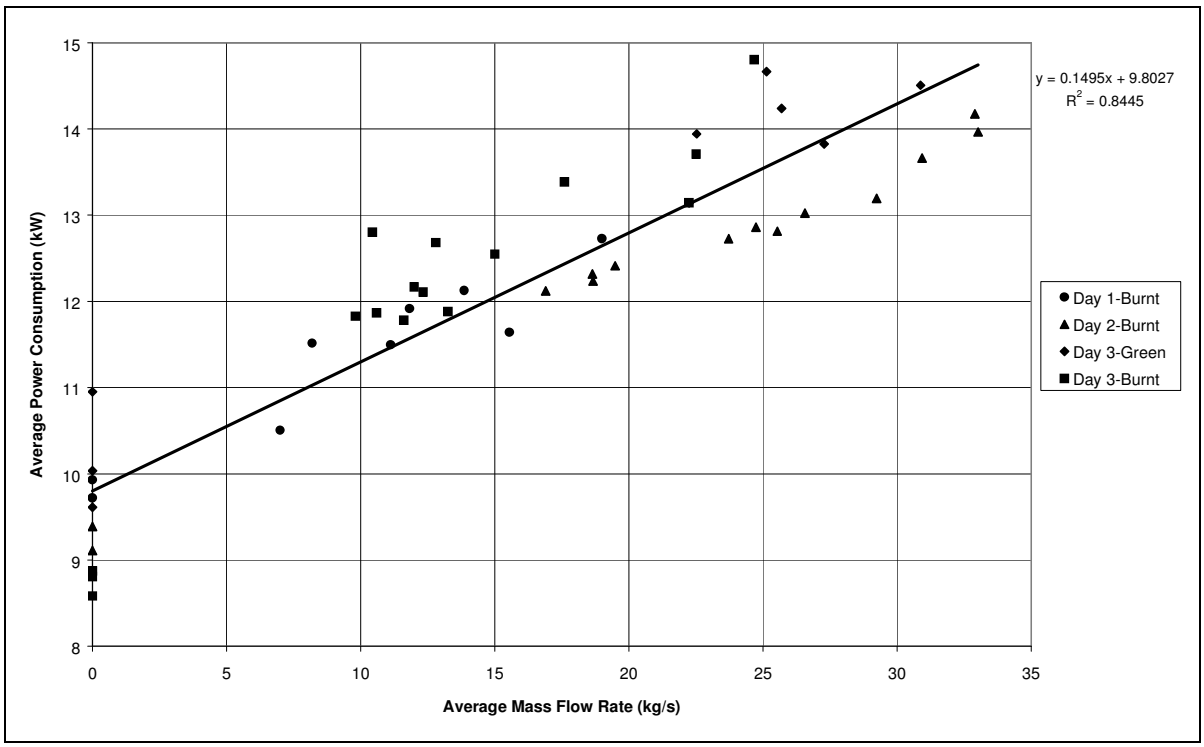

Figure 5-8. Calibration results of the chopper power measurements (Note nonzero y axis).

5.4.2 Elevator Power

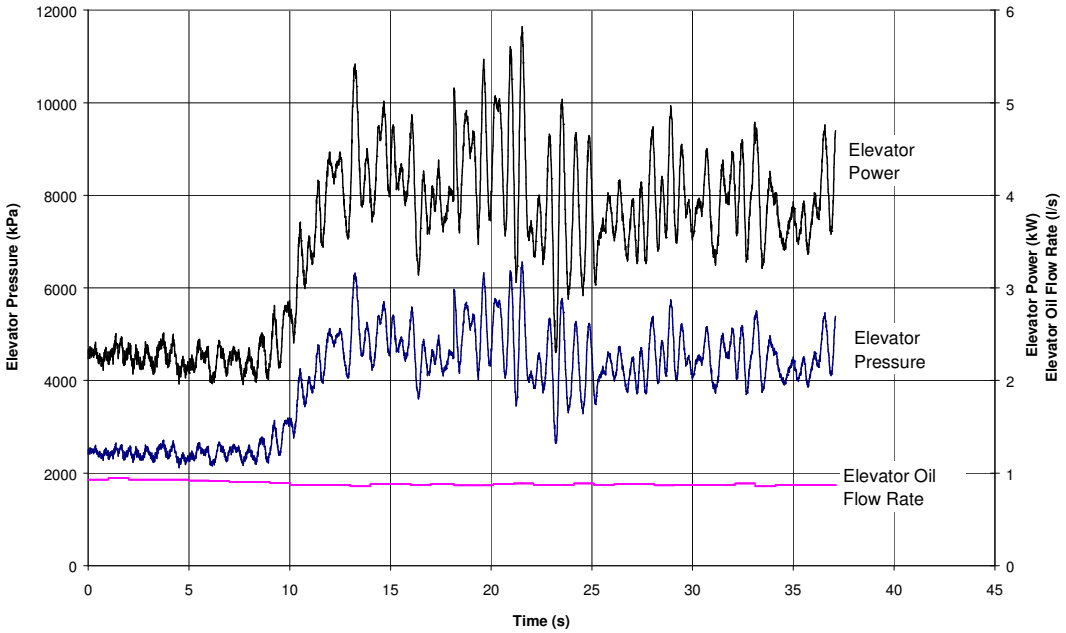

Figure 5-9. Typical data from the beginning of a run for the elevator power measurements.

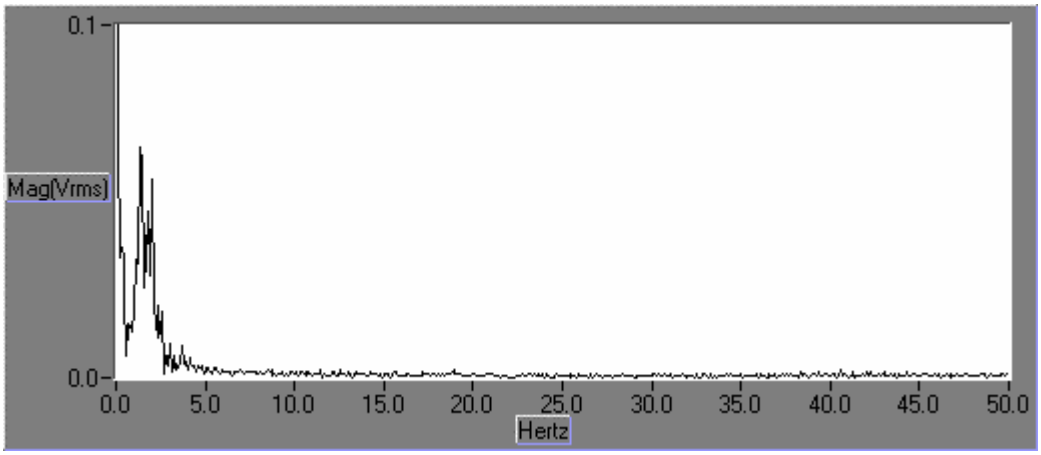

Figure 5-10. Frequency spectrum of the elevator pressure signal during normal cane flow conditions.

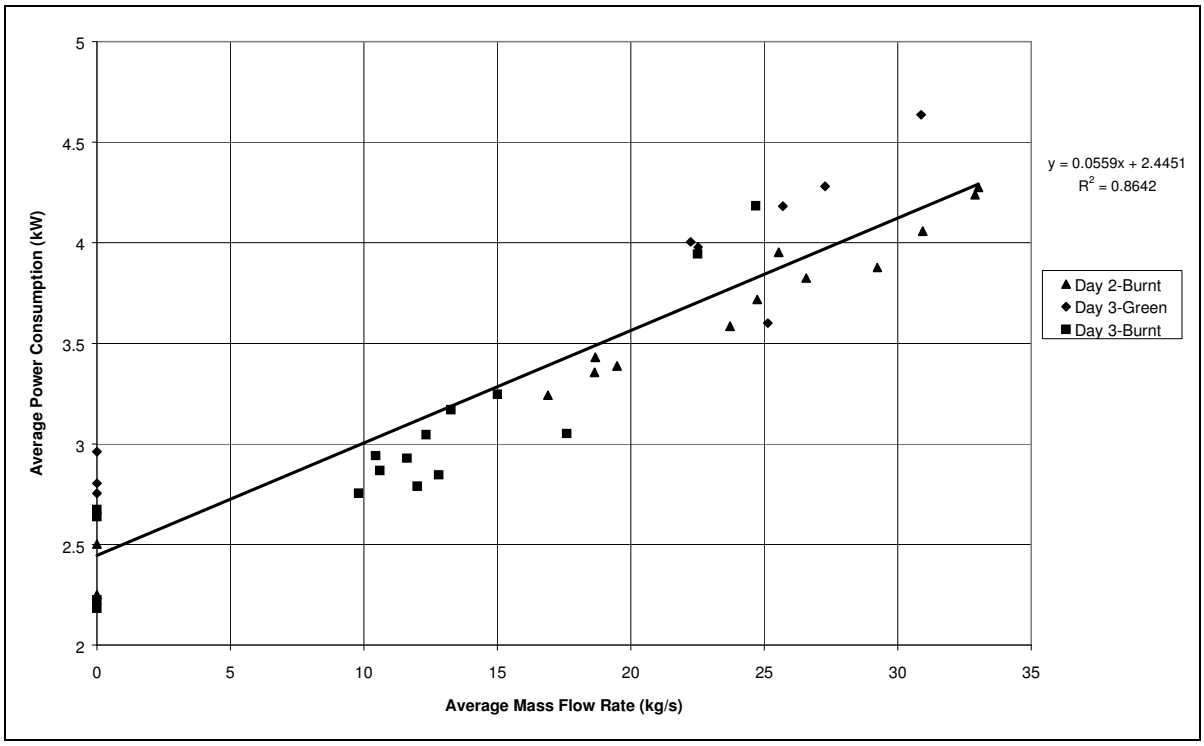

Figure 5-11. Calibration results of the elevator power measurements.

5.4.3 Feed Roller Separation

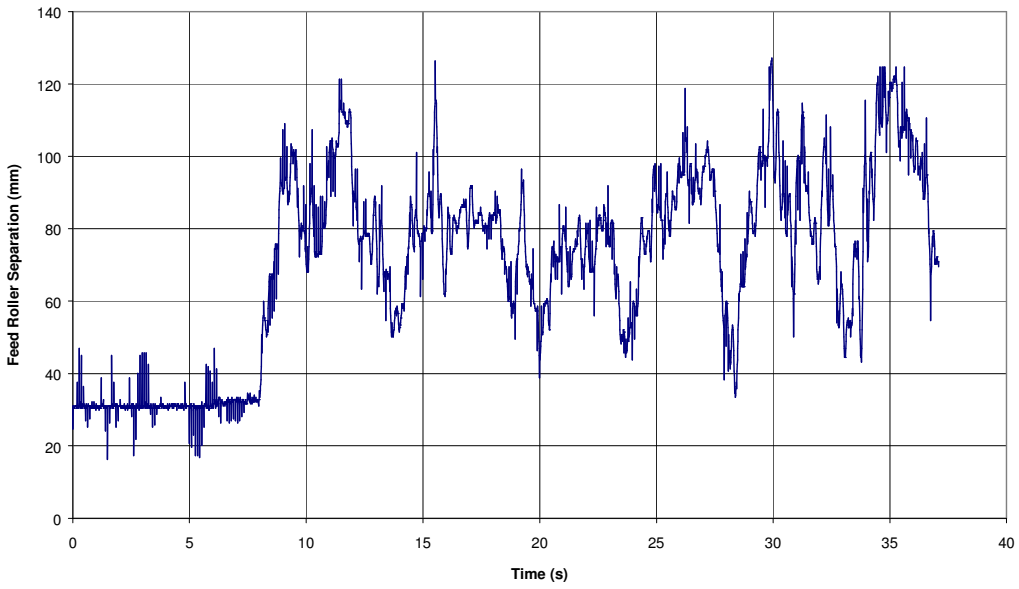

Figure 5-12. Typical data from the beginning of a run for the Feed Roller Separation measurements.

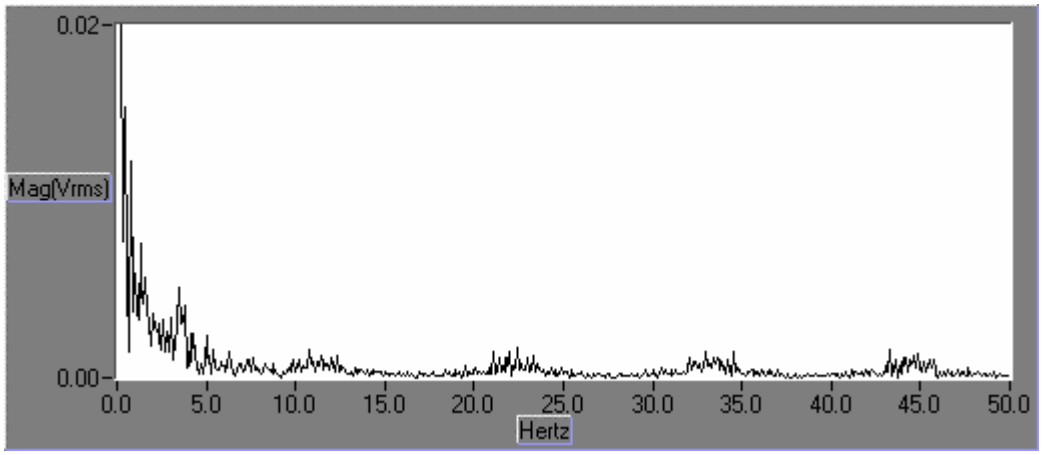

Figure 5-13. Frequency spectrum of the Feed roller Separation signal during normal cane flow conditions.

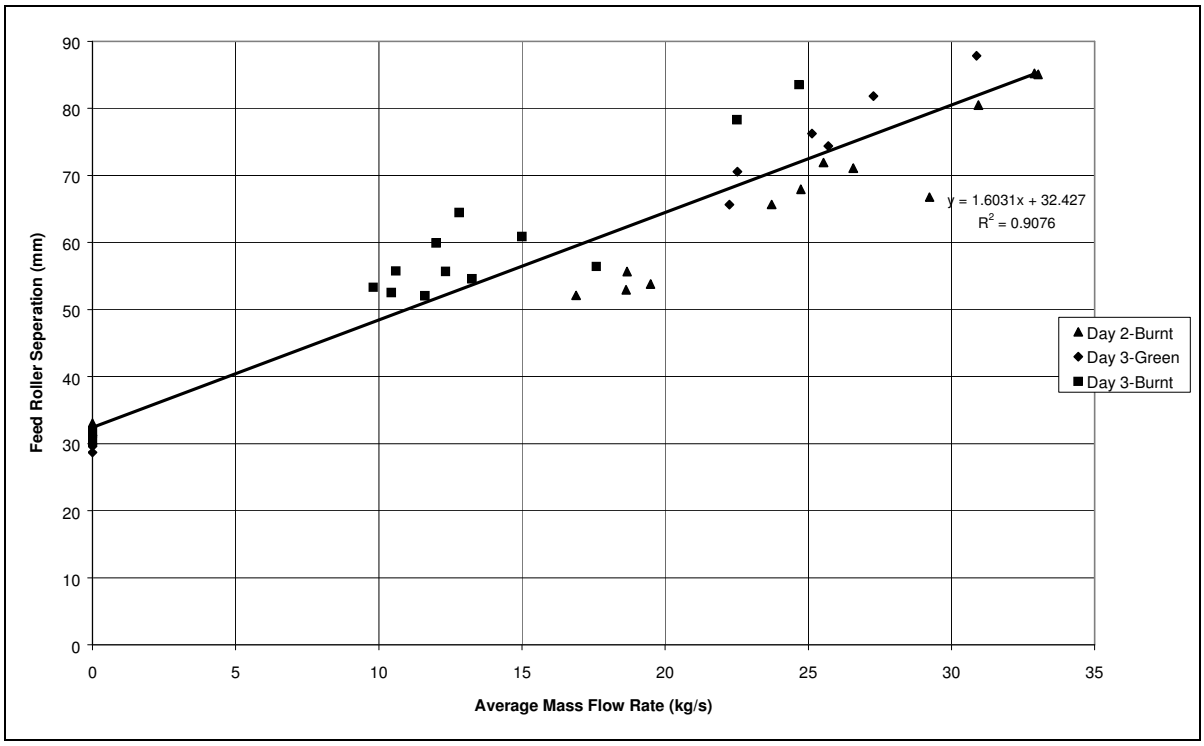

Figure 5-14. Calibration results of the feed roller separation measurements

5.4.4 Weigh Pad

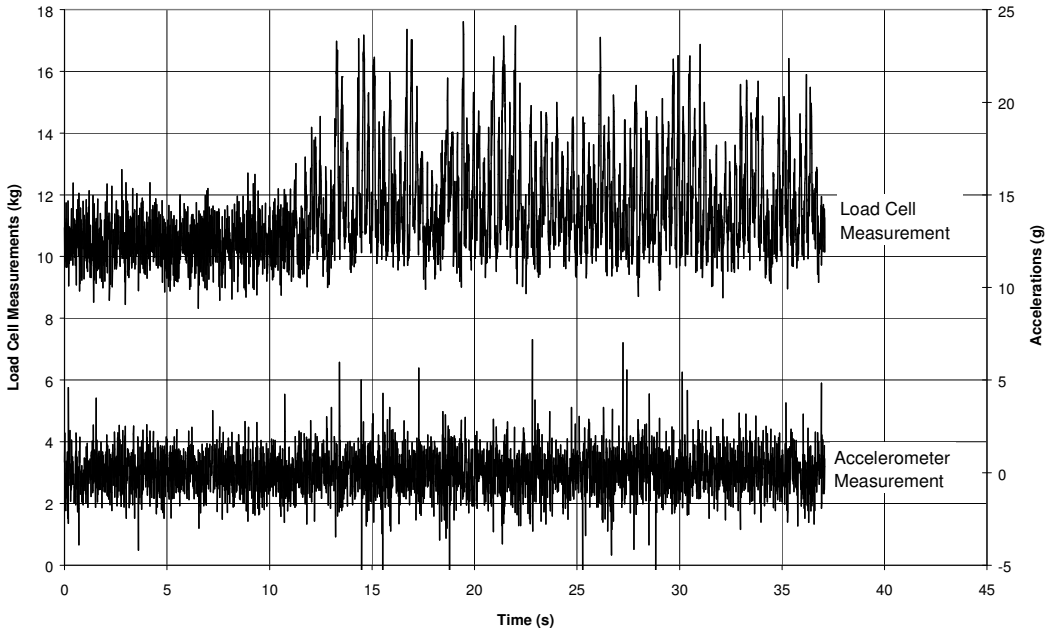

Figure 5-15. Typical data from the beginning of a run for the weigh pad measurements.

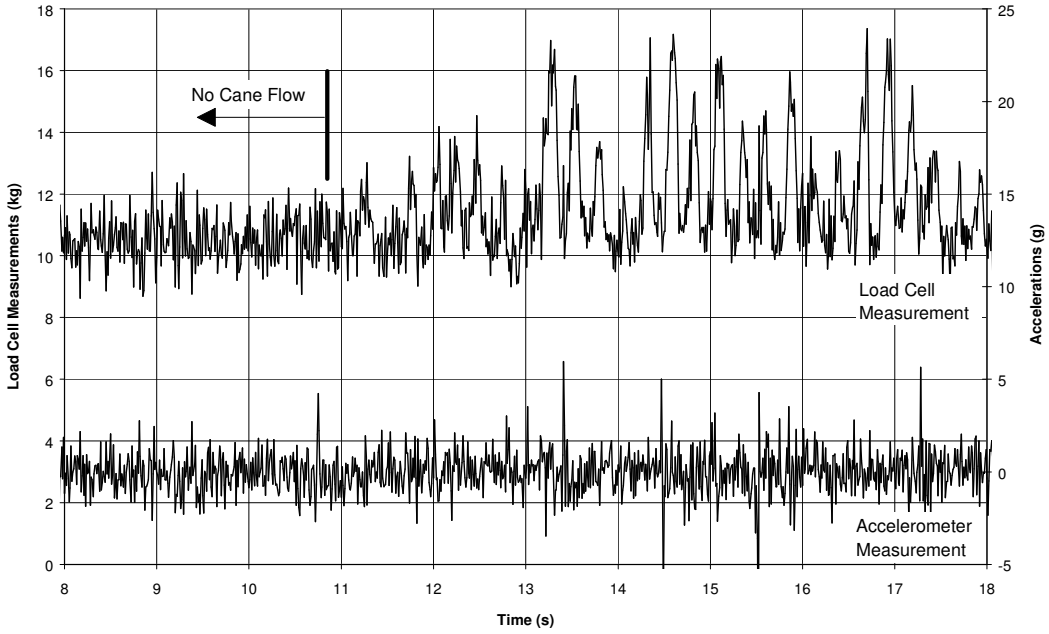

Figure 5-16. Zoomed view of the data in Figure 5-15 showing the peaks in the load cell measurements as cane travels over the weigh pad.

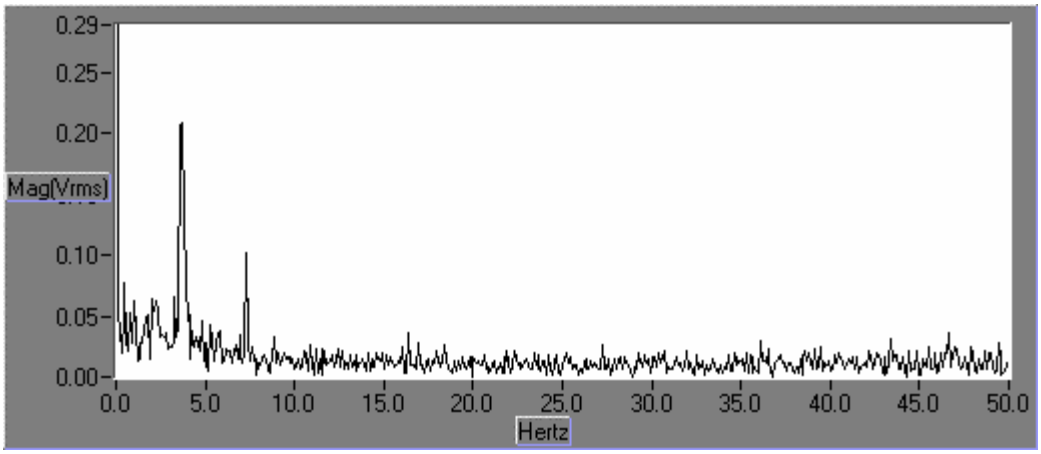

Figure 5-17. Frequency spectrum of the weigh pad signal during normal cane flow conditions.

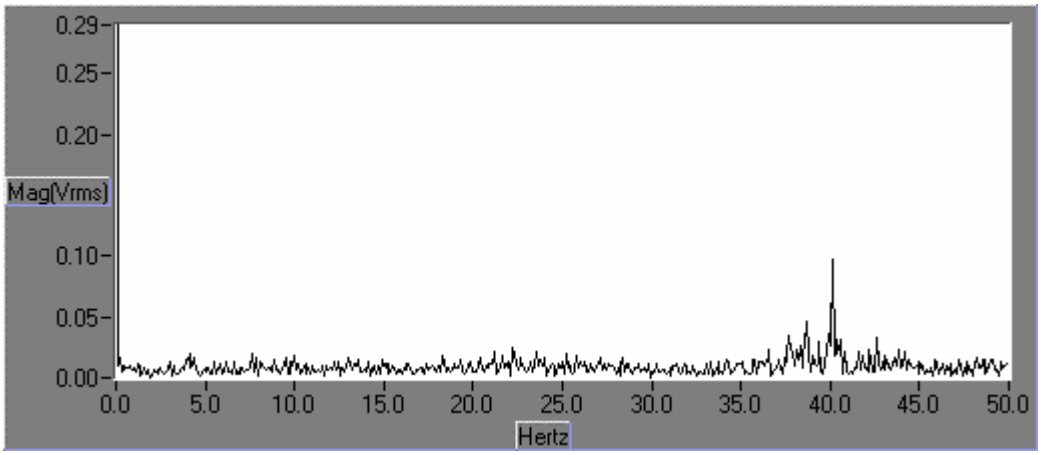

Figure 5-18. Frequency spectrum of the weigh pad signal during free running conditions.

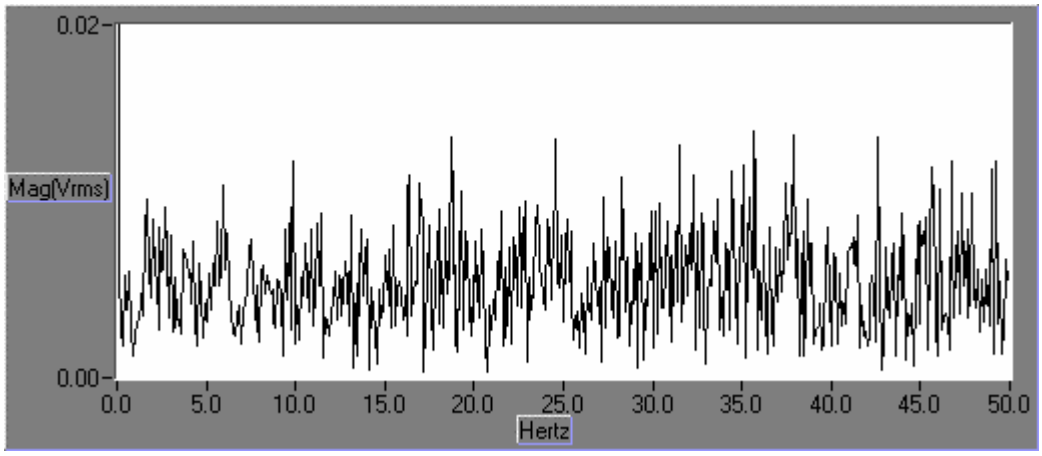

Figure 5-19. Frequency spectrum of the weigh pad accelerometer signal during normal cane flow conditions.

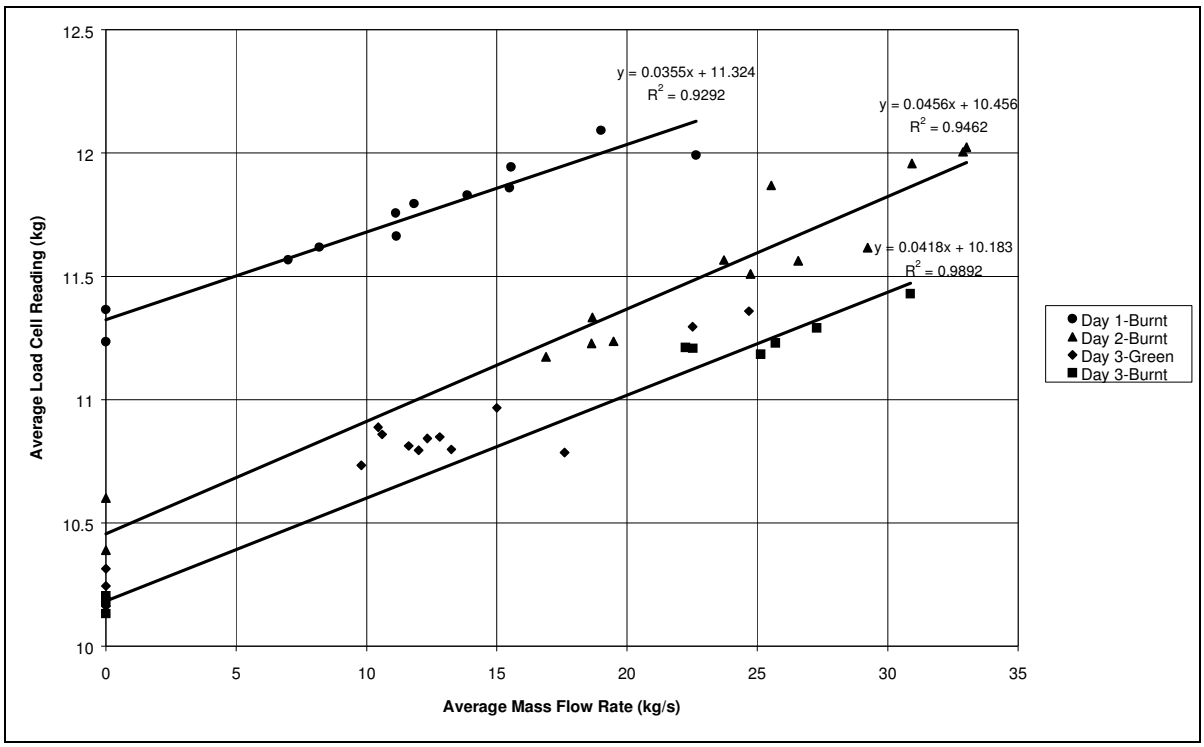

Figure 5-20. Calibration results of the weigh pad measurements.

Table 5-1. Summary of Results

Technique	Calibration Line		R^2	Std Error
	Intercept, I	Slope, m		(kg/s)
Chopper Power	9.80 kW	0.149 kW/(kg/s)	0.84	4.18
Elevator Power	2.44 kW	0.056 kW/(kg/s)	0.86	4.08
Feed Roller Separation	32.4 mm	1.60 mm/(kg/s)	0.91	3.36
Weigh Pad*	10.45 kg	0.046 kg/(kg/s)	0.95	3.33

* Note: Weigh pad results are taken from Day 2 as a general indicator of the results.

5.5 Discussion

The results from the previous section will be discussed individually for each sensing technique.

Firstly it should be noted that for this trial the test area for each run is not in accordance with the area stated in the accuracy specification of the previous chapter. For this trial, the test area for each run was 150 m^2 (100 m long x 1.5 m wide) which is larger than the 100 m^2 specified in the accuracy goal. The reason for this is that the trial was carried out prior to the development of the accuracy goal. The difference in area in a practical sense is relatively insignificant. Based on the theory presented in Chapter 3, the results of this trial should be 1.2 times better than a trial conducted over a test area of 100 m^2. This can be calculated using the assumption that error decreases proportional to the square root of the measurement area.

Before examining the calibration results the error sources in the testing process should be recognised. This will define the magnitude of the error bars that could be placed on the graphs. The error bars can be plotted along two axes, being the X-axis, which is the average mass flow rate and the Y-axis, which was the sensor output. The X-axis is calculated by measurements of the total mass harvested and the time of harvest. The total mass harvested can have significant errors introduced from a number of sources including:

- A proportion of sugar cane and trash that is measured by the chopper and feed roller sensors is lost out of the primary extractor fan. This loss can be as high as 20 % at high mass flow rates. In this situation where the harvester was not tested to its limit then the loss would be lower, estimated in the area of 5 %. This inaccuracy would produce a

negative error on the X-axis of this magnitude.

- Sugar cane and trash is also lost out of the secondary extractor fan. This material is measured by all sensors but not recorded in the weigh truck. This total weight can be estimated to average approximately 5 % and will produce a negative error also.

- Sugar cane can also be lost over the side of the weigh truck through operator error. This problem was exacerbated by the relatively inexperienced operators. In the worst case, these losses could have introduced a negative error of 5 %.

The other measurement used to calculate the average mass flow is the time of harvest. The error for this measurement would be less than 2 seconds. On an average run time of 45 seconds this could result in an error of 4.4 %. This error would also appear in the same magnitude on Y-axis. This is because the average sensor reading is calculated by dividing the integrated sensor output by the total time of the run. Therefore any error in the measurement of harvest time would affect both axis measurements proportionally and therefore not impact on the calibration results.

Therefore from this analysis the X-axis error bar would be 15 % in the positive direction for the feed roller separation and chopper power techniques and 10 % in the positive direction for the elevator power and weigh pad sensor.

The Y-axis also has error introduced from the transducers used for the measurements. The manufacturers specification for the transducers accuracy were:

- Pressure transducers: ±0.25 % error full scale.
- Load cells: ±0.1 % error full scale.

Also, due to the discrete acquisition of the sensor signal at 100 Hz, the worst-case error was 1 % (0.1 s/1s) for every four revolutions of the relevant shaft. This random error would average out over the whole run to be much smaller.

These specifications indicate the errors in the Y-axis of the calibration graphs are largely less than 1 % and much smaller than these on the X-axis. These uncertainties must be taken into account when analysing the results of the trials.

5.5.1 Chopper Power

Due to electrical difficulties, the transducer designed to measure the hydraulic pressure at the outlet of the chopper motors failed. This prevented the differential pressure across the chopper motors being accurately calculated. Subsequently, the pressure transducer at the inlet of the motors was the only measurement available to estimate chopper power. As the feed roller system of the harvester followed the chopper system in the hydraulic circuit, the hydraulic pressure measured at the inlet of the chopper motors includes the pressure required to drive the feed roller system. Therefore all calculations of chopper power include the power consumption of the feed roller system. It is postulated that the power consumption of the feed roller system would be dependent on the mass flow rate in any case, and that therefore the results would still be useful.

Figure 5-6 displays the example data for the chopper sensors. There is a distinct increase in power as the harvester begins to cut cane at the 7 second mark, levelling off at the 10 second mark as the relatively steady state flow rate commence. The chopper pressure reading is quite erratic and noisy, which is also reflected in the power results. A distinct clipping of the data is present at 10,000 kPa. This is due to the hydraulic pressure increasing above the upper limit of the transducer and data acquisition system. This did not affect the result significantly as the limit is breached infrequently and only at the higher flow rates produced during this run but rarely during the rest of the trials. This artefact is also exhibited in the calculated power signal as expected.

The calculated power signal is quite noisy with spikes at a relatively high frequency. These spikes would be due to the individual chops of the chopper, which occur at a rate of 8 Hz (2 bladed chopper rotating at 4 revolutions per second). The lower frequency variations are due to the fluctuation in the cane flow rate through the chopper, which can vary significantly over short periods. These observations are also supported by Figure 5-7, which shows the frequency spectrum of the chopper pressure signal. A distinct peak is found at approximately 8 Hz while lower frequency components are found below 2.5 Hz. Some higher frequency signal is also found above 30 Hz, which is most likely due to the action of the hydraulic motors and pumps.

Another interesting observation from Figure 5-6 is the relatively high power requirement to operate the chopper system with no cane compared to the typical operating level with cane flow. The free running power was about 9 kW while the operating range peaked at 18 kW

but averaged to approximately 15 kW. This ratio of 0.6 indicates a low operating efficiency and can have a serious impact on the use of this technique for measuring mass flow rate. Small fluctuations or drift in the free running power will effectively cause a shift in the calibration line for this technique. With this ratio of free running power to operating power, a 10 % drift in the free running power will result in a similar full scale error in the mass flow rate measurement. Any number of factors including change in hydraulic oil temperature to the build-up of foreign matter in the system could conceivably cause this change in the free running power. One technique to minimise this problem would be to regularly update the calibration line with the most up to date free running measurement. This could be carried out manually if this value changes slowly and is only required once or twice daily. However if this value changed more swiftly, then an automatic updating technique would need to be introduced. The end of each row provides an opportunity to zero this technique.

In Figure 5-6 a notable reduction in the chopper oil flow rate occurs as the run progresses. This reduction in flow rate is displayed with more resolution in Figure 5-5 where it appears to reduce by approximately 10 % of its initial value. It is evident that the flow rate drops as the harvester begins to move and then drop further as the crop is harvested. This reduction in oil flow rate would be roughly proportional to the reduction in engine speed as the harvester's power load increases. This result indicates the importance of monitoring oil flow rate for accurate calculation of hydraulic power in this situation. An assumption that the oil flow rate remains the constant over all operating conditions could lead to power measurement errors in the order of 10 %.

The calibration line derived for the chopper power measurements is given in Figure 5-8. This line was calculated by fitting a linear trend-line through all the data points. There is a large degree of scatter in the data and therefore a large amount of error. When the data are separated into the different conditions of each day then some patterns emerge. The Day 2 results appear to follow a unique calibration line with a lower gradient than the overall calibration. This is primarily due to the fact that the cane harvested was burnt and of variety Q96. This indicates that the different conditions have a significant affect on the slope of the calibration line. The full extent of this effect due to the variation caused by other factors such as measurement error is hard to quantify. Green cane has a higher power requirement due to the additional material chopped that is then removed by the secondary extractor fan. Also different varieties are known to have different levels of hardness and therefore varying requirements for chopping power. The chopper power technique would therefore need to be calibrated for each different condition to be useful for yield mapping purposes. That is, changes in crop variety, green/burnt cane and even crop age would have to be calibrated.

Every time a new field is entered the sensor would have to be recalibrated. This is not so different from grain yield monitors where this is standard practice.

The other notable fact in Figure 5-8, is the degree of variation in the free running power measurements of the chopper system. These measurements appear along the Y-axis at zero cane flow. This measurement cannot obviously be affected by varying crop conditions as no cane is flowing through the machine. It is function of the friction in the chopper system. This variation is a significant source of error for the calibration curves. As stated previously an auto zeroing technique would be required for this sensing technique to be useful.

If the effect of the different crop conditions and the drift in the free running reading is removed from the data in Figure 5-8, then there is significantly less error. This remaining error could be accounted for with the measurement error on the X-axis. (15 % as discussed above). Overall this sensor gave a coefficient of determination (R^2) of 0.84 (Table 5-1), which is less than desirable but still provided a valuable indicator of mass flow rate. A standard error of 4.18 kg/s for this sensor is the highest of all those measured. However this is not a fair comparison with the other techniques as the elevator and feed roller techniques were trialed over fewer conditions and the weigh pad result was only calculated over one day.

5.5.2 Elevator Power

The example data from the elevator power measurements given in Figure 5-9 have the same features as the chopper power equivalents. There is an obvious increase in power as the cane begins to enter the system near the 10 second mark. This is roughly 2 to 3 seconds behind the chopper system due to the time required to fill the elevator. The pressure signal does show a strong frequency component at roughly 2 Hz, which is supported by the frequency spectrum given in Figure 5-10. The hydraulic motors rotate at roughly this speed and are therefore the probable source of this frequency component. The elevator does offer the same sort of lower frequency variations as the chopper power, due largely to the variation in sugar cane flow rate. These fluctuations are somewhat smoother than those for the chopper power measurements as the elevator holds approximately 3 seconds worth of cane from the chopper system. This characteristic would act to form a moving average of the chopper power signal.

The elevator pressure does not approach the 10,000 kPa limit as the system operates at a

much lower pressure than the chopper system. The power consumption of the elevator is also much less than the chopper system. For the elevator the free running power consumption was approximately 2.25 kW while the operating power was around 4 kW. Again there is a high ratio between the free running power and the operating power. This fact can cause the same problems with the calibration as mentioned in the chopper power discussion.

Figure 5-9 also displays the reduction in the oil flow rate as harvesting begins. Figure 5-5 shows this reduction more closely where the reduction appears in line with the chopper reduction, at roughly 10 %. Again the cause of this is the reduction in the engine speed of the harvester as discussed in the chopper power discussion. This reduction means that it is important to monitor oil flow rate to correctly measure the hydraulic power during harvesting.

Figure 5-11 displays the calibration results for the elevator power measurements. Again there is significant scatter around the calibration line. The most obvious cause of this scatter is the variation in the free running power. This variation is as large as the variation in all the other calibration data. This result indicates that if the variation in the free running power requirement could be reduced or monitored then the majority of the error for this technique could be removed. The elevator is constructed from a multitude of rotating and sliding elements, all of which produce friction. This results in a high proportion of the elevator power being required to overcoming the friction force. Also, this force can change significantly due to changes in the components of the elevator such as the elevator chain and foreign matter build up. This results in significant change in the free running power occurring over a short period. A better technique would be to try to monitor the free running power of the elevator and use this to update the calibration line. To be useful this would need to ideally occur every few minutes but at worst every 20 minutes. This maybe difficult to implement, as the elevator would need to be emptied and running for at least 5 seconds which rarely occurs in typical harvesting situations.

Table 5-1 shows that the elevator power technique achieved a R^2 of 0.86 and a standard error of 4.08 kg/s, which is slightly better than the chopper power but worse than the other two techniques. If the variation in the free running power of this technique can be reduced or monitored, the accuracy could improve dramatically.

5.5.3 Feed Roller Separation

The feed roller results given in Figure 5-12 are as expected. At the beginning of the data there is a distinct baseline that occurs when there is no cane flow. This baseline is relatively stable with some high frequency noise superimposed. This noise is an artefact of the sensor design and is caused by harvester vibrations. The baseline is well defined and stable because the feed rollers rest against a fixed 'stop' when there is no cane passing through the harvester. As cane begins to flow there is significant increase in feed roller separation, which approaches the 120 mm maximum. The lower frequency fluctuations in Figure 5-12 are due to irregular "feeding" of sugar cane through the harvester.

Figure 5-13 shows the frequency spectrum of the feed roller separation signal with most of the signal occurring below 5 Hz. This is due to the variation in the "feeding" rate of sugar cane through the harvester. Figure 5-13 also shows some signal at 11 Hz increments. This is higher frequency noise that is an artefact of the sensor design.

Figure 5-14 shows a significant scatter in the data points and a distinct difference between burnt and green cane. Sugar cane harvested green has up to 30 % more extraneous material than a burnt crop (Ridge and Dick, 1988). This extraneous matter is passed through the feed rollers before being removed by the extractor fans. This results in a larger feed roller separation for the same mass flow rate measured at the weigh truck.

Table 5-1 shows that this technique produced an R^2 of 0.91 and a standard error of 3.36 kg/s. This is a substantial improvement on the power measurement techniques for such a simple technique. Although the method is volumetric, the benefit of this technique is its simplicity. This technique has a stable baseline but the gradient of the calibration line is significantly affected by crop conditions. If this technique is to be used to sense mass flow rate then factors affecting its accuracy such as cane density variation and feed rate variations need to be examined.

5.5.4 Weigh Pad

Figure 5-15 shows that there is a significant amount of noise in the weigh pad signal, but there is a distinct increase in signal magnitude at the 11 second mark, when cane begins to

flow. Figure 5-16 gives a closer view of this data. In this figure, as the cane begins to flow, a signal pulse is apparent at a frequency of approximately 4 Hz. This is the rate at which the elevator flights travel over the weigh pad. As the flight passes, the mass reading drops back to close to the original baseline as expected.

Frequency analysis of the free running data (first 11 seconds of Figure 5-15) indicates that the noise is spread across the spectrum but there is a distinct peak in the 40 Hz region (Figure 5-18). This is most probably due to the vibrations from the secondary extractor fan, primary extractor fan or harvester engine. An unbalanced fan blade on one of the extractor fans could cause such noise, particularly from the secondary extractor fan because of its close proximity to the weigh pad.

Figure 5-17 shows that there is significant weigh pad signal at 4Hz. This is due to the rate that the elevator flights pass over the weigh pad.

The acceleration data (in Figure 5-15) display a significant amount of variation with readings of up to ±5g. The noise spectrum of the acceleration data (Figure 5-19) is broad, indicating no specific band of noise. Note the acceleration readings fluctuate around an average of 0 g. This is due to the AC coupling design of the sensor. It would be difficult to correct the mass measurements using this acceleration data, as there appears to be no correlation.

Figure 5-20 shows the calibration results for the weigh pad sensor. The results are widely scattered. However there are three distinct calibrations lines with similar gradients. The major difference between the calibration lines is the shift in the baseline values. The shift was caused by adjustments to the load cell mountings, which were carried out each morning before testing. The loads on the two load cells were adjusted (using turn buckles) to equalise the load cell readings.

A drawback of this particular weigh pad design is the very slight gradients that were obtained from the calibration lines. Compared to the baseline readings of approximately 10 kg the gradient was only approximately 0.04 kg/(kg/s). This could be improved by reducing the weight of the weigh pad.

Results from Day 3 shows that different harvesting techniques (i.e. green or burnt) do not affect the weigh pad calibration. This is expected, as the primary extraction fan should remove most of the trash found in green cane before it reaches the weigh pad.

Overall the results from the weigh pad were mixed but provided sufficiently positive results to continue the research into this technique.

Weigh pad technique suffers from very small load cell sensitivity to flow rate, drift in free running readings and susceptibility to mechanical noise.

5.6 Conclusion

From these trials the main conclusions that can be drawn are:

1. Both power techniques for the chopper and elevator suffer from drifting free running values that seems to be a source of significant error.

2. Feed roller separation has a stable free running volume but the calibration line slope is significantly affected by crop conditions, the “gulping “ of cane by the harvester which results from non-uniform feed and when large stools holding dirt or clumps of stubble pass through the rollers.

3. The weigh pad technique suffers from very small load cell sensitivity to flow rate, drifting in free running readings and susceptibility to mechanical noise.

4. All of the techniques offer potential but none produce results near the accuracy goal.

5. Further analysis of the weigh pad technique is required to optimise the design for improved accuracy.

Chapter 6 – Development of Preliminary Sugar Cane Yield Maps And Their Agronomic Application

6.1 Introduction

After the preliminary success of measuring mass flow rate during the field trials, an opportunity arose to install a complete yield mapping system on a harvester within a commercial operation for the 1996 harvest season. This opportunity was accepted, in part to gain experience with the technology of yield mapping, but also to provide insights into the agronomic and economic case for yield mapping. As the weigh pad sensor required further development at this stage, the chopper and elevator power were used as a measure of mass flow rate. This work is discussed in this chapter, along with an associated survey of soil chemistry, and an analysis of the economic benefits to follow up variable rate soil amelioration. The dissertation then continues on to describe the analysis and improvement of the weigh pad sensor and its subsequent incorporation into a commercial yield mapping system.

This is essentially the first known application of precision agriculture to sugar cane. The site was a 1000 ha farm operated by DAVCO Farming, Ayr, North Queensland, Australia. For this chapter, a single field was selected to be representative of the whole farm. The 117 ha field is defined as Field 7A in farm plans.

The chapter is divided into three sections describing the site-specific procedures carried out in the field. These were yield mapping, directed soil sampling and variable rate application. For the yield mapping a unique system was developed to produce the first ever yield maps of sugar cane. Next, the soil sampling was carried out with the assistance of the yield map. The

results of the soil tests indicated a strong negative correlation of crop yield with the sodium content and the magnesium content of the soil. Variable rate technology was subsequently used to apply gypsum with the aim of overcoming these yield-limiting factors. Finally, to show the viability of precision agriculture in this situation, a simple economic analysis was conducted using three scenarios.

6.2 Yield mapping

A prototype yield mapping system for the chopper sugar cane harvester was developed and tested during the full 1996 harvest from June to December in the Burdekin region to establish its reliability and demonstrate the potential of yield mapping for better informing management decisions. Yield maps were developed for a total of 700 ha. This chapter presents the maps developed for a 117 ha field that displayed significant spatial yield variation.

The prototype equipment consisted of:

- A laptop computer;
- GPS receiver (Trimble GeoExplorer, 6 channel);
- Differential GPS correction receiver (Fugro Starfix's Omnistar system);
- PCMCIA data acquisition card;
- Sensor signal conditioning;
- Pressure sensor on chopper hydraulics;
- Pressure sensor on elevator hydraulics; and
- Ground speed sensor (RIMIK)

Sensors and hardware were fitted to the farm's 1997 model CAMECO cane harvester. The sensor outputs were conditioned and then acquired by the data acquisition card in the laptop computer. The ground speed was measured by a magnetic pickup on the front wheel of the harvester. The GPS receiver received differential GPS correction from the Differential GPS Correction receiver and then passed the corrected GPS readings onto the laptop computer through RS-232 communication connections. The laptop computer was a Pentium 100 running Microsoft Windows 95. The total cost of the hardware was $13000, with $9000 accounted for by the DGPS components.

A major focus of this research was to continue earlier work on developing a reliable mass

flow sensor, because the mass flow rate of cane through the harvester is the major measurement required for yield calculations. In the previous work (Cox *et al.*, 1996) it was found that the power consumption of the chopper and elevator systems of a mechanical harvester are strong linear indicators of the mass flow rate through the machine. On the basis of these results it was decided to use both these techniques in the prototype system. Hydraulic power is the product of pressure and motor speed, but the hydraulic system of a harvester and the operating procedures mean that motor speeds remain relatively constant. Therefore, in order to simplify the requirements for data acquisition, only hydraulic pressures were measured.

The weigh pad sensor was not used as a mass flow sensor as this trial was conducted early on in the research project. This was prior to the weigh pad being fully researched and designed as discussed in previous chapters. There were also concerns about reliability and failure that could cause considerable damage to the elevator of the harvester. The principles used here apply to the weigh pad sensor equally.

The software to operate the whole system was written by the author in National Instrument's LabView®. The display provided useful information to the harvester driver and a graphical user interface enabled easy operation. The primary purpose of the software was to collect the information and save it to the hard drive of the computer in a standard ASCII file format. Information required for the purpose of yield mapping was collected and recorded each second. The data were saved to a 540 Mb hard drive that had the capacity to store three months of data. Operation was automatic, with no input being required by the harvester driver. However, visual information was available on such measurements as the instantaneous yield, total yield for the day, total areas harvested for the day and harvester speed.

Information recorded each second included:

1. Global Positioning System Position and Fix Data: NMEA-0183 Output Message GPGGA.
2. Global Positioning System Course Over Ground and Ground Speed Data: NMEA-0183 Output Message GPVTG.
3. Sensor Readings:
    a. Real time yield calculation using rough calibration on chopper sensor reading, t/ha.
    b. Elevator pressure sensor reading, kPa.
    c. Chopper pressure sensor reading, kPa.

d. Ground speed sensor reading, m/s.

Table 6-1 shows a sample of the data collected. Appendix F details the format of the data strings.

Table 6-1. Sample of data collected by the yield mapping system.

```
$GPGGA,194506.28,1941.90653,S,14713.57325,E,2,03,1.4,19,M,55.6,M,5.28,0004*46,
$GPVTG,094,T,086,M,3.26,N,6.05,K*49$,
197.88,4167.55,10617.49,  1.64,  0.00
$GPGGA,194507.34,1941.90661,S,14713.57420,E,2,03,1.4,19,M,55.6,M,6.34,0004*47,
$GPVTG,095,T,087,M,3.24,N,6.01,K*4F$,
201.35,4377.31,10597.61,  1.61,  0.00
$GPGGA,194508.43,1941.90679,S,14713.57615,E,2,03,1.4,19,M,55.6,M,5.43,0004*47,
$GPVTG,093,T,085,M,3.24,N,6.01,K*4B$,
201.54,4489.43,10603.85,  1.61,  0.00
$GPGGA,194509.43,1941.90689,S,14713.57615,E,2,03,1.4,19,M,55.6,M,5.43,0004*47,
$GPVTG,093,T,085,M,3.24,N,6.01,K*4B$,
169.67,4412.26,9477.30,  1.58,  0.00
$GPGGA,194510.43,1941.90699,S,14713.57790,E,2,03,1.4,19,M,55.6,M,7.43,0004*4E,
$GPVTG,093,T,085,M,3.06,N,5.66,K*49$,
180.12,4290.36,9814.50,  1.58,  0.00
```

A linear calibration equation was applied to the chopper pump hydraulic pressure and elevator pump hydraulic pressure measurements to attain the mass flow rate reading for each sensor. The calibration factors of the linear calibration equation were calculated by post processing the recorded data on a PC in the office. The post processing procedure consisted of:

1. Examine the pressure readings to define the baseline or free running reading which becomes the intercept of the linear calibration equation. E.g. the chopper pressure is 1000 kPa when the harvester is running at normal operating speed but with no cane being harvested.
2. The pressure readings above the baseline for each second over a day are summed up to calculate the total 'work' require to process the cane over the day. e.g. The chopper pressure reading for one second was 1600 kPa hence the pressure reading above the baseline (1000 kPa) was 600 kPa.s. Adding this value up for each second of actual harvesting in the day would on average total maybe 16,600,000 kPa.s.
3. Calculate the calibration scale factor by dividing the total mass of cane harvested for the day as measured at the sugar mill by total work. E.g. 1000,000 kg ÷16600000 kPa.s = 0.0602 kg/kPa.s.
4. Apply the calibration equation to all the pressure readings (each second) to calculate the mass flow rate in kg/s. E.g. 600 kPa.s x 0.0602 kg/kPa.s = 36.1 kg/s
5. Calculate yield for each reading based on the mass flow rate and the ground speed and the row spacing. E.g. (36.1 kg/s ÷1000 kg/t) ÷ (3m/s x 1.5m ÷ 10000 m^2/ha) =

80 t/ha.

For the chopper yield calculations in Step 5 above, a time delay of two seconds was applied to the ground speed reading to account for the difference in time between when the cane is cut from the ground and when it is measured by the chopper pressure sensors. For the elevator calculations a time delay of 4 seconds was applied. This delay is discussed in more detail in previous chapters.

This post processing procedure was conducted for each day of harvesting. The procedure produced a data file that had the GPS location and the yield measurement for both the chopper and the elevator.

Yield maps were produced using ESRI's Arcview®, a general-purpose GIS package. The author used Arcview's programming language, Avenue, to develop a program to import the data and then smooth it. The smoothing technique consisted of placing a 20 m by 20 m grid over the field and calculating the average of all the yield reading in each grid cell. Approximately 100 data points were found in each grid cell. More complicated interpolation techniques were not implemented due to the significant computation time required for even this simple smoothing technique. In total the 117 ha field considered here contained approximately 350,000 data points.

6.2.1 Results

A purpose of the testing was to gain an insight into the accuracy and reliability of the system for measuring yield. This was carried out by accumulating the sensor reading over each day and plotting it against the total cane cut for the day as measured by mill weights. Calibration results for the chopper and elevator sensors for the 117 ha field are shown in Figure 6-1 along with 10 % error bars to indicate the confidence limit.

Figures 6-2 and 6-3 show the yield maps produced using the chopper and elevator measurements respectively, grid size being 20 m x 20 m. The average yield of the field was 122 t/ha. Figure 6-4 is a processed form of a colour aerial photograph of the same field presented for visual comparison with the yield maps. The contrast of the photograph has been adjusted to emphasise the lower yielding areas, which are lightly coloured, with the high yielding areas being dark. This photograph was taken in 1994, two crop cycles before

the yield maps were produced. However the yield variations are expected to be consistent from season to season due to the underlying problem relating to sodic soil.

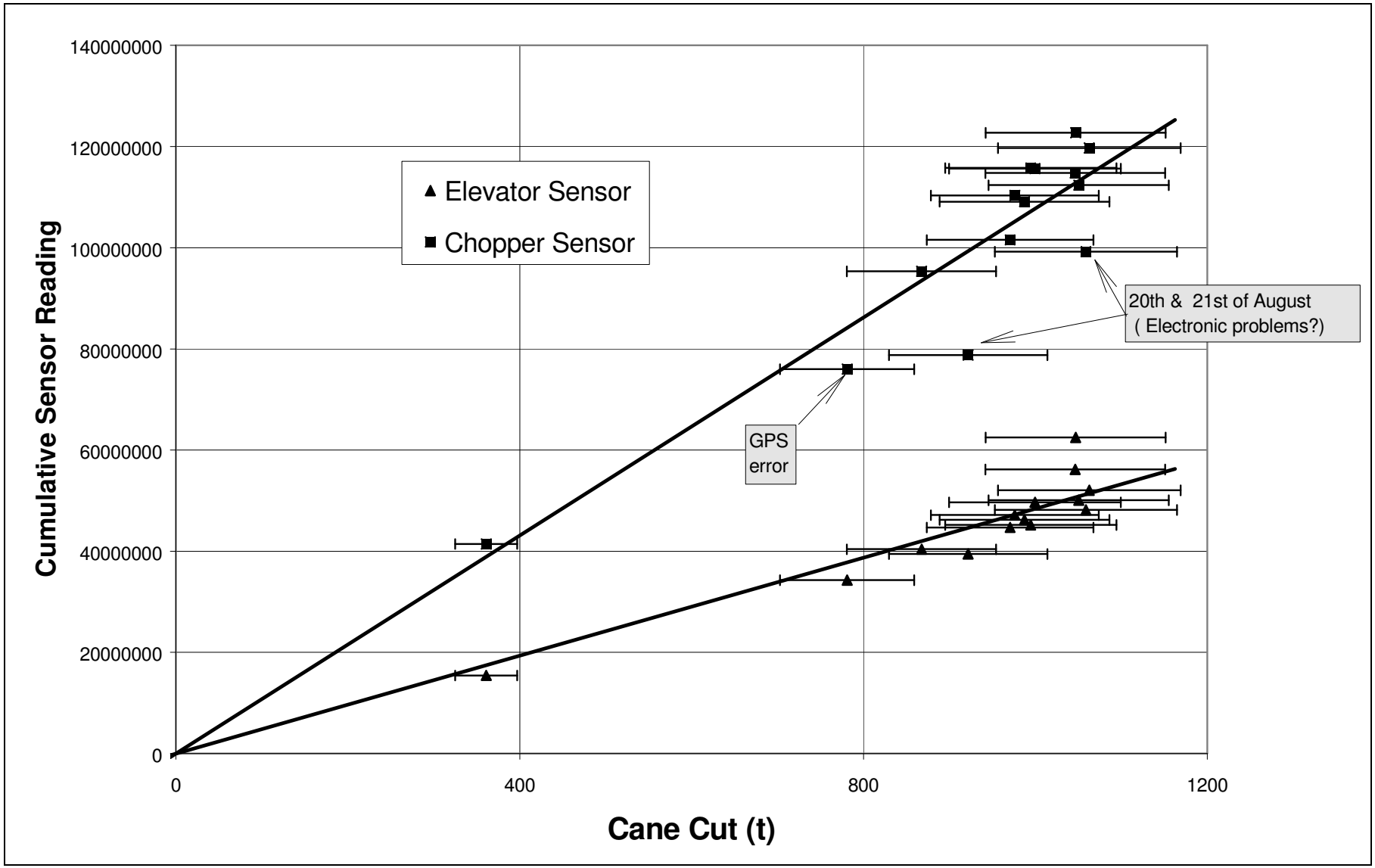

Figure 6-1. Correlation of daily calibration results (10% error bars).

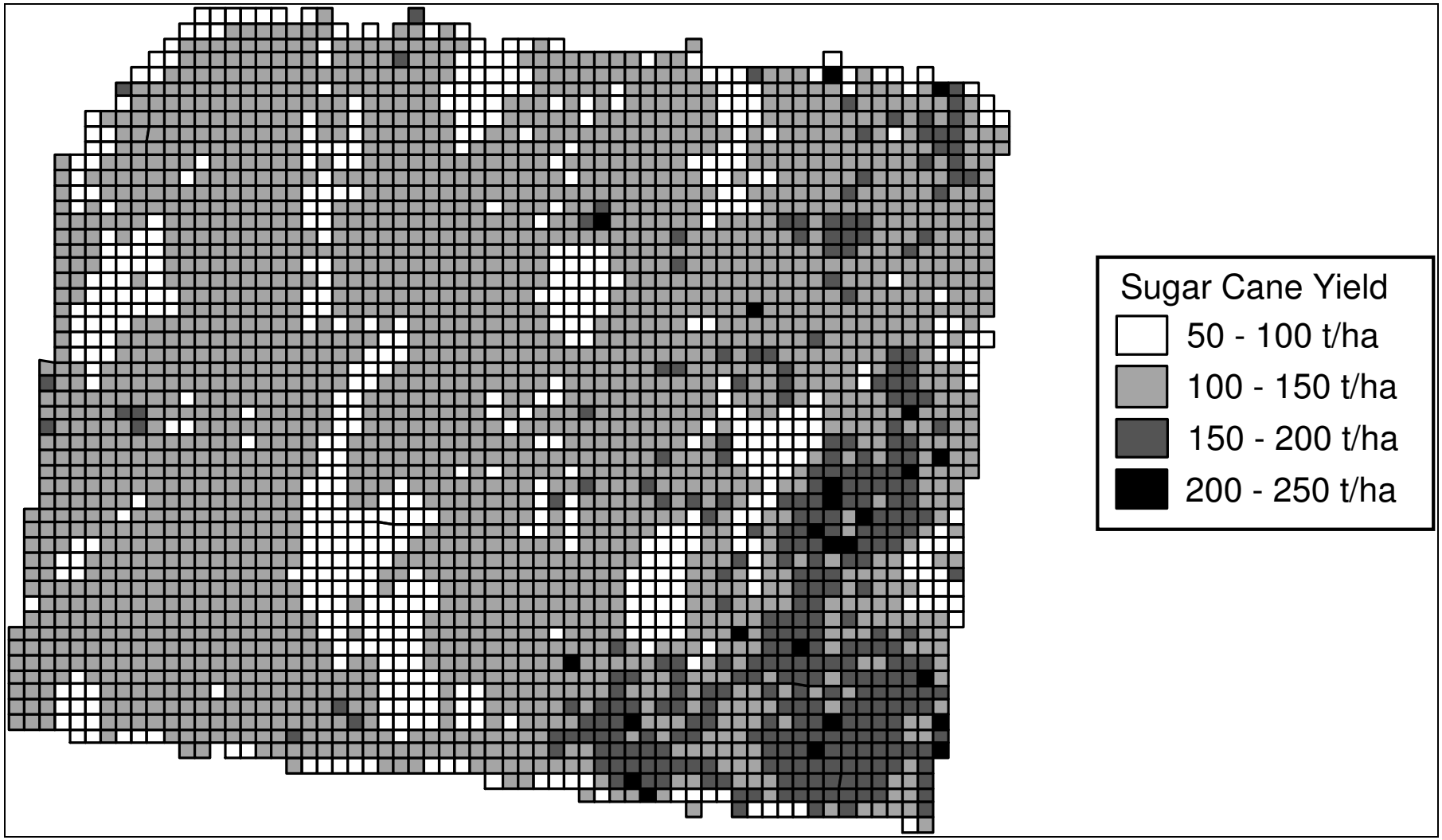

Figure 6-2. Yield Map produced using the Chopper measurement.

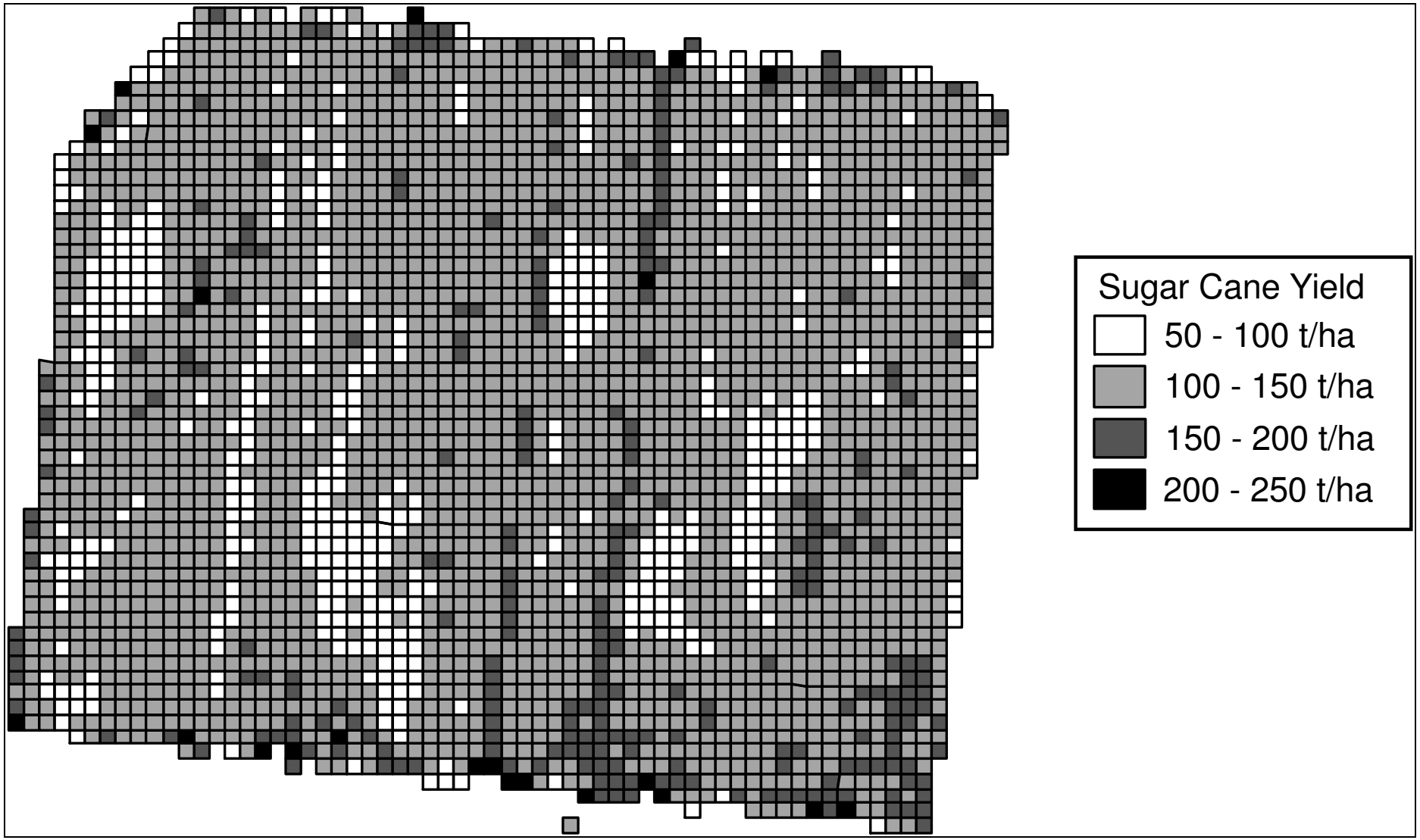

Figure 6-3. Yield Map produced using the Elevator measurement.

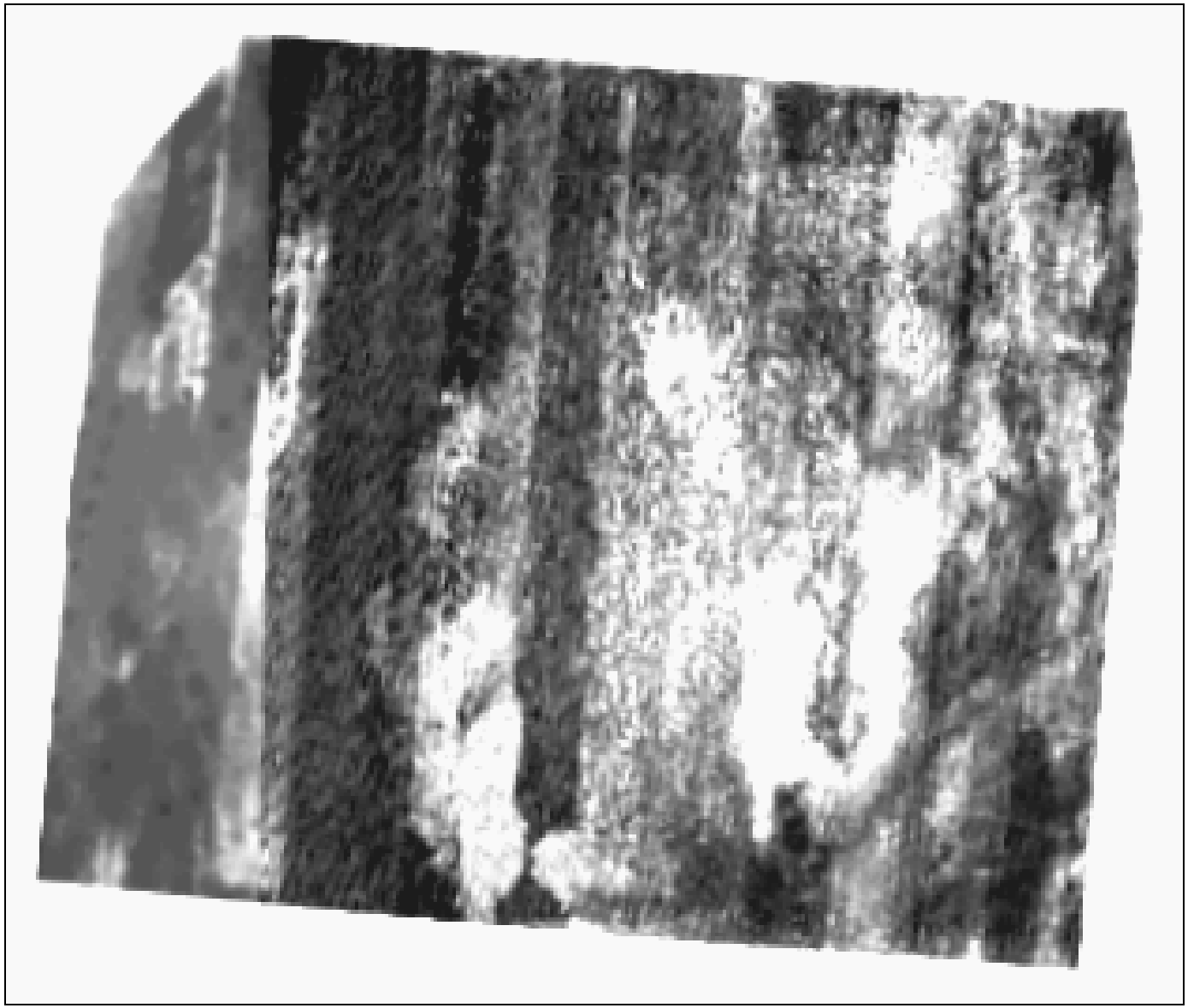

Figure 6-4. Aerial photo of the yield mapped field.

6.2.2 Discussion

The prototype system operated successfully over the full season with data gathered for more than 700ha. Minor problems, relating to the electronics, did cause the loss of some data. The cane harvesting environment is hostile so any yield monitoring system must be robustly designed to cope with these conditions.

The DGPS components worked extremely well, incurring no major problems. Through general observation the location accuracy appeared to be within a five metre range most of the time. Through the season, the GPS receiver did lose positioning capabilities for approximately one hour periods, but this did not become a major problem.

Figure 6-1 shows the daily calibrations over a 14 day period. The narrow spread of the data points around the respective calibration lines indicates that the sensing techniques performed satisfactorily. The exceptions are noted on the graph and are due to problems encountered with the GPS and electronics. As shown by the error bars, approximately 90 % of the data points lie within 10 % of the respective calibration lines. This figure shows that the chopper and elevator sensors measure daily harvest amounts accurately to within 10 %.

Figure 6-2 is the yield map produced from the chopper measurement and shows a significant spatial variation in yield. The areas that stand out on the maps are the lower yielding patches throughout the field and the higher yielding section at the bottom right hand corner. The yield map produced using the elevator sensor is shown in Figure 6-3. There are obvious similarities and differences between the two maps. The lower yielding areas are similar in shape and position, however the elevator map does not indicate the high yielding area at the bottom right hand corner. The other marked difference is shown on the elevator map where two high yielding lines only one square wide can be seen in the field. These erroneous data are believed to be due to a major shift in the calibration of the elevator sensor, caused by a build up of mud or other matter in the elevator producing higher power readings than usual.

Figure 6-4 shows an aerial photograph of the same field taken two seasons before the yield maps were produced. The low yielding points indicated by light areas in the photo coincide with the low yielding areas indicated on the yield maps. Although the aerial photo cannot provide conclusive evidence that the yield maps are accurate over the entire field, it does give confidence in defining the lower yielding areas. Scouting of this field four months after

harvest also provided visual evidence that the yield maps were relatively correct in the positioning of the high and low yield areas.

This research showed that yield maps could be produced for sugar cane using standard yield mapping principles.

6.3 Directed Soil sampling

The history of this field should be discussed to provide an insight into the cause of the yield variation. The field is situated in the newly developed Burdekin River Irrigation Area (BRIA) and has been in production for seven years. Prior to this it was laser levelled to improve irrigation and drainage. It is this levelling which has caused the higher areas to be "scalped" of their topsoil and the lower area to be filled. The scalping exposed highly sodic subsoil that has poor structure and greatly reduced infiltration and water holding capacity. This severely limits yield in these areas, particularly under fully irrigated conditions. A cut/fill map has shown that these scalped areas occur in the same places as the lower yielding areas on the yield map. The largest yields are found in the south-eastern corner of the paddock where the area was filled with up to 0.5m of imported topsoil. With this history, the farmer expects that the yield variation is due to the adverse effect of sodicity on soil structure, and plans to rectify the problem with variable rate gypsum amelioration. The soil sampling provides evidence to support this line of action.

For this section the grid yield map was further processed in the contouring package, Surfer® to produce a black and white map suitable for publication. The resultant yield map (Figure 6-5) showed significant signs of yield variation. In the field under study the average yield was 120 t/ha and the yields were normally distributed around this value with a standard deviation of 25 t/ha. The lowest yield was 70 t/ha ($2100/ha) and the highest was 190 t/ha ($5700/ha). It was encouraging to find a close correlation between the high and low yield areas found on the yield map and those displayed on an infrared aerial photo of the field taken previously.

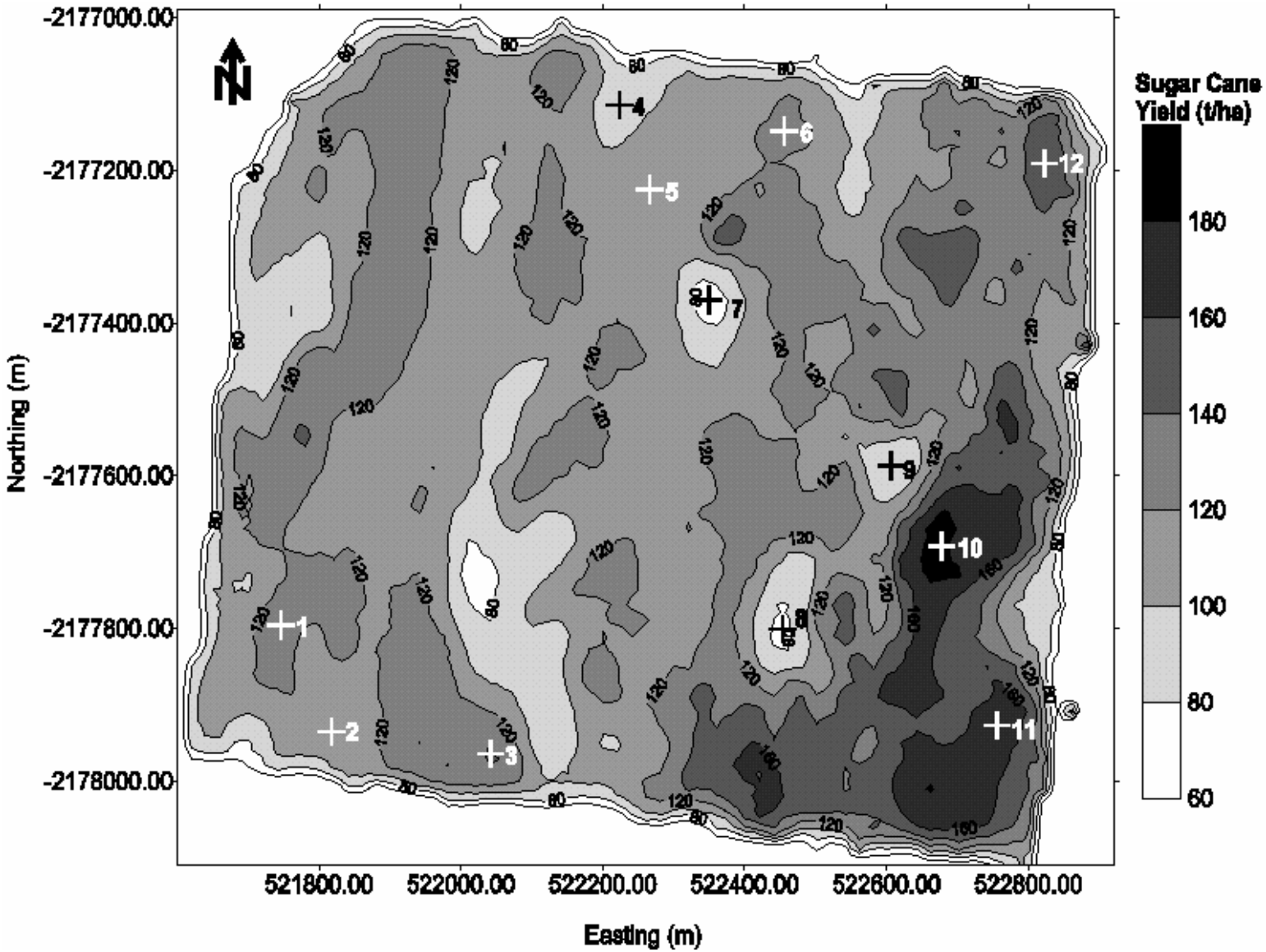

Figure 6-5. Yield map of field under study with soil sample positions marked.

Pocknee et al. (1996) defined the process of directed soil sampling as dividing a field into smaller units as required by, and based on, the patterns present within the field, and then of sampling each of these units individually. In this case the maps available to determine the 'patterns present within the field' were a yield map, a laser-levelling cut and fill map, soil survey map and infrared aerial photos of a mature crop. After examination it was believed the yield map represented the most recent and representative information. Therefore based on the yield map it was decided to choose 12 sample locations over the field. The sites were chosen to cover the full representation of the yield variation. From the yield map six different yield intervals were definable. They were 60-80 t/ha, 80-100 t/ha, 100-120 t/ha, 120-140 t/ha, 140-160 t/ha and 160-220 t/ha. Two replicate sites were selected for each yield interval, making a total of twelve sampling sites. The selected sites are shown on the yield map.

Differential GPS technology was used to navigate to the selected positions. At these sites, five samples were taken within a radius of 15 m and mixed together to give a representative sample. The sampling method involved a coring tube and a jackhammer. Samples were taken at a depth of 0-25 cm and 25-50 cm on advice from extension staff (Ham, G. pers. comm., 2 Sept 1996).

The total of 24 samples (12 sites X 2 soil depths) were dried and sent to the INCITEC soil laboratory in Brisbane. The soil samples (0-25 cm) were analysed for: Soil Colour (Munsell), Soil Texture, pH, Organic Carbon, Nitrate Nitrogen, Sulfur, Phosphorus (BSES), Phosphorus (Colwell), Potassium, Calcium, Magnesium, Sodium, Chloride, Electrical Conductivity, Copper, Zinc, Manganese, Iron and Boron. From these results the Cation Exchange Capacity, Calcium/Magnesium Ratio, ESP and Electrical Conductivity (se) were calculated. A summary of the soil analysis results is given in Appendix G.

A simple linear regression was conducted for each soil variable versus yield. For analysis purposes the yield of the sample points was taken as the median of the yield range appropriate to that point. For example, point 1 lies on the yield range 120-140 t/ha and therefore the yield is taken as 130 t/ha.

The results of the correlation analysis confirmed what was expected but also provided additional information. Of the top soil parameters analysed, sodium, chloride, electrical

conductivity, Ca/Mg Ratio and calculated electrical conductivity (se) were significantly correlated with crop yield ($F<0.01$). Magnesium and ESP were marginally correlated with yield (approx. $F=0.05$). Of these variables the best linear correlation came from sodium and calculated electrical conductivity (se) accounting for 69 % and 67 % of the variation respectively.

The strong negative correlation of yield with sodium is expected and will be discussed later. The strong negative correlation of electrical conductivity with yield is caused by the effect of sodium on electrical conductivity rather than the direct effect of electrical conductivity on yield. The high negative chloride correlation is related to the inability of the high sodic soils to leach the chloride from the topsoil. The only positive correlation with yield was found with the Ca/Mg ratio due to the positive effect of Ca on the sodic soil.

Of the subsoil variables measured, most were significantly correlated ($F<0.01$) with yield. They were: pH, sulphur, phosphorus, magnesium, sodium, electrical conductivity, CEC, ESP and Ca/Mg Ratio. The uncorrelated variables were potassium, calcium and potassium (nitric). The strong correlation of yield with most of the variables is due to the interdependence between them. This interdependence is primarily due to the weak leaching nature of the soil. The highly sodic soils allow less infiltration and therefore less leaching, resulting in higher concentrations of the measured parameters.

An interesting correlation was the negative relationship of phosphorus with yield. This could be due to a build up of residual phosphorus in lower yielding areas after seven years of uniform application. This result would indicate that variable rate application of this input could take advantage of this factor and save on input costs.

As noted above, the correlation of yield with sodium was strong, accounting for 62 % of the variation. Surprisingly the best correlation was found with magnesium, accounting for 75 % of the yield variation.

The high sodium content of these soils is not believed to be toxic to cane plants. Instead, the effect on yield is manifested through deterioration of soil structure. Increasing levels of Exchangeable Sodium Percentage (ESP) cause clay particles to disperse when the soil is wet. This is associated with sealing and crusting of surface soils, and dense subsoil clays that resist penetration by roots. Even if water does penetrate the surface the water is held strongly in very small pores formed in the dispersed soil making it difficult for roots to withdraw this water and the end result of sodicity is water stress. Both water infiltration and water storage in the soil are reduced. When a sodic soil is wet, the clay is dispersed and has a very low

bearing capacity. When dry, sodic soils are very hard and poorly structured.

Figure 6-6 shows the sodium and magnesium levels (top and subsoil average) plotted against the crop yield. Although sodium has a strong overall negative correlation to yield, the relationship is not as linear or obvious as expected. Below a yield of 130 t/ha the relationship is pronounced, but above 130 t/ha there seemed to be little or no reduction in sodium for a large increase in yield. This raised the question as to what is causing the 70 t/ha reduction from 200 t/ha down to 130 t/ha when sodium seems to be relatively constant. At this point the effect of magnesium was examined more closely.

At the higher yield levels the relationship of yield with magnesium was very pronounced (Figure 6-6). The water content for dispersion of a magnesium-sodium soil is only about half that of calcium-sodium soil (Bakker and Emerson, 1973). This is also supported by Ellis and Cardwell (1935) who note that magnesium as opposed to calcium may promote the dispersion of clay from a soil. The combination of magnesium with the sodium is likely to magnify the adverse soil properties that lead to a reduced yield. In fact, Bakker and Emerson (1973) state that 'it is clearly inadequate, when attempting to define a sodium affected soil, to use ESP (exchangeable sodium percentage) as the only criterion. However, to give equal weight to sodium and magnesium does not seem justified'. In Figure 6-6 it is assumed that magnesium is only 'half as bad' as sodium and therefore when plotted together, magnesium is weighted as half it's actual soil proportion i.e. (0.5 Mg + Na). The linear correlation of this quantity with yield is notable, having an R^2 of 0.96.

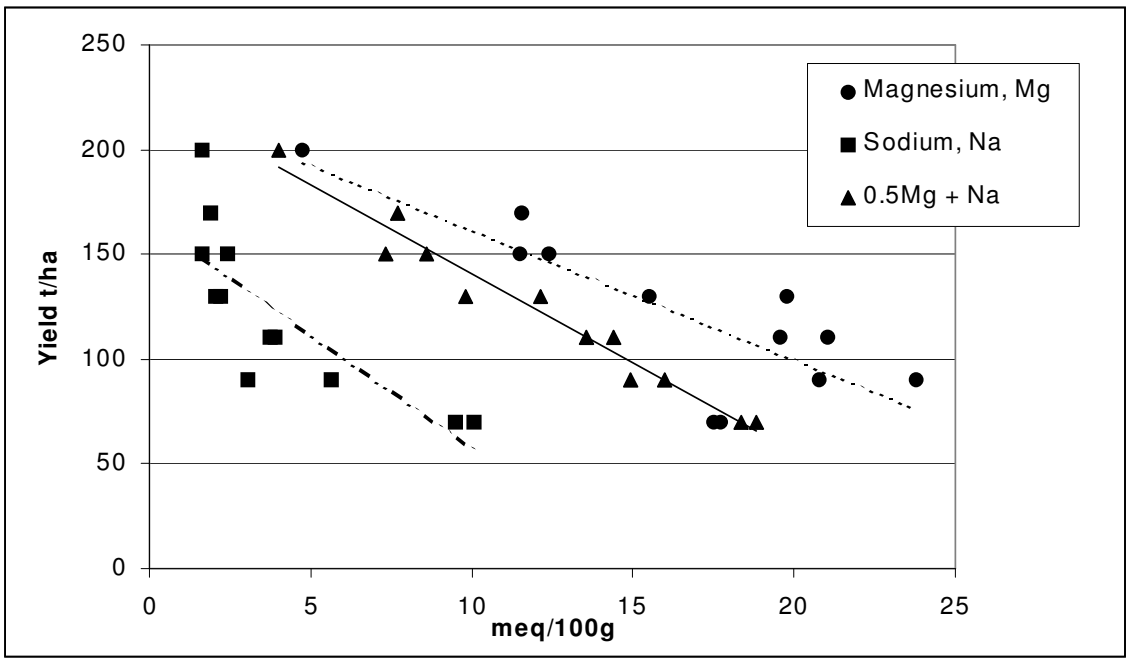

Figure 6-6. Linear correlation of crop yield with magnesium (Mg), sodium (Na) and a combination of magnesium and sodium (0.5Mg + Na).

Table 6-2. Correlation results between yield, magnesium and sodium.

Variable	Gradient, m ((t/ha)/(meq/100g))	Intercept, c (t/ha)	R^2
Magnesium, Mg	-6.1496	222.87	0.68
Sodium, Na	-10.921	165.93	0.64
Combination 0.5 Mg + Na	-8.4557	225.13	0.96

Another important point that this work revealed is the futility of using random soil samples when making input recommendations at the block level. If soil sampling were conducted randomly across this field in an attempt to gauge the level of sodicity, the resultant data would be pointless due to the randomness of the soil parameters that would result. Even if numerous samples were mixed together there is no guarantee that a representative sample would be achieved. Therefore, that individual or mixed soil samples should not be used to make blanket field recommendation for crop inputs. This may be a reason for the general distrust by farmers of soil analysis results. The use of yield maps can greatly improve sampling strategies and in doing so provide a great deal more agronomic information on which to base recommendations, even at the field scale.

6.4 Variable Rate Application

The soil analysis results have shown a clear negative relationship between the sodium and magnesium content of the soil and crop yield. Now this relationship can be used to develop a prescription for the field.

Sodic soils are probably the most expensive soils to reclaim. To reclaim the soil, sodium must be leached away and replaced with calcium. To do this, subsurface drainage is necessary to allow sodium to leach from the soil. Gypsum is applied at rates of up to 25 t/ha and is used as a calcium source. The next step is to rip with a tine ripper to open the soil without turning it over. These actions will allow water to move through the soil, removing sodium and replacing it with calcium.

The current technique for gypsum application is the use of a ten tonne spreading truck fitted with hydraulically driven rate control. A variable rate controller was purchased to automatically control the gypsum rate as defined by an application map. The application map was exactly the same as the yield map given in Figure 6-5, except that the legend was adjusted to represent the gypsum requirements. These requirements were calculated using the prescription equation defined in Figure 6-7. This equation was developed by defining the two endpoints. These were, 20 t/ha of gypsum for the worst areas yielding 70 t/ha and no gypsum (0 t/ha) for the best areas yielding 190 t/ha. Between these points the prescription rate was assumed to be linear. This prescription is not based on any scientific facts except that these are the usual rates specified for blanket applications.

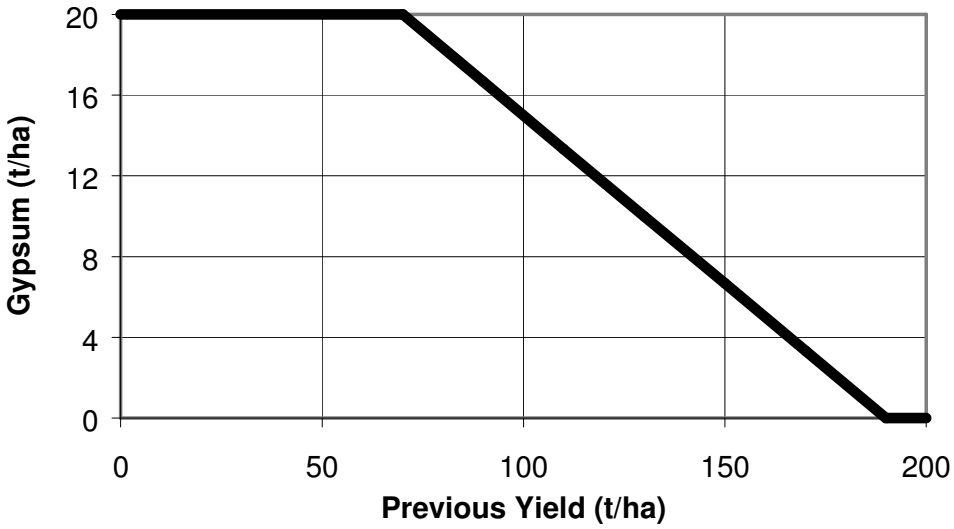

Figure 6-7. Recommendation equation for gypsum application

6.4.1 Economics

At the normal application rate of 10 t/ha, gypsum application costs $1000/ha, and is therefore a high cost input. This offers the possibility for substantial economic benefit if the gypsum application rate can be controlled according to needs. By reducing the amount of gypsum required, input costs will be reduced, while optimum placement of gypsum will increase production.

For this economic analysis, the economic return is calculated for gypsum being applied at an optimum rather than a blanket rate. Three scenarios are compared, and the cost of each is calculated as the cost of the crop input (gypsum) and the cost of lost production if insufficient input is applied. These scenarios are:

1. Precision agriculture optimised gypsum distribution so that the correct amount of gypsum is applied in each area. There is no production lost and there is no over application cost.
2. Application of gypsum with a blanket distribution at the maximum recommended rate of 20 t/ha. This results in no production loss but there is an over application cost on most of the field.
3. Application of the same total amount of gypsum as the precision agriculture optimised Scenario 1 except as a blanket application over the field. The input cost is the same as for the Scenario 1 but there are production losses as some areas are under applied.

A number of assumptions were made in the analysis. Firstly, it was assumed that the prescription equation given in Figure 6-7 is optimal. That is, if gypsum is applied at a greater rate than given by the prescription then it is wasted. Also if the gypsum is applied at a rate less than the prescription, then loss in production results. The rate of production loss is assumed to be 2.5 tonne of cane per year per tonne/ha of gypsum not applied. This figure is calculated from measured yield increases of 25 t/ha for gypsum application rates of 10 t/ha (Ham, 1986). For these calculations it has been assumed that one gypsum application is sufficient for one cane crop cycle of 5 years. Therefore every 1 t/ha of gypsum under-applied results in 12.5 t/ha of lost cane production over the 5 years. With the price of sugar cane at $30/t, this implies a total loss in returns of $375/ha over the 5 years.

The yield distribution used for the calculations is shown in Figure 6-8 and comes directly from the yield map in Figure 6-5. The shape of this distribution determines how much gypsum is applied under Scenario 1. It also determines how much gypsum is over applied in Scenario 2 and how much lost production results from Scenario 3. The flatter the distribution (higher variability) the greater the advantage of adopting precision agriculture.

The total cost of implementing precision agriculture was calculated as $5829 ($49.82/ha). This figure is calculated in Table 6-3 and takes into account all costs associated with precision agriculture including yield mapping, soil sampling and variable rate application. The costing assumptions are quite conservative and even if this figure was doubled it would not affect the outcome of the analysis substantially.

Table 6-3. Cost associated with application of precision agriculture to the field under study.

Item		Cost ($/ha)	Cost ($ for 117ha field)
Cost of yield mapping			
Capital Cost			
Yield monitor, $8 000 at 200ha per year over 5 years*		8.00	936.00
DGPS $4000 at 200ha per year over 5 years*		4.00	468.00
Beacon Differential Correction		0	0
Mapping Cost		6.00	702.00
	Total	18.00	2106.00
Cost of soil sampling			
Sampling Cost			
DGPS already purchased		0	0
Soil coring hardware $4000 at 200ha per year over 5 years*		4.00	468.00
Labour 2 men x 1 days labour x $150		-	300.00
Soil analysis 24 samples x $50		-	1200.00
Data analysis and prescription map Generation		10.00	1170.00
	Total	-	3138.00
Cost of variable rate application			
Capital Cost			
VRT controller $5000 at 200 ha per year over 5 years*		5.00	585.00
DGPS Already purchased		0	0
	Total	5.00	585.00
	Overall Total	$49.82	$5829.00

* Note: Assumes hardware is used for remediation of 200ha per year for 5 years before obsolescence, which is quite feasible for a large farm or cooperative.

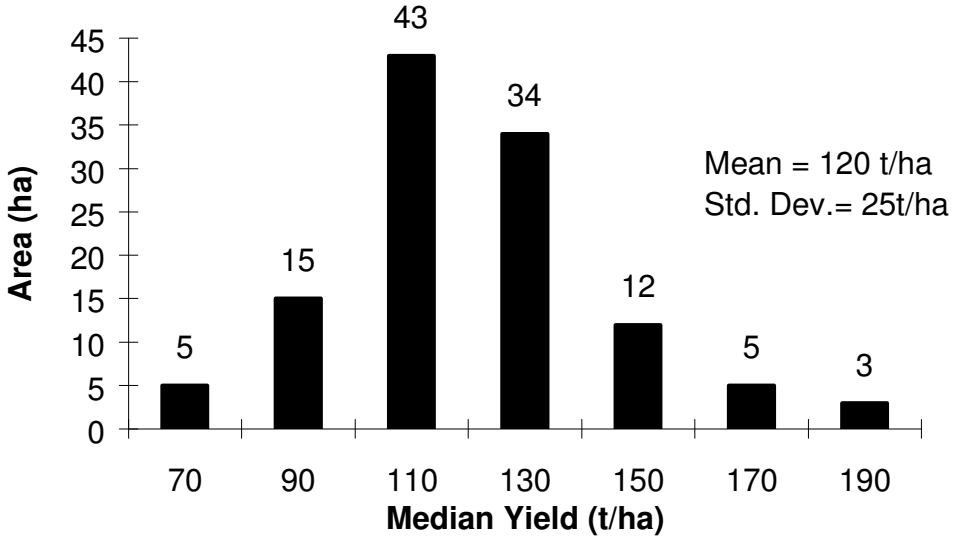

Figure 6-8. Histogram of crop yield for the field under study.

The outcomes of the calculations for the three scenarios are shown in Figure 6-9. The total cost of Scenario 1 over the field was $141,829 ($1212/ha). Scenario 2 (20 t/ha blanket application) resulted in $234,000 ($2000/ha) total cost. In Scenario 1 a total of 1360 t was applied, which when spread evenly over the 117 ha field is equivalent to 11.62 t/ha. Scenario 3 therefore involved 11.62 t/ha blanket application and its cost totalled $207,656 ($1775/ha). These results clearly show the benefit of precision agriculture, with Scenario 1 showing an improvement of $92,171 ($788/ha) over Scenario 2 and a $65,827 ($563/ha) improvement over 11.62 t/ha blanket in Scenario 3. These savings are measured over 5 years.

This is however, a very simple analysis that incorporates several assumptions. Field trials need to be conducted to develop a better recommendation equation and crop response curve. A more accurate assessment of these factors would result in a much more reliable and robust economic analysis. However, with the information that is available this economic analysis provides a reasonable estimate of the benefits of precision agriculture in this situation. This form of information could be applied to any crop situation to gauge the potential savings. The main variables are the level of variability, the cost of the input and the value of the crop. If all of these variables are high then significant savings are possible with precision agriculture.

A limitation of this simplistic analysis is that it assumes yield response will be constant from year to year. Work by a number of researchers including Lark *et al.* (1999) and Moore and

Tyndale-Biscoe (1999) show that climate variability can greatly influence the potential gains. These studies have been undertaken in rain feed crops where rainfall difference from year to year can significantly affect yield. However in the fully irrigated case study given here, rainfall variability is less significant and the simplistic analysis presented is still useful.

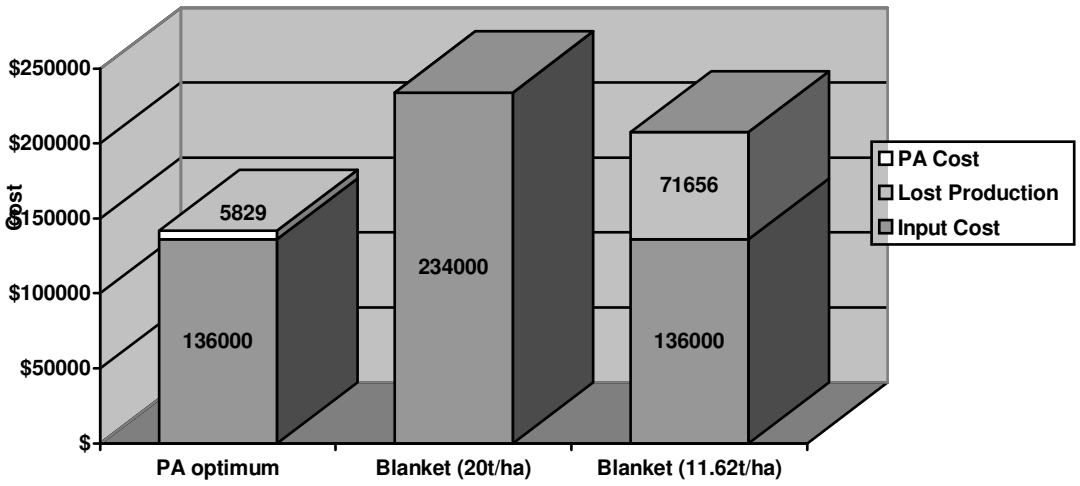

Figure 6-9. A cost comparison of various of application scenarios over 5 years for the field under study.

6.5 Conclusions

A case study was carried out to assess the potential for applying precision agriculture principles to sugar cane. A field was selected and various precision agriculture techniques applied to it. Firstly yield mapping was conducted. This involved developing the first yield mapping system for sugar cane that operated for two seasons with positive results. The resultant yield map of the field under study displayed significant yield variation from 70t/ha to over 190 t/ha. Soil sampling was then conducted to determine the cause of the yield variation. Linear correlation analysis of soil parameters against yield found results, which confirmed what was suspected. High sodium levels in the soil were producing a soil with poor structure, which minimises water infiltration and storage. Magnesium played a significant part in the problem and exacerbating the effect of sodium. Based on these results variable rate gypsum application has been conducted. Economic analysis of the situation has shown benefits resulting from precision agriculture of at least $563/ha over five years when compared with standard management of blanket input application.

This chapter has demonstrated the importance of yield mapping for the application of precision agriculture to sugar cane. Although the mass flow rate sensing techniques used have limitations, useful yield maps were produced. This indicates that the desired accuracy goal set previously may not have to be achieved to produce useful yield maps. The field trials of Chapter 5 showed that the weigh pad offers significant potential for measuring mass flow rate. The next chapter begins a detailed analysis of the sensor with the aim of overcoming limitations and improving its accuracy and reliability.

Chapter 7 - Dynamic Response of the Weigh Pad Sensor

7.1 Introduction

The preliminary field trials on the weigh pad sensor given in Chapter 5 showed that the dynamic environment of the harvester induced substantial noise in the sensor measurement. This dynamic environment has numerous sources including low frequency components caused by the travel of the harvester across a field and higher frequency components caused by mechanical components of the harvester such as the harvester engine, hydraulic motors, rotating shafts and gears, moving chains etc. These sources produce negative and positive accelerations on the structure of the weigh pad. The result of these accelerations is fluctuating forces on the load cell. This makes it difficult to accurately measure the mass of sugar cane on the weigh pad.

This chapter examines this problem by modelling the weigh pad's dynamic response and conducting laboratory trials to support the theory. The outcome is an optimised sensor design based on the understanding of the impact of dynamic conditions. Field trials were then conducted on this optimised weigh pad design. The results indicate that measurement error due to the harvester dynamic environment can be reduced to acceptable levels.

7.2 Nature Of The Problem

The significance of dynamics on the weigh pad sensor is shown in Figure 7-1. This graph shows weigh pad output signal from the preliminary trials (see Chapter 5). The

measurements were taken during no cane flow (i.e. harvester operating all functions but no cane being harvested). The variation in the signal is due entirely to the mechanical noise, in and around the weigh pad structure. The raw data were collected at 100 Hz. Analysis of this raw data shows a standard deviation of 0.81 kg. When compared to typical harvesting flow rates of 25 kg/s (theoretical load cell reading of 1.125 kg, due to cane), this would result in errors of 144 %, 2 sigma ((2 x 0.81)/1.125). Filtering the data with a simple one second moving average reduced the standard deviation of the readings to 0.15 kg but this still resulted in an equivalent error of 27 %, 2 sigma, ((2 x 0.15)/1.125).

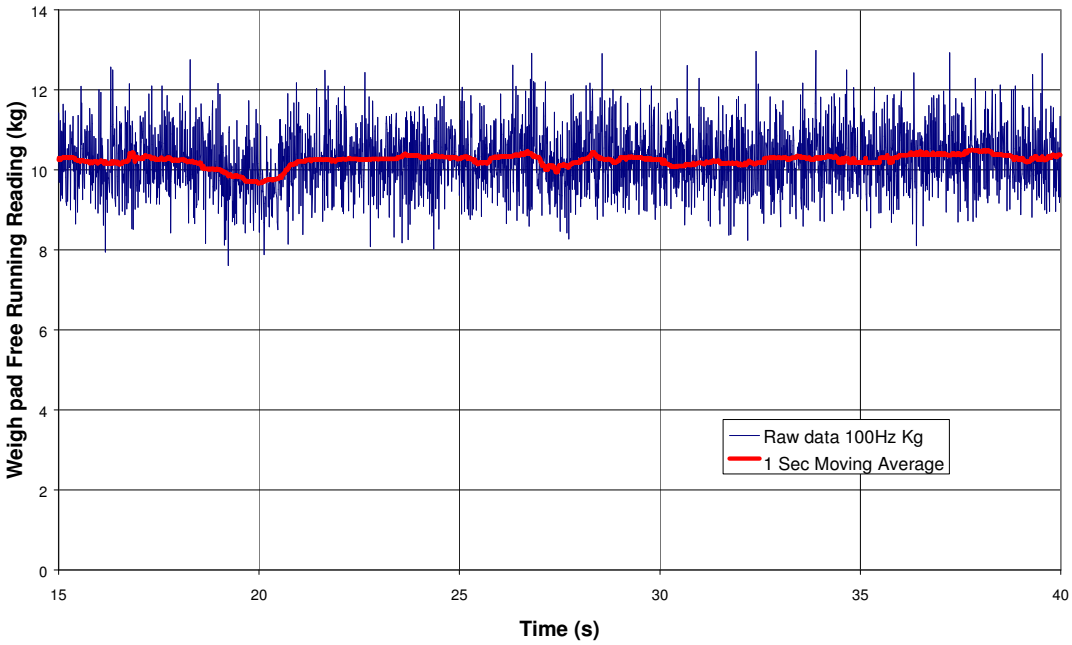

Figure 7-1. Raw weigh pad signal under zero cane flow conditions (free running) along with the filtered equivalent.

Figure 7-2 shows similar data to Figure 7-1 but also shows sensor output during normal cane flow conditions. The average sugar cane flow rate in the first half of the graph is approximately 35 kg/s. This equates to an average load cell measurement, due to cane, of 1.575 kg. The standard deviation of the noise is again 0.81 kg. Therefore the instantaneous error is 103 %, 2 sigma, ((2 x 0.81)/1.575).

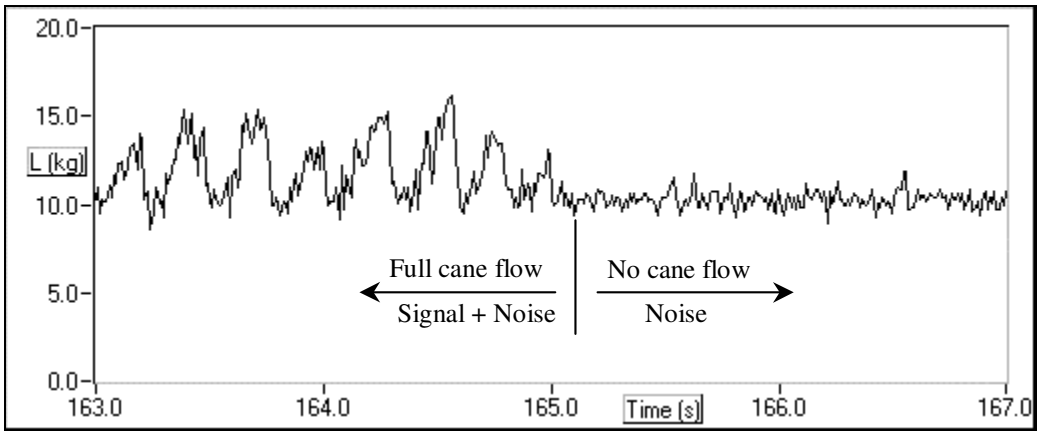

Figure 7-2. Weigh pad signal displaying the noise superimposed on the mass flow rate signal.

These results show that mechanical noise does have a large impact on the instantaneous accuracy of the weigh pad sensor. This high error allows significant room for improvement hence the aim of the analysis described in this chapter is to reduce this error to an acceptable level. Filtering the data appears to significantly reduce error and this relationship is examined further in this chapter.

7.3 Theory

The weigh pad sensor's reaction to vibrations can be modelled using three theoretical assumptions, defined here as:

- the acceleration-error relationship,
- the acceleration characteristics and
- the error-time relationship.

7.3.1 Acceleration-Error relationship

The free body diagram given in Figure 7-3 can explain the effect of weighing in a dynamic situation. The force acting on the load cell is due to a combination of the mass of cane and the weigh plate mass. Under stationary conditions the acceleration on the parts is 1g and the force on the load cell is equivalent to the weight of both parts. Assuming the acceleration is 1g and knowing the mass of the weigh plate, the mass of cane can easily be calculated. This

is the typical operation of scales where the mass of the weigh structure is 'tared off' the reading before measurements are made and a force measurements is converted to mass measurement assuming an acceleration of 1 g. However, under dynamic conditions, the acceleration on the objects varies from the usual 1 g. This change in acceleration creates a different force on the load cell. This variation in force is the source of the weighing error and from Figure 7-3 is related to both the mass of the weigh plate and the mass of cane. From this simple model we can develop an equation that describes the magnitude of error resulting from dynamic accelerations. This relationship is developed below and shown in Equation 7.1.

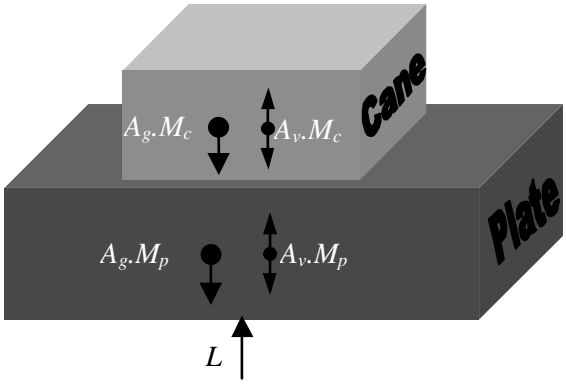

where L is the load cell reaction [N];
A_g is the acceleration due to gravity [g];
A_v is the acceleration due to vibration [g];
M_c is the mass of cane [kg]; and
M_p is the mass of the weigh plate [kg].

Figure 7-3. Free body diagram of weigh pad system.

From the free body diagram:

$$\begin{aligned} L &= A_g.M_p + A_v.M_p + A_g.M_c + A_v.M_c \\ &= A_g(M_p + M_c) + A_v(M_p + M_c) \end{aligned}$$

The error due to the dynamic load on the load cell is the above equation minus the force of the actual mass under gravity:

$$\begin{aligned} Error\ (\mathrm{N}) &= L - (M_p + M_c).A_g \\ &= (M_p + M_c).A_g + A_v(M_p + M_c) - (M_p + M_c).A_g \\ &= A_v(M_p + M_c) \end{aligned}$$

Therefore the error as a percentage of the measurand, M_c is:

$$\text{Error } (\%) = \frac{A_v (M_p + M_c)}{M_c . A_g} \quad 100 \qquad \textbf{(Equation 7.1)}$$

This equation requires two assumptions to be correct. These are:

- The cane mass acts as a homogeneous lump.
- The cane mass is always in contact with pad and never airborne.

When these assumptions are true the acceleration exerted on the cane and the plate is the same. While these assumptions may not be totally correct they are suitable approximations to produce a simple model.

This equation also does not take into account the slope of the weigh pad. For the bench testing given in Section 7.4 the weigh pad was horizontal so this is approroriate.

7.3.2 Acceleration Characteristics

The nature of the accelerations exerted on the weigh pad can be defined by three assumptions.

Assumption 1*: The integral of the accelerations due to vibration, A_v, over an infinite time interval is zero.*

Written mathematically as:

$$\int_{t=0}^{t \to \infty} A_v(t) \mathrm{d}t = 0$$

This assumption can be developed by the following mathematics:

The movement of the weigh pad in the vertical direction (z) over an extended time period is zero. That is:

$$\Delta z = 0$$

$$\therefore \frac{dz}{dt} = 0$$

$$\therefore \frac{dz^2}{dt^2} = 0$$

Hence the net vertical acceleration due to vibration over an extended period of time is zero. This means the positive and negative accelerations cancel each other out over time. The implication of this assumption is extremely important for the accuracy of the weigh pad sensor. It means the effect of the dynamic accelerations becomes a less and less significant source of error as the measurement time increases. If applied to Equation 7.1, when *Av* is zero then error (%) is also zero.

The next assumption shows that an infinite period of time is not required to reduce the error to an acceptable level.

Assumption 2: *The distribution of the accelerations due to vibration, A_v, about the mean of zero can be assumed to be random with a normal distribution (Gaussian).*

This assumption can be supported by analysis of acceleration measurements taken on the elevator of a harvester (see Figure 7-4). These measurements were acquired with a piezoelectric accelerometer at 2000 Hz on an Austoft 7000 harvester, while running the harvester at normal engine operating speed with all functions running such as the elevator. The harvester was stationary throughout the sample time. It is obvious that significant accelerations are present, at times exceeding 10 g. Figure 7-5 shows the frequency spectrum of this data which indicates the accelerations are spread across a wide range of frequencies and therefore literally random.

Figure 7-6 shows the Gaussian distribution of the acceleration data. It has a mean very close to zero of 0.3 g and a standard deviation of 2 g. Analysis of measurements taken on another harvester (Cameco manufacturer) have given similar results with a larger standard deviation of 3.5 g. The mean of 0.3 g is significantly different to zero but expected as the sample time was only 2.5 seconds. This agrees with Assumption 1 that indicates that the mean will tend towards zero as the sample time increases.

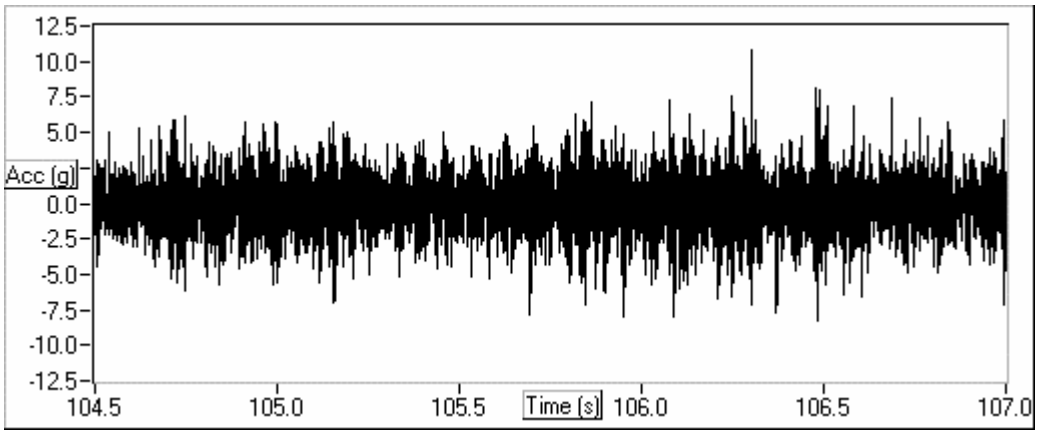

Figure 7-4. Acceleration measurements taken on the Elevator of a sugar cane harvester.

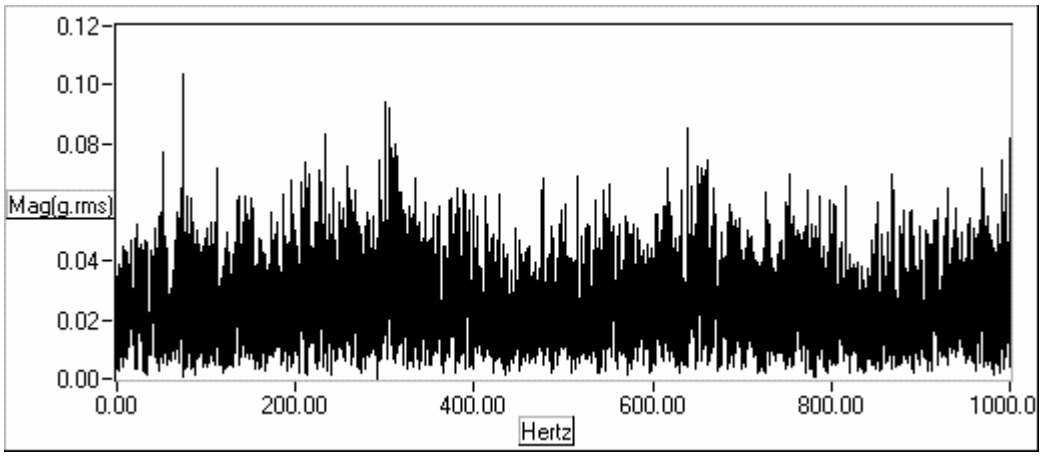

Figure 7-5. Frequency Spectrum of the acceleration data.

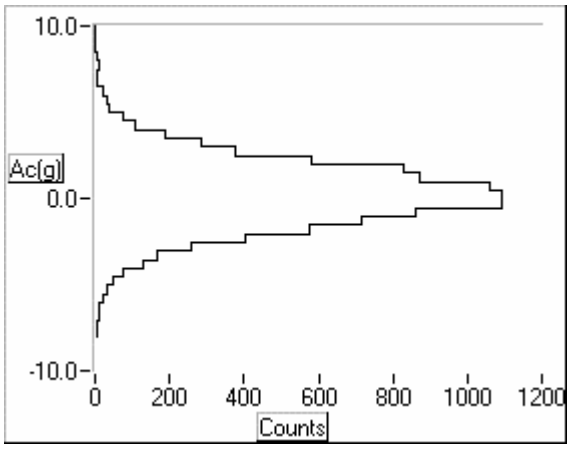

Figure 7-6. Histogram of acceleration data showing a mean of 0.3 g and a standard deviation of 2.0 g.

7.3.3 Acceleration-Time relationship

Following on from the previous set of assumptions a relationship between accelerations and averaging time can by developed. Due to the Gaussian nature of the accelerations there is a simple relationship between the standard deviation of all accelerations and the mean acceleration of a subsample.

Any elementary statistics text (for example Freund, 1992, p294) states a theory about the *sampling distribution of the mean*. This theory states that the mean of a random sample of a population is equal to the mean of the population with a sampling error of:

$$\sigma_x = \frac{\sigma}{\sqrt{n}} \qquad \textbf{(Equation 7.2)}$$

where σ_x is the standard error of the mean

σ is the standard deviation of the population;

n is the sample size.

This equation shows that the standard deviation of the distribution of the sample mean decreases when, n, the sample size, is increased. This means that when n becomes larger the expected values of the sample mean are closer to the population mean.

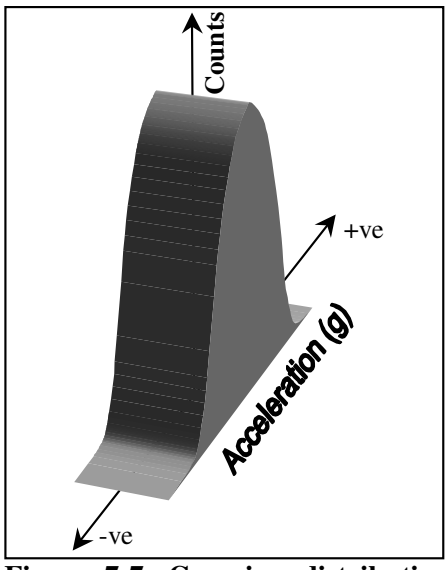

Figure 7-7. Gaussian distribution of the total population of accelerations due to vibrations.

To put this in the context of the weigh pad, if the entire population of the accelerations due to

vibrations are sampled (from time, t = 0 to t = ∞) the mean will be 0 g. However if a smaller proportion of this population is sampled then the calculated mean will be close to the mean of the population, but contain some sampling error. This sampling error represents the net acceleration exerted on the weigh pad sensor over the sampling period. The relationship between sampling error and the sample size is given in Equation 7.3 and shown graphically in Figure 7-8.

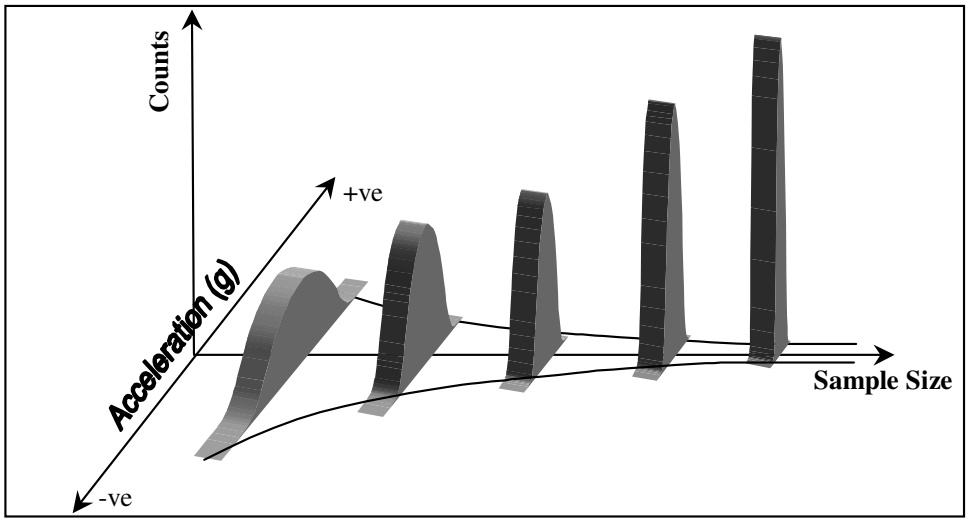

Figure 7-8. Relationship between acceleration distribution and sample size.

$$A_v = \frac{K}{\sqrt{t_s}} \qquad \textbf{(Equation 7.3)}$$

where A_v is the acceleration due to vibration [g];
K is the standard error of the mean of A_v for a sample time of 1 sec [g.t $^{1/2}$];
t_s is the sample time [s].

For the data shown in Figure 7-4, K can be calculated as:

$$\begin{aligned} K &= \sigma(A_v)\sqrt{t_s} \\ &= 3.5g\sqrt{\frac{1}{2000\text{Hz}}} \\ &= 0.078\ \text{g.t}^{1/2} \end{aligned}$$

This value would be different for each harvester and affected by the condition of the vibration sources on the harvester such as engine, fans, chains and sprockets. It may also be

significantly larger for tracked machines compared to rubber wheeled machines. Also this value could be affected by paddock conditions (i.e. rougher paddock gives higher accelerations). For the purpose of this analysis this value of K = 0.078 g.t $^{1/2}$ will be used as the typical value for the magnitude of the accelerations exerted on the weigh pad.

7.3.4 Mathematical Model

From the theoretical assumptions stated above the following relationship between standard error SE [%], average time and mass applied can be defined as:

$$\mathrm{SE}\,(\%) = \frac{K}{\sqrt{t_s}} \cdot \frac{(M_c + M_p)}{M_c} 100$$

(Equation 7.4)

This equation shows there are some different ways to reduce the error of the sensor. These are:

1. Minimise K by introducing dampening into the sensor system (e.g. shock absorbers)
2. Minimise the mass of the weigh pad, M_p
3. Increase the sample time, t_s. This option is limited by the spatial resolution desired for the yield maps. Over the target area of 100m^2 at a normal operating speed of 8 kph and a row width of 1.5 m this leaves 30s for averaging measurements.

7.4 Bench Testing

7.4.1 Materials and Method

Laboratory bench tests were conducted to test the theory developed in the previous section. The apparatus used for these experiments is shown in Figure 7-9. Each of the items displayed is now described.

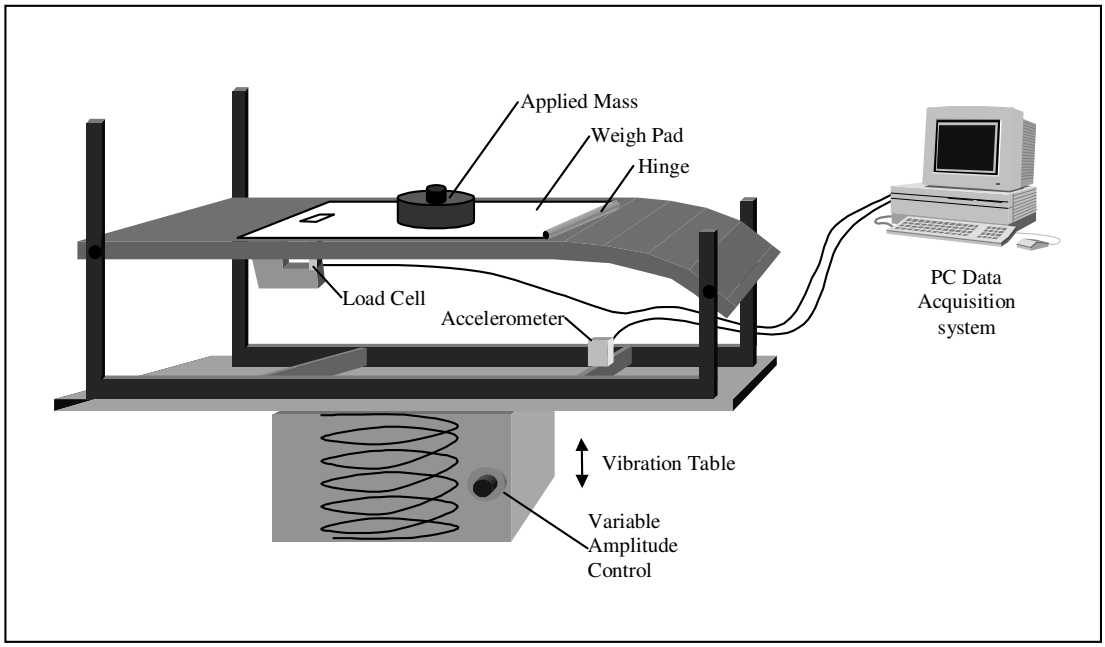

Figure 7-9. Apparatus for vibration bench testing of the weigh pad.

To simulate vibration, the weigh pad was mounted on a vibration table. The table's usual purpose was to agitate concrete samples for civil engineering experiments, however it possessed the necessary features to carry out the weigh pad testing. The table consisted of an electromagnetic coil driving a steel platform on which test objects could be placed. The coil produced accelerations in the vertical direction with a fixed frequency of approximately 50 Hz and with adjustable amplitude of between ±3 g and ±5 g. An external knob controlled the amplitude.

The weigh pad was mounted securely on the vibration table with a specially designed frame (see Appendix C). To prevent the amplification of the acceleration forces from the table to the weigh pad, the frame was significantly over designed to maximise its natural frequency well above the 50 Hz driving frequency. The weigh pad design that was examined during the bench testing is displayed in Figure 7-10. The weigh plate, suspended outer section and elevator flooring were all made out of 4 mm plate mild steel. The outer section was suspended from the elevator flooring by the six isolation mounts. These mounts were designed to dampen the vibration occurring on the elevator flooring and therefore reduce the accelerations that occur at the weigh plate/ load cell. The dimensions of the weigh plate were 700 mm by 300 mm. The load cell was a piezoelectric type. This load cell type was chosen as it has a very high natural frequency and fast response time, which allowed the frequency response effects of the load cell to be removed from the testing to focus on the weigh pad response.

The accelerometer was mounted securely on the support frame to measure the accelerations produced by the vibration table. The accelerometer was also a piezoelectric type with a ±50 g measurement range.

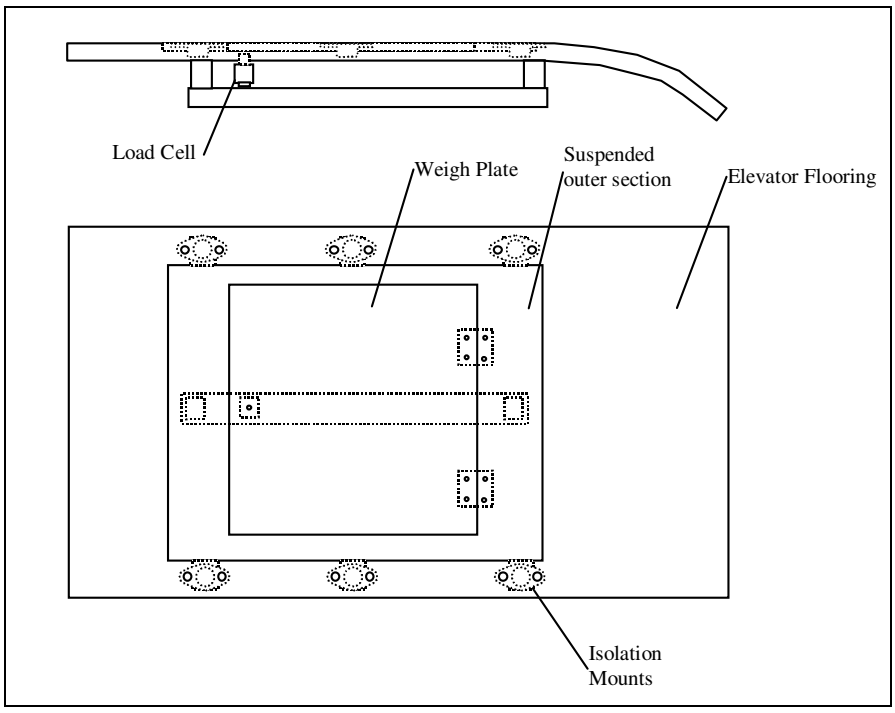

Figure 7-10. Weigh pad design examined in bench tests.

The data acquisition system was comprised of a Windows based personal computer with a National Instruments 12 bit data acquisition card. The data acquisition software was written in Labview® and acquired the load cell and accelerometer signals at an acquisition rate of 500 Hz and logged them to a file for later analysis.

The experiments were designed to test the vibration/error relationship described in Equation 7.4. The variables in this equation are acceleration amplitude, *Ac*, mass of cane, *Mc* and mass of pad, *Mp*. During the experiment the acceleration amplitude was varied from ±3 g to ±5 g in 5 steps. The mass of cane, Mc, was simulated by steel weights bolted to the centre of the weigh pad. The weights applied altered from 0 to 10 kg in 2 kg steps. A random experiment was designed by selecting one of the five acceleration settings randomly then conducting the experimental runs with the six different cane weights conducted randomly. Then the next acceleration setting was selected randomly and the procedure repeated until all five

acceleration settings were tested. In all, this resulted in 30 runs that were each carried out for 2 minutes and saved to a computer file.

The bench testing was designed to be carried out in controlled conditions, removing some of the complexities and variables that affect the sensor operation in the field. It was decided to use steel weights bolted to the centre of the weigh pad to simulate sugar cane, thus removing the complexity of sugar cane flow while retaining the effect of varying sample masses.

7.4.2 Results

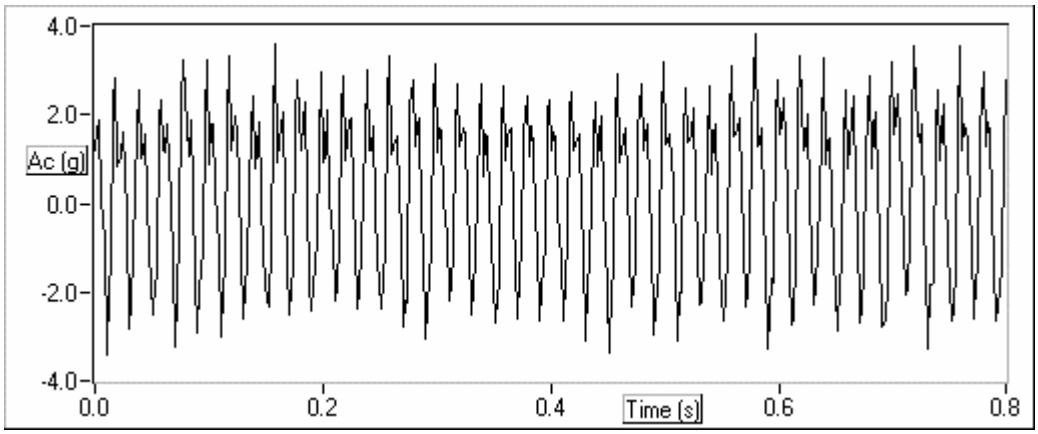

Figure 7-11. Typical accelerometer measurements on the weigh pad during testing.

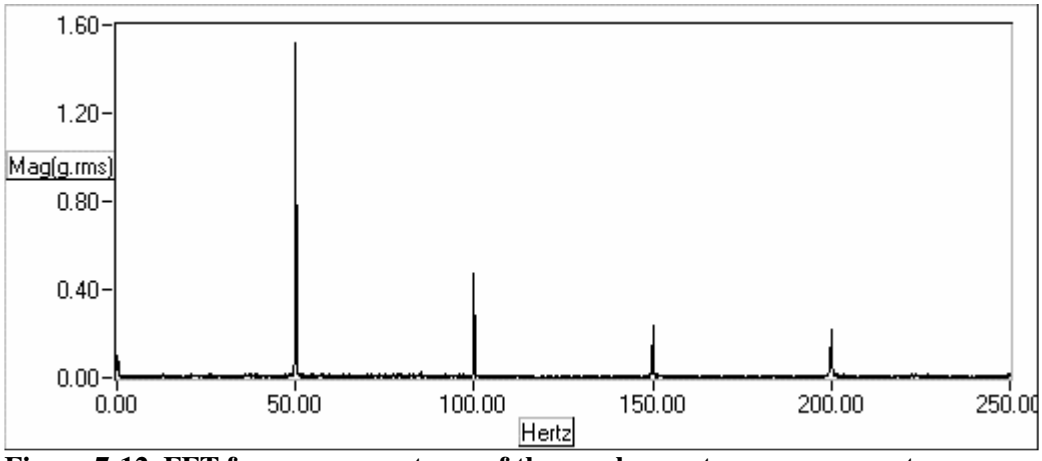

Figure 7-12. FFT frequency spectrum of the accelerometer measurements.

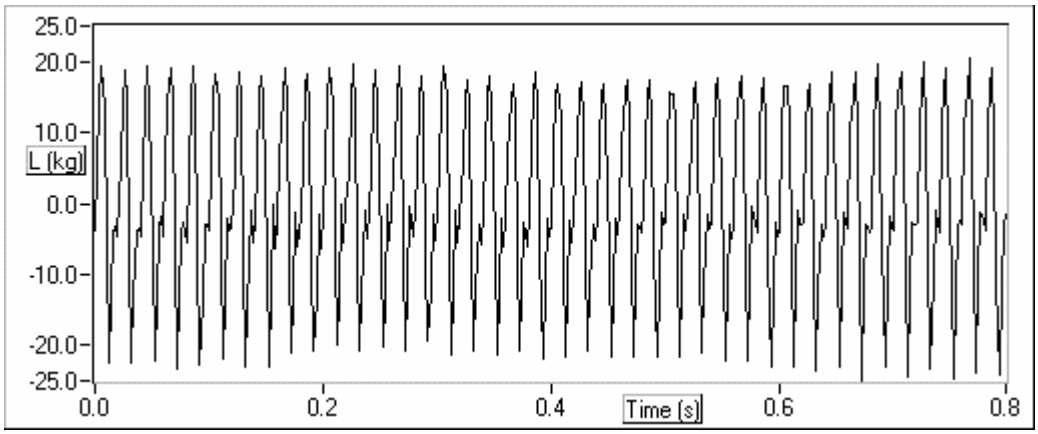

Figure 7-13. Typical load cell measurements on the weigh pad during testing.

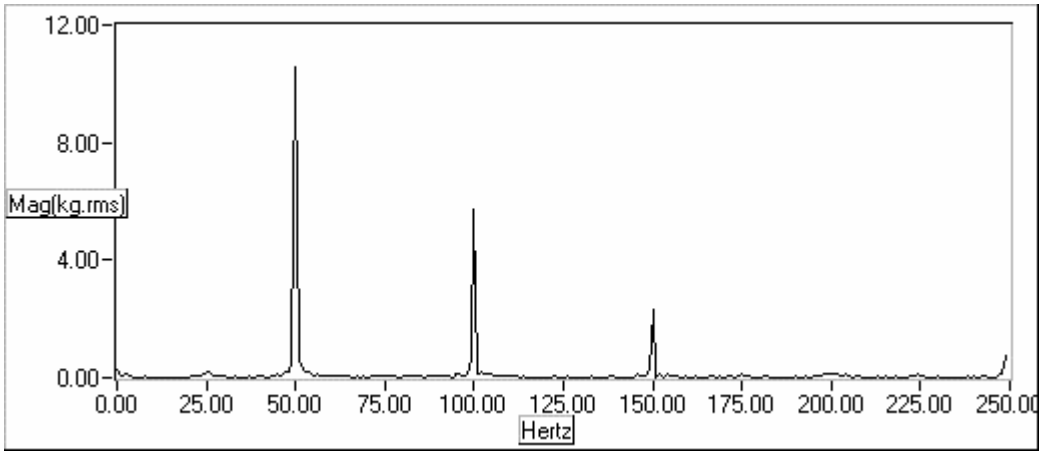

Figure 7-14. FFT frequency spectrum of the load cell measurements.

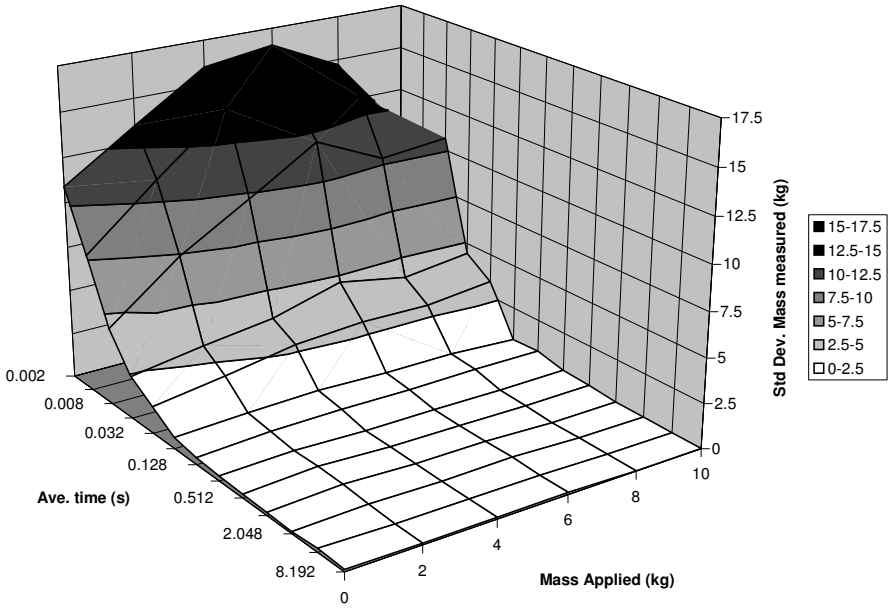

Figure 7-15. Results of bench test for lowest acceleration setting.

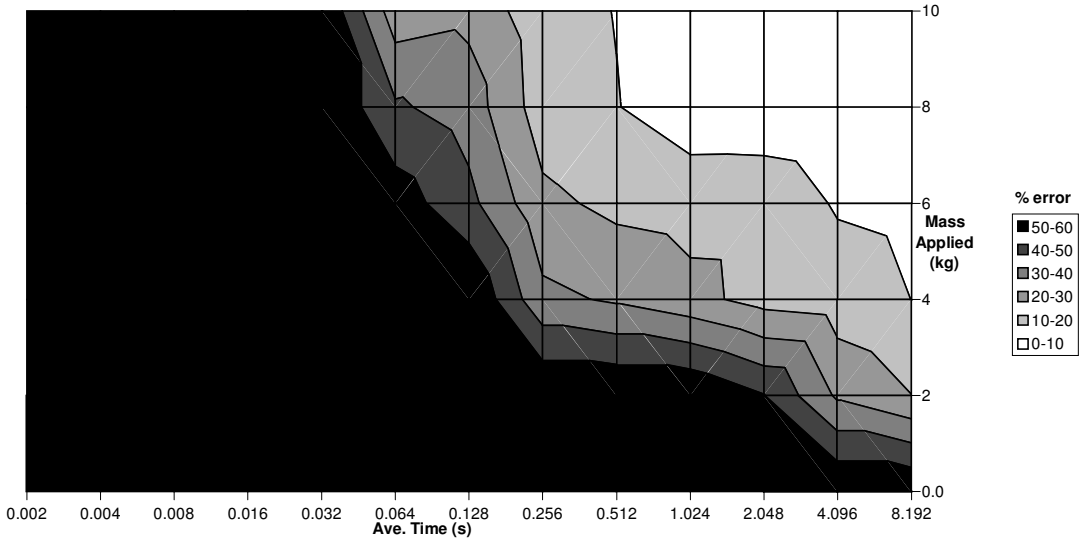

Figure 7-16. Experimental relationship between average time, the mass applied and percent error in measurement for lowest acceleration setting.

Percent Error, E [%],calculated as:

$$E = \frac{2S}{\frac{1}{2}\mathrm{M_a}} \cdot 100 \qquad \textbf{(Equation 7.5)}$$

where S is the standard deviation of the mass measured [kg]; and
M_a is the mass applied [kg].

Note: In Equation 7.5 M_a is multiplied by ½ due to the hinged weigh pad design which results in only half the mass applied is actually measured by the load cell.

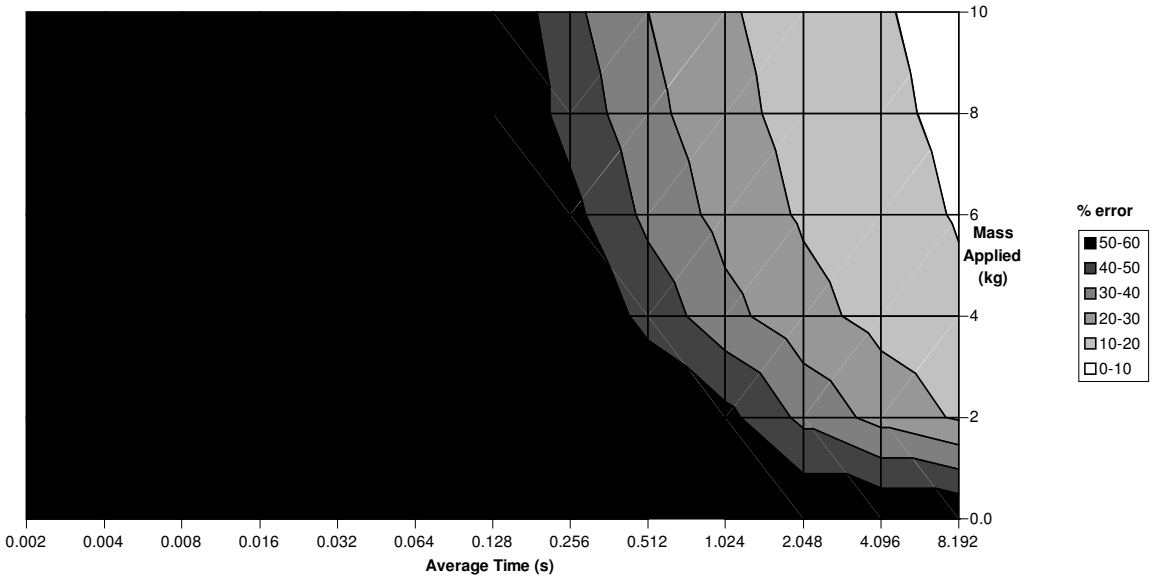

Figure 7-17. Modelled relationship between average time, the mass applied and percent error in measurement for lowest acceleration setting.

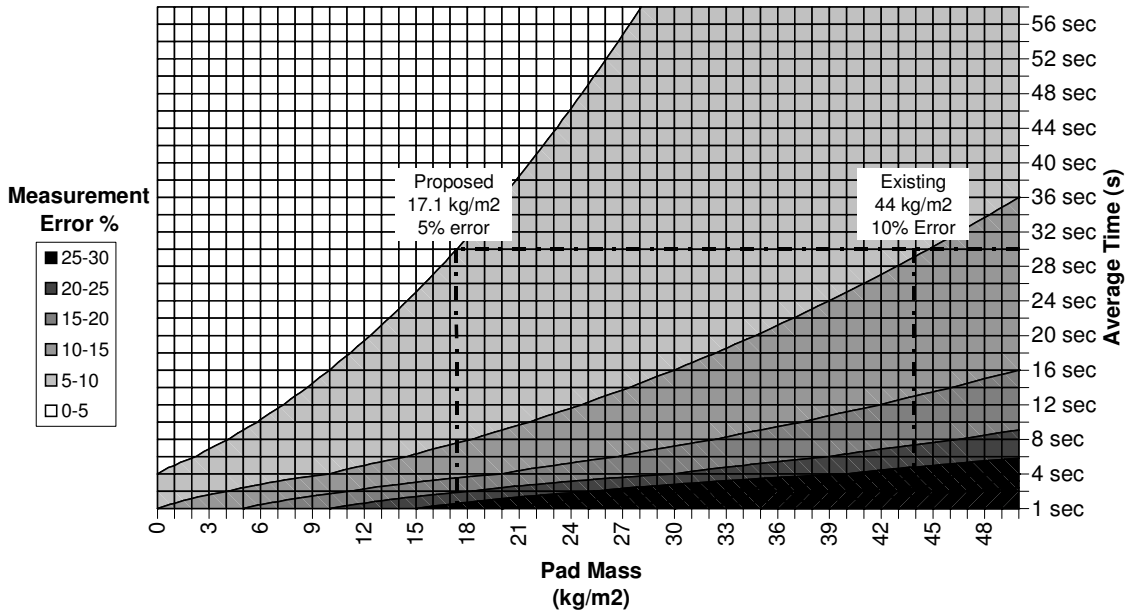

Figure 7-18. Modelled relationship between measurement error, weigh pad mass and average time.

7.4.3 Discussion

Figure 7-11 shows a typical accelerometer output during a test run. For this particular run the vibration table was set at the lowest acceleration setting ranging from –3 g to +3 g roughly. The signal is sinusoidal in appearance with some attenuation at the signal peak. Figure 7-12 shows the frequency spectrum of this signal. Clearly the main frequency component is at 50 Hz with additional components at 100 Hz, 150 Hz and 200 Hz. The 50 Hz driving frequency is probablyy related to the frequency of the 240 V mains power. Ideally the testing would have been carried out over a range of frequencies but due to a limitation of the vibration table this was not possible.

Figure 7-13 shows the load cell output for the same time period shown in Figure 7-11. The signal is also sinusoidal in shape ranging from –20 kg to +20 kg. As expected the frequency spectrum of this signal is similar to the frequency signal of the accelerometer. Figure 7-14 shows the primary component at 50 Hz with additional components at 100 Hz and 150 Hz although there is no obvious component at 200 Hz. The attenuation of the signal at 200 Hz is probably a function of the weigh pads dampening characteristics of higher frequencies.

Figure 7-15 shows the experimental results for the lowest acceleration setting (approx ±3 g). Four other graphs of similar appearance were produced from the other acceleration settings. These graphs are not shown, as they were of similar appearance except for an increase in magnitude in the vertical Z-axis. The graphs have some interesting features.

Firstly, at the 0.002 seconds average time the standard deviation of the mass measured increased as the mass applied increases to a maximum applied mass of 6 kg and then reduced at 8 kg and 10 kg. Based on the model stated in Section 7.3.4, this should continue to climb at a linear rate. The natural frequency of a system is related to its spring constant and excited mass. Therefore if the driving frequency and spring constant is fixed, the mass can be varied until the driving frequency becomes the natural frequency. This coincided with the 6 kg applied weight because the additional weight coupled with spring constant of the system caused the natural frequency of the weigh pad system to coincide closely with the 50 Hz driving frequency. This is illustrated by the equation below:

$$f_n = \sqrt{\frac{k}{M_a + M_p}} \cdot \frac{1}{2\pi} \qquad \textbf{(Equation 7.6)}$$

where f_n is the natural frequency of the system [hz];
k is the spring constant [N/m];
M_a is the mass applied [kg]; and
M_p is the mass of the weigh pad [kg].

Therefore, when $f_n = 50\text{hz}, M_a = 6kg$ and $M_p = 3kg$:

$$\begin{aligned} k &= (f_n.2\pi)^2.(M_a + M_p) \\ &= (100\,\pi)^2.(6+3) \\ &= 887 \text{ kN/m} \end{aligned}$$

This calculation shows that the spring constant maybe an important characteristic of the weigh pad. The calculated spring constant of 887 kN/m may too low resulting in amplifed mechanical noise and increased errors.

Another feature of Figure 7-15 is the effect of averaging on Z-axis data. The standard deviation of mass measured decreases rapidly as the average time increases. An average time of only 0.128 seconds decreases the standard deviation of mass measured by over 90 %

compared to that measured at 0.002 seconds. For the average time of 8.192 seconds the standard deviation of mass measured appears to have reduced close to zero. Closer examination shows the standard deviation of mass measured is 0.1 kg for the 2 kg mass applied. This is equivalent to an error of 10 % for 95 % confidence. This value was calculated using Equation 7.5. Applying this equation to all the results shown in Figure 7-15 produces Figure 7-16.

Figure 7-16 has some obvious and expected relationships. For example, the percentage error reduced as the average time increases and also as the mass applied increases. The percent error is infinity at the applied mass of 0 kg.

Figure 7-17 shows the modelled equivalent of Figure 7-16 using Equation 7.4. Comparison of these figures shows the contour lines are similar in shape with the lowest error in the top right corner. Error reduces from the bottom left corner as average time and mass applied increases. The most obvious differences occur when the mass applied is greater than 2 kg. The percentage error calculated for the experimental results is lower than the modelled results, for the same average time. Put another way the average time required to produce the same error is lower for the experimental results compared to the modelled results. This difference is due to the attenuation or dampening of the accelerations at the higher mass applied (as previous discussed).

The similarity of Figure 7-16 and Figure 7-17 support the error model proposed in Equation 7.4, although it appears conservative at the higher mass flow rates. The typical cane flow through a harvester under normal conditions is 25 kg/s, which is equivalent to approximately 6 kg applied to this weigh pad design. At this level the error model is conservative by approximately 50 %, but can be used to predict the reduction in error possible by reducing the weigh pad mass. This is shown graphically in Figure 7-18. The graph shows the reduction in error possible when the weigh pad mass is reduced and the average time is increased. Assuming the target average time of 30 seconds (previously discussed) the current weigh pad design, with a mass of 44 kg per m^2 of surface area, achieves an error of 10 %, due to dynamics. To get to the desired maximum error level of 5 % the weigh plate mass per unit surface area needs to be reduced to at least 17.1 kg per m^2 of surface area.

The desired ‘mass’ of the weigh plate is specified as ‘mass per unit area’ because the surface area of the weigh plate is also critical to accuracy. As the surface areas of the plate can change depending on it designed length and width the desired mass cannot be simply given in terms of kg. A designer could simply reduce the length and width to satisfy the

specification but this will also reduce the signal obtained from the sugar cane flow and defeat the purpose of reducing mass. Therefore the mass has to be specified as mass per unit area of the plate (kg/m^2).

Based on Figure 7-2 it was suggested that a band pass filter to accept frequencies around 4 Hz and reject all others would result in the signal that is desired. This was briefly examined and found not to work because at higher mass flow rates the sugar cane continually covers the weigh pad (i.e. space between elevator flights is covered with cane). This leads to the signal not being restricted to the 4 Hz area and a component tending to 0 Hz (continual mass). Therefore a band pass filter would give results that are non-linear and less sensitive at higher flow rates.

7.4.4 Conclusions

From the theoretical and experimental analysis there are a number of conclusions:

- Firstly, that the weigh plate should be made as light as possible to minimise the error due to dynamic conditions. Based on testing results, the mass of the pad needs to be less than 17.1 kg per m^2 of surface area is required to achieve less than 5 % error 95 % of the time with 30 seconds of averaging.

- Secondly, electronic analogue filters rather than mechanical devices should be used to reduce the noise due to dynamic conditions. A low pass filter with a cut-off frequency of approximately 1 Hz will be as effective as any other technique. Shock absorbers or rubber mounts should not be used, as they cause a natural frequency that potentially could amplify error at certain frequencies.

- The weigh pad should be as rigid as possible to maximise its natural frequency. This will minimise the chance of amplifying noise present at lower frequencies.

A new weigh pad sensor was designed based on these conclusions. This design is discussed in Section 7.6, along with the field trials designed to determine if the changes actually improve its accuracy.

7.5 Real Time Correction Using Acceleration Measurements

Acceleration measurements offer the potential to improve the accuracy of the weigh pad in real time. Raw load cell measurements can theoretically be corrected using measurements from an accelerometer attached on or near the weigh pad sensor on the harvester. The theory behind the technique is shown below.

$$L = (A_v + A_g).\frac{1}{2}(M_c + M_p)$$

$$\Rightarrow M_c = \frac{2L}{(A_v + A_g)} - M_p \qquad \textbf{(Equation 7.7)}$$

To test this theory, this equation was applied to a sample of data collected during the bench testing previously discussed. For this data the acceleration setting was approximately ±3 g with 3 kg applied to the weigh pad.

Figure 7-19 shows the results of the test. The figure covers 0.2 seconds of time. The acceleration data can be seen oscillating at approximately 50 Hz between ±3 g. The load cell measurement can be seen oscillating at approximately 50 Hz between –19 kg to +15 kg. The acceleration and load cell data appear in phase as expected. The corrected signal can be seen in this figure going outside the Y-axis scale. The full extent of the corrected data can be seen in Figure 7-20. This result ranged from 1300 kg to –500 kg. This is obviously incorrect with the actual mass applied of only 2 kg. The large spikes in the corrected results occur when the accelerometer measurement is close to zero. This is because the accelerometer measurement is a denominator in Equation 7.7 and therefore the correct mass approaches infinity. If the system followed theory then the load cell measurement would approach zero at the same time. However, a slight phase difference between the two signals results in the large erroneous spikes in the correct result.

For this technique to work, the acceleration signal would need to be smoothed to keep it positive around 1g and prevent it crossing the X-axis. Averaging the acceleration measurements over a period of 1 to 5 seconds could do this.

This technique would only slightly improve the accuracy of the weigh pad. For example if the error is 5 % over 30 seconds of averaging, then with real time correction the error may reduce to say 4 %. This improvement in accuracy would not warrant the added complexity of the accelerometer. An accelerometer may have more potential in removing any bias due to change in slope of the weigh pad sensor. This technique was thoroughly examined by McCarthy (1998).

Ideally the accelerometer should have been attached to the weigh plate but it was attached to the support frame as shown in Figure 7-9. The closer the accelerometer is to the weigh plate, the higher the chance of getting a true measurement of the accelerations exerted on the weigh plate. The difference in position for this testing could result in a difference in phase and frequency between the signals measured by the accelerometer and load cell. This phase difference means the two signals would be slightly offset in time. For this system, the offset is probably less than 0.01 s (see differences in peaks and troughs of measured mass and acceleration signal in Figure 7-19). This will result in significant errors when applying Equation 7.7 to signals with higher frequencies (e.g. greater than 50 Hz) but at lower frequencies (e.g. less than 1 Hz) the small time offset will have less impact. This was an oversight in the testing and it is recommended if these trials were to be replicated the accelerometer be mounted on the weigh plate close to the load cell.

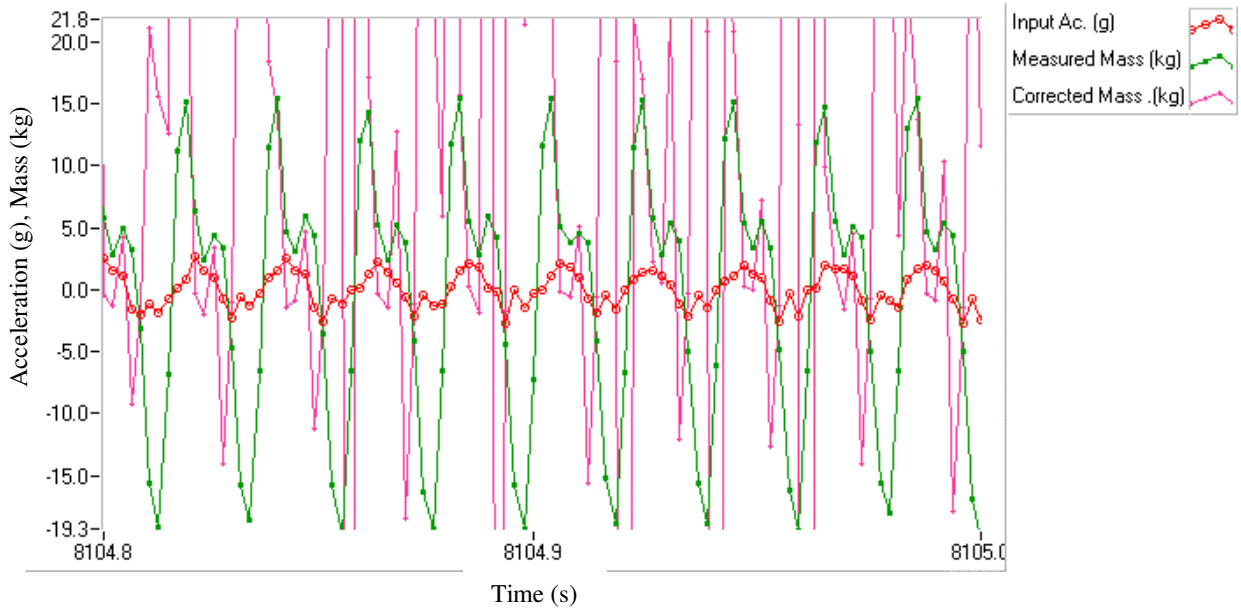

Figure 7-19. Accelerometer and load cell signals along with the corrected mass reading (off scale)

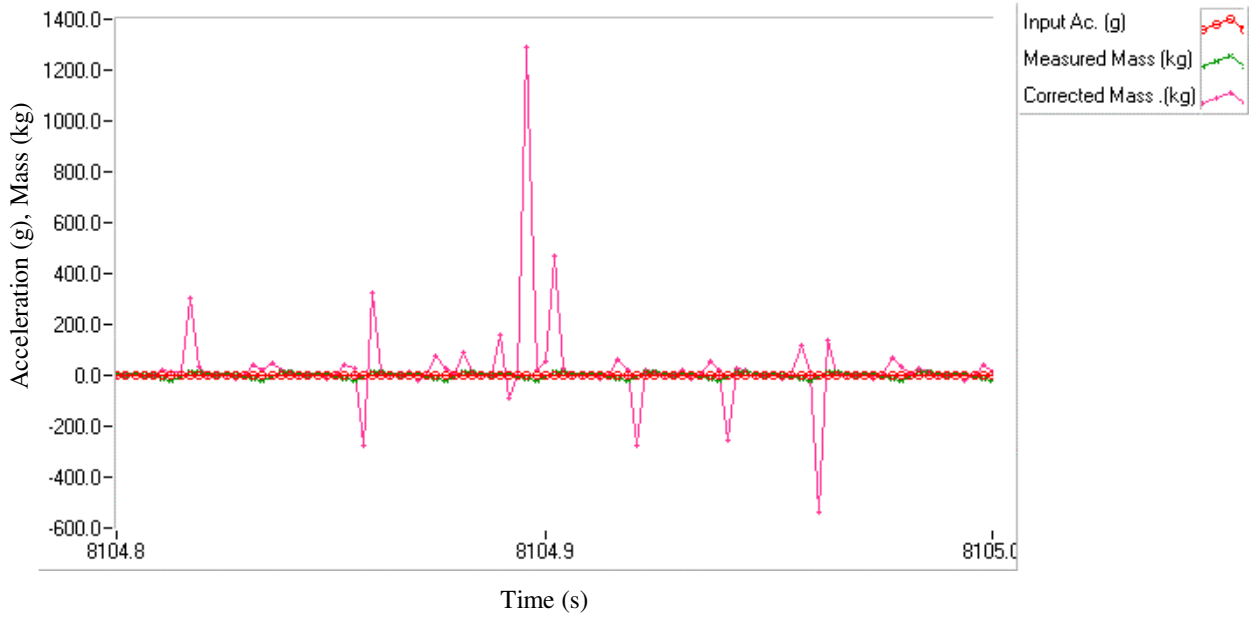

Figure 7-20. Signals shown in Figure 6.19 with y scale adjusted to fit corrected mass reading.

7.6 Field Trials

7.6.1 Introduction

A theoretical model was developed to understand the effect of dynamics on the accuracy of the weigh pad sensor. Bench testing has validated this model. Based on these results a lighter and more rigid weigh pad was designed and manufactured. The new weigh pad was constructed of rectangular hollow section (RHS) aluminium frame covered by 6 mm thick High Density Polyethylene (HDPE) plastic. This design had a mass of 5.1 kg or 19.8 kg/m^2. This was slightly heavier than the 17.1 kg/m^2 stated previously. Attempts were made to reduce the mass even further by using fibre composite material such as fibreglass sandwiched balsa wood, however there were problems finding a suitable material to protect the fibreglass from wear.

Drawings of the weigh pad design are shown in Appendix D.

7.6.2 Materials and Method

The field trials were undertaken during the 1st to 5th and 22nd to 26th September 1997 in Bundaberg, on Fairymead Plantation. Trials were conducted in both burnt and 'green' cane. The burnt cane was of variety Q96 with an average crop yield of approximately 120 t/ha. The green cane was also of variety Q96 producing a low average crop yield of approximately 65 t/ha.

Each trial consisted of a series of runs, with each run defined as a 70 m long row of cane, harvested into the weigh truck. During each run, the electrical output from each of the sensors was digitally sampled at a rate of 100 samples per second and recorded onto the hard drive of a laptop computer. Software was written in National Instrument's Labview® to control the data acquisition. Each run was carried out at a different ground speed to achieve a range mass flow rates through the sensors. A 1996 model Austoft 7000 rubber wheeled cane harvester was used, fitted with the three separate sensing techniques previously discussed. An overview of the sensors installed is shown in Figure 7-21.

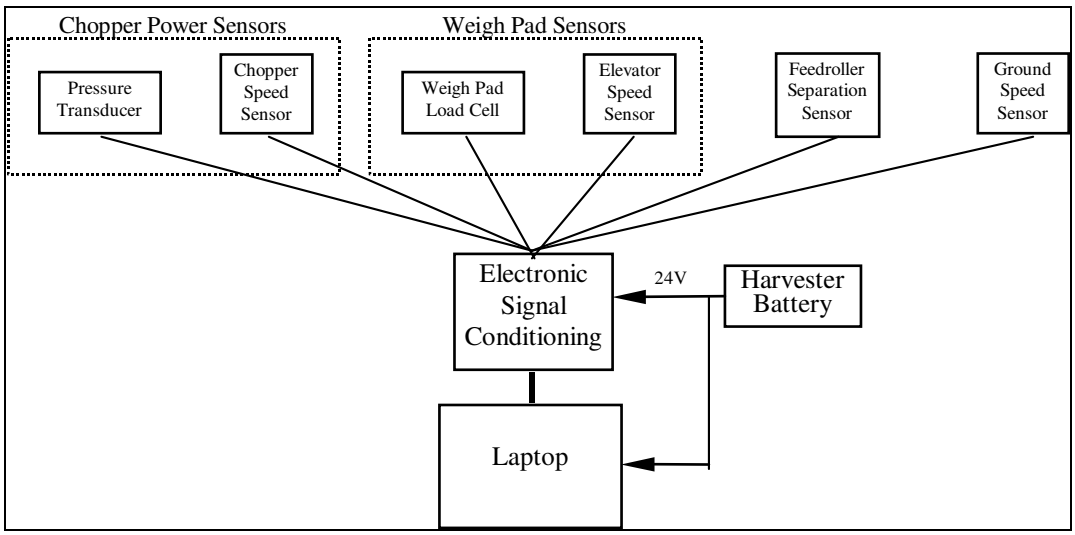

Figure 7-21. Block diagram of the instrumentation installation on the cane harvester.

The analysis of the data occurred in the office using a PC. A program was written using National Instrument's Labview® to calculate the average reading for each sensor, for each run. The time of flow was defined as the time from when the cane was first sensed by the feed roller separation sensor to when the last portion of cane passed over the weigh pad.

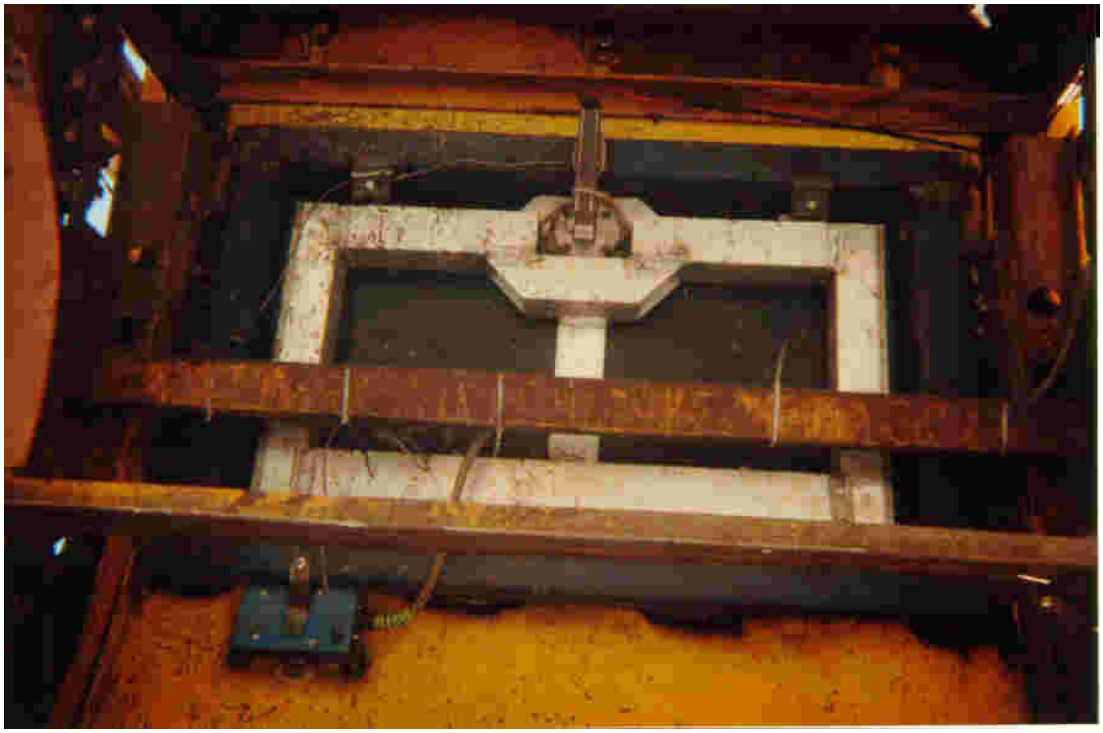

Figure 7-22. The weigh pad installed in the harvester (viewed from underneath the elevator)

7.6.3 Results

The results are divided into two areas; 1) Mass flow calibration curves and 2) Cumulative mass comparisons charts. The Mass flow calibration curves are graphs of average mass flow rate, as measured from the weigh truck, versus the average sensor output during the run. The average mass flow rate calculated for each run was defined as:

$$\text{Average Mass Flow Rate (kg / s)} = \frac{\text{Weigh Truck Measured Mass (kg)}}{\text{Time of Flow(s)}}$$

(Equation 7-8)

Each run produces a single point on these graphs. The calibration curves are the line of best fit through these data points. The cumulative mass comparison charts are calculated by applying these mass flow calibration curves to the average sensor output for each run. The outcome is a bar graph comparing the total mass as measured by the weigh truck to the total mass as measured by the respective sensors. Only the results for the weigh pad sensor are

shown in the sections below. Results from the other sensors were analysed but are not relevant to this section.

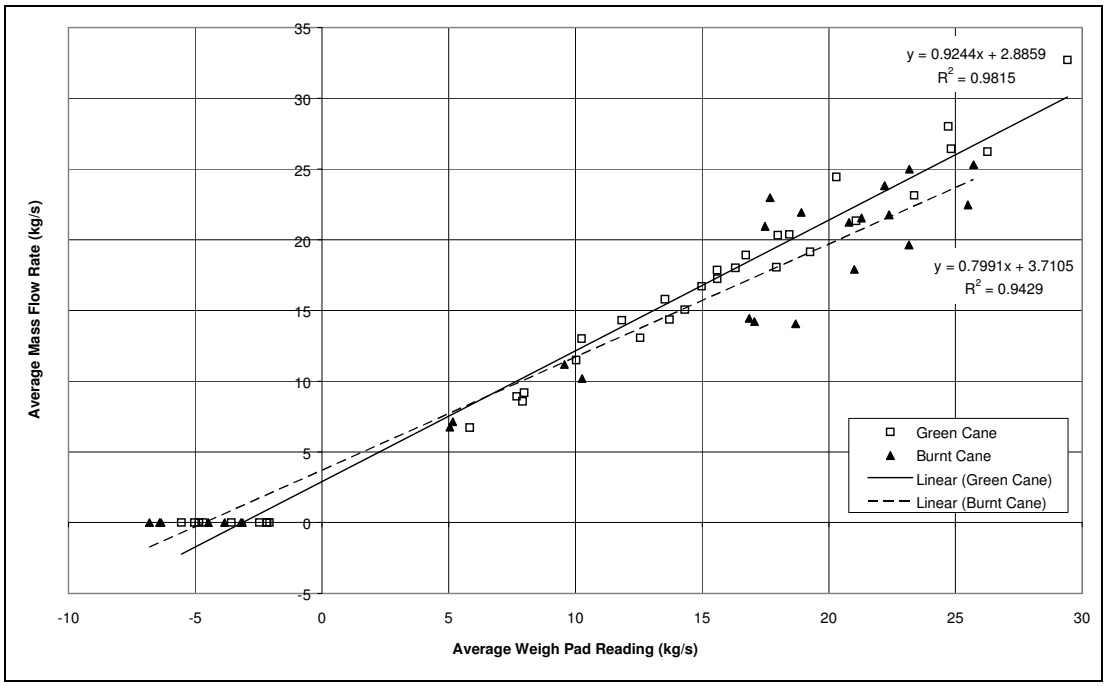

Figure 7-23. Average mass flow rate versus average weigh pad reading in kilograms per second.

The average weigh pad reading (kg/s) shown in Figure 7-23 was calculated using the formula below:

$$m_f = \frac{M}{l}.s \qquad \textbf{(Equation 7.9)}$$

where m_f is the mass flow rate [kg/s];

M is the mass as measured by the load cell [kg] calculated using the load calibration function below;

l is the length of the weigh pad in the direction of the elevator [m]; and

s is the speed of the elevator [m/s] calculated using the elevator speed calibration function below.

Load cell calibration function:

$$M = 1.523.V + 1.007$$ **(Equation 7.10)**

where V is the signal conditioning output for the load cell [V].

This calibration function was determined by placing weights of known mass in the centre of the weigh plate and recording the voltage output. The weigh pad was installed in the elevator of the harvester with the elevator in field operating position in terms of it slope to horizontal. The harvester engine or other components were not operating.

Elevator speed calibration function:

$$s = \frac{d}{\mathrm{t}}$$ **(Equation 7.11)**

where d is distance travelled by elevator per sprocket revolution, 0.566m; and
t is time per revolution [s].

Table 7-1. Summary of calibration results from weigh truck trials.

Sensor	Gradient, m	Intercept, I	R^2
Weigh Pad Green Cane	0.924 (kg/s)/(kg/s)	2.886 (kg/s)	0.98
Weigh Pad Burnt Cane	0.799 (kg/s)/(kg/s)	3.711 (kg/s)	0.94

The cumulative mass comparison graphs (Figure 7-24 and Figure 7-25) give an indication of the accuracy of the sensor when compared to the harvested totals for each run. The lighter coloured bars on the left represent the actual mass of cane as measured by the weigh truck. The darker coloured bars on the right represent the mass of cane as calculated using the calibration curves of the previous section applied to the sensor measurements. Five percent error bars are also displayed to represent the accuracy goal that was aimed for.

Note for some runs that no weigh truck mass has been given. These runs are defined as the 'free running' test to measure the sensor output during no cane flow. These runs were typically 30 s to 60 s in duration. If the results indicate a mass reading during these runs then the sensor output had drifted from the zero reading of the calibration curve.

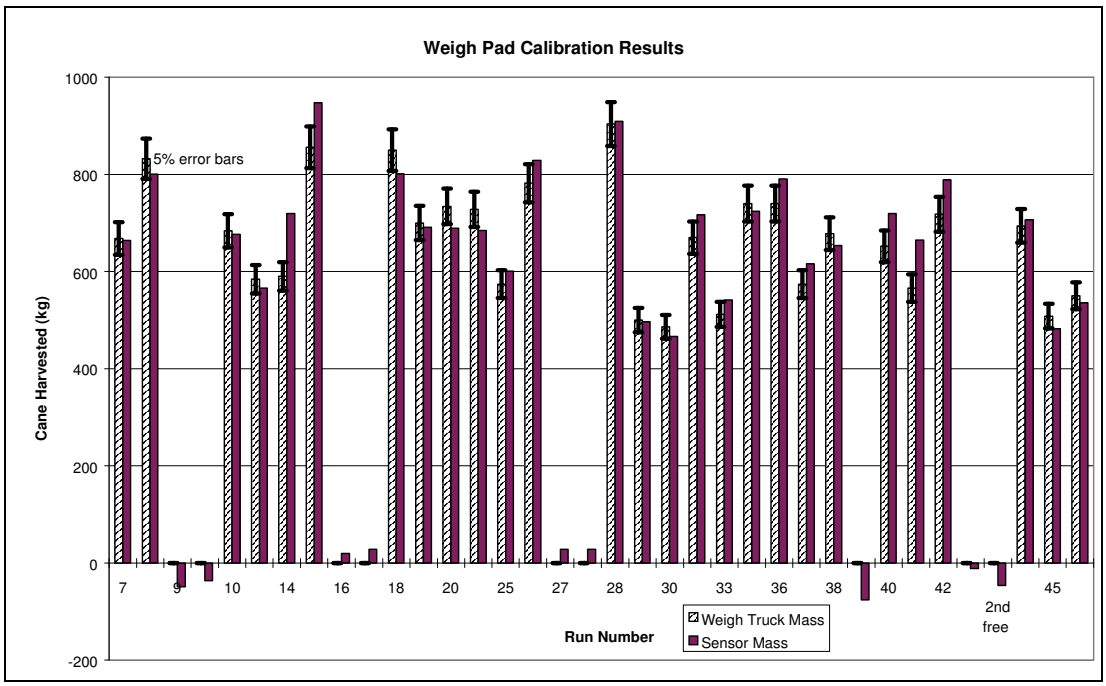

Figure 7-24. Cumulative mass comparison for weigh pad in green cane

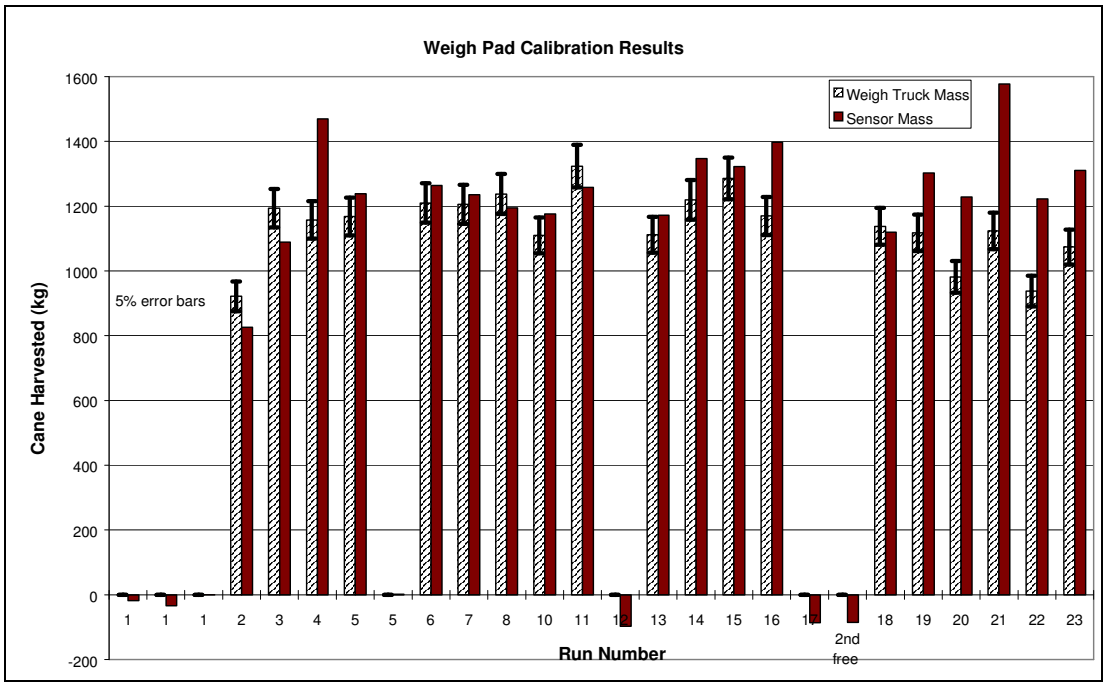

Figure 7-25. Cumulative mass comparison for weigh pad in burnt cane

Table 7-2. Summary of accuracy statistics from weigh truck trials.

Sensor	Average Absolute Error (%)	95 % Probability Error (%)	Average Absolute Yield Error (t/ha)
Weigh Pad Green	5.8	14.6	3.8
Weigh Pad Burnt	13.0	28.4	11.7

Average Absolute Error, AAE [%], was calculated as:

$$\text{AAE} = \frac{\sum \left| \text{Error for each run} \right|}{\text{Number of runs}}$$

$$\text{where Error for each run [\%]} = \frac{(\text{Sensor Mass [kg]} - \text{Weigh Truck Mass [kg]})}{\text{Weigh Truck Mass [kg]}} 100$$

The 95 % Probability Error is the percentage error within which 95 % of the results fall. This represents the accuracy statistic we are aiming to get below the 5 % mark as discussed in previous chapters. It is calculated using elementary statistics as:

$$95\% \text{ Probability Error [\%]} = 2 \sqrt{\frac{\sum (\text{Error For Each Run} - \text{Mean Error})^2}{\text{Number of Runs} - 1}}$$

Average Absolute Yield Error, AAYE[t/ha] was calculated as:

$$\text{AAYE} = \frac{\sum \left| \text{Error for each run} \right|}{\text{Number of runs}}$$

$$\text{where} \quad \text{Error for each run [t/ha]} = \frac{(\text{Sensor Mass (t)} - \text{Weigh Truck Mass(t)})}{\text{Area (ha)}}$$

$$\text{Area} = 100 \text{m}^2 = 0.001 \text{ ha}$$

7.6.4 Discussion

Mass Flow Calibration Curves

The weigh pad results were encouraging overall however there were a number of interesting characteristics of the calibration curve (Figure 7-23). The first characteristic is the positioning of the cluster of points just left of the graph origin. These points are defined as 'free running' readings and are measured by operating the harvester at normal operating engine speed, with all harvestings functions running as normal, but with no cane flow. The harvester was not normally moving along the ground either. These readings are necessary to define the origin of the calibration line. The point of interest is the positioning of these free running values left of the zero of the X-axis. The X-axis zero is the weigh pad reading taken under static conditions with no harvester operation. This indicates there is a discrepancy between the zero reading taken during normal harvester operation and when the harvester is not operating at all. These results were initially very perplexing however after extensive investigation the difference was found to be caused by a negative force on the weigh pad. This negative force was caused by a negative pressure (relative to atmospheric pressure), on the topside of the weigh pad. This negative or suction pressure was caused by the secondary extractor fan of the harvester as shown in Figure 7-26. During harvesting the fan removes extraneous leaf material from the harvested cane by creating an updraft through the material as it falls off the end of the elevator. To create this updraft the fan generates a negative pressure on the inlet relative to the outlet. This negative pressure impacts on the weigh pad by causing a negative force on the load cell that is proportional to the pressure.

This outcome is of concern, as the operation of the secondary extractor fan appeared to significantly effect the calibration and therefore accuracy of the weigh pad sensor. Attempts to minimise this effect are discussed in the next chapter.

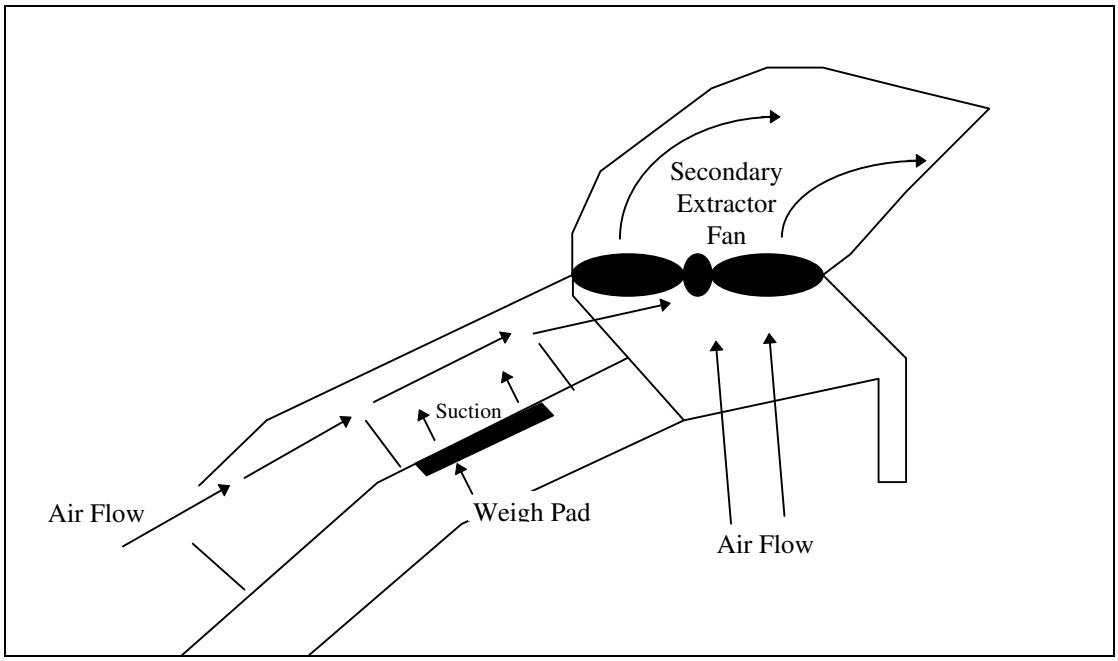

Figure 7-26. Effect of the secondary extractor fan on the weigh pad.

Another point of concern regarding the free running measurements was the extent of the variation. The variation of 5 kg/s (from –7 kg/s to –2 kg/s on the Y-axis) is equivalent to 20 % error full scale. It was expected that these readings would exhibit minimal variation as they are not subjected to noise sources present during harvesting, such as additional accelerations, dynamics of cane flow, etc. The magnitude of variation found at zero flow was as large as the variation found at any flow rate throughout the calibration range. This indicates that most of the error found in the calibration data is also present during no flow. Therefore, if the cause of the scatter of the free running data can be deducted and reduced then the accuracy of the sensor over the full operating range may be improved also. This is examined closely in the next chapter.

Another characteristic of interest in Figure 7-23 is the significantly higher error or scatter found in the data measured while harvesting burnt cane (R^2 = 0.94) compared to the data from the green cane harvesting (R^2 = 0.98). The difference could be due to a number of factors. A possible reason for the difference is that the burnt cane was harvested after some light rain. This resulted a build up of foreign matter around the edge of the weigh pad as shown in Figure 7-27. The consequence of this build-up is an additional force on the load cell and therefore an error in the measurement of the mass flow. This indicates that the current weigh pad design may be susceptible to the build up of foreign matter.

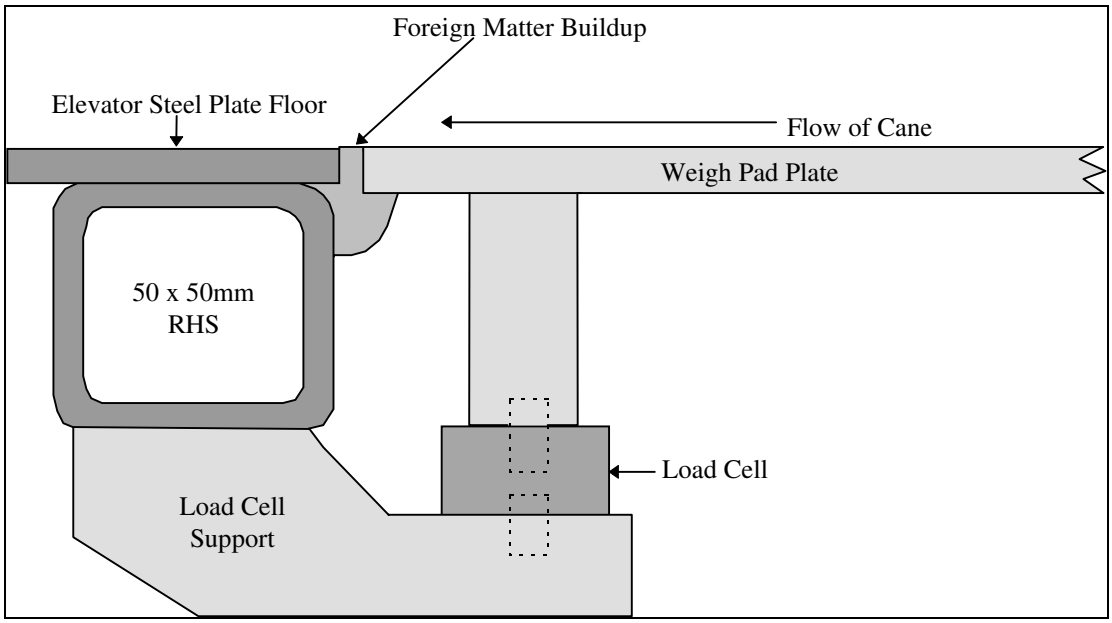

Figure 7-27. Foreign matter build-up around hinged weigh pad

The final point to note about Figure 7-23 is the slope of the calibration lines. The slopes are 0.92 for the green cane and 0.80 for the burnt cane. If the results were to agree with theory, the calibration lines should have a gradient of 1.0. A factor less than 1.0 indicates the weigh pad is measuring a flow rate higher than the actual flow rate. This could be due to a number of factors:

a) The elevator flights may be coming in contact with the weigh plate surface resulting in a positive force on the load cell. Stalks of cane being wedged under the flights can exacerbate this problem.

b) The secondary extractor fan can remove up to 5 to 10 % by weight of extraneous matter from the cane flow. This material would be weighed by the weigh pad but not recorded in the weigh truck. This would have the most effect on the green cane, which has more extraneous matter.

c) The negative force on the weigh pad due to the suction pressure may not be as great during harvesting. The presence of the cane flow may affect the pressure gradient between the secondary extractor fan and the weigh pad.

Cumulative Mass Comparison

Figure 7-24 and Figure 7-25 give an indication of the accuracy of the weigh pad in measuring the cumulative mass flow for each of the runs conducted. For these results to meet

the accuracy goal of less than 5 % error, 95 % of the time, most of the 'calculated mass' bars (95 % of them) should lie within the 5 % error bars shown on the graphs. This is not the case for both figures. This is reflected in the statistics in Table 7-2. The 95 % probability error is 14.6 % for green and 28.4 % for burnt.

The other accuracy statistics shown in Table 7-2 are far more encouraging. The average absolute error of 5.8 % in green cane is acceptable. Also the average absolute error measured in tonnes per hectare was only 3.8 t/ha. This would be a good figure to use when recommending the sensor to farmers as most would be satisfied with this level of accuracy in yield maps. A much higher level of accuracy is required if the sensor is to be used for on farm experiments and agronomic trials. Note that with PA equipment a different approach can be taken to agronomic trials that allows much larger sample sizes and therefore lower accuracy results can detect statistically significant differences.

7.7 Conclusion

A theoretical model has been developed to model the effects of acceleration dynamics on the accuracy of weigh pad sensor. Laboratory bench testing has shown support for the mathematical model. From the theoretical and experimental analysis a number of conclusions were drawn:

- The weigh pad should be made as light as possible to minimise the error due to dynamic conditions.
- Electronic analogue filters should be used to reduce the noise due to external acceleration.
- The weigh pad should be as rigid as possible to maximise its natural frequency.

A new weigh pad sensor was designed based on these conclusions. Field trials were carried out to determine if the changes actually improve its accuracy. The results indicate the effects of external accelerations dynamics have been significantly reduced. However, the accuracy achieved during the field trials is not within the accuracy goal. The main factor limiting accuracy is a drift in the sensor zero or base line value of the sensor. This problem is analysed closely in the next chapter.

Also examined was the potential of real time acceleration measurements to improve the

accuracy of the weigh pad. The results showed for this technique to work, the acceleration signal would need to be smoothed to keep it positive around 1 g. Averaging the acceleration measurements over a period of 1 to 5 seconds using a moving boxcar filter or moving average could do this. However it is estimated that the improvement in weigh pad accuracy would only be marginal and an accelerometer may have more potential in removing any bias due to change in slope of the weigh pad sensor (an inclinometer could also be used to do this).

Chapter 8 - Effect of the Secondary Extractor Fan on the Weigh Pad

8.1 Introduction

As stated in the previous chapter baseline drift appears to be the largest error source in the weigh pad calibration. The baseline drift is caused by a number of factors including the secondary extractor fan of the harvester, which induces a fluctuating negative pressure on the weigh pad. This problem was examined to determine the extent of the problem and to enable solutions to be proposed.

The secondary extractor fan is designed to remove extraneous leaf matter from the flow of sugar cane billets. Extraneous matter is removed by the fan inducing airflow through the billeted sugar cane as the cane falls from the top end of the elevator. The location of the extractor fan is shown in Figure 8-1. The weigh pad is positioned approximately one metre away from the secondary extractor fan. Figure 8-2 shows the position of the weigh pad relative to the secondary extractor fan. Also shown on Figure 8-2 is the shroud which covers the elevator for 2m before the secondary extractor fan. The shroud is designed to reduce Air Flow A (see Figure 8-2) and increase Air Flow B that is required to clean the cane. In doing this, the shroud sets up a pressure gradient from the secondary extractor fan back to the opening of the shroud (at Air Flow A on Figure 8-2). The pressure at the shroud opening is close to atmospheric, while the pressure at the underside of the extractor fan is negative. Therefore, the pressure on the topside of the weigh pad is negative, somewhere between the two. The pressure on the underside of the weigh pad is atmospheric. Therefore the pressure differential between the top and underside of the weigh pad induces a negative force on the weigh pad load cell. This force is equal to the pressure differential between the top and underside of the weigh pad multiplied by the surface area of the weigh pad.

Results from the previous chapter indicate the suction force applied by the secondary extractor fan is significant and in the order of twenty five per cent of the normal operating load on the weigh pad due to sugar cane flow. The suction force can be removed from the calibration by rezeroing the weigh pad sensor when the secondary extractor fan is operating. However, measurement error arises when the suction force changes over time and causes baseline drift. The suction force can change for a number of reasons including a change in engine speed that in turn will cause a change in secondary extractor fan speed and a change in the flow rate of cane through the elevator and secondary extractor fan. The objective of this research is to analyse the effect of the secondary extractor fan on the weigh pad and develop methods to minimise it.

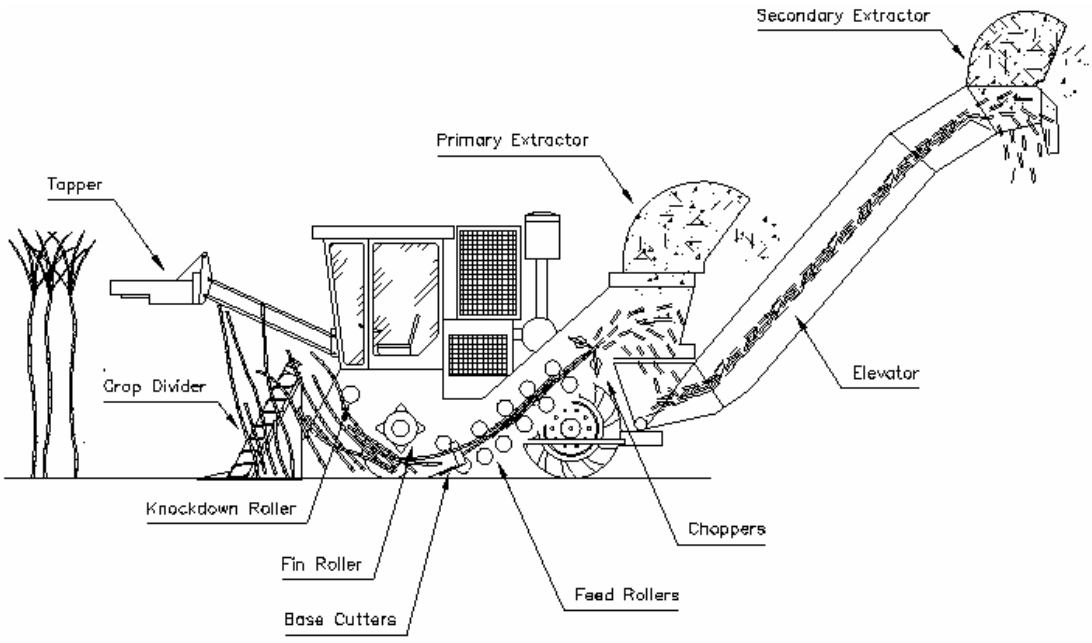

Figure 8-1. Position of the secondary extractor fan on the harvester.

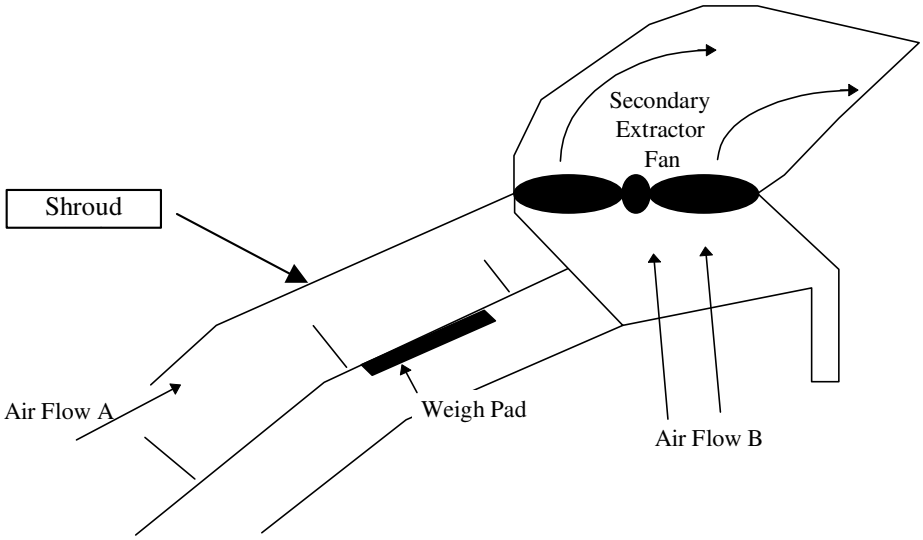

Figure 8-2. Position of the secondary extractor fan, weigh pad and shroud.

The magnitude of the effect of the secondary extractor fan on the weigh pad can be shown by Figure 8-3 to Figure 8-6. Figure 8-3 shows the weigh pad load cell signal with the harvester operating normally, but with no cane flow. The variation in load reading is due to the secondary extractor fan. Note the zero in the Y-axis was defined as the average of this signal over a 30 second period. The load reading with the secondary extractor fan off is approximately 19N. The signal in Figure 8-3 has a strong frequency component at approximately 4 Hz as confirmed by the frequency spectrum shown in Figure 8-4. This frequency component is due to the elevator flights passing over the weigh pad and interfering with the airflow. When a flight is directly over the centre of the weigh pad, the suction force is the strongest (negative peak of signal at approximately –17 N) and when the flights are positioned either side of the weigh pad the suction force is the weakest (positive peak of signal at approximately +17 N). When compared to a datum of +19 N (fan off) this suction force changes from –2 N to –36 N or averages at –17 N. Over the surface area of the weigh pad (0.29 m^2) these forces are equivalent to negative pressures of 7 Pa, 124 Pa and 59 Pa, respectively.

Figure 8-5 shows the weigh pad load cell signal with the harvester operating normally and with a typical cane flow rate of approximately 25 kg/s. The frequency spectrum in Figure 8-6 shows the main frequency component at 4 Hz. Comparing the signal in Figure 8-3 to that in Figure 8-5 shows that the suction force is a very significant force in the weigh pad measurement.

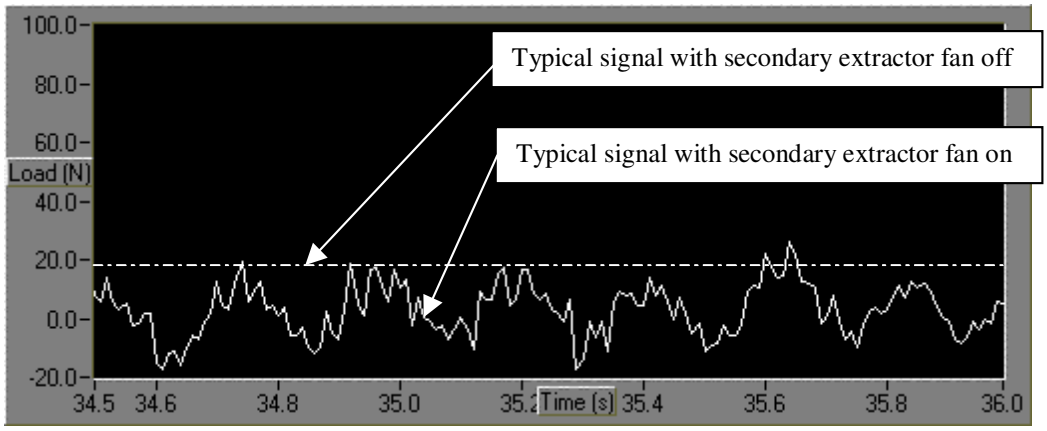

Figure 8-3. Weigh pad load cell measurement for no cane flow.

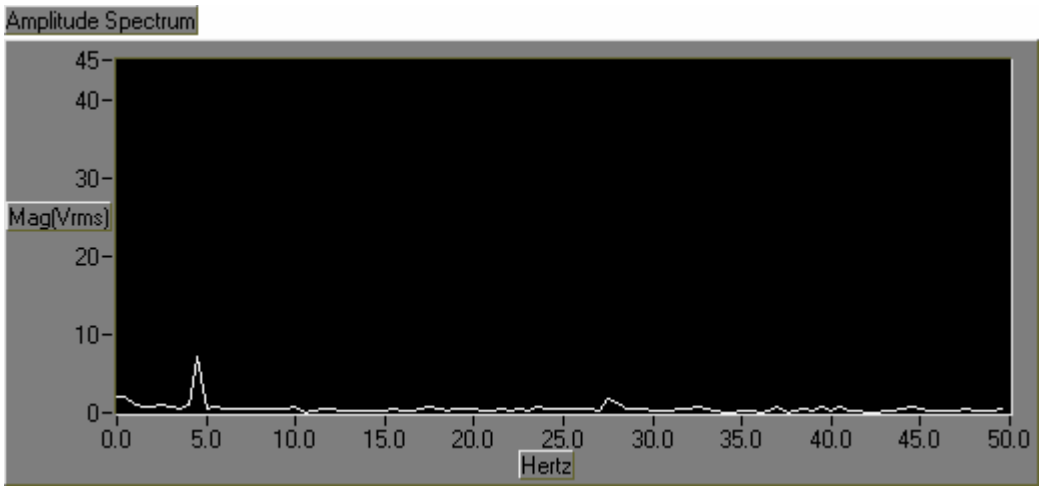

Figure 8-4. Frequency spectrum of the load cell measurement for no cane flow.

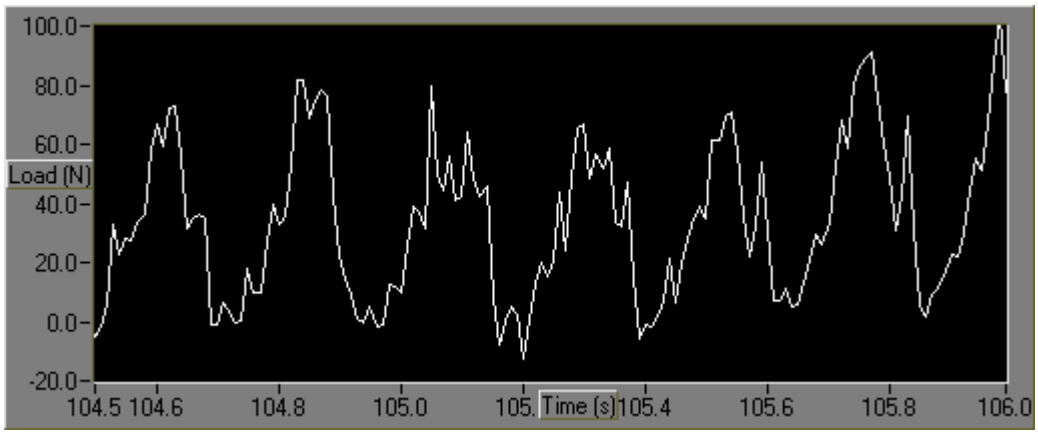

Figure 8-5. Weigh pad load cell measurement for flow rate around 25kg/s.

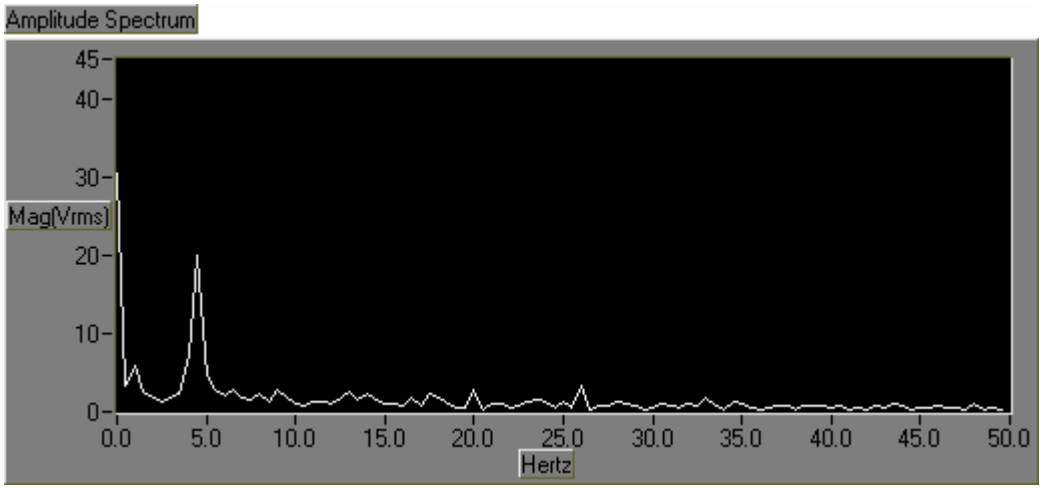

Figure 8-6. Frequency spectrum for Weigh pad load cell measurement for flow rate around 25kg/s.

8.2 Potential Solutions

There are three potential options to reduce the effect of the secondary extractor fan. They are:

1. **Perforated Pad**

   By making the weigh pad perforated, air will be able to flow through it. This will reduce the pressure differential between the top and bottom side of the weigh plate.

   Advantages:

   - Simple

   Disadvantages:

   - Perforations may become blocked or would be covered by elevated cane that would experience the negative forces.
   - Would have to use steel which may increase the weigh plate weight
   - Would have to use steel which has does not have the non-stick properties of HDPE plastic
   - May decrease the performance of the secondary extractor fan

2. **Curtain**

   By placing a vertical curtain between the weigh pad and the secondary extractor fan

(See Figure 8-7), the pressure above the weigh plate would be reduced. The curtain should be flexible so not to cause an obstruction to cane flow. Rubber would be a suitable material.

Advantages:

- Simple
- Cheap
- Easy to install/replace
- May increase the performance of the secondary extractor fan

Disadvantages:

- May wear out
- Air may still flow around the curtain reducing its effectiveness

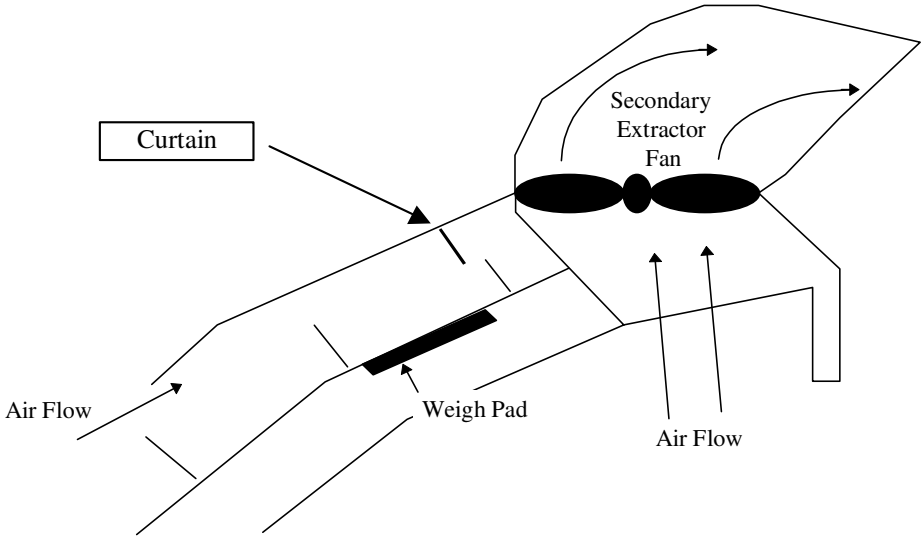

Figure 8-7. Use of a curtain to reduce the impact of the extractor fan on the weigh pad.

3. Vents

By incorporating vents into the area around the weigh pad as shown in Figure 8-8, air will be able to flow through to the extractor fan. This will have the effect of equalising the pressure difference between the volume under the shroud and the atmospheric pressure outside. The net result would be a reduction of the suction force on the weigh plate.

Advantages:

- Simple

Disadvantages:

- Requires significant equipment and work to retrofit
- May decrease the performance of the secondary extractor fan

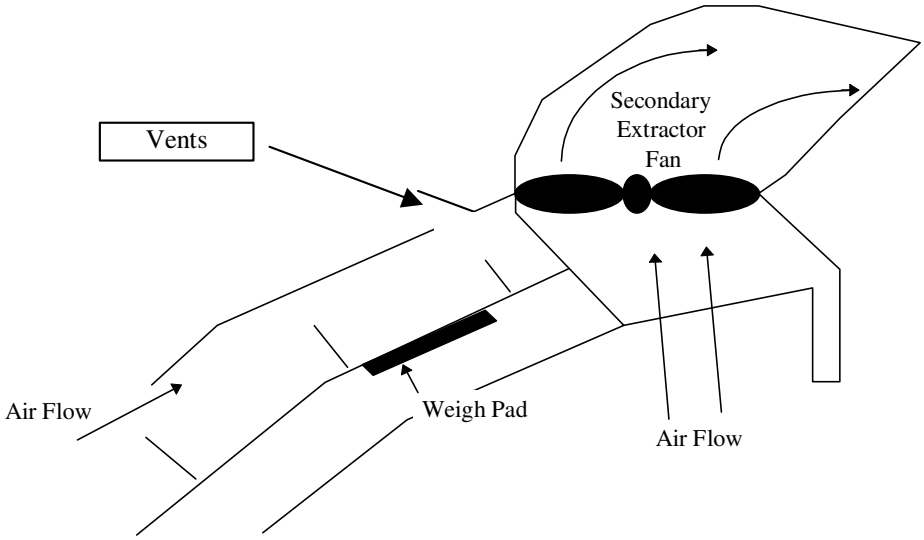

Figure 8-8. Use of a vents to reduce the impact of the extractor fan on the weigh pad.

Importantly, any method adopted should not significantly reduce the cleaning operation or efficiency of the secondary extractor fan. The curtain appeared to be the simplest option to adopt and may even improve the performance of the secondary extractor fan. Therefore this option was examined. The method and results are shown below.

8.3 Materials and Method

A fully functional Austoft 7000 cane harvester was used in the study. The secondary extractor fan was positioned to discharge the out flowing air directly behind the elevator. Air pressures at various points around the secondary extractor fan, weigh pad and elevator were measured with an inclined manometer filled with water. The air velocity was also measured at various points around the secondary extractor fan, weigh pad and elevator with a hand

held instrument. A hand held instrument was also used for measuring the secondary extractor fan speed. These instruments were used to measure various parameters during operation of the harvester with and without the curtains in place.

Two curtain configurations were tested; short and long. The short curtain (170 mm long) was long enough to hang from the shroud to the top of the elevator flights. The long curtain (450 mm long) was long enough to hang from the shroud to the floor. The curtains were the full width of the elevator and were made of 6 mm thick rubber bolted to 25 mm x 25 mm angle iron as shown in Figure 8-10 (for short curtain design).

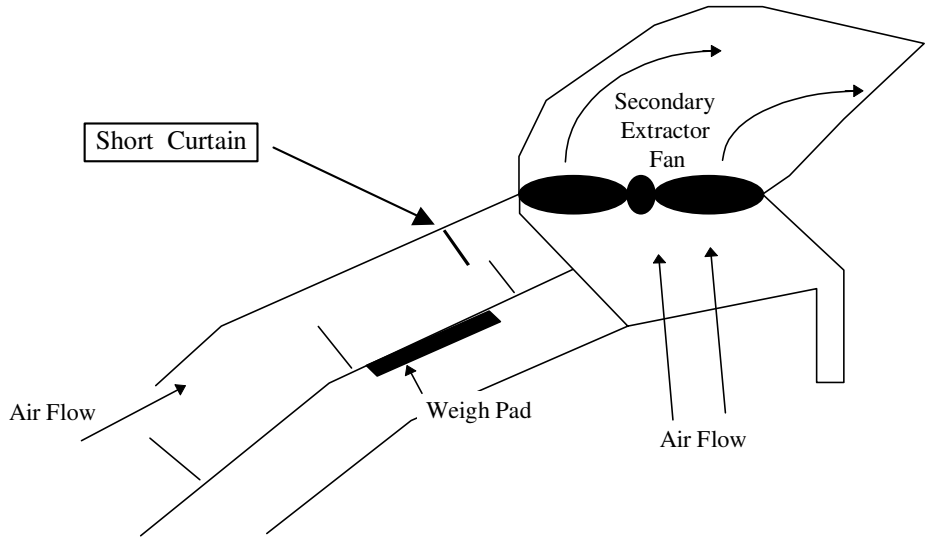

Figure 8-9. Typical installation of the short curtain.

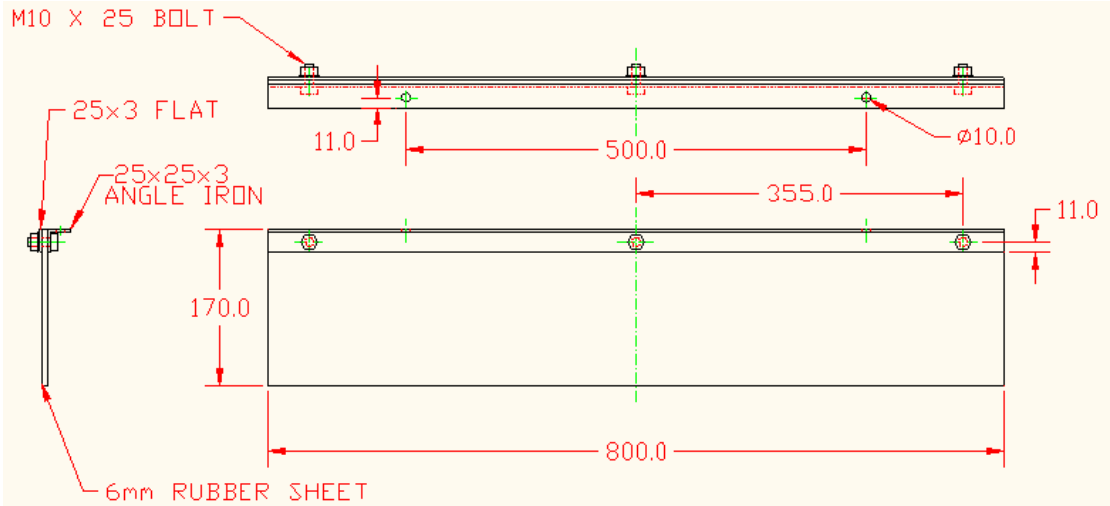

Figure 8-10. Typical Short curtain design.

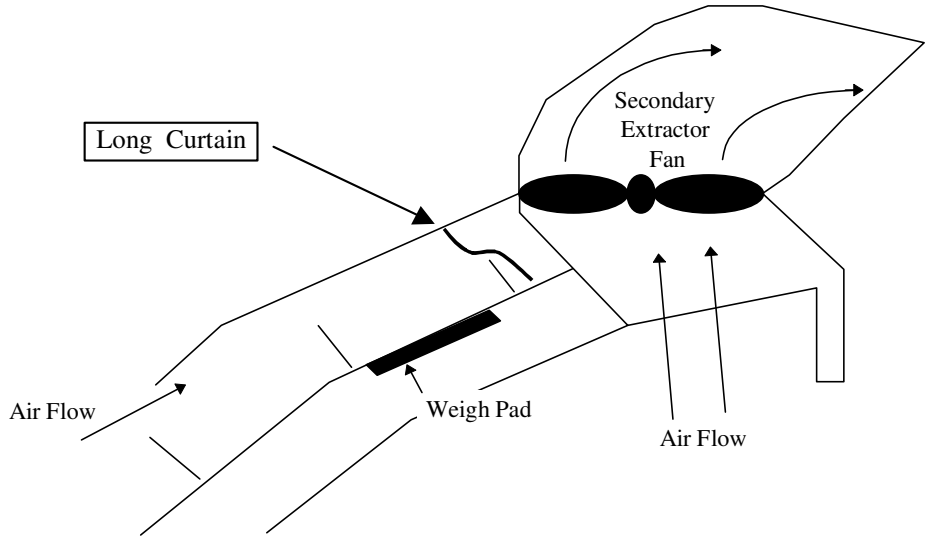

Figure 8-11. Typical installation of the long curtain.

8.4 Results

Figure 8-12 shows the relationship measured between the harvester engine speed and the secondary extractor fan speed. Figure 8-13 shows the relationship measured between the secondary extractor fan speed and the average air speed on its inlet side and outlet side. Also shown is the relationship between the secondary extractor fan speed and the pressure measured on the inlet side of the fan.

Figure 8-14 shows the air speed profile measured above the weigh pad, from the floor of the elevator (0 mm) to the shroud (330 mm). The measurements were taken at three points across the width of the elevator (250 mm left of centre line, on centre line, 250 mm to the right of the centre line, looking up the elevator) to show the variation. The typical height of the elevator flights on the vertical axis is also shown.

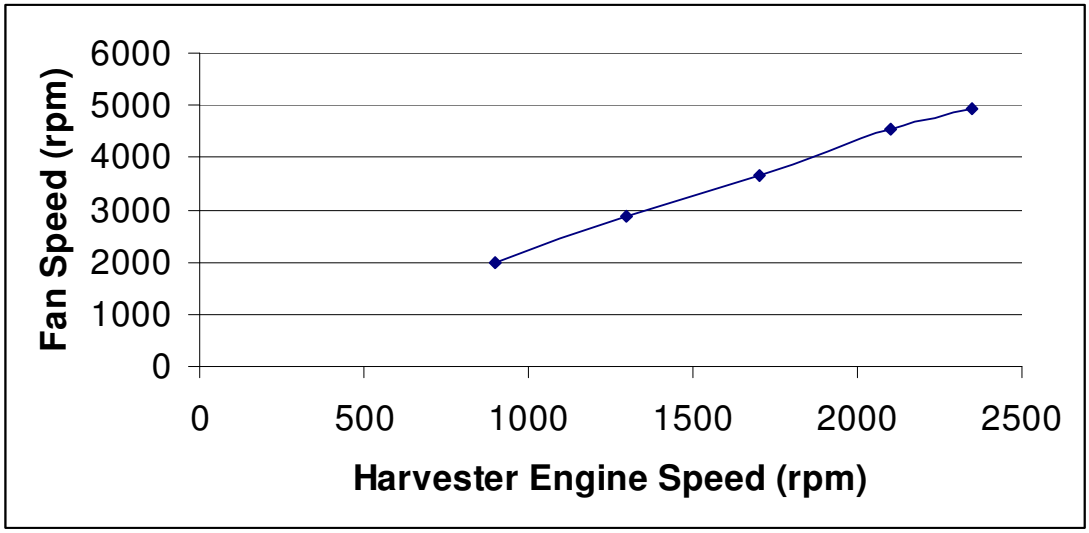

Figure 8-12. Relationship between harvester engine speed and secondary extractor fan speed.

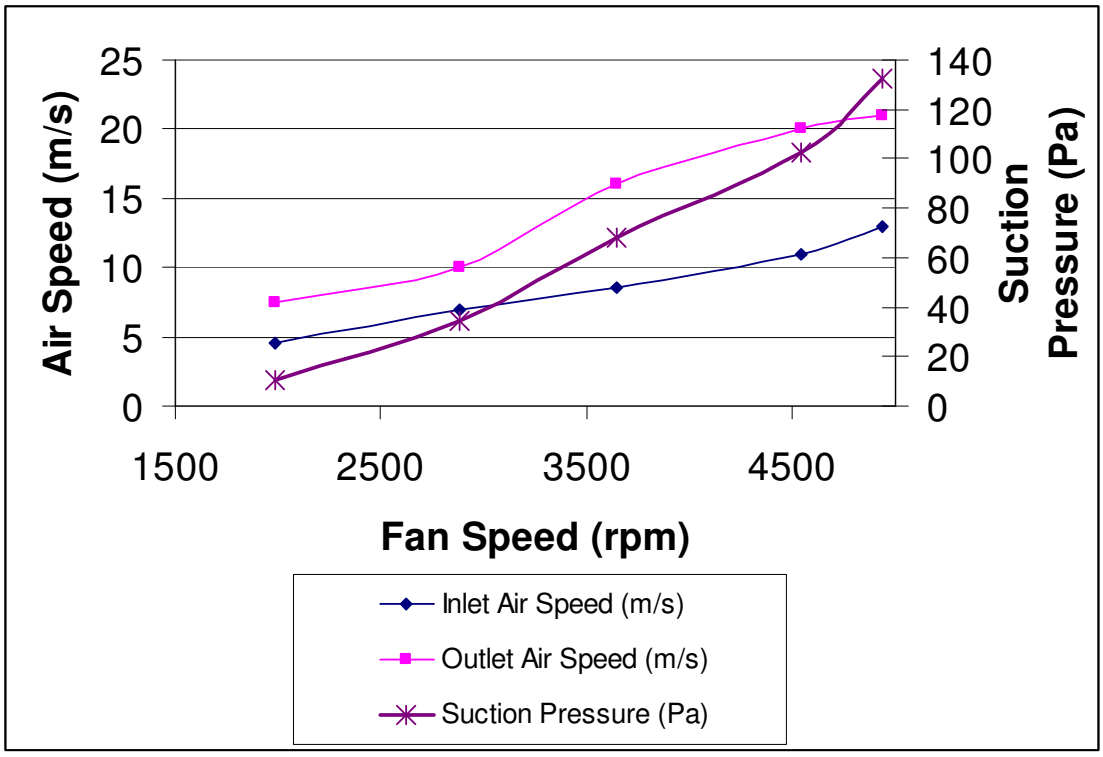

Figure 8-13. Relationship of secondary extractor fan speed to air speed and suction pressure.

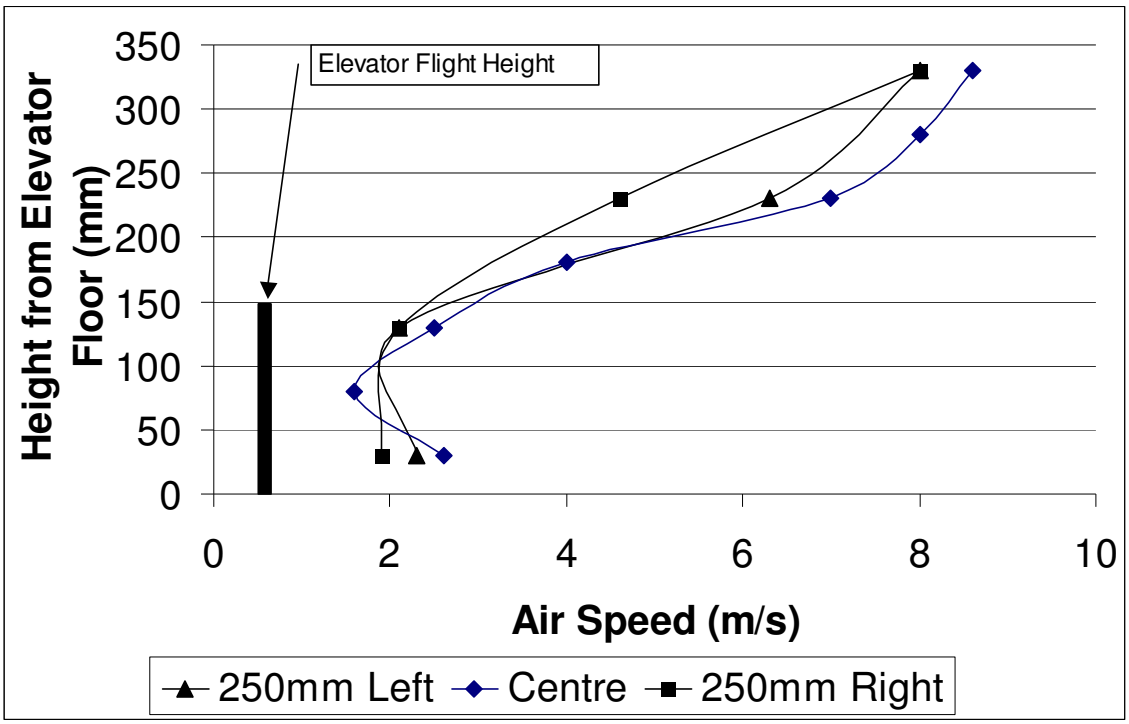

Figure 8-14. Air speed profile from the floor of the elevator to the shroud.

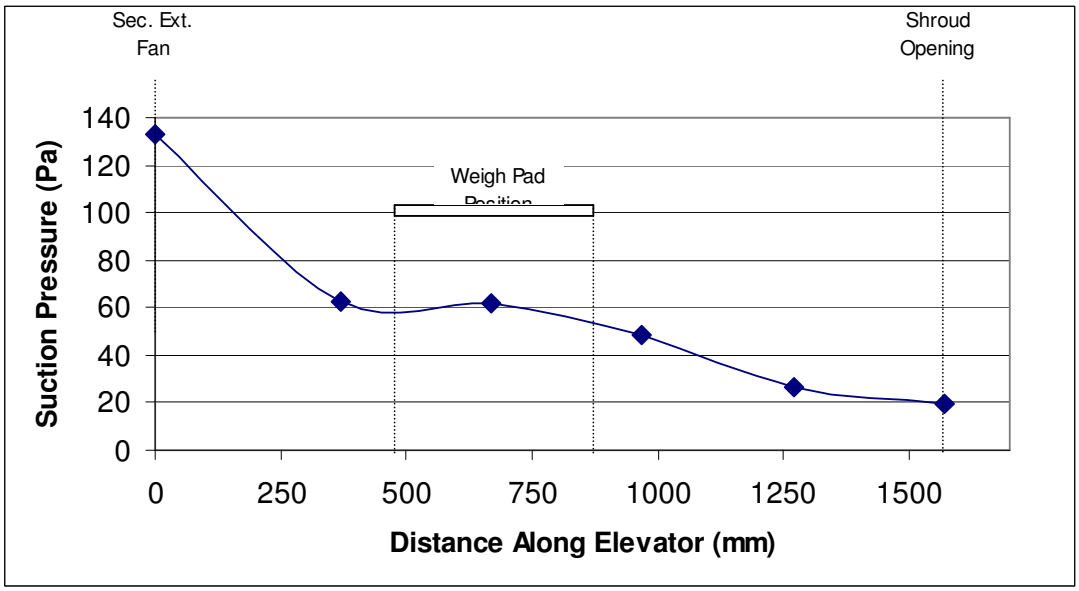

Figure 8-15. Pressure gradient measured along the elevator.

Figure 8-15 shows the suction pressure measured at various points along the elevator. The readings were measured at floor level along the centre line at six points ranging from the opening at the start of the shroud (0 mm), to the opening at the secondary extractor fan (1570 mm). Note Figure 8-3 indicated the suction pressure varies at a frequency of approximately 4

Hz. The inclined manometer did not have a dynamic response in this range and averaged the air pressures. Therefore the results given here should be considered as the average air pressure over time.

Figure 8-16 shows the pressure measured along the elevator for three different curtain positions. The three positions of the curtain along the horizontal axis are also shown. The typical position of the weigh pad along the horizontal axis is also shown. Figure 8-17 shows the same results except for the long curtain design.

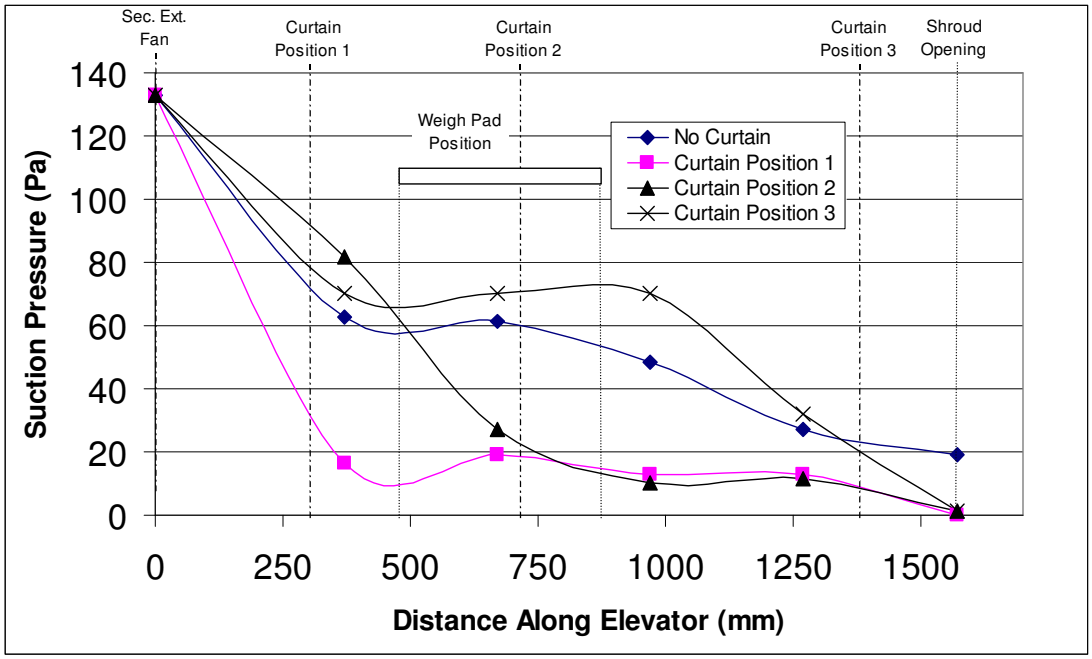

Figure 8-16. Effect of short curtain on pressure measured along the elevator for different curtain positions.

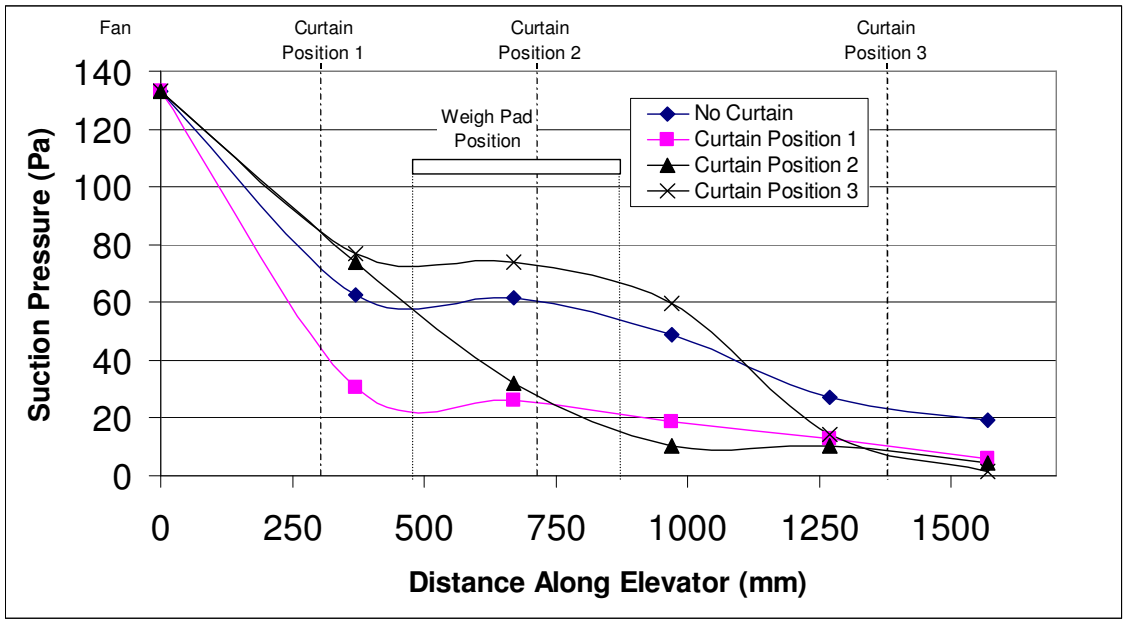

Figure 8-17. Effect of long curtain on pressure measured along the elevator for different curtain positions.

8.5 Discussion

There was a linear relationship between harvester engine speed and secondary extractor fan speed as shown by Figure 8-12. This indicates any change in engine speed will result in a proportional change in secondary extractor fan speed. Changes in engine speed can occur for a number of reasons but are mainly due to different throttle settings by the operator or a reduction in engine speed when the harvester is operating under different loads whilst harvesting. As shown in Figure 8-13, the suction pressure on the inlet of the secondary extractor fan increases with increase in the secondary extractor fan speed. Therefore any change in engine speed affects the secondary extractor fan speed, which in turn affects its suction pressure, which in turn affects the baseline reading of the weigh pad sensor.

Figure 8-13 shows the inlet and outlet air speeds of the secondary extractor fan increase in a somewhat linear fashion as the secondary extractor fan speed increase. The outlet speed is greater than the inlet speed and the difference increases as the secondary extractor fan speed increases. The suction pressure increases as the secondary extractor fan speed increases. The maximum suction pressure without curtains was 137 Pa. There was a large change in pressure of 30 Pa between 4500 rpm and 4900 rpm. This means that if the secondary extractor fan speed drops only 8%, the suction pressure drops 23%. This change would have

a large impact on the baseline value of the weigh pad.

Figure 8-14 shows there are higher air speeds towards the shroud and the low speeds towards the floor. This is likely due to the elevator flights being an impediment to the airflow closer to the floor. This air speed profile changes as the elevator flights pass. The suction pressure on the weigh pad also changes as the elevator flights pass. This is most likely the reason for the change in baseline reading shown in Figure 8-3, as the elevator flights pass over the weigh pad. Figure 8-14 shows the variation in air velocity across the elevator width is not great.

The pressure gradient along the elevator beneath the shroud covering the upper part of the elevator, as shown in Figure 8-15, was as expected with the low suction pressure at the shroud opening, increasing towards the secondary extractor fan. The average suction pressure over the position of the weigh pad was 58 Pa. Over the surface area of the weigh pad (0.29 m^2) this theoretically produces a negative force of 17 N. This agrees very closely with the results in Figure 8-3 that previously were shown to have an average suction force of 17N.

Figure 8-16 shows that the short curtain can significantly change the pressure gradient between the secondary extractor fan and the shroud opening. Generally the curtain increased the suction pressure on the secondary extractor fan side and reduced the negative pressure effects over the weigh pad. The best position for reducing the suction pressure at the weigh pad was Position 1, between the weigh pad and the secondary extractor fan. In this case, the average suction pressure on the weigh pad dropped 74% to less than 15 Pa. The worst position was Position 3, where it actually increased the suction pressure on the weigh pad.

The long curtain also increased the suction pressure on the secondary extractor fan side and reduced the negative pressure effects over the weigh pad. The best position for reducing the suction pressure at the weigh pad was Position 1. In this position it reduced the average suction pressure on the weigh pad 69% to 18 Pa. This was not quite as effective as the short curtain mainly because the long curtain fluttered considerably as it was contacted by the passing flights.

8.6 Conclusion

A linear relationship exists between harvester engine speed and secondary extractor fan speed. Therefore, any change in engine speed effects the secondary extractor fan speed which in turn effects its suction pressure and hence effects the baseline reading of the weigh pad sensor.

A pressure gradient exists along the elevator with the high suction pressure at the secondary extractor fan and decreasing suction pressure towards the shroud opening. The average suction pressure over the position of the weigh pad was 58 Pa, which equates to a negative force of 17 N.

The short curtain is effective in reducing the negative force on the weigh pad due to the secondary extractor fan by 74% from 17 N to 4.4 N. This load, as a proportion of the weigh pad load during normal cane flow, equates to a reduction from approximately -25% of the reading to -6%. The short curtain is recommended for it minimises the impact of the secondary extractor fan on the baseline drift of the weigh pad. Any change in this suction force will have a much smaller effect on the baseline reading of the weigh pad.

Chapter 9 - Weigh Pad Sensor Final Design

9.1 Introduction

Based on the results of research conducted on the weigh pad concept discussed in the previous chapters, this chapter outlines the main design considerations for the weigh pad sensor. Based on these considerations a sensor design is proposed and detailed drawings are given along with the critical parts required. The typical sensor installation is also explained.

9.2 Design Considerations

Extensive investigations have been carried out on the weigh pad concept. This has led to some important recommendations that should be taken into account when designing such a sensor.

9.2.1 Light Weight

The operating environment of the harvester applies a significant amount of mechanical noise to the weigh pad sensor. This impacts adversely on the accuracy of the sensor. The best way to minimise this adverse effect is to keep the weight of the weigh plate as low as possible. This reduces the effect of the noise on the sensor reading.

This consideration is the reason for the current aluminium design with a lightweight plastic surface. This design maintains a strong structure while keeping the weight down. Keeping the mass of the pad to less than 14 kg per m^2 of surface area is advised. This will keep the errors due to mechanical noise to reasonable levels.

9.2.2 Strength

The weigh pad must be designed with considerable strength to maintain sensor accuracy and for general operation. The accuracy of the sensor can be reduced if the actual weigh plate is designed with a low structural stiffness. This will lead to a low natural frequency that will amplify the effect of any low frequency mechanical noise. For example a piece of flat steel 3 mm thick will have a low natural frequency in the range that can effect the accuracy of the sensor. The current weigh plate design with a 40 x 40 mm RHS aluminium frame provides the necessary structural stiffness.

Weigh plate strength is also required to prevent failure and excessive deflection when large load are applied to the sensor. This is particularly necessary for the corners of the weigh plate on the edge opposite to the hinges.

9.2.3 Reliability

Reliability is a concern with the design of any component. The reliability of the weigh pad has two major aspects. The first is related to the failure that can cause harvester shutdown and the second is related to the failure that can result in data loss or erroneous data.

A minimal chance of failure that can cause harvester shut down is important. The major design consideration to prevent this is to provide bi-directional stops that prevent excessive deflection of the weigh plate. These elements are usually implemented to protect the load cell from excessive deflection that is detrimental to its operation, however in this case the prevention of failure of the whole sensor and elevator structure is necessary. The negative load stop is particularly important as it prevents the lifting of the weigh plate into the path of the elevator flights that would result in major failure. For the weigh pad design that is given in this chapter, the over/under load stop has been implemented near the load cell and can be viewed in the Load Cell Mount Assembly Drawing given later in this chapter. There is only

±1 mm deflection allowed for correct operation of the load cell. To keep this fine tolerance free from foreign matter the stops must be enclosed within a weatherproof cover.

A second form of failure would be one resulting in data loss or erroneous data. This failure is not as crucial as the previously discussed form of failure, however its probability should be minimised. This can be achieved by selecting sensor parts that are water, dust and vibration proof. Such selection is of particular importance to the load cell and electronic components. Cane harvesters are periodically cleaned down with high-pressure water and therefore electrical components must be extremely water proof with a rating of IP65 or better. Harvesters on tracks also provide considerable vibration that has caused electrical components to be shaken from PCB boards in trials. Electronic boards therefore should contain surface mount components and/or be sealed/secured with an epoxy resin.

The sensor should also be designed for minimal maintenance or adjustment requirement. This will ensure that the sensor will operate without operator input. If the sensor does require service, it should allow the rapid removal and fitting of parts when required. The current design implements various features to make this possible, including the four bolts to remove and/or adjust the height of the pad and a single bolt to undo the weigh plate from the load cell and allow the plate to hinge up and allow easy access to the components.

9.2.4 Foreign Matter Build-up

Foreign matter can build-up around the weigh pad sensor and affect its operation. The build up of foreign matter usually only affects the accuracy of the sensor output but not the operation of the harvester. The types of foreign matter build-up are dirt/mud, sugar cane tops and leaf trash and pieces of sugar cane billets.

The surface of the weigh plate is made of Ultra High Molecular Weight PolyEthylene (UHMW PE) that was chosen for, among other factors, its non-stick characteristic. Under most operating environments this prevents the build up of foreign matter over the surface of the weigh plate. Under certain conditions this can be a significant problem, particular in wet conditions where some soils have the tendency to adhere to steel surfaces. Should this occur it would severely affect the sensor accuracy if the elevator flights came into contact with this material adhered to the weigh plate surface.

The build-up of dirt/mud around the edge of the weigh plate can also cause problems with the accuracy of the weigh pad. This would affect the baseline or zero value of the sensor. This problem can be minimised by allowing generous tolerances around the edge and beneath the weigh plate to allow the foreign material to fall away. A gap of 7 mm around the edge of the weigh plate was found to give the optimum balance between allowing dirt/mud to pass through while preventing cane/trash particles from jamming between the plate and the elevator floor. A chamfered, rounded or rebated back side to the weigh pad can also assist in trash clearance, however as the plate is worn down the gap can increase which can restrict the life of the plate.

Hinging the weigh pad from the back instead of the front is another design feature that has been incorporated to minimise the effect of dirt/mud build-up around the edge of the weigh plate. Although this method may appear to make the weigh plate more vulnerable to failure by connection by the elevator flights, it does improve dirt/mud tolerance. By having the hinges at the back this allows the front of the weigh pad to be positioned slightly lower (2 mm) than the surface of the elevator floor (see Figure 9-1). The rear of the plate is also positioned slightly below the floor (1 mm). The main benefits is that mud tends to fall onto the weigh plate surface and travel to the rear of the weigh plate where mud build-up does not significantly affect the reading of the load cell and therefore accuracy.

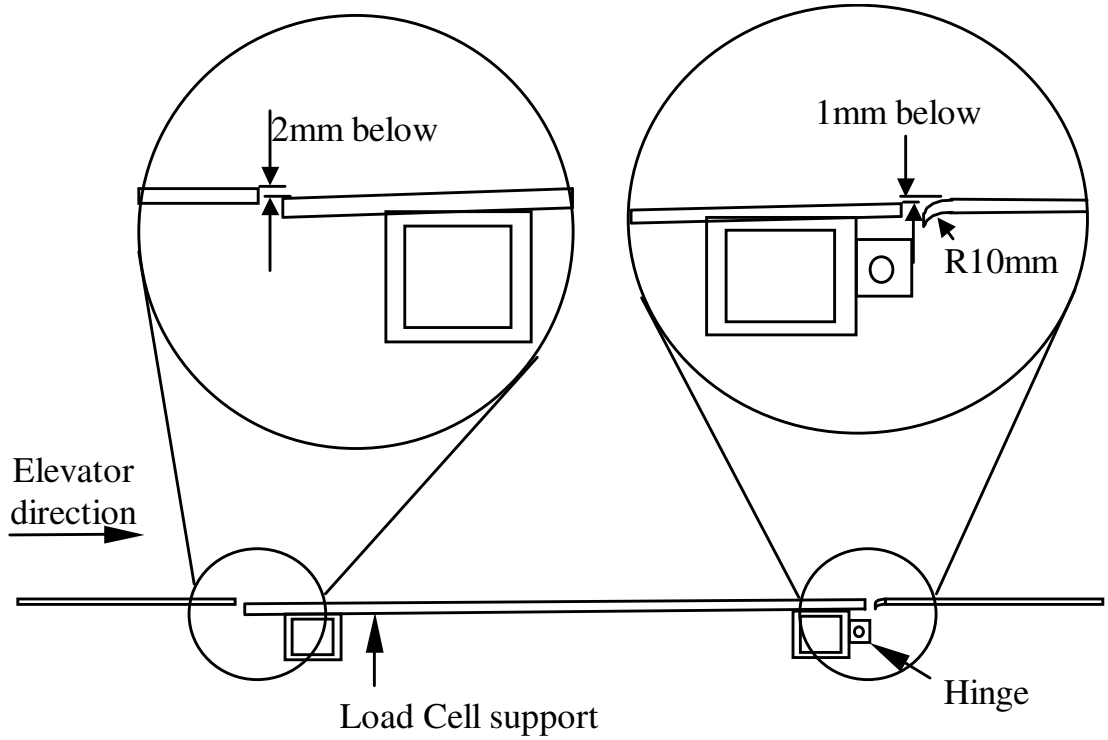

Figure 9-1. Weigh pad located to minimise effect of foreign matter build-up on sensor

accuracy.

A good clearance below the edge of the weigh plate surface is also important. This allows the foreign matter to fall through without building up. Therefore, the weigh plate surface and the elevator floor should have at least 10 mm clearance around the edges as shown in Figure 9-2.

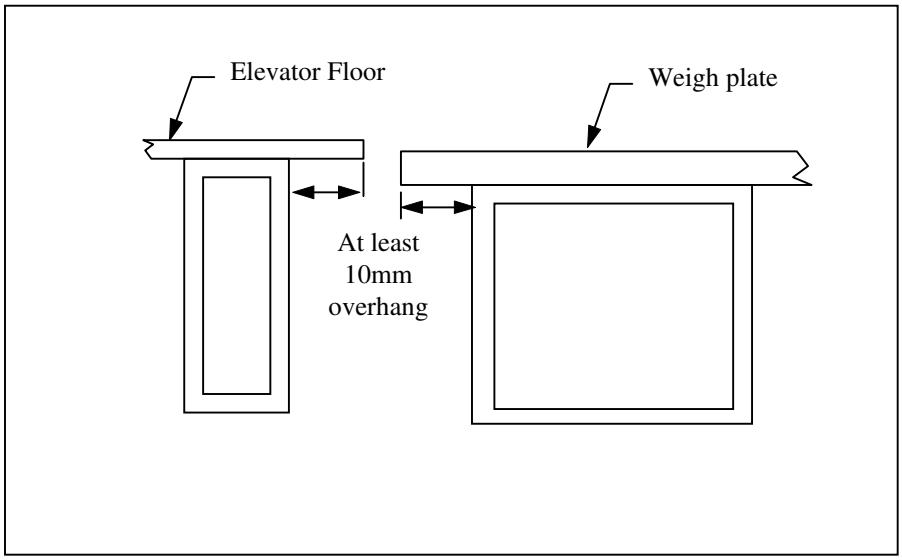

Figure 9-2. Overhang required to prevent mud/foreign matter build up around the edge of the weigh pad.

9.3 Sensor Design

The weigh pad assembly drawing is given on the following page. Following this is the load cell mount assembly drawing.

Appendix F is a report titled “Sugar Cane Yield Monitor Development: Final Report and Recommendations”. This report was presented to Case Austoft, Bundaberg to detail the proposed sensor design and recommendations for commercial application. The report includes detailed drawings for each of the components of the weigh pad sensor along with a parts list.

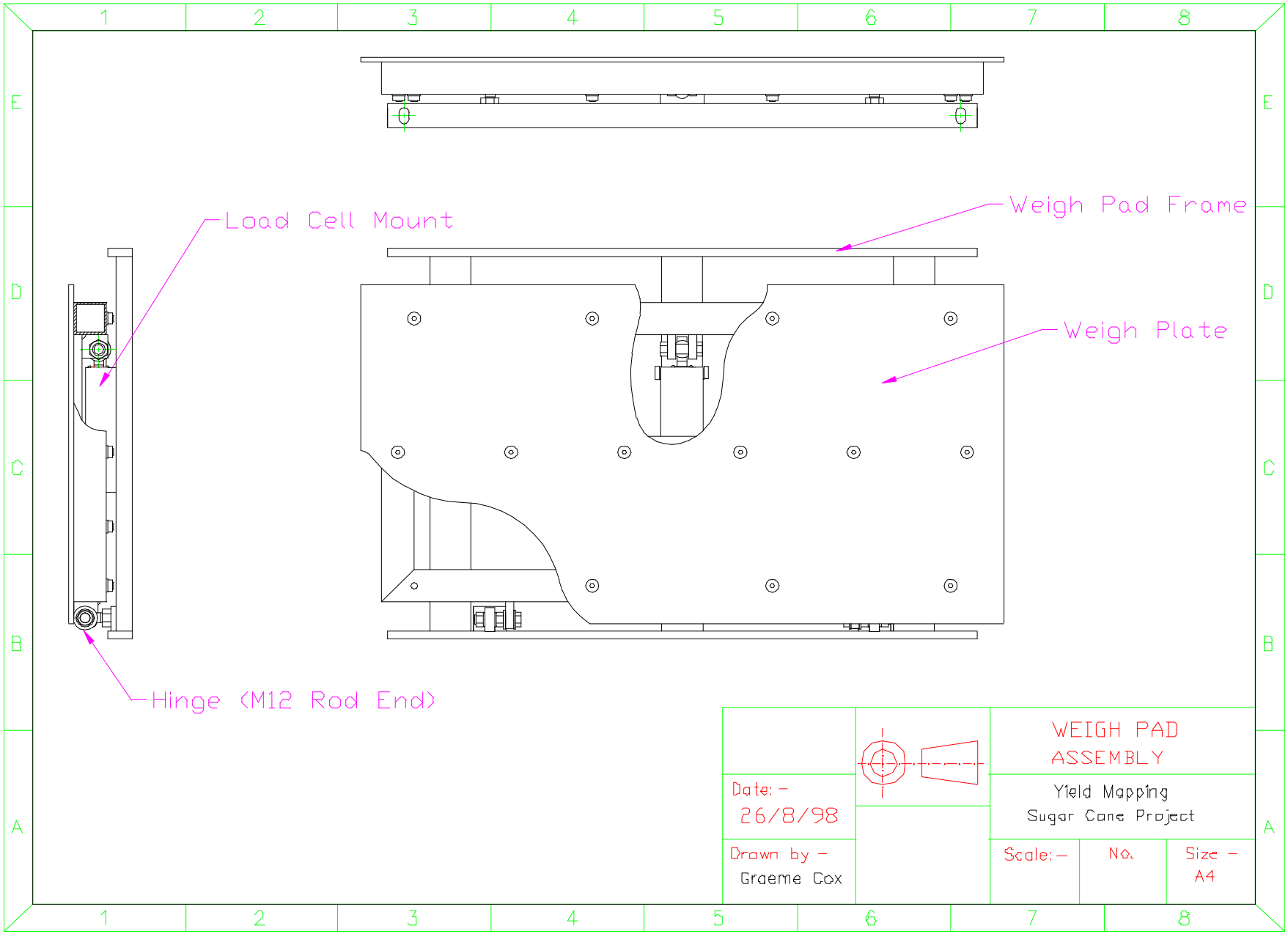
Load Cell Mount
Weigh Pad Frame
Weigh Plate
Hinge (M12 Rod End)
WEIGH PAD ASSEMBLY
Yield Mapping
Sugar Cane Project
Date: -
26/8/98
Drawn by -
Graeme Cox
Scale: -
No.
Size -
A4

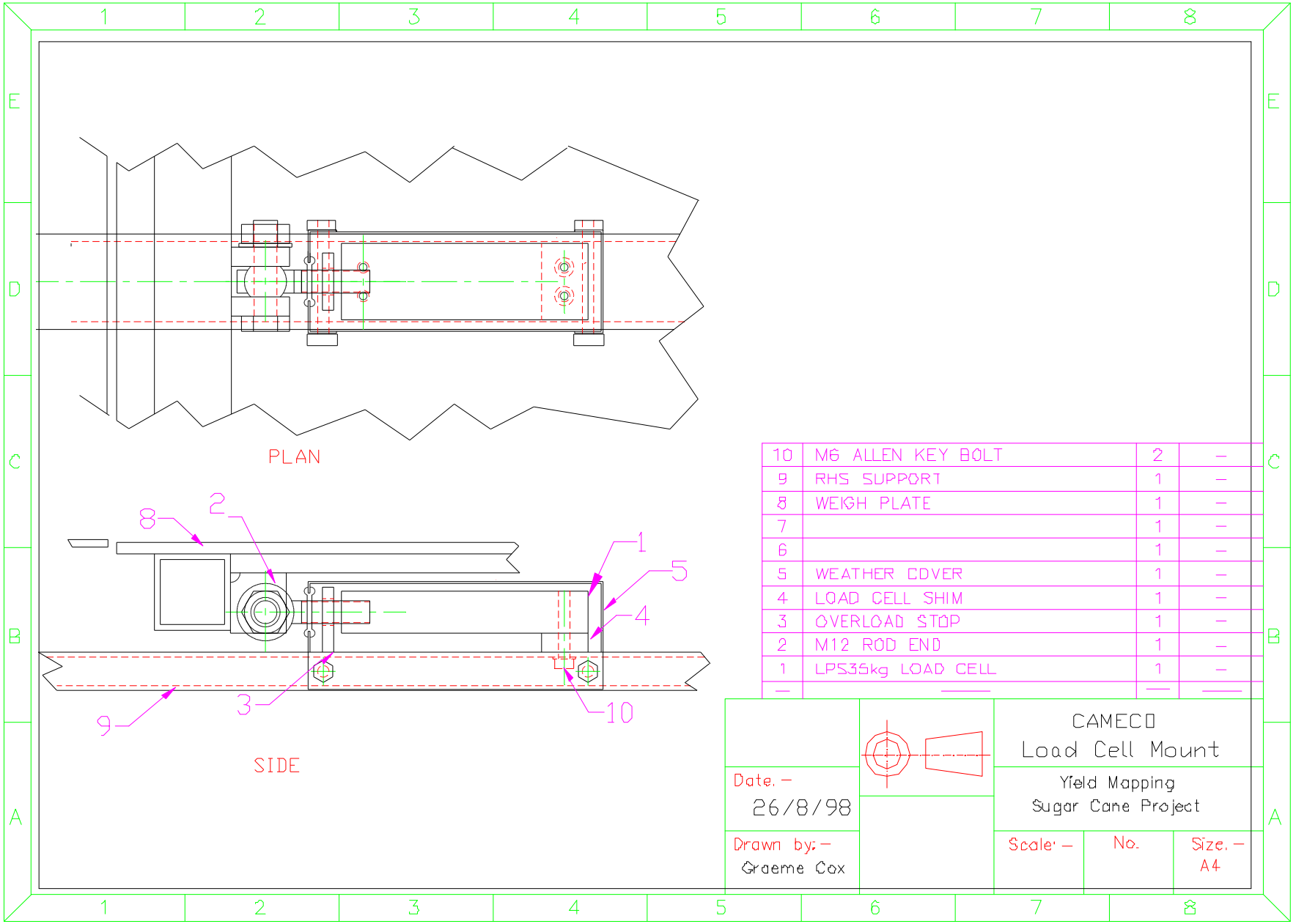

10	M6 ALLEN KEY BOLT	2	–
9	RHS SUPPORT	1	–
8	WEIGH PLATE	1	–
7		1	–
6		1	–
5	WEATHER COVER	1	–
4	LOAD CELL SHIM	1	–
3	OVERLOAD STOP	1	–
2	M12 ROD END	1	–
1	LPS35kg LOAD CELL	1	–
—	———	—	———

CAMECO
Load Cell Mount
Yield Mapping
Sugar Cane Project

Date. –
26/8/98

Drawn by: –
Graeme Cox

Scale: –

No.

Size. –
A4

9.4 Sensor Installation

This sensor design was used in a number of prototype yield monitor systems. These systems and the trials are discussed in the next chapter. The typical sensor installation for these trials is shown below.

Installation in an Austoft machine requires an extended elevator to be fitted. Installation of the weigh pad in such an elevator requires the existing floor section to be removed and replaced by the floor section with the weigh pad attached. This can be done with the elevator in a fully assembled state however installation is much simpler if such is carried out when the elevator is stripped down with no elevator chain in place. The attachment of the weigh pad sensor to the Austoft elevator floor is shown on the following page. Figure 9-3, Figure 9-4 and Figure 9-5 are photographs of the sensor installed in a harvester.

[Intentionally left blank]

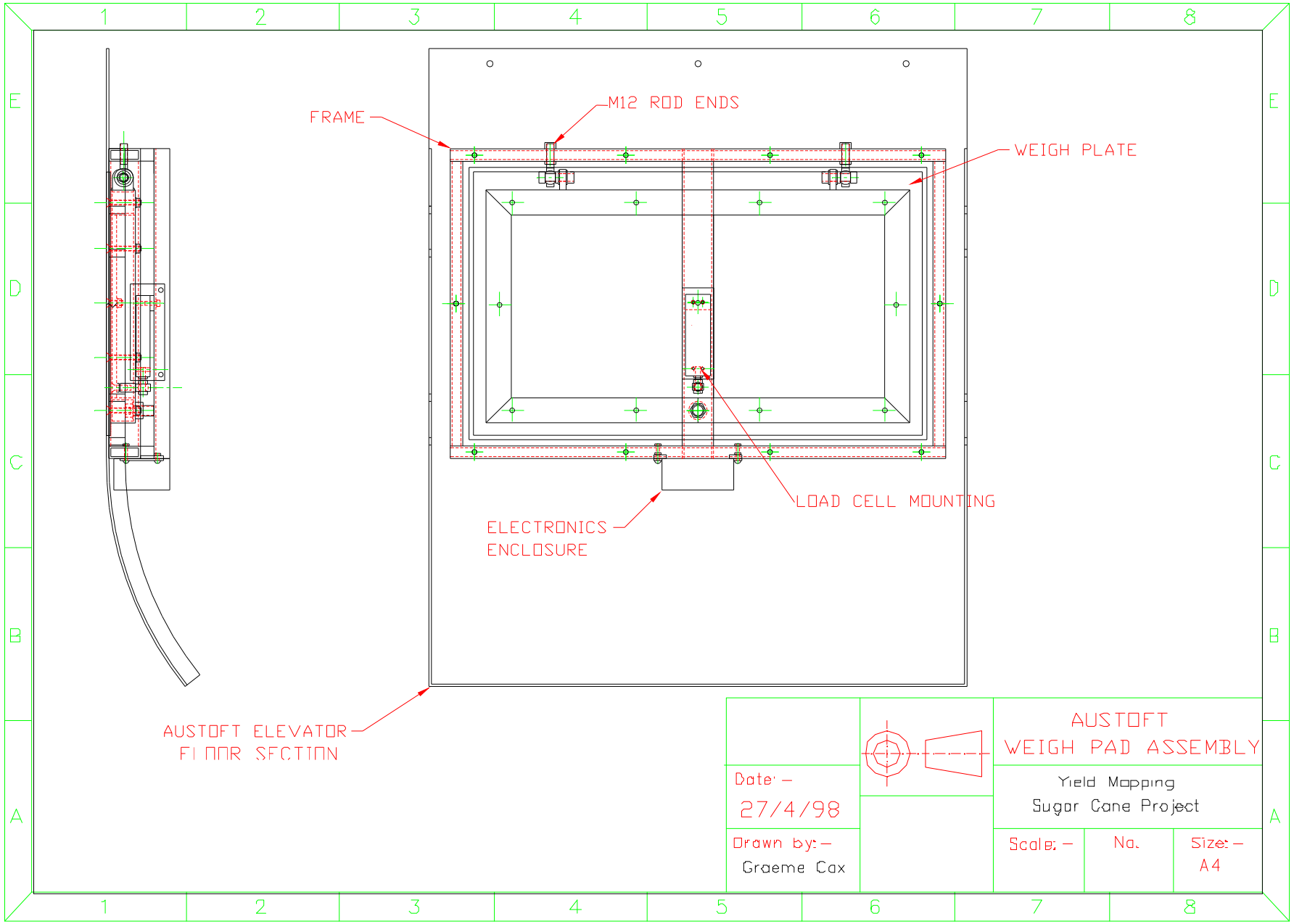
FRAME
M12 ROD ENDS
WEIGH PLATE
LOAD CELL MOUNTING
ELECTRONICS ENCLOSURE
AUSTOFT ELEVATOR FLOOR SECTION
AUSTOFT
WEIGH PAD ASSEMBLY
Yield Mapping
Sugar Cane Project
Date: –
27/4/98
Drawn by: –
Graeme Cox
Scale: –
No.
Size: –
A4

Figure 9-3. Underside view of weigh pad installed in an Austoft harvester.

Figure 9-4. Topside view of weigh pad installed in a Cameco harvester.

Figure 9-5. Close-up view of the load cell mount assembly installed on a Cameco harvester.

9.5 Conclusion

Based on the results of research conducted on the weigh pad concept, a sensor design is proposed and detailed in this chapter. The main design considerations are:

1. Minimise the weight of the weigh plate to reduce sensor error due to vibration.
2. Maximise the strength of the sensor to maximise its natural frequency and therefore eliminate the potential for low frequency accelerations/vibrations to affect accuracy.
3. Maximise the reliability of the sensor so not to negatively affect harvester operation and the supply of accurate and reliable yield data.
4. Minimising the effect of foreign matter build up on sensor accuracy.

Based on these considerations a sensor was designed and detailed drawings are given along with the critical parts required. The typical sensor installation was shown.

This sensor design was used in a number of prototype yield monitor systems. These systems

and the trials are discussed in the next chapter.

Chapter 10 - Prototype Yield Mapping System

10.1 Introduction

The previous chapters have described the design and development of weigh pad sensor to measure the mass flow rate of sugar cane through the chopper harvester. The next step is to develop a full yield mapping system to produce sugar cane yield maps. As outlined in Chapter 3, a yield mapping system or yield monitor incorporates all the components required to collect the data required for the production of yield maps. As shown in Figure 10-1, these include a mass flow sensor (in this case the weigh pad sensor), a ground speed sensor, a DGPS receiver, a yield display/monitor and data logger.

The objectives of this chapter's research was to:

a) Develop a yield mapping system for sugar cane incorporating the weigh pad sensor.
b) Test the accuracy of the sugar cane yield mapping system under field conditions in a commercial operation.
c) Test the reliability of the sugar cane yield mapping system under field conditions in a commercial operation.

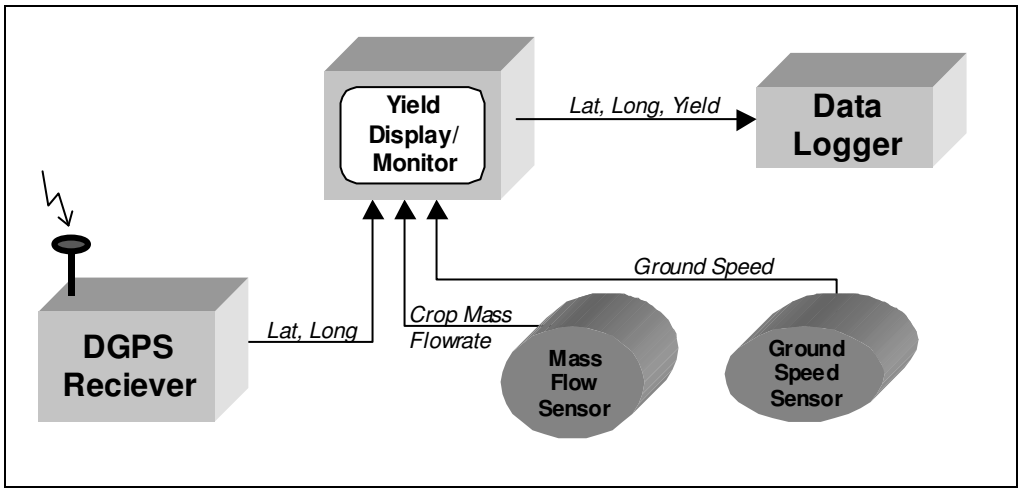

Figure 10-1. Yield mapping system components.

10.2 Materials and Method

For research purposes, the author had previously developed a yield mapping system using a laptop computer based data acquisition system. This system is discussed in detail in Chapter 6. For commercial application it was decided to use a commercially available yield mapping system and incorporate the weigh pad sensor. Microtrak's Grain-Trak system was selected.

Microtrak is an agricultural electronics manufacturer based in the USA. The Grain-Trak system is their commercial yield mapping system developed for grain harvesters. The system acquires signals from a mass flow rate sensor and a ground speed sensor to calculate instantaneous crop yield. This information is displayed on an LCD display and then logged along with GPS location coordinates (if available) to a PCMCIA flash RAM card, every one to three seconds. This system had all the necessary features to easily integrate with the weigh pad sensor to produce a reliable and practical system for yield mapping sugar cane. Figure 10-2 shows the Grain-Trak yield display that was used as the interface to the operator for calibration and measurement display.

Figure 10-2. The Microtrak Grain-Trak display/interface.

The weigh pad sensor was interfaced with the Grain-Trak system. A low pass filter with a cut-off frequency of 1 Hz was applied to the voltage signal outputted by the load cell signal conditioning circuit. The resulting voltage signal was then converted from the to a 0-5 V frequency signal, with the frequency signal proportional to the voltage. The frequency ranged from 400 Hz to 1200 Hz for the full range of the load cell.

Three identical yield mapping systems as described above were fitted to three harvesters for the entire 5 month harvest season for 1998. The reliability and operation of the systems was monitored with site visits and feedback from the operators. Problems encountered with the system are discussed in section 10.4.2.

The systems were calibrated by the standard Grain-Trak calibration procedure. This involved four steps:

a) Setting the baseline or zero value (defined as the 'null' value in Grain-Trak manual) of the weigh pad sensor. This was carried out by running the harvester at operating engine speed (full throttle) with all harvester functions running as normal including the elevator and then triggering (by the press of a button) the Grain-Trak console to record the weigh pad reading for 7 seconds. This step was also carried out every few hours of operation to remove any baseline shift.
b) Reset the load counter on the Grain-Trak display to zero.
c) Harvest a known mass of sugar cane. In most cases, the mass of harvested cane for a full day was used. This mass is measured at the sugar mill.
d) Adjust the calibration factor on the Grain-Trak display until the mass as recorded by the yield mapping system matched the mass measured by the weigh trailer.

The internal software of the Grain-Trak system used a linear calibration function. Therefore, a baseline reading and one calibration factor was required, calculated from a single load mass measurement.

10.2.1 Accuracy Trial

A trial was carried out on the 14/9/98 to test the accuracy of the yield mapping system under field conditions in a commercial operation. The accuracy was determined by comparing the yield mapping system mass totals with the mass of cane harvested into the 14 t capacity haul-out bins. The yield mapping system was installed on the Arriga District Harvesting Company's Austoft 7000 series harvester. The site was a cane farm at Mareeba, North Queensland, Australia. The harvested cane was variety Q117, unburnt and in favourable dry ground conditions.

During an 8-hour harvest shift, the mass of sugar cane harvested into each of the 35 haul-out bins was recorded (as measured by the weigh trailer) along with the mass as measured by the sugar cane yield mapping system. These masses were compared as shown in the next section.

10.3 Results

The results for the trials are given in Figure 10-3. From these results the accuracy of the system was estimated.

The Absolute error for each bin measurement was calculated as:

$$\text{Absolute Error}(\%) = \left| \frac{\text{Yield monitor measured bin weight} - \text{Mill weigh bridge bin weight}}{\text{Mill weigh bridge bin weight}} 100 \right|$$

Table 10-1 and Table 10-2 gives accuracy statistics calculated from the results presented in Figure 10-3. Figure 10-4 gives a typical yield map produced from the prototype systems.

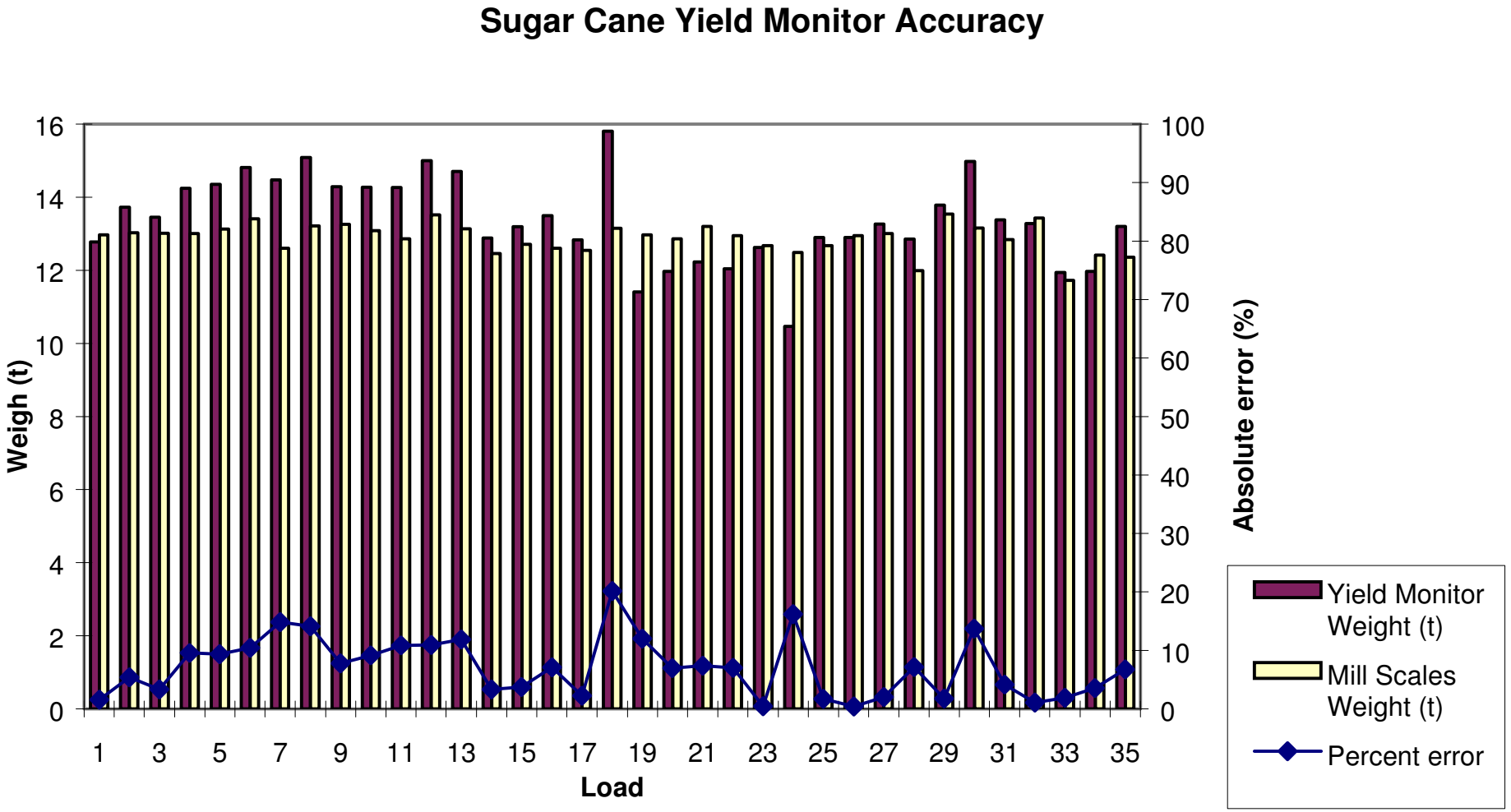

Figure 10-3. Comparison of yield monitor measurements with haul out bin weights.

Table 10-1. Accuracy of the yield monitor over each bin.

Total Number Of Bins	35
Average Bin Weights	12.9 t
Average Absolute Error	7.2 %
Standard Deviation Of Error	8 %
Error with 95% Confidence	16 %

Table 10-2. Accuracy of the yield monitor over the whole day.

Yield monitor cumulative mass	468.75 t
Mill weigh bridge cumulative mass	450.88 t
Difference	17.87 t
Error	+3.9 %

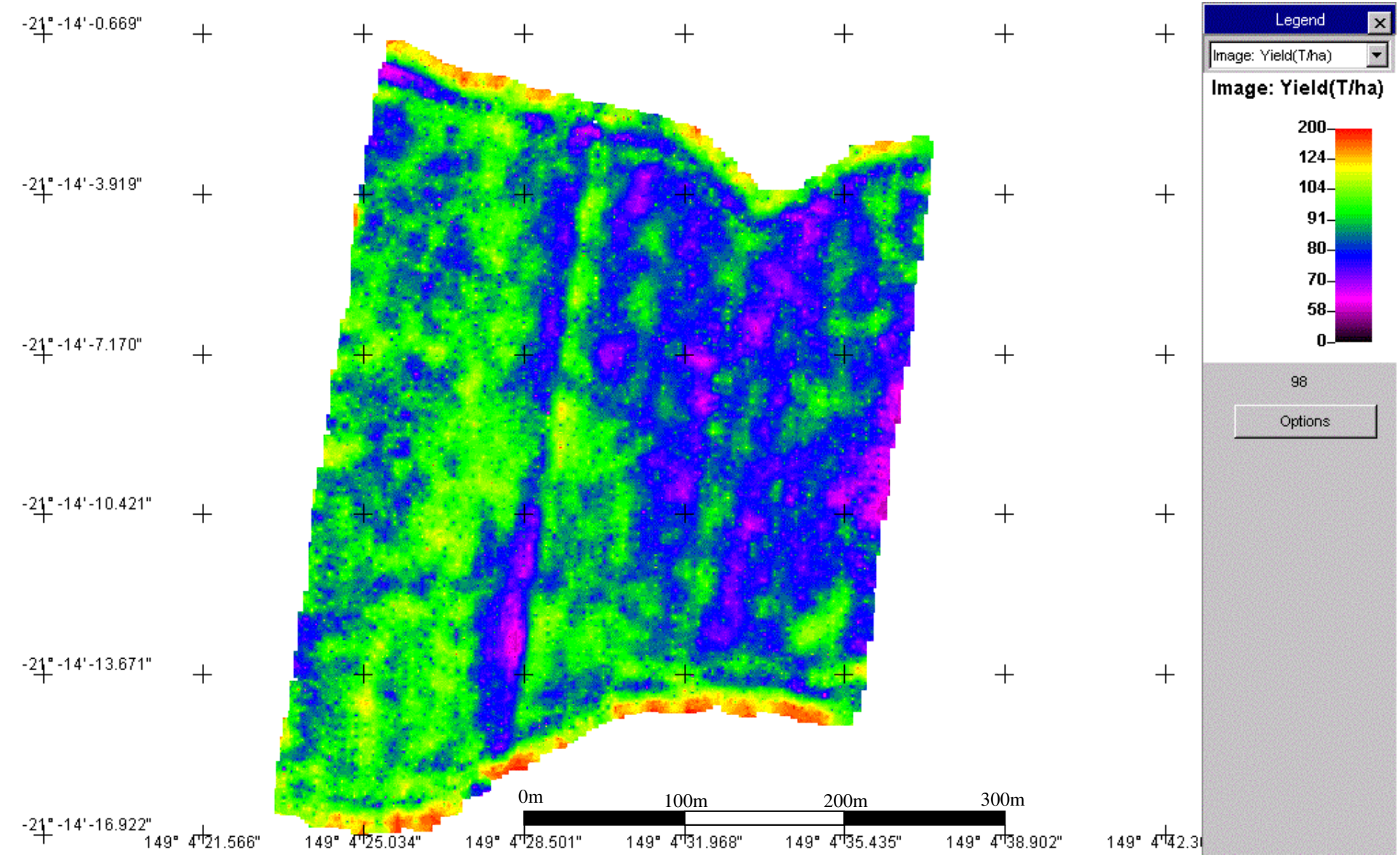

Figure 10-4. Typical yield map produced by prototype yield mapping systems. (Courtesy of D.Pollock, Pivot Agriculture, 2001)

10.4 Discussion

10.4.1 System Accuracy

The accuracy trial confirmed the level of accuracy being achieved by the weigh pad sensor was not close to the accuracy goal stated previously. In this case the error for 95 % confidence was 16 %. Assuming an average weight of 14 t per bin and an average yield of 100 t/ha, the area harvested for each bin was approximately 1400 m^2. The accuracy goal previously stated was less than 5 % error with 95 % confidence over a measurement area of $100m^2$.

Although the accuracy achieved was not to the desired research goal, the harvester operator and farm manager were satisfied with the level of accuracy achieved. The logic behind this was the fact that yield variations within the paddock typically ranged more than 200 % (i.e. from 60 t/ha – 180 t/ha). A yield map constructed with data of the accuracy level measured above produced yield maps with satisfactory detail to make management decisions.

The result for the day of +3.9 % error was encouraging and indicated the improved accuracy of the system over larger measurement areas.

10.4.2 Weigh Pad Sensor Operation

The weigh pad sensor operated satisfactorily on the three prototype systems. Two notable problems were encountered which affected the accuracy of the weigh pad measurements. These were baseline drift and flight contact. There are two potential techniques to overcome these problems. One is to incorporate an auto-zeroing method to overcome baseline drift and the second is to incorporate a type of “batch weighing” to overcome the problem of flight contact. These techniques are outlined below.

Auto-Zero

Most weighing systems incorporate auto-zeroing functions to minimise the error due to drift

in this zero value. In the weigh pad situation this is vital as the zero can drift significantly over a period of minutes for a number of reasons including foreign matter build up. Figure 10-5 shows thin cane stalks wedged in the leading edge of the weigh pad, which is a typical cause of baseline drift.

Auto-zeroing involves monitoring the tare value of the weigh pad sensor and setting the value as the zero for the mass flow rate calculations. A possible technique to enable auto-zeroing would be to remove a single flight from the elevator and as the space left by this flight passes the weigh pad, trigger a zero reading. This would result in a zero measurement occurring every five seconds. At the time of writing this technique has subsequently been successfully developed and is used on current commercial yield monitors.

The removal of a flight will only reduce the capacity of the elevator by 5 %, which is acceptable. To regain this capacity the elevator could be sped up 5 % or the width of the elevator increase by 5 % at manufacture.

Figure 10-5. Leaf matter wedged between the weigh plate edge and the elevator floor.

Batch Weighing

In wet conditions or in green cane harvesting, foreign matter such as mud and/or trash can build up on the lower edge of the elevator flights (See Figure 10-6, Figure 10-7, Figure 10-8, and Figure 10-9 for examples). This material places the flights in contact with the weigh plate and the downward force produces erroneous mass flow rate measurements. The current signal processing technique uses the average load cell output over each second to calculate the average mass flow rate. This technique is susceptible to the effect of the elevator flights. To overcome this problem, the signal processing could be changed to measure only when the flights are not over the weigh pad. This would only be a fraction of a second as each flight passes. The only problem with this technique is that the hinged weigh pad design could not be used. A design that is uniformly sensitive to weight along its full length is required otherwise a non-linear calibration curve will result. A proximity sensor is also required to measure the position of each flight as it approaches the weigh pad.

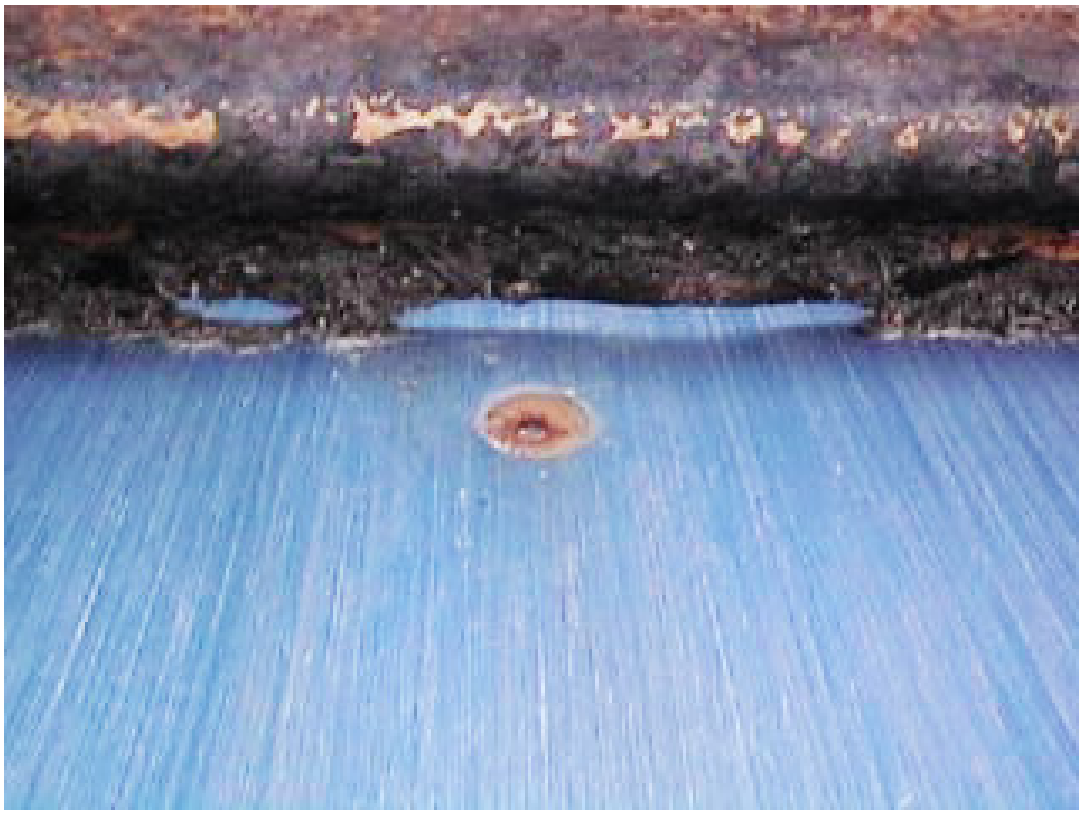

Figure 10-6. Clearance between the weigh plate and an elevator flight, viewed from behind the flight in the direction of elevator travel.

Figure 10-7. Build up of extraneous matter (mainly mud) on the base of an elevator flight just prior to travelling over the weigh plate. (Viewed from above and in front of the flight).

Figure 10-8. Build up of extraneous matter (mud and leaf matter) on the base of an elevator flight. (Viewed from above the flight).

Figure 10-9. Piece of sugar cane billet wedged under an elevator flight just prior to travelling over the weigh plate. (Viewed from in front of the flight).

10.4.3 Yield Mapping System

Changes Specific to Microtrak Grain-Trak Yield Monitor

During the 1998 season the Microtrak Grain-Trak console worked well with the weigh pad sensor. It has all the necessary features to be used for yield mapping of sugar cane. There are some minor software modifications that could be implemented to improve the operation in sugar cane. These are:

1. Prevent the cumulative mass totals from incrementing once the run/hold switch is on hold. Currently the console is set up for grain yield mapping where the grain can continue to flow past the mass flow sensor for up to 30 seconds after the machine has stopped harvesting. In sugar cane harvesting where the run/hold switch is operated by the on/off operation of the elevator, mass flow stops immediately when the elevator is stopped. However the Microtrak console continues to accumulate the extra mass after the elevator has been shut down.

2. Change the lag time in the yield calculation to 5 seconds as explained below.
3. Have the option to use GPS derived ground speed measurements as explained below.

GPS Ground Speed

Currently, the standard technique for measuring ground speed for yield mapping is a proximity sensor on a wheel or track. In the sugar cane harvesting environment this sensor can be difficult to maintain in wet weather conditions. For this reason it would be desirable to have the option to use the ground speed as measured by the GPS receiver. Initially when yield mapping first began this was not advisable as the accuracy of the DGPS receivers was not good enough. However, the latest receivers have improved considerably to be as good or better than the traditional means of measuring speed.

GPS systems such as the Trimble AgGPS 132 are quoted to achieve speed accuracy's of 0.16 kph or 0.044 ms^{-1} (Trimble Inc., 1998). This would produce an error of 2.3 % when compared to the average harvesting speed of 7 kph or 1.94 ms^{-1}. This is satisfactory and would be comparable to the accuracy of the current methods. The recent removal of "Selective Availability" on the GPS may have improved the accuracy even further.

Lag Time

There is a lag between the time when the cane is cut at the base cutters and when it is weighed by the sensor. This lag can be important for two reasons. The first is related to the calculation of the yield on a point by point basis and the second is related to the alignment to the correct GPS coordinates. In the first case the yield is calculated by the mass flow rate divided by the harvester ground speed as shown in Equation 3.1. For yield to be calculated accurately it is important to be able to align the mass flow rate measurement with the correct ground speed measurement. For the most accurate and strictest application of Equation 3.1, the mass flow rate of cane at the base cutters should be divided by the ground speed at the same time. This is not possible, as the mass flow rate sensor is not situated at the base cutters. There is a time delay of approximately 5 seconds between when the cane is cut at the base cutters and when is measured at the weigh pad. This delay must be incorporated into the yield calculation and is done by simply delaying the ground speed measurement by 5 seconds. As the yield measurements will be delayed by 5 seconds using this technique, the GPS coordinates should also be delayed so that they coincide with the correct yield measurements. In sugar cane yield mapping this delay is not as much of a problem as in

grain yield mapping where the delay can range from 10 to 30 seconds.

Convolution of the harvested material within the harvester can lead to difficulties for yield monitoring other crops such as grain and peanuts. In these cases the crop material takes significant time to be threshed from extraneous matter and can have a number of routes through the threshing process. Boydell *et al.* (1995) closely examined the dynamics of peanut flow through a peanut combine and showed that the mass flow rate measured by a sensor could be by deconvoluted using simple first order system response equations. This problem is not significant for sugar cane yield mapping and does not warrant further analysis at this point.

Data Storage and Processing

Sugar cane yield mapping is slightly different to yield mapping in grain crops. The major difference is the narrow width of harvest in sugar cane (1.5 m). This narrow width leads to cane yield mapping producing 4 times as much data as grain yield mapping. For this reason the time which each yield reading represents can be extended. In grain yield mapping it is advised to record yield measurements each second. In cane however, it is recommended to average the data over 3 seconds. This will reduce the amount of data and save on processing time and transfer time. This will not reduce the accuracy of the yield information, as the data needs to be significantly smoothed during the map production stage in any case.

Yield Map Production

Sugar cane has some inherent advantages and disadvantages for the production of yield maps when compared to yield maps produced from grain harvesters. These include:
Advantages:

1. There are more yield measurements for the same unit area harvested. This can lead to better accuracy or improved resolution of the yield map.
2. Convolution of the mass flow rate signal is not a big problem as in grain harvesters.

Disadvantages:

1. More points to process and store for the same unit area harvested. This leads to increased processing time and increased hardware cost.
2. More stopping and starting during harvest, which can lead to convolution problems

and timing problems and subsequently extra yield measurement errors.

After the data are collected on the harvester, they must be computer processed to produce the actual yield map. During this stage the data are smoothed from the point yield data to a contour map or something similar. This is a crucial process in yield map production to achieve meaningful maps. The smoothing averages out a lot of the noise that is present in each individual yield reading. The larger the area the data is smoothed over, the more accurate the yield map becomes. Obviously, however, too much smoothing diminishes the value of the yield map. For the current weigh pad sensor it is advisable to smooth or average the data over an area of at least 400 m^2 to get useful results. This equates to an area of 20 m x 20 m or a search radius of 11 m.

10.5 Conclusion

A yield mapping system was developed for sugar cane incorporating the weigh pad sensor. Three identical systems were constructed and installed on three harvesters for the 1998 cane harvester season. The results show sugarcane can be yield mapped using general yield mapping principles. No special techniques are required just a reliable mass flow sensor. The Microtrak Grain-Trak console worked satisfactorily with the weigh pad sensor. It has all the necessary features to be used for yield mapping of sugar cane. There are some minor software modifications that could be implemented to improve the operation in sugar cane.

The level of accuracy being achieved by the yield mapping system was less than 16 % error, with 95 % confidence, over measurement areas of approximately 1400 m^2. Although the accuracy achieved was not to the desired research goal, yield maps were produced with satisfactory detail to make management decisions.

The reliability of the sugar cane yield mapping system under field condition in a commercial operation was satisfactory. However, the auto-zeroing and batch weigh techniques should be tested to improve the reliability of the weigh pad readings during wet harvesting conditions.

After note: At the time of writing the features recommended in section 10.4.3 have been implemented in a specialised data logger/display developed specifically for this task. This was developed by the NCEA for Case Austoft as part of the commercialisation efforts.

Chapter 11 – Conclusion

11.1 Review

Yield mapping was reviewed for the theory involved, the technology required, its justification, and previous developments. The main limiting component in applying yield mapping to sugar cane was the lack of a suitable flow rate sensor. The other components of a yield mapping system could be developed or modified to suit the specific requirement of sugar cane.

Existing mass flow rate techniques for yield mapping other crops were reviewed. The nature of the measurement errors for these sensors was closely examined. The errors found in yield mapping systems could generally be classed as random. However, this error reduces as the measurement time or harvest area increases. These findings indicated that stating the accuracy of a yield monitor mass flow rate sensor using only the average error can be misleading. The accuracy of a yield monitor or mass flow rate sensor needs to be defined by three factors:

1. Percentage error of measurement
2. Confidence limit of this value (e.g. 95% of the time).
3. Area over which the measurement is made.

The functional and performance requirements of a sugar cane mass flow sensor were outlined. Important functional requirements included robust and simple calibration, and ability to operate properly in rough, dusty and moist conditions. Performance requirements have been defined as the accuracy of the mass flow sensor. Based on a review of the accuracy of grain mass flow sensors and assumptions concerning the measurement accuracy

required for agronomic purposes in sugar cane, a desirable and achievable accuracy goal for the sugar cane mass flow sensor was proposed as:

- less than 5% cumulative measurement error,
- 95% of the time (2 standard deviations),
- measured over a 100 m^2 harvest area.

Existing mass flow sensors for other crops were reviewed. Based on this review four potential techniques were proposed to measure the mass flow rate of sugar cane through the chopper harvester. These techniques were defined as:

1. Chopper Power Measurement

   Uses the hydraulic power required to chop the sugar cane into billets as an indicator of the mass flow rate.

2. Elevator Power Measurement

   Uses the hydraulic power required to elevate the billeted sugar cane into the 'haul-out' vehicle as an indicator of the mass flow rate.

3. Volumetric Measurement

   Uses the separation distance between the feed rollers of the harvester feed train as a volumetric indicator of the mass flow rate.

4. Mass Measurement

   Involves weighing the cane flow through the elevator of the harvester as it passes over a weighing platform defined as the 'weigh pad'.

Initial field trials were carried out on each of these techniques. The primary objective of the trials was to compare the performance of the four sensing techniques to assess their potential accuracy, limitations and problems. The four techniques were tested simultaneously by placing various sensors on a single harvester and comparing the sensor outputs with the mass flow rate as measured by a weigh truck. From these trials the main conclusions were:

- Both the chopper power and elevator power techniques suffered from drifting baseline values that seem to be a source of significant error. The calibration line slope was also significantly affected by crop conditions.
- The feed roller separation technique had a stable baseline value but the calibration line slope was significantly affected by crop conditions.
- The weigh pad technique suffered from very small load cell sensitivity to flow rate, drifting in baseline readings and susceptibility to mechanical noise/acceleration dynamics.

All techniques offered potential but none produced results close to the accuracy goal. The

weigh pad technique offered the most potential for improvement and potential to accurately measure the mass flow rate with a single calibration under all conditions. Therefore it was decided the weigh pad technique warranted further analysis to optimise the design for accuracy.

An opportunity arose to install a complete yield mapping system on a harvester within a commercial operation. This opportunity was accepted to assess the potential for applying yield maps to the agronomic management of sugar cane. A field was selected to act as a case study. Yield mapping was firstly conducted on the field. This involved developing an experimental yield mapping system. Because the weigh pad sensor required further development at this stage, chopper and elevator power were used as a measure of mass flow rate. The resultant yield map displayed significant yield variation from 70t/ha to over 190t/ha. Soil sampling was then conducted to determine the cause of the yield variation. Linear correlation analysis of soil parameters against yield found results that confirmed what was suspected. High sodium levels in the soil were producing a soil with poor structure, which minimised water infiltration and storage. Magnesium played a significant part in the problem and exacerbating the effect of sodium. Based on these results a variable rate gypsum application map was developed. Economic analysis of the proposed variable rate gypsum application has shown a benefit of at least $563/ha over a five year period, when compared with standard management of blanket gypsum application.

Further analysis on the weigh pad sensor involved examining the dynamic response of the weigh pad sensor. Theory was developed to mathematically model the effects of acceleration dynamics on the accuracy of weigh pad sensor. The model defined the relationship between measurement error, time that the measurements are averaged over and the mass being measured. This equation shows there are some different ways to reduce the error of the sensor. These were:

- Minimise the magnitude of the acceleration applied to the weigh pad sensor by introducing shock absorbers into the sensor system.
- Minimise the mass of the weigh plate.
- Increase the sample time. This option is limited by the spatial resolution desired for the yield maps. Over the target area of $100m^2$ at a normal operating speed of 8kph and a row width of 1.5 m this leaves 30s for averaging measurements.

Laboratory bench testing supported the mathematical model. From the theoretical and experimental analysis a number of conclusions were drawn:

- The weigh pad should be made as light as possible to minimise the error due to

dynamic conditions.

- Electronic analogue filters should be used to reduce the noise due to external acceleration.
- The weigh pad should be as rigid as possible to maximise its natural frequency.

A new weigh pad sensor was designed based on these conclusions. Field trials were carried out to determine if the changes actually improved its accuracy. The results indicated the effects of external accelerations dynamics were significantly reduced. However, the accuracy achieved during the field trials was not within the accuracy goal. The main factor limiting accuracy was a drift in the baseline value of the sensor.

The potential of real time acceleration measurements to improve the accuracy of the weigh pad was examined. The results showed for this technique to work, the acceleration signal would need to be significantly smoothed over time to keep its magnitude positive around 1g. Averaging the acceleration measurements over a period of 1 to 5 seconds could do this. The improvement in weigh pad accuracy using this technique however would only be marginal. An accelerometer was concluded to have more potential in removing any bias due to change in slope of the weigh pad sensor. This was examined by McCarthy (1998).

The baseline drift of the weigh pad was caused by a number of factors including the secondary extractor fan of the harvester, which induced a negative pressure on the weigh pad. This problem was examined to determine the extent of the problem and propose solutions. A pressure gradient was found to exist along the harvester elevator with low suction pressure at the shroud's lower opening and increasing to high suction pressure at the secondary extractor fan. This resulted in the pressure on the topside of the weigh pad being negative, somewhere between the two. The pressure on the underside of the weigh pad was atmospheric or close to it. Therefore the pressure differential between the top and underside of the weigh pad induced a negative force on the weigh pad load cell. This force was equal to the pressure differential between the top and underside of the weigh pad (58 Pa) multiplied by the surface area of the weigh pad (0.29 m^2), which equated to a negative force of 17 N. This load, as a proportion of the weigh pad load during typical cane mass flow rates (50 N), equated to over 30% of the reading.

A rubber curtain placed between the weigh pad and the secondary extractor fan was proposed to minimise this suction force. The curtain reduced the negative force on the weigh pad due to the secondary extractor fan by 74% (from 17 N to 4.4 N). This load, as a proportion of the weigh pad load during normal cane flow, equates to reduction from around

-34% of the reading to -9%. The curtain was recommended for use to minimise the impact of the secondary extractor fan on the baseline drift of the weigh pad.

Based on the results of research conducted on the weigh pad concept, a sensor design was proposed and detailed. The main design considerations were:

1. Minimise the weight of the weigh plate to reduce sensor error due to mechanical noise/dynamics.
2. Optimise the strength of the sensor so that its natural frequency was great enough to minimise the potential for low frequency accelerations/vibrations to affect accuracy.
3. Maximise the reliability of the sensor so not to negatively affect harvester operation and the supply of accurate and reliable yield data.
4. Minimising the effect of foreign matter build up on sensor accuracy.

Detailed drawings were given along with the critical parts required. The sensor installation methods for the two common types of chopper harvesters were also given.

A yield mapping system was developed for the sugar cane chopper harvester incorporating the weigh pad sensor, a ground speed sensor, a DGPS receiver, a yield display/monitor and data logger. A commercially available yield mapping system for grain harvesters (Microtrak's Grain-Trak) was interfaced with the weigh pad to achieve this. Three identical systems were constructed and installed on three harvesters for the 1998 cane harvest season. The results showed sugar cane could be yield mapped using standard yield mapping principles. No special techniques are required except a reliable mass flow sensor.

The level of accuracy being achieved by the yield mapping system had less than 16% error, with 95% confidence, over 0.14 ha. Although the accuracy achieved was not to the desired research goal, yield maps were produced with satisfactory detail to make agronomic management decisions.

The reliability of the sugar cane yield mapping system under field condition in a commercial operation was satisfactory. However, two techniques were proposed (auto-zeroing and batch weigh techniques) to improve the reliability of the weigh pad readings during wet or adverse harvesting conditions.

11.2 Conclusions

This research has been very successful in achieving the stated objectives. The first sugar cane yield mapping system in the world has been developed. This system is being commercially adopted by the largest sugar cane harvester manufacturer in the world, CASE Austoft.

The specific objective of developing a reliable means for measuring mass flow rate through a chopper sugar cane harvester have been accomplished with the weigh pad sensor. Measurement from this sensor were combined with GPS information to derive yield mapping data. GIS techniques were used to develop the first sugar cane yield maps in the world.

The accuracy goal of less than 5% error for 95% of the samples harvested over an area of $100m^2$ was not achieved by the prototype system (16% error for 95% of samples measured over an area of $1400m^2$, see Section 10.4.1) but yield maps from data of the systems were useful for agronomic purposes.

11.3 Recommendations for Further Research

As discussed in Chapter 10, there are two problems which can significantly affected the accuracy of the weigh pad sensor. These were defined as 'baseline drift' and 'flight contact'. Two potential techniques are proposed to overcome these problems. One is to incorporate an 'auto-zeroing' method to overcome baseline drift and the second is to incorporate a type of 'batch weighing' to overcome the problem of flight contact. More details on problems and techniques are given in Chapter 10. It is recommended these techniques be tested in the field.

The 'auto-zeroing' method and some other features recommended in Chapter 10 have subsequently been implemented in a specialised data logger/display developed specifically for this task. This was developed by the NCEA for Case Austoft as part of the commercialisation efforts. Case Austoft is continuing to conduct research and development on the system and is intending to make the yield mapping system available as a standard item on new harvesters and a retrofit unit on existing harvesters in the near future.

References

@g/Innovator Online, 1996, 'Yield monitor manufactures' [Online], Available from: http://www.agriculture.com/technology/, [Accessed 9/9/2001]

Ag Leader, 1997, *Grain Yield Monitor Product Literature*, Ag Leader, Ames, IA, USA

Agco, 1998, *Precision Agriculture*, [Online], Available from: http://www.agco.com/pa [Accessed March, 1998]

Algerbo, P., & Ehlert, D., 2000, Evaluation of Yield Sensing Systems for Potato Harvesters, Proceedings of the Fifth International Conference on Precision Agriculture. ASA-CSSA-SSSA, St. Paul, MN.

Anonymous, 1994, *Precision Agriculture Web Page*, [Online], Soil Science Department of the University of Minnesota, Available from: gopher://gopher.soils.umn.edu:70/00/ssfm/about, [Accessed March, 1996]

ANZECC, 1992, *Australian water quality guidelines for fresh and marine waters*. Australian and New Zealand Environment and Conservation Council. Canberra.

Arslan, S. & Colvin T.S., 2002, An Evaluation of the Response of Yield Monitors and Combines to Varying Yields, Precision Agriculture Journal, 3 (2): 107-122, Kluwer Academic Publishers

Asgrow Seed Company, 1997, *Comparison of Weigh Wagon and Yield Monitor Results*, [Online], Available from: http://www.asgrow.com/AsgrowFarms/CFR97CnYldMon1.html [Accessed 27/11/1997]

Auernhammer, H., Demmel, M., Muhr, T., Rottmeier, J. & Wild, K. 1994, 'Site Specific Yield Measurement in Combines and Forage Harvesting Machines', In: *Proceedings of the International Conference on Agricultural Engineering*, Milano, 29th Aug. - 1st Sept., 1994. part 2, ppa. 698 - 699.

Bakker, A.C. & Emerson, W.W., 1973, 'The comparative effects of exchangeable calcium, magnesium, and sodium on some physical properties of aggregates from subsoils of red-brown earths. II. The permeability of Shepparton soil and comparison of methods'. *Aust. J. Soil Res.* 11, 143-50

Benjamin, C.E., Price, R.R. & Mailander, M. P. 2001. *Sugar Cane Yield Monitoring System.* ASAE Paper No. 011189. ASAE, St. Joseph MI.

Benlloch, J.V., Sánchez, A., Christensen, S. & Walter, A.M., 1996, *Weed mapping in cereal crops using image analysis techniques.* AgEng Conference, Madrid, 1996, Paper 96G-0.47, 9 pp.

Birrell, S.J., Sudduth, K.A., & Borgelt, S.C. 1996, 'Comparison of sensors and techniques for crop yield mapping', *Computers and Electronics in Agriculture*, Vol. 14 1996, pp. 215-233.

Borgelt, S.C., & Sudduth K.A. 1992, *Grain Flow monitoring for in-field yield mapping*. ASAE/SAE paper no. 92-1022.

Boydell B., Vellidis G., Perry C., Thomas, D.L., & Vervoort, R.W. 1995, 'Dynamics of peanut flow through a peanut combine', In: *Proceedings of the third international conference on Precision Agriculture*, 1996, Robert P.C., Rust R.H. & Larson W.E., (ed.) Minneapolis, MN June 23-36,1996.ASA, CSSA, SSSA Madison, WI

Bramley, R.G.V. & Johnson, A.K.L. 1996, 'Land use impacts on nutrient loading in the Herbert River'. In *Proceedings of a conference on the Downstream Effects of Land Use*, Rockhampton, April 1995', (Eds. A.G. Eyles, H.M. Hunter & G.E. Rayment). (Department of Primary Industries, Queensland: Brisbane)

Campbell, R.H., Rawlins, S.L., & Han, S. 1994, *Monitoring methods for potato yield mapping*. ASAE Paper No. 941584. ASAE Winter Meeting (1994). Atlanta, Georgia, December 12-15, 1994.

Clark, S.J., Schrock, M.D. & Young, S.C. 1987, *Agricultural Engineering Research for Agriculture 2000*. ASAE/SAE paper no. 87-2016.

Colvin, T.S., Karlen D.L. & Tisher, N. 1991, 'Yield variability within field in central Iowa'. In: *Automated Agriculture for the 21st Century, Proceedings of the 1991 symposium*, pp 366-372 ASAE publication No 1191, ASAE St Joseph MI USA.

Cora, J.E., and Marques J, 2000, *The Potential for Precision Agriculture for Soil and Sugarcane Yield Variability in Brazil*, Proceedings of the Fifth International Conference on Precision Agriculture. ASA-CSSA-SSSA, St. Paul, MN.

Cox, G., Harris, H., Pax, R. & Dick, R. 1996, 'Monitoring cane yield by measuring mass flow rate through the harvester'. *Proc. Aust. Soc. Sugar Cane Technol.* 1996 Conference

De Baerdemaeker J., Delcroix & Lindemans, P. 1985, *Monitoring the grain flow on combines*, Paper presented at Agri-mation Conference and Exposition, Feb. 1985, Chicago. ASAE Pub. 01-85.

Doerge, T. 1997, 'Weigh Wagon vs. Yield Monitor Comparison', *CROP INSIGHTS* · Vol. 7 · NO. 17, [Online], Available from: http://www.pioneer.com/usa/technology/i970801.htm, [Accessed 2/11/98]

Doerge, T. 1999, 'Yield Monitor Calibration Update and Guidelines for Collecting Pioneer Strip Trial Data', *CROP INSIGHTS* · Vol. 9 · NO. 16, [Online], Available from: http://www.agriculture.com/technology/thisweek/1999/pio_monitors99.html, [Accessed 9/9/2001]

Durrence, J. S., Hamrita, T. K., & Vellidis, G. 1999, A Load Cell Based Yield Monitor for Peanut Feasibility Study, Precision Agriculture Journal 1 (3): 301-317, Kluwer Academic Publishers

Ehlert, D., 2000, *Measuring Mass Flow by Bounce Plate for Yield Mapping of Potatoes*, Precision Agriculture Journal 2 (2): 119-130, Kluwer Academic Publishers

Ellis, J.H., & Cardwell, O.G. 1935, 'Magnesium clay solonetz'. *Trans 3rd int. Congr. Soil Sci.* Vol. 1, pp. 348-50.

Forcella, F. 1993, 'Value of managing within-field variability'. In: *Proceedings of Soil Specific Crop Management*. April 14-16, 1992. Minneapolis, MN. P.C. Robert, et al., editors. ASA, CSA, SSSA. Madison, WI. pp. 125-132.

Freund, J.E. 1992, *Mathematical Statistics*, Prentice Hall Inc, Upper Saddle River, USA

Ham G.J. 1986, 'Modifying irrigation water for soils with low infiltration rates'. *Proc. Aust. Soc. Sugar Cane Technol.* 1986 Conference

Hammer, G. 1993, 'Crop Modelling - Current Status and Implications for Sugar Cane', In: *Proc. Aust. Soc. Sugar Cane Technol.* 1993, Watson Ferguson and Company, Brisbane.

Harrison, J.D, Birrel, S.J., Sudduth, K.A. & Borgelt S.C. 1992, *Global positioning System Applications for site specific farming research*. ASAE paper no 92-3615 , ASAE, St Joseph, MI

Higgins, M., Fehlhaber, L., Honor, I. & Kean, J. 1992, *The basics of the Global Positioning System and its application in land management where 1m to 10m accuracy is required*,

Queensland Department of Lands, Brisbane

Howard, K.D., Pringle, J.L., Schrock, M.D., Kuhlman, D.K. & Oard. D.L. 1993, *An elevator based grain flow sensor*. Presented at the 1993 International Winter Meeting. ASAE Paper No. 931504. ASAE, 2950 Niles Road, St. Joseph, MI 49805-9659.

Humbert, R.P. 1968, *The Growing of Sugar Cane*, Elsevier, Amsterdam

Keating, B.A., Vallis, I., Parton, W.J, Catchpoole, V.R., Muchow, R.C., & Robertson, M.J. 1994, 'Modelling and its application to nitrogen management and research for sugarcane'. *Proc. Aust. Soc. Sugar Cane Technol*., 1994 16:131-142.

Lark, R.M., Bolam, H.C., Mayr, T., Bradley, I., Burton, R.G.O. and Dampney, P.M.R. 1999, *Analysis of yield maps in support of field investigations of soil variation*. Proceedings of the 2nd European Conference on Precision Agriculture. pp 151–161.

Larson W.E., Tyler, D.A. & Nelson, G.A. 1991, 'Using GPS satellites for precision navigation', In: *Automated Agriculture for the 21st century, Proceedings of the 1991 symposium*, pp.201-208 ASAE publication No 1191, ASAE St Joseph MI USA

Leicia Inc. 1995, *GPS Product data sheets*, Torrence, California

Lemne, K. 1992, *Technology for yield variability measurement*, ASAE Paper No. 92-1543, ASAE, St Joseph, MI

Liu, W., Upadhyaya, S.K., Kataoka, T. & Shibusawa. S. 1996, 'Development of a texture/soil compaction sensor'. In: *Proceedings of the third international conference on Precision Agriculture*, 1996, Robert P.C., Rust R.H. & Larson W.E., (ed.) Minneapolis, MN June 23-36,1996.ASA, CSSA, SSSA Madison, WI pp. 617-630.

Lowenberg-DeBoer, J., & Swinton, S.M. 1995, *Economics of Site-Specific Management in Agronomic Crops*, Department of Agricultural Economics, Michigan State University, Michigan

Males, W.P., & Clive, P.R. 1996, 'Maintaining the international competitiveness of the Australian Sugar Industry'. In: *Sugarcane: Research Towards Efficient and Sustainable Production*. (Eds. Wilson, J.R., Hogarth, D.M., Cambell, J.A. & Garside, A.L.). (CSIRO Devision of tropical crops and pastures, Brisbane). pp. 3-5

Massey Ferguson Group Limited. 1993, *Yield Mapping System, MF 30/40 series combines*

McCarthy, S. 1998, *A Two Axis Inclinometer*, BEng Thesis, University of Southern Queensland.

Milby, R. 1997, *Mark II Agronomy*. Green Plan Analyst.

Missotten, B., Strubbe, G. & De Baerdemaeker, J. 1996, 'Accuracy of grain and straw yield mapping'. In: *Site-specific management for agricultural systems*. P.C. Robert, R.H, Rust, & W.E. Larson (ed.) Madison, WI: ASA, CSSA, SSSA p713-722

Mitchell, A.W., Reghenzani, J.R., Hunter, H.M. & Bramley, R.G.V. 1996, 'Water quality and nutrient fluxes from river systems draining to the Great Barrier Reef Marine Park'. In: *Proceedings of a conference on the Downstream Effects of Land Use*, Rockhampton, April 1995', (Eds. A.G. Eyles, H.M. Hunter & G.E. Rayment). (Department of Primary Industries, Queensland: Brisbane)

Moore, G.A., and J.P. Tyndale-Biscoe. 1999. Estimation of the Importance of Spatially Variable Nitrogen Application and Soil Moisture Holding Capacity to Wheat Production, *Precision Agriculture 1 (1)* p.27-38

Muchow, R.C., & Rebertson, M.J. 1994, 'Relating crop nitrogen uptake to sugarcane yield'. *Proc. Queensl. Soc. Sugar Cane Technol.*, 1994, 16:122-130.

Pagnano, N.B., & Magalhaes, P.S.G., 2001. *Sugarcane Yield Measurement*. Faculdade de Engenharia Agricola – Unicamp – Campinas – SP, Brasil 13083-970. 3rd European Conference on Precision Agriculture Proceedings, pp. 839-844. Montpellier, France.

Perrson, S. 1987, *Mechanics of cutting plant material*, ASAE Monograph No 7, ASAE Michigan, USA

Pocknee, S., Boydell, B.C., Green, H.M., Waters D.J. & Kvien, C.K. 1996, 'Directed Soil Sampling'. In: *Proceedings of the third international conference on Precision Agriculture*, 1996, Robert P.C., Rust R.H. & Larson W.E., (ed.) Minneapolis, MN June 23-36,1996.ASA, CSSA, SSSA Madison, WI

Rawlins, S.L., Campbell, G.S., Campbell, R.H. & Hess, J.R. 1995, 'Yield mapping of potato'. In: *Proceedings of Site-Specific Management for Agricultural Systems*. 2nd annual conference. March 27-30, 1994, Minneapolis, MN. ASA-CSSA-SSSA. Madison, WI. pp. 59-68.

Reichenberger, L. 1995, *Site specific is sweet on beets*, [Online], Available from: http://www.agriculture.com/sfonline/archive/archive.html, [Accessed 10/6/1995]

Reid, R.L.(ed.) 1990, *The Manual of Australian Agriculture*, 5th ed. Macarthur Press, Australia

Reyns, P., Missotten, B., Ramon, H., & De Baerdemaeker, J. 2002, A Review of Combine Sensors for Precision Farming, Precision Agriculture Journal 3 (2): 169-182, Kluwer Academic Publishers

Ridge, D.R. & Dick R.G. 1988, 'Current research on green cane harvesting and dirt rejection by harvesters'. *Proc. Aust. Soc. Sugar Cane Tech*. 1988 8:19-24

Russnogle, J. 1991, *Sky Spy : Gulf war technology pinpoints fields and yields*, Top Producer. November, 1991. P12-14

Saraiva, A. M., Hirakawa, A. R., Cugnasca, C. E., Pierossi, M. A. & Hassuani, S. J., 2000, *A Weighing System for Grab Loaders for Sugar Cane Yield Mapping*, Precision Agriculture Journal 2 (3): 293-309, Kluwer Academic Publishers

Schueller, J.K. & Wang, M.W. 1994, 'Spatially-variable fertilizer and pesticide application with GPS and DGPS', *Computers and Electronics in Agriculture*, Vol. 11 (1996), pp. 69-83.

Schumacher, J.A. & Froehlich, D.P. 1989, *Computer controlled chemical application in controlled traffic fields*. ASAE Paper No. 89-1606, ASAE, St Joseph, MI

Shropshire G., Peterson C. & Fisher, K. 1993, *Field experience with differential GPS*, ASAE paper 93-1073 ASAE, St Joseph, MI

Stott, B.L., Borgelt, S.C. & Sudduth, K.A. 1993, *Yield determination using an instrumented Claas Combine*, ASAE paper no. 93-1507. ASAE, St Joseph, MI

Strubbe, G.J., Missoten, B. & DeBaerdemaeker, J. 1996, 'Mass flow measurement with a curved plate at the exit of an elevator'. In: *Proceedings of the third international conference on Precision Agriculture*, 1996, Robert P.C., Rust R.H. & Larson W.E., (ed.) Minneapolis, MN June 23-36,1996.ASA, CSSA, SSSA Madison, WI pp. 703-712.

Sydenham, P.H., Hancock N.H., & Thorn, R. 1989, *Introduction to Measurement Science and Engineering,* John Wiley, UK.

Trimble. Inc, 1998, *Ag132 GPS Receiver Product data sheets*, California

Vansichen, R. & De Baerdemaeker, J. 1993, A measurement technique for yield mapping of corn silage, *Journal of Agricultural Engineering Research*, Vol. 55.

Verburg, K., Keating, B.A., Bristow, K.L., Huth, N.I., Ross, P.J. & Catchpoole, V.R., 1996, 'Evaluation of Nitrogen fertiliser management strategies in sugar cane using APSIM-SWIM'. In *Sugarcane: Research Towards Efficient and Sustainable Production*. (Eds. Wilson, J.R., Hogarth, D.M., Cambell, J.A. & Garside, A.L.). (CSIRO Devision of tropical crops and pastures, Brisbane). pp. 200-202

Walter, J.D., Hofman, V.L. & Backer, L.F. 1996, 'Site-specific yield monitoring', In: *Proceedings of the third international conference on Precision Agriculture*, 1996, Robert P.C., Rust R.H. & Larson W.E., (ed.) Minneapolis, MN June 23-36,1996.ASA, CSSA, SSSA Madison, WI pp. 835-844.

Weiss, N.A. & Hasset, M. 1986, *Introductory Statistics*, Addison-Wesley Publishing Company, USA

Wendte, K.W., A. Skotnikov, & Thomas, K.K., 2001. *Sugar Cane Yield Monitor*. United States Patent No. 6272819. August 14, 2001

Wilcox, J. 1998, 'Charts illustrate yield monitor vs scaled weights results', *AgInnovator News* 13-FEB-98, [Online], Available from: http://www.agriculture.com/subscribe/basic/aginnovator/AgInnovator.cgi?FNC=News__Ahtnews_html___3512, [Accessed 2/11/98]

Wollonhaupt, N.C. & Bucholz, D.D. 1993, 'Profitability of Farming by Soils', in *Soil Specific Crop Management*, ASA-CSSA-SSA, Madison WI, USA

Wood, R.A. 1990, 'The roles of nitrogen, phosphorus and potassium in the production of sugarcane in South Africa'. *Fertiliser Res.* 26: 89-98

Zillman, S.R. 1996, *Development of a method for the mass flow measurement of sugar cane*, BEng Thesis, University of Southern Queensland.

Appendices

Appendix A: Feed Roller Separation Sensor Design and Calibration

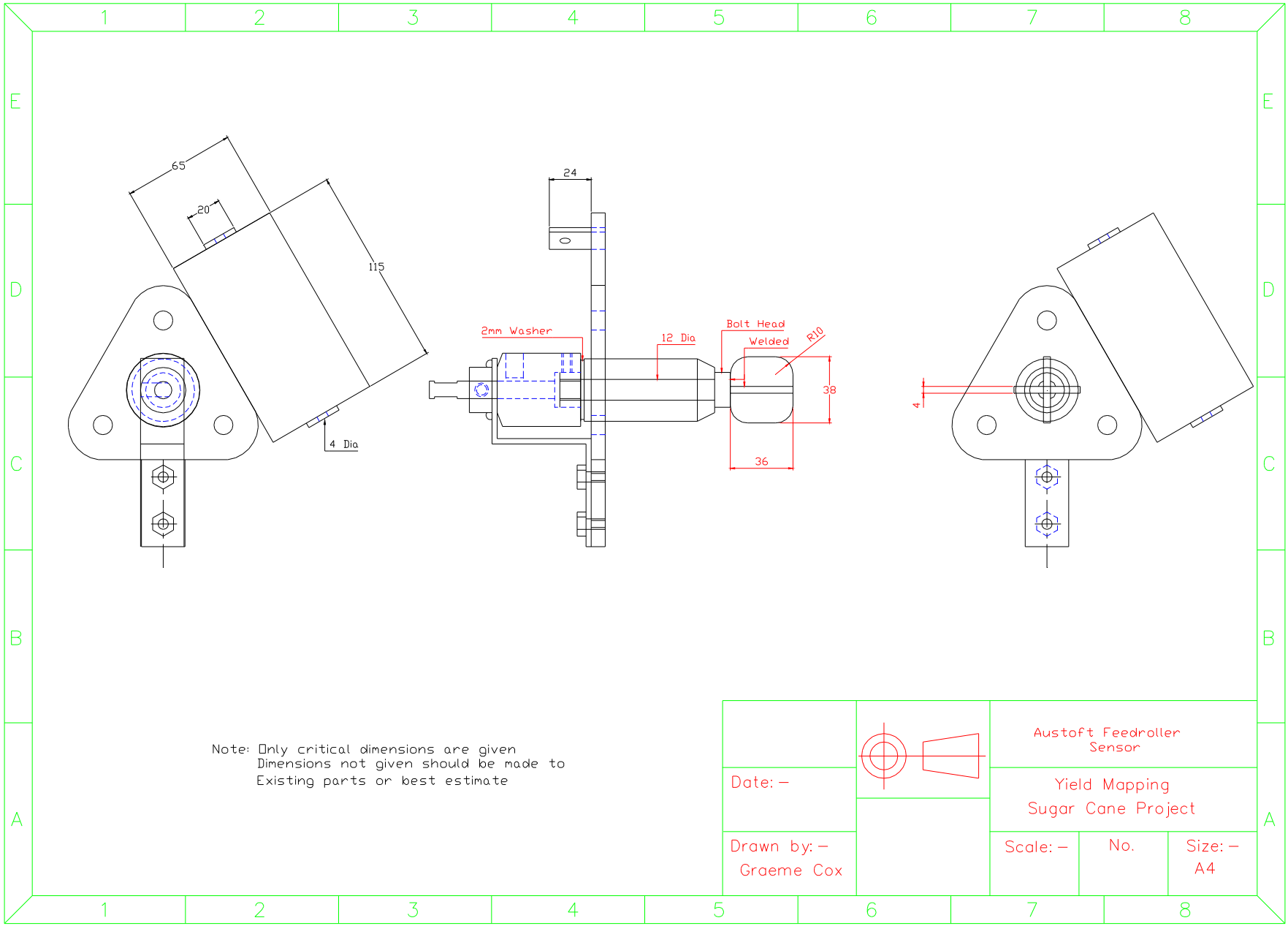
65
20
115
4 Dia
24
2mm Washer
12 Dia
Bolt Head
Welded
R10
38
36
4
Note: Only critical dimensions are given
Dimensions not given should be made to
Existing parts or best estimate
Austoft Feedroller
Sensor
Date: –
Yield Mapping
Sugar Cane Project
Drawn by: –
Graeme Cox
Scale: –
No.
Size: –
A4

Feed Roller Sensor Calibration

Angle (deg)	Sensor Output (V)	Sinusoid Trendline (V)	Feedroller Separation (mm)
0	3.48	3.51	-4.9
12.5	3.46	3.49	-28.6
19.5	3.4	3.47	-38.2
42.1	3.31	3.34	-49.8
51.5	3.24	3.26	-45.4
61.5	3.15	3.17	-35.1
70.5	3.06	3.07	-21.0
80.25	2.96	2.96	-0.9
85.7	2.9	2.90	12.2
90	2.85	2.85	23.5
96	2.78	2.78	40.4
99	2.75	2.75	49.3
102	2.71	2.71	58.5
108	2.65	2.65	77.5
111	2.61	2.61	87.4
114	2.58	2.58	97.4
117	2.55	2.55	107.6
119.5	2.52	2.52	116.2
122.75	2.49	2.49	127.4
125.6	2.46	2.46	137.3
128.5	2.43	2.43	147.4
131.5	2.41	2.41	157.9
134.5	2.38	2.38	168.3
142.5	2.32	2.32	195.9
148.7	2.29	2.28	216.6
156.7	2.24	2.23	242.2
163.5	2.21	2.21	262.6
169.2	2.19	2.19	278.5
174.5	2.18	2.18	292.1
179	2.19	2.17	302.7

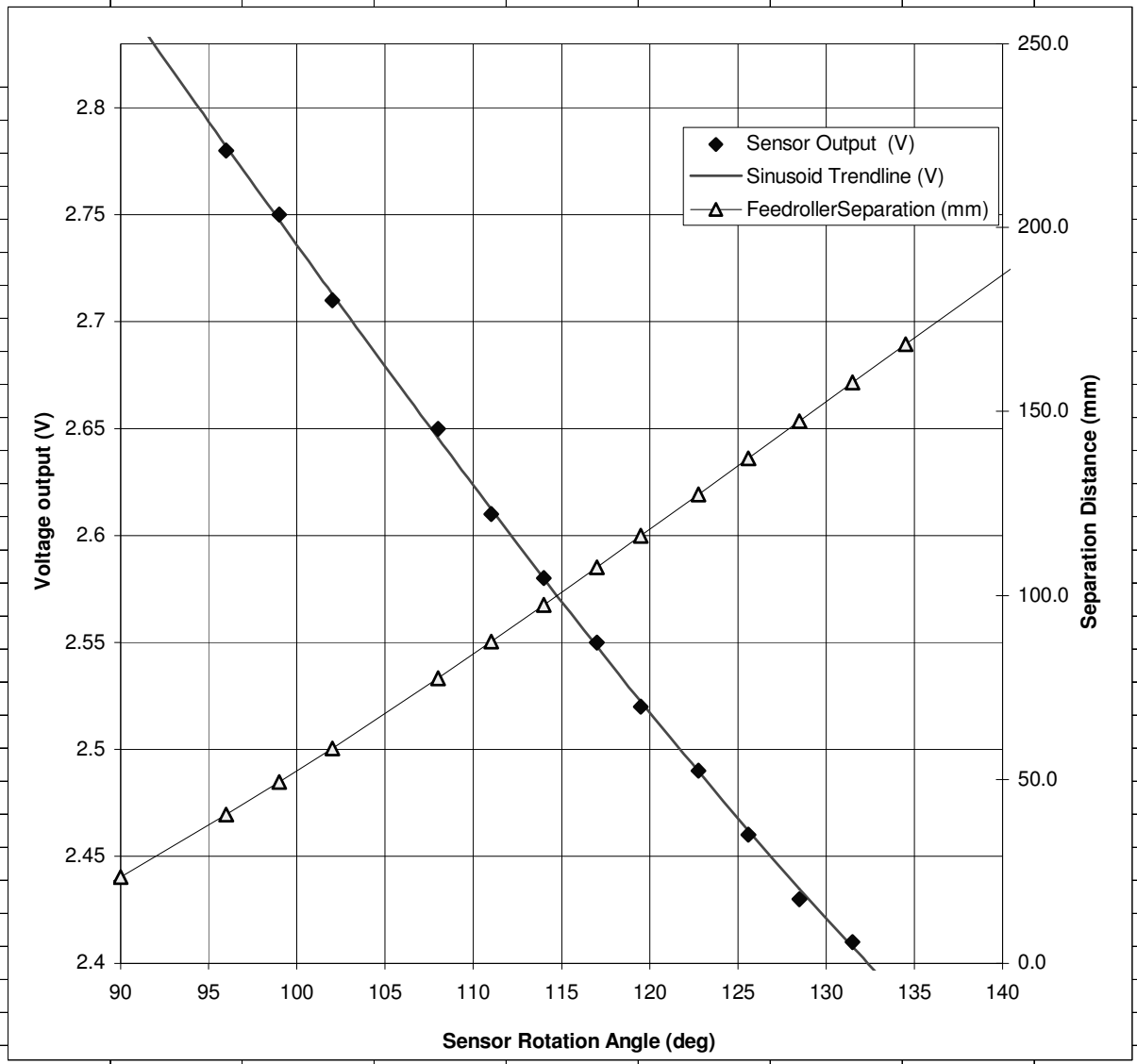

Appendix B: Field Trials Sensor Signal Conditioning

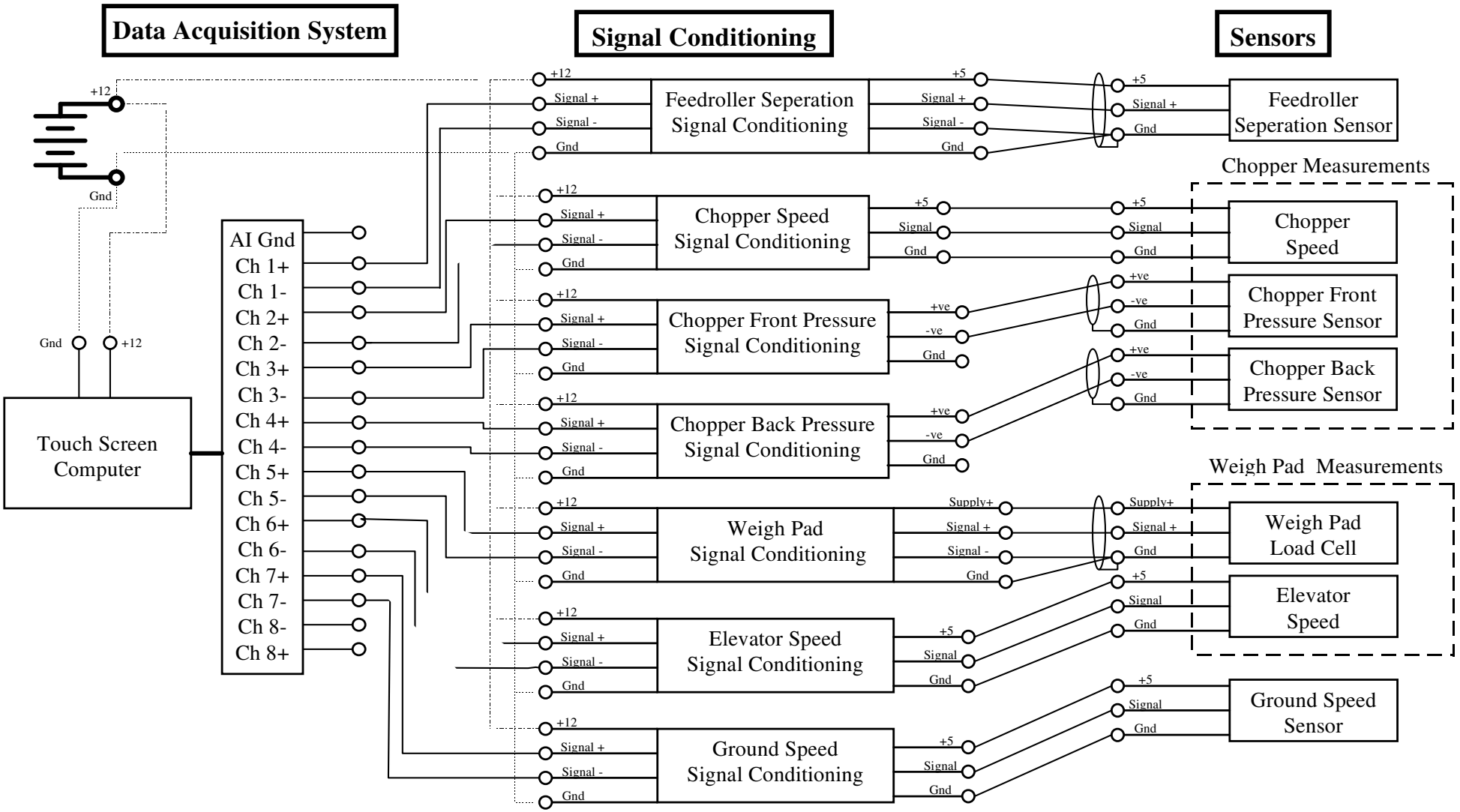
Data Acquisition System
Signal Conditioning
Sensors
+12
Gnd
Gnd
+12
Touch Screen Computer
AI Gnd
Ch 1+
Ch 1-
Ch 2+
Ch 2-
Ch 3+
Ch 3-
Ch 4+
Ch 4-
Ch 5+
Ch 5-
Ch 6+
Ch 6-
Ch 7+
Ch 7-
Ch 8-
Ch 8+
+12
Signal +
Signal -
Gnd
Feedroller Seperation Signal Conditioning
+5
Signal +
Signal -
Gnd
Feedroller Seperation Sensor
Chopper Measurements
Chopper Speed Signal Conditioning
Signal
Chopper Speed
Chopper Front Pressure Signal Conditioning
+ve
-ve
Chopper Front Pressure Sensor
Chopper Back Pressure Signal Conditioning
Chopper Back Pressure Sensor
Weigh Pad Measurements
Weigh Pad Signal Conditioning
Supply+
Weigh Pad Load Cell
Elevator Speed Signal Conditioning
Elevator Speed
Ground Speed Signal Conditioning
Ground Speed Sensor

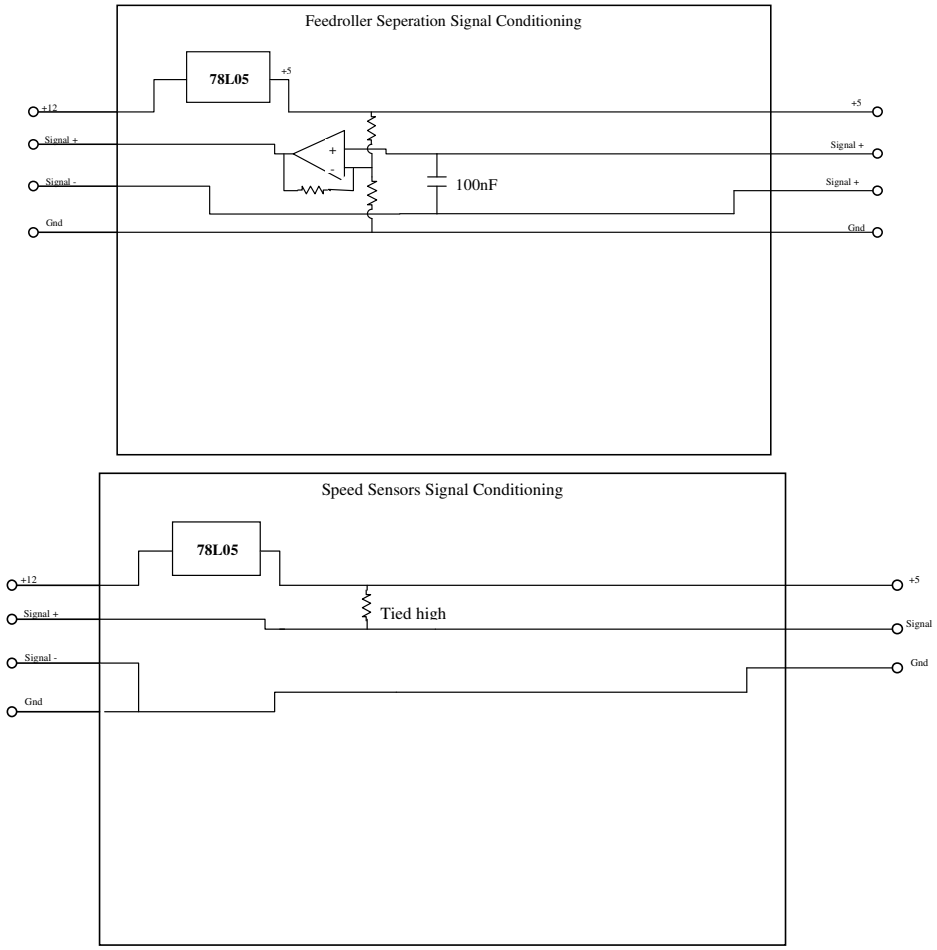

Note: Standard wiring for the 78L05 was used to produce out +5V from +12V in. The actual resistors and capacitors used to do this is not given in these diagrams as this is a standard procedure.

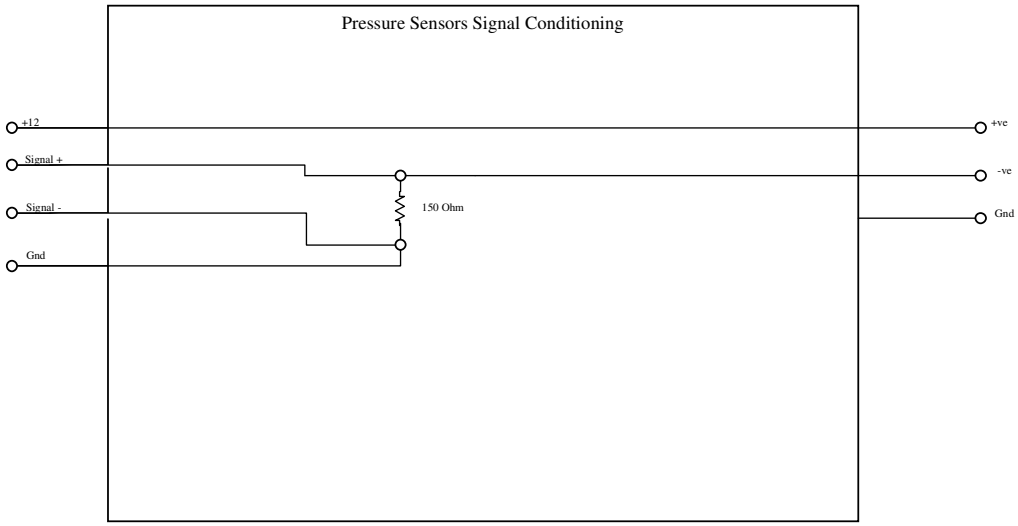
Pressure Sensors Signal Conditioning
+12
Signal +
Signal -
Gnd
150 Ohm
+ve
-ve
Gnd

Appendix C: Vibration Testing Frame

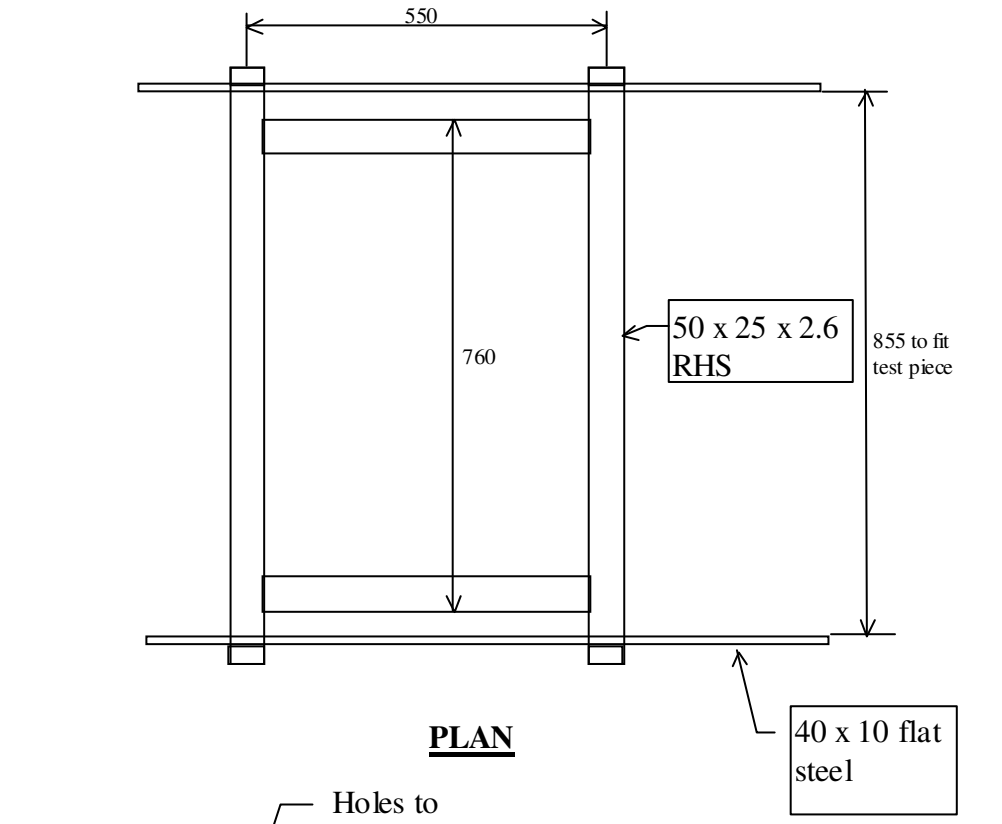

PLAN

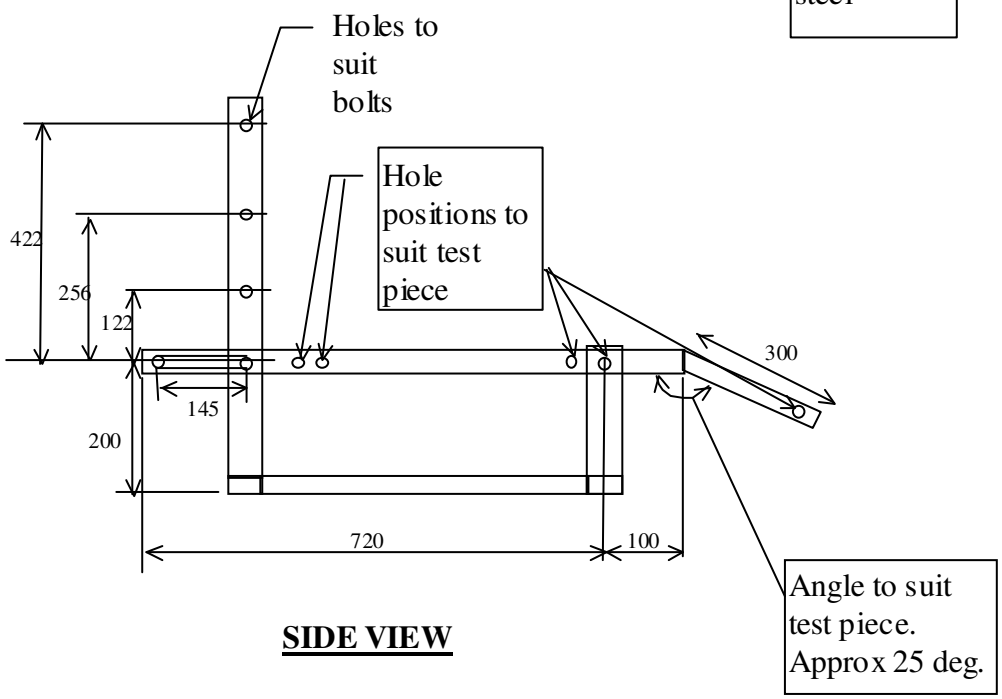

SIDE VIEW

All dimensions in millimetres.

Appendix D: 1997 Weigh Pad Design

All dimensions in millimetres unless otherwise stated.

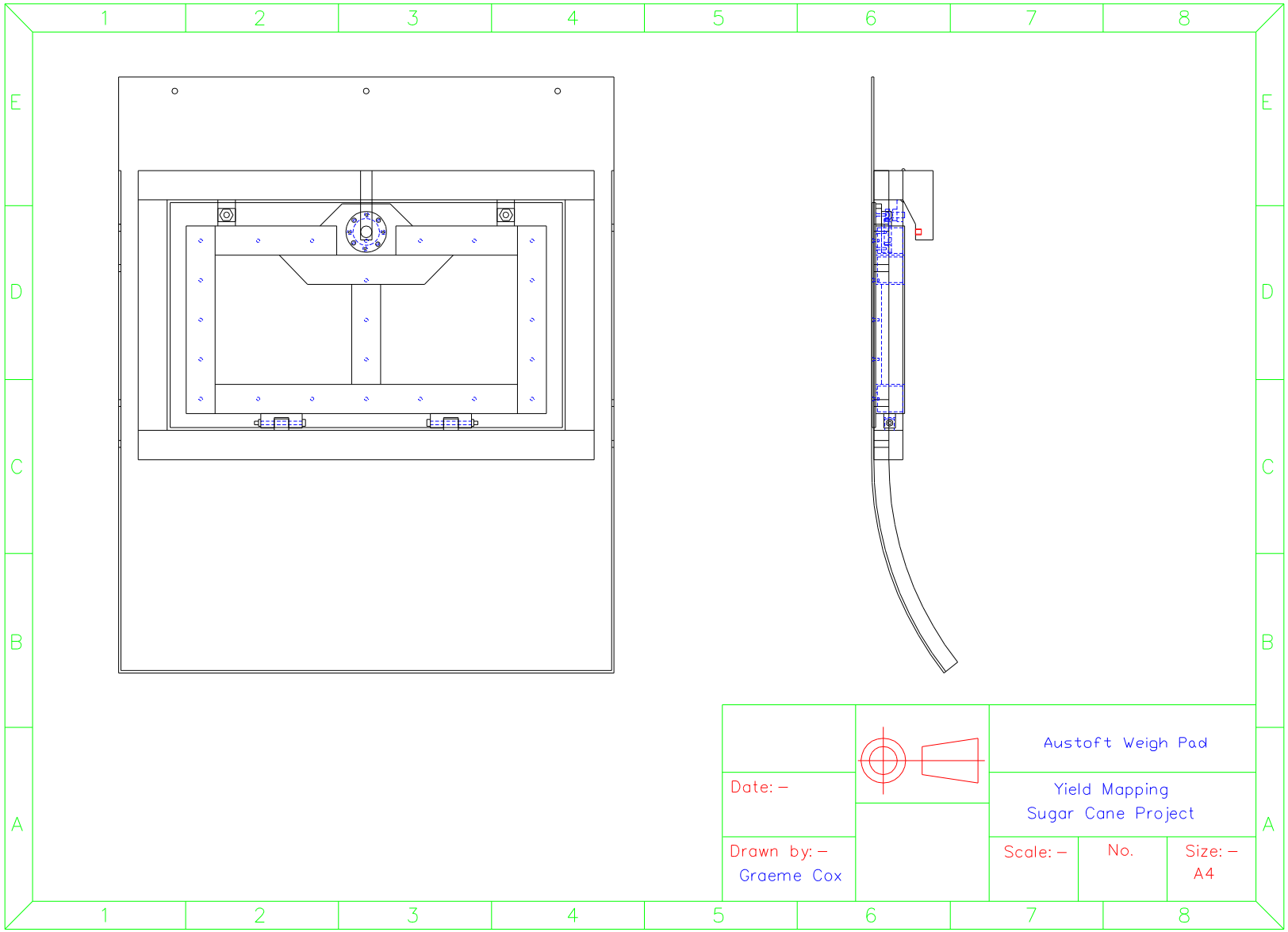
1
2
3
4
5
6
7
8
E
D
C
B
A
Austoft Weigh Pad
Date: –
Yield Mapping
Sugar Cane Project
Drawn by: –
Graeme Cox
Scale: –
No.
Size: –
A4

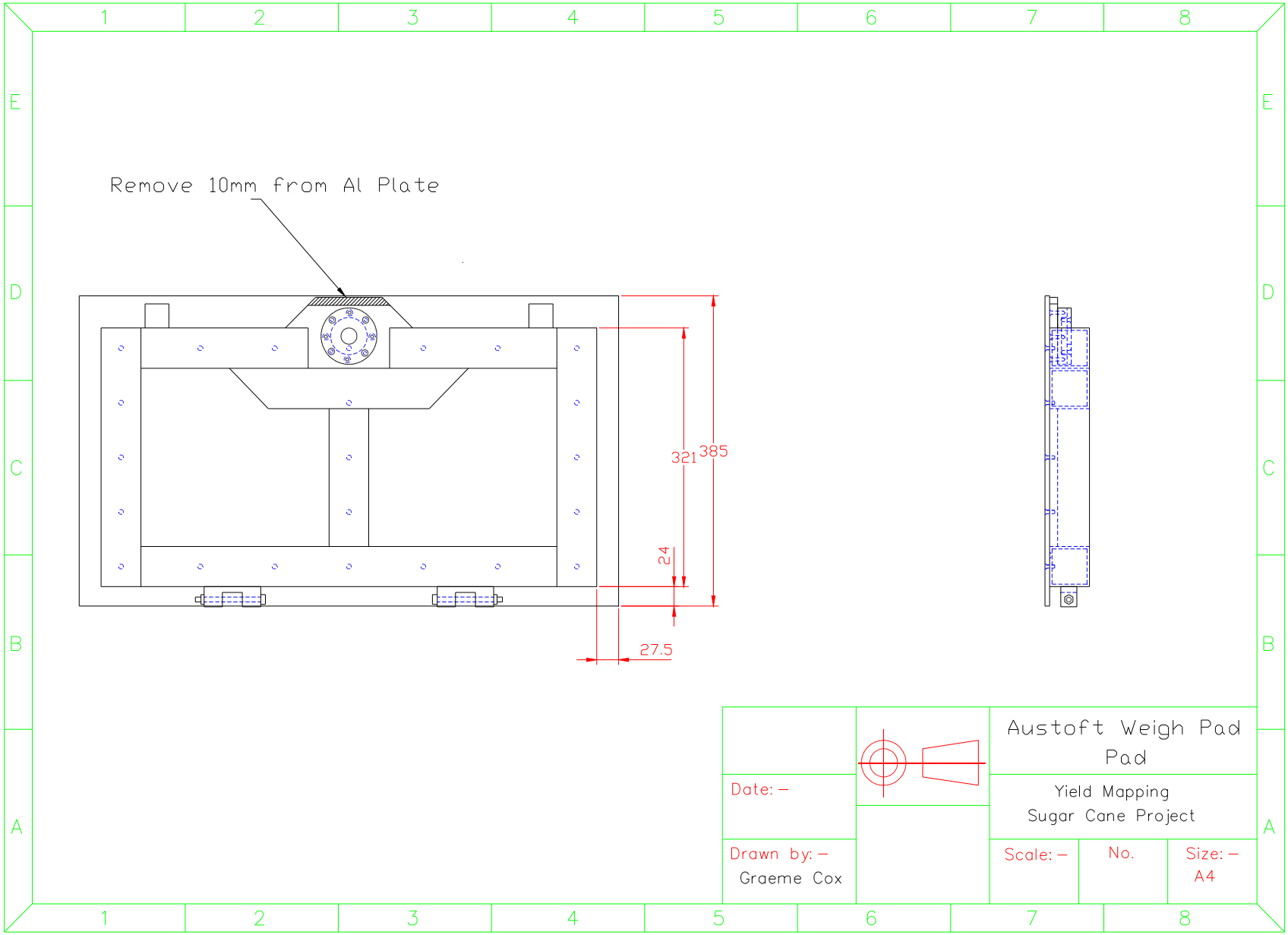
1
2
3
4
5
6
7
8
E
D
C
B
A
Remove 10mm from Al Plate
385
321
24
27.5
Austoft Weigh Pad Pad
Yield Mapping
Sugar Cane Project
Date: –
Drawn by: –
Graeme Cox
Scale: –
No.
Size: –
A4

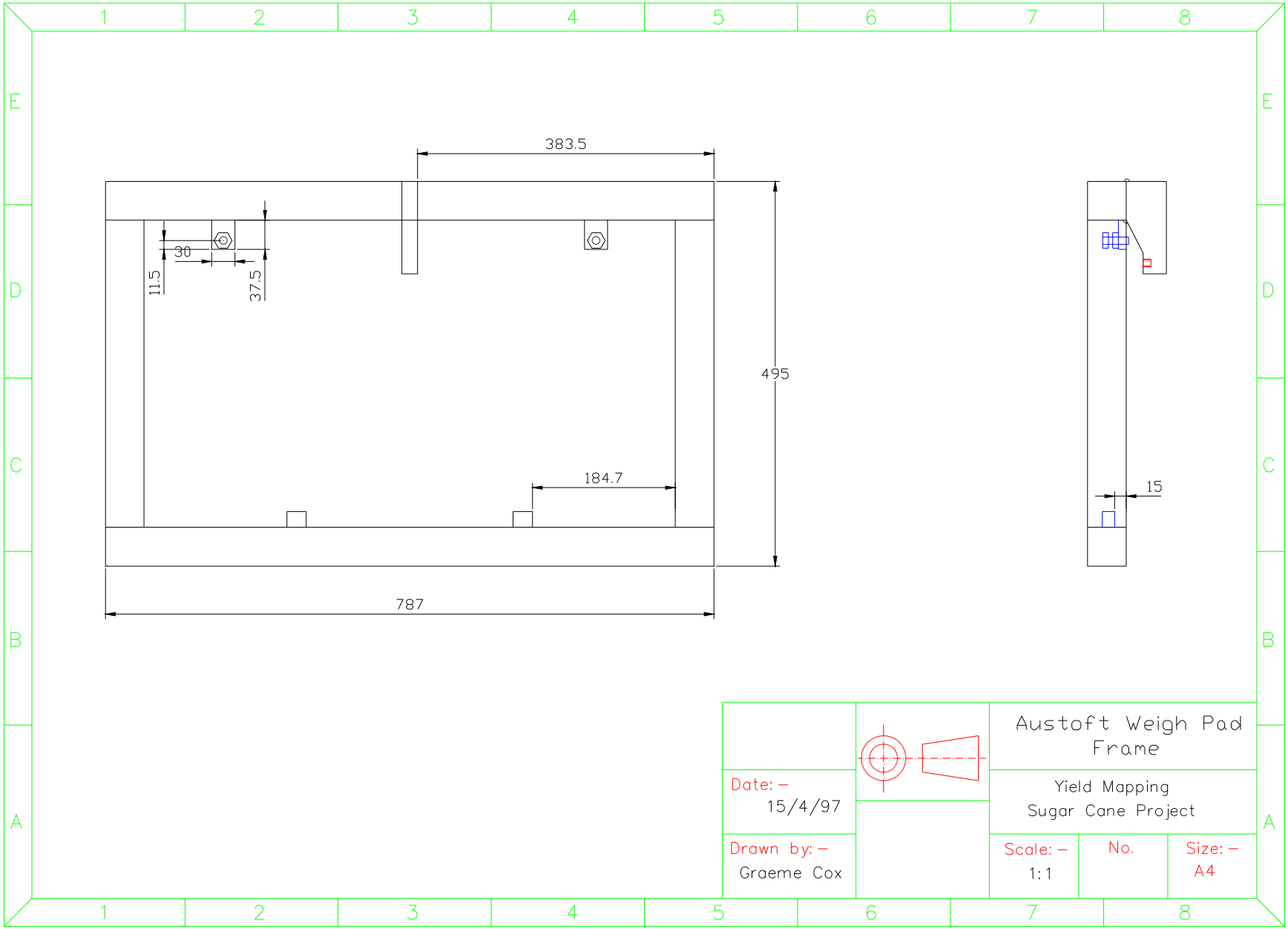
1
2
3
4
5
6
7
8
A
B
C
D
E
383.5
30
11.5
37.5
495
184.7
787
15
Austoft Weigh Pad Frame
Yield Mapping
Sugar Cane Project
Date: –
15/4/97
Drawn by: –
Graeme Cox
Scale: –
1:1
No.
Size: –
A4

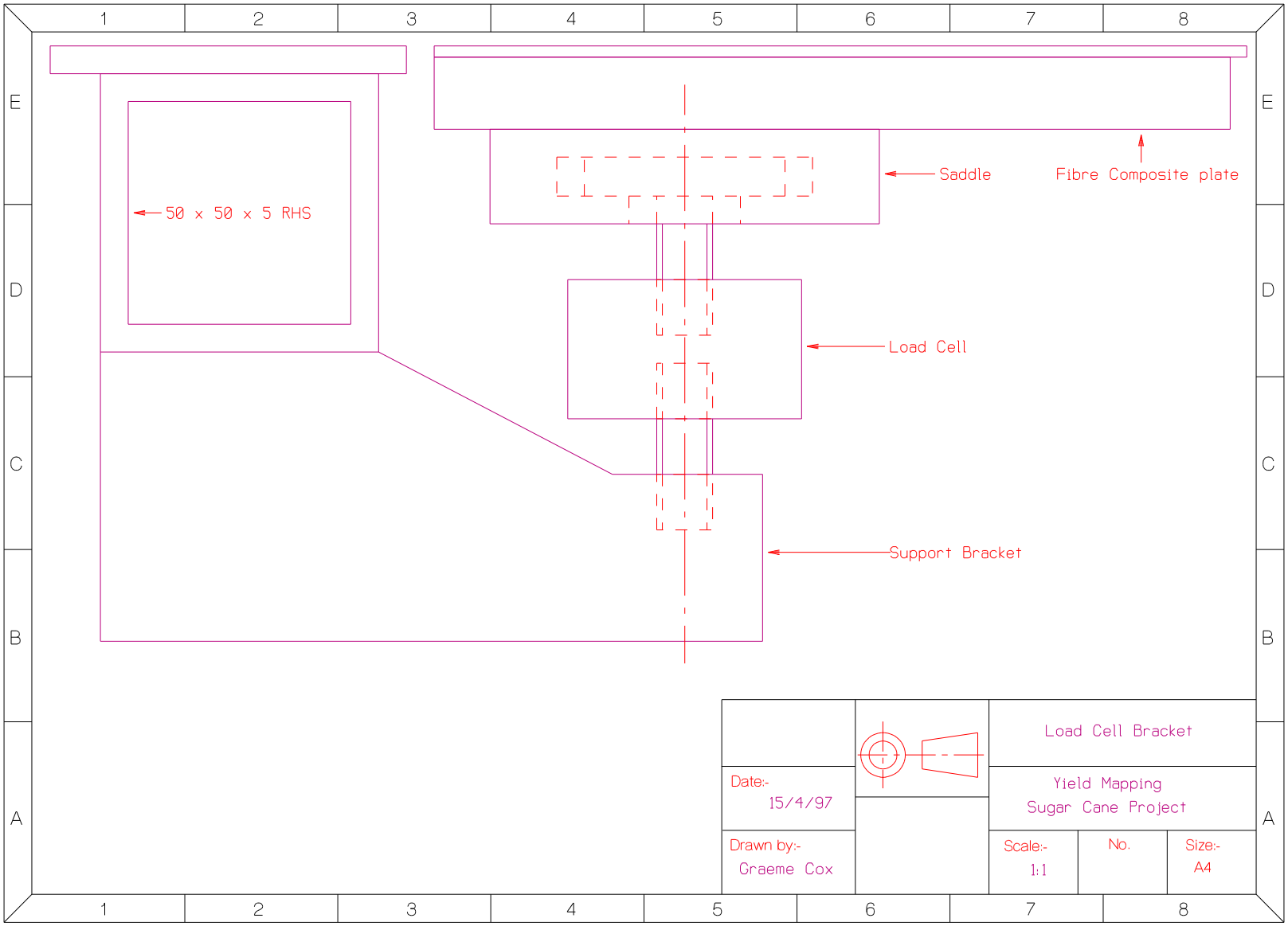
1
2
3
4
5
6
7
8
E
D
C
B
A
50 x 50 x 5 RHS
Saddle
Fibre Composite plate
Load Cell
Support Bracket
Load Cell Bracket
Date:-
15/4/97
Yield Mapping
Sugar Cane Project
Drawn by:-
Graeme Cox
Scale:-
1:1
No.
Size:-
A4

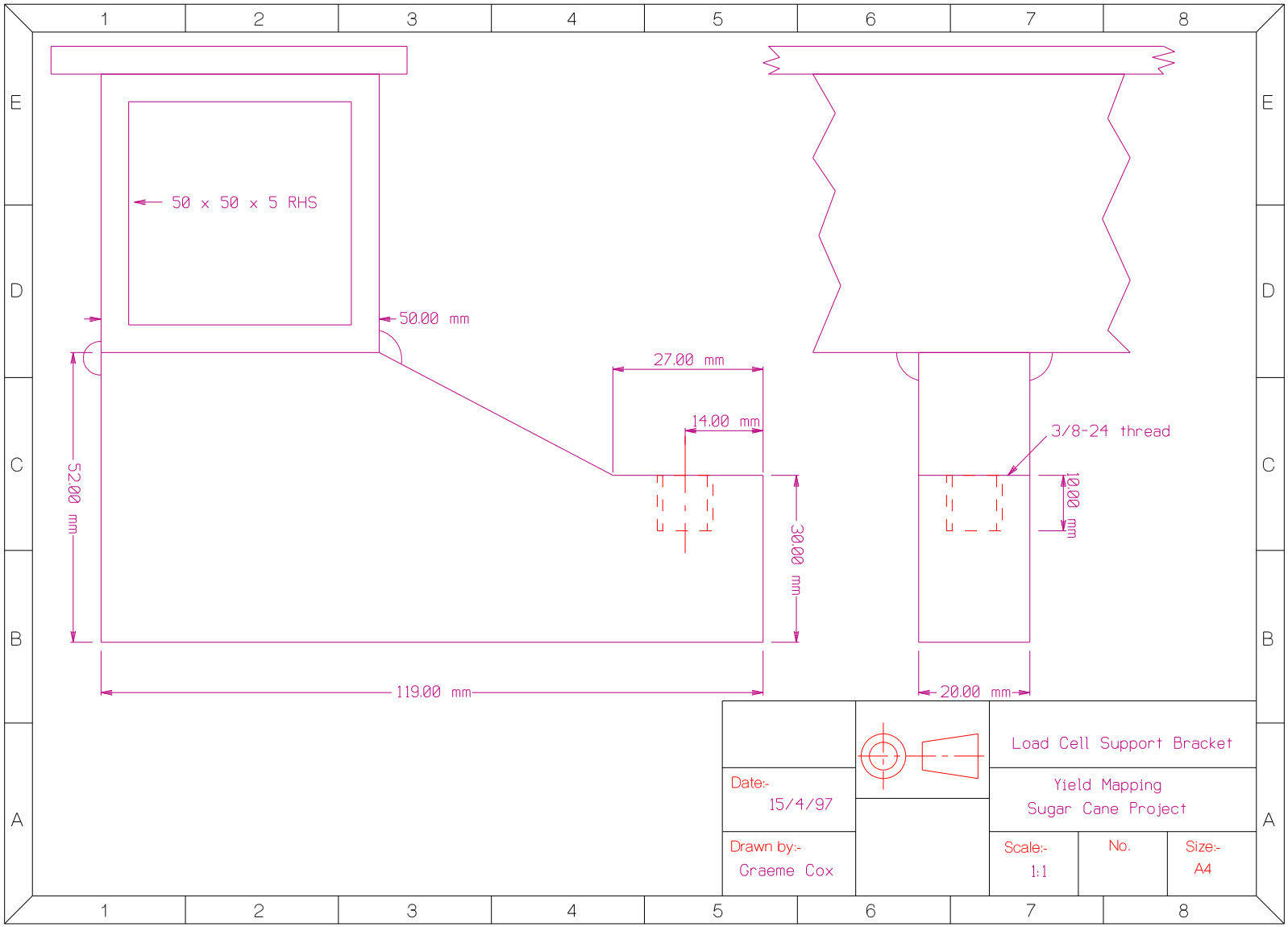
1
2
3
4
5
6
7
8
E
D
C
B
A
50 x 50 x 5 RHS
50.00 mm
27.00 mm
14.00 mm
3/8-24 thread
52.00 mm
30.00 mm
10.00 mm
119.00 mm
20.00 mm
Load Cell Support Bracket
Date:-
15/4/97
Yield Mapping
Sugar Cane Project
Drawn by:-
Graeme Cox
Scale:-
1:1
No.
Size:-
A4

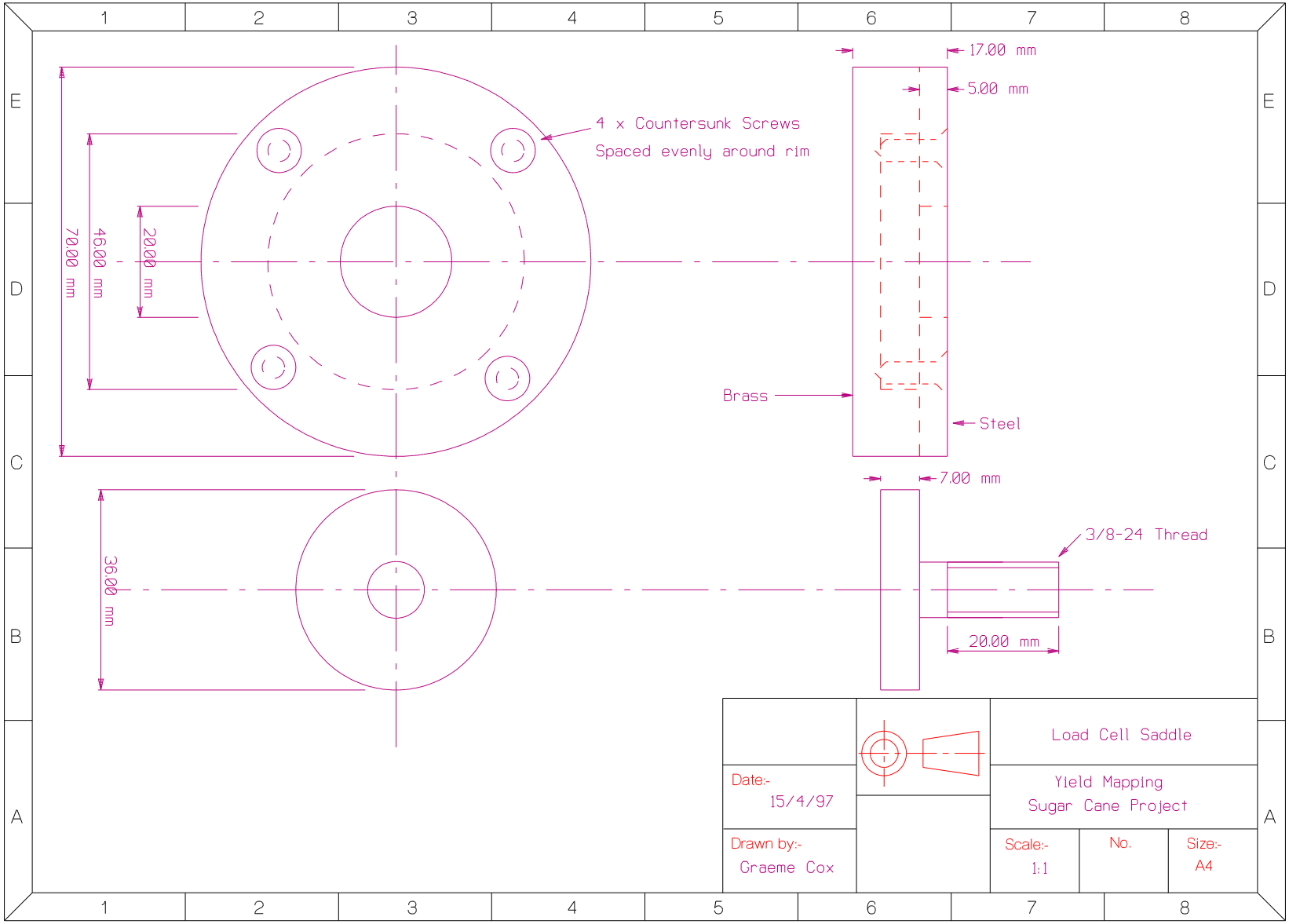
1
2
3
4
5
6
7
8
A
B
C
D
E
4 x Countersunk Screws
Spaced evenly around rim
70.00 mm
46.00 mm
20.00 mm
17.00 mm
5.00 mm
Brass
Steel
7.00 mm
3/8-24 Thread
36.00 mm
20.00 mm
Load Cell Saddle
Date:-
15/4/97
Yield Mapping
Sugar Cane Project
Drawn by:-
Graeme Cox
Scale:-
1:1
No.
Size:-
A4

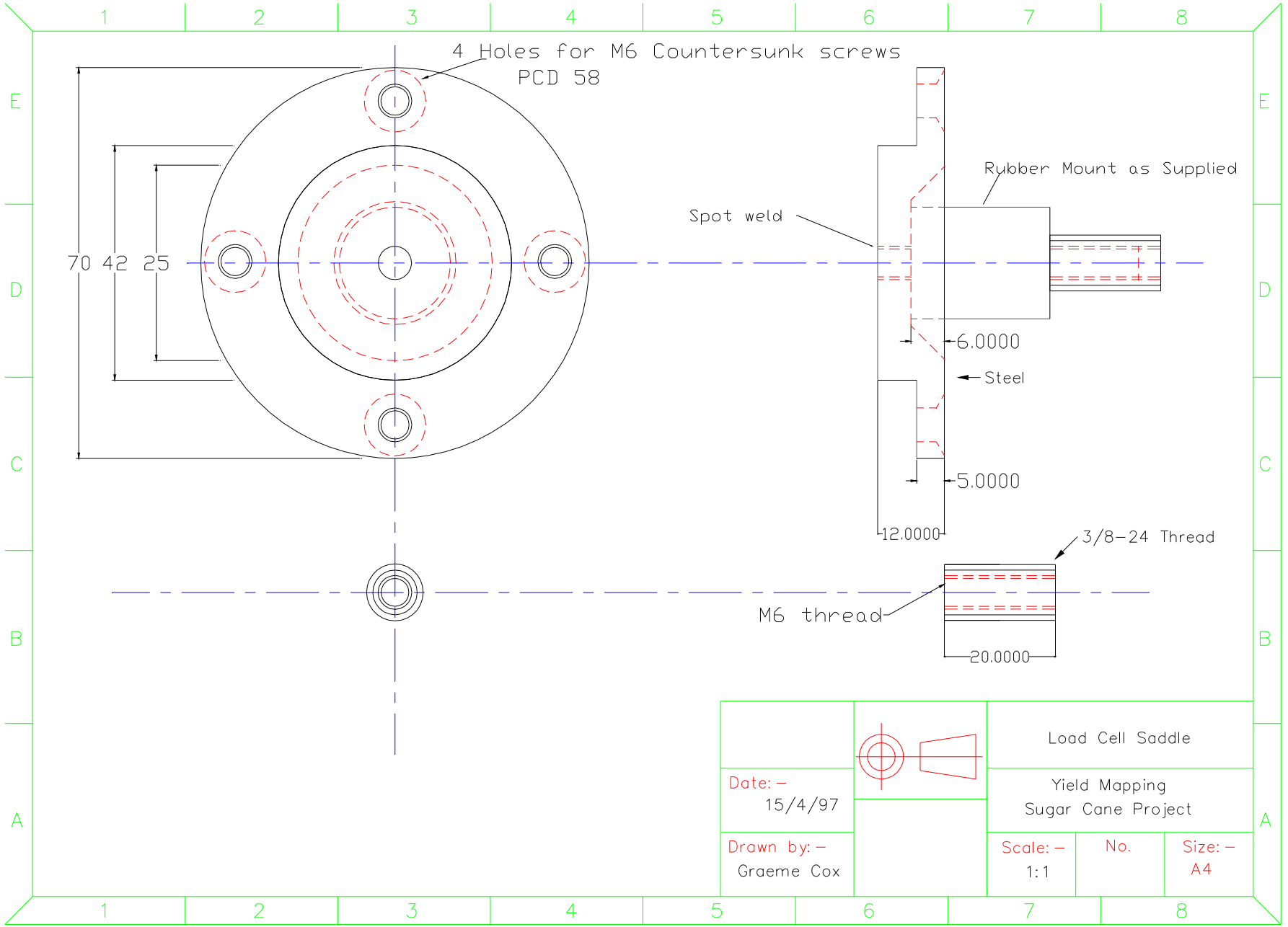
4 Holes for M6 Countersunk screws
PCD 58
70 42 25
Rubber Mount as Supplied
Spot weld
6.0000
Steel
5.0000
12.0000
3/8-24 Thread
M6 thread
20.0000
Load Cell Saddle
Date: –
15/4/97
Yield Mapping
Sugar Cane Project
Drawn by: –
Graeme Cox
Scale: –
1:1
No.
Size: –
A4

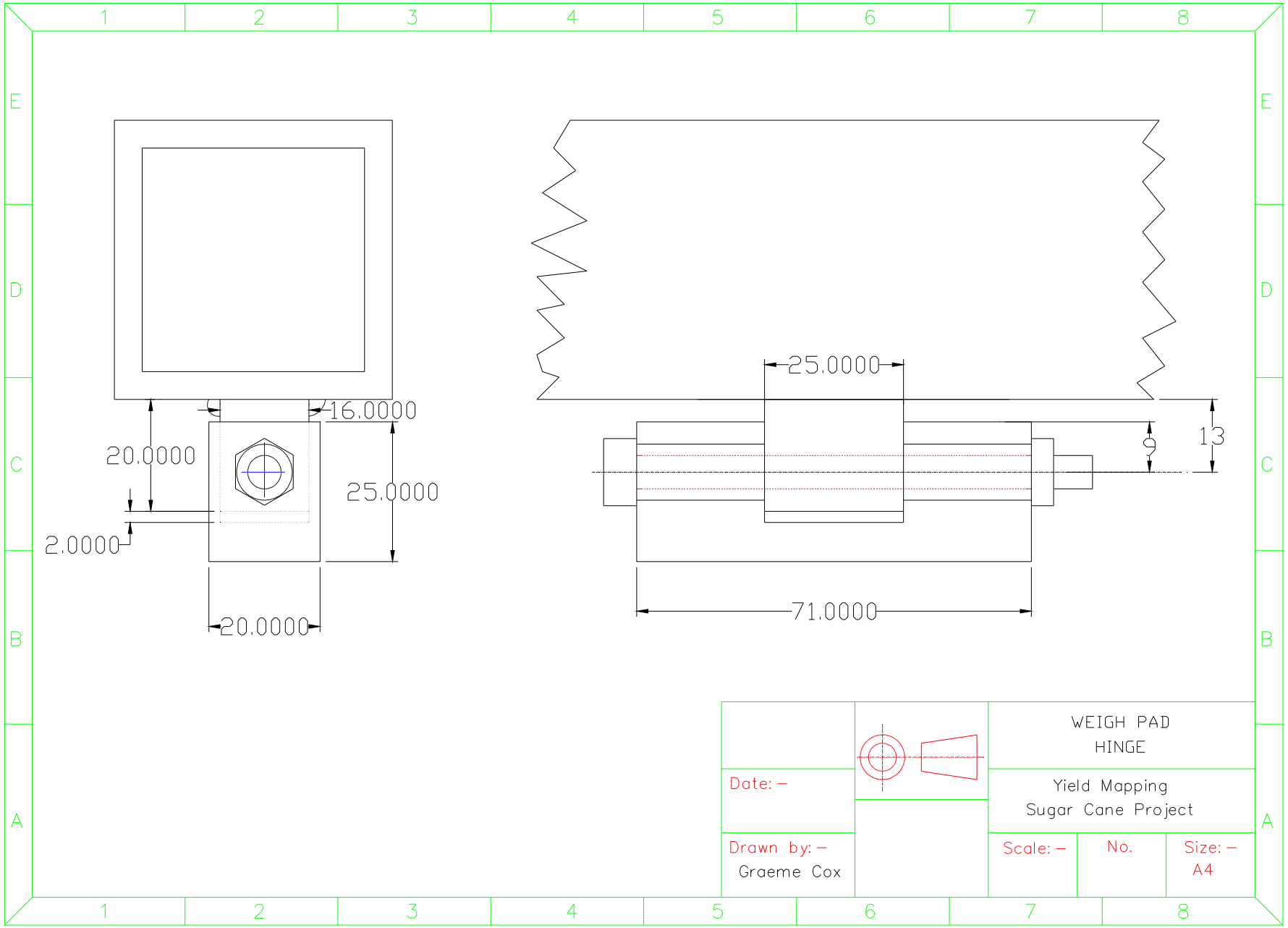
1
2
3
4
5
6
7
8
E
D
C
B
A
16.0000
20.0000
25.0000
2.0000
20.0000
25.0000
9
13
71.0000
WEIGH PAD
HINGE
Date: –
Yield Mapping
Sugar Cane Project
Drawn by: –
Graeme Cox
Scale: –
No.
Size: –
A4

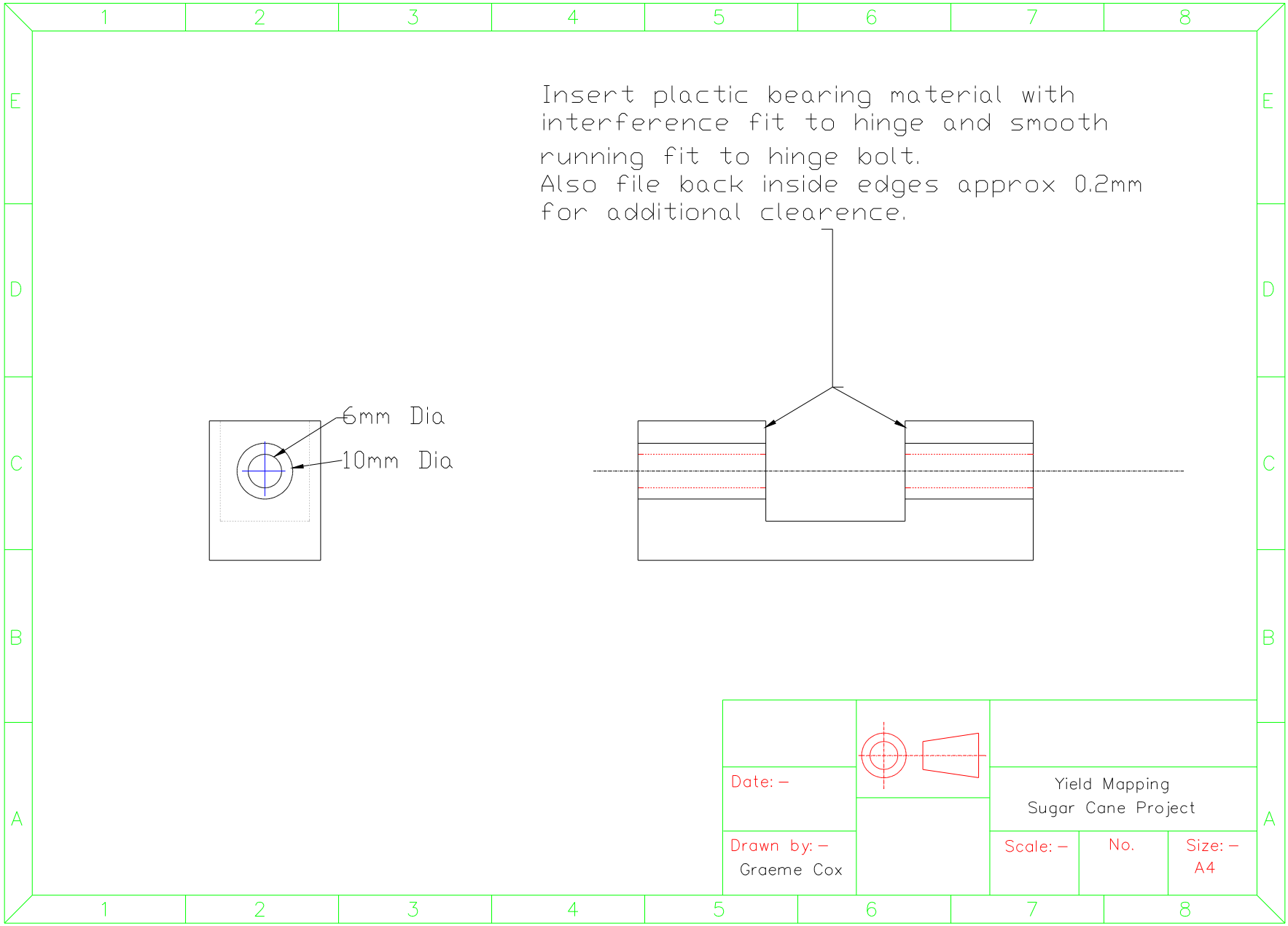
Insert plactic bearing material with interference fit to hinge and smooth running fit to hinge bolt.
Also file back inside edges approx 0.2mm for additional clearence.
6mm Dia
10mm Dia
Date: –
Yield Mapping
Sugar Cane Project
Drawn by: –
Graeme Cox
Scale: –
No.
Size: –
A4

Appendix E: 1997 Fixed Weigh Pad Design

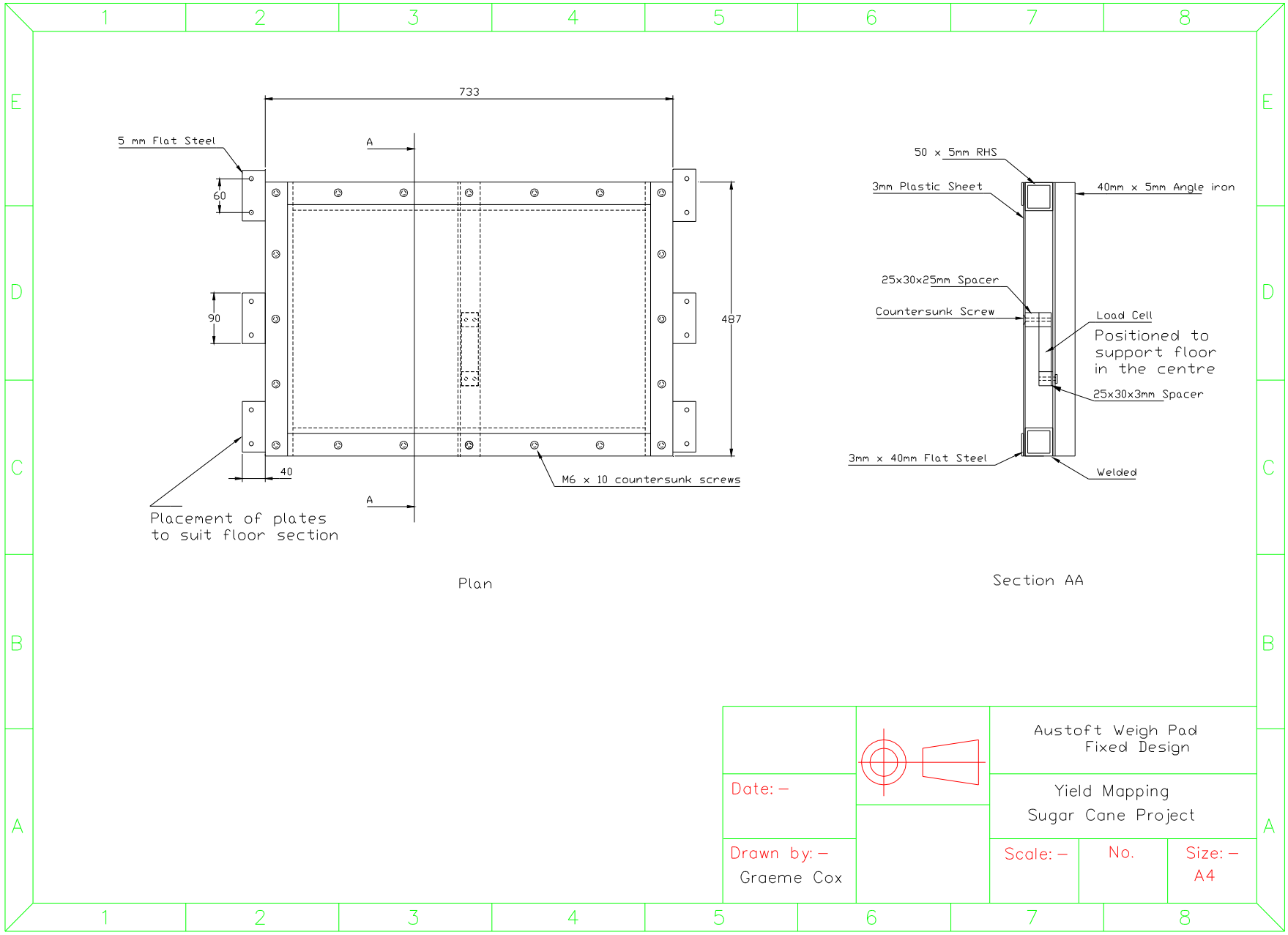
733
5 mm Flat Steel
A
60
90
487
40
M6 x 10 countersunk screws
Placement of plates
to suit floor section
Plan
50 x 5mm RHS
3mm Plastic Sheet
40mm x 5mm Angle iron
25x30x25mm Spacer
Countersunk Screw
Load Cell
Positioned to
support floor
in the centre
25x30x3mm Spacer
3mm x 40mm Flat Steel
Welded
Section AA
Austoft Weigh Pad
Fixed Design
Date: –
Yield Mapping
Sugar Cane Project
Drawn by: –
Graeme Cox
Scale: –
No.
Size: –
A4

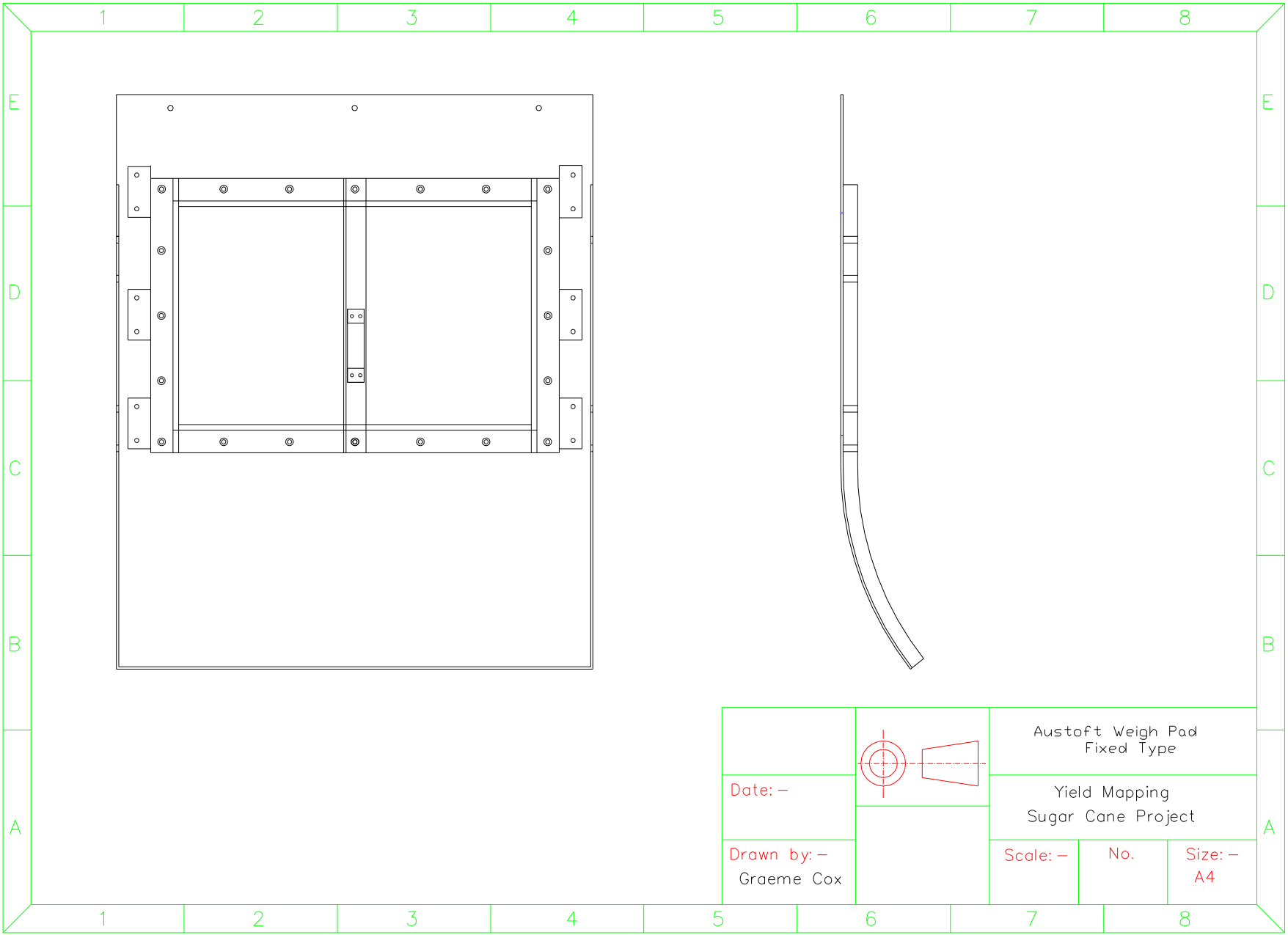
1
2
3
4
5
6
7
8
E
D
C
B
A
Austoft Weigh Pad
Fixed Type
Date: –
Yield Mapping
Sugar Cane Project
Drawn by: –
Graeme Cox
Scale: –
No.
Size: –
A4

Appendix F: Yield Monitor Data File Format

TABLE G.1 Sample of data collected by the yield mapping system.

```
$GPGGA,194506.28,1941.90653,S,14713.57325,E,2,03,1.4,19,M,55.6,M,5.28,0004*46,$GPVTG,094,T,086,M,3.26,N,6.05,K*49$,197.88,4167.55,10617.49,1.64,  0.00
$GPGGA,194507.34,1941.90661,S,14713.57420,E,2,03,1.4,19,M,55.6,M,6.34,0004*47,$GPVTG,095,T,087,M,3.24,N,6.01,K*4F$,201.35,4377.31,10597.61,  1.61,  0.00
$GPGGA,194508.43,1941.90679,S,14713.57615,E,2,03,1.4,19,M,55.6,M,5.43,0004*47,$GPVTG,093,T,085,M,3.24,N,6.01,K*4B$,201.54,4489.43,10603.85,  1.61,  0.00
$GPGGA,194509.43,1941.90689,S,14713.57615,E,2,03,1.4,19,M,55.6,M,5.43,0004*47,$GPVTG,093,T,085,M,3.24,N,6.01,K*4B$,169.67,4412.26,9477.30,  1.58,  0.00
$GPGGA,194510.43,1941.90699,S,14713.57790,E,2,03,1.4,19,M,55.6,M,7.43,0004*4E,$GPVTG,093,T,085,M,3.06,N,5.66,K*49$,180.12,4290.36,9814.50,  1.58,  0.00
```

String Format $GPGGA,<1>,<2>,<3>,<4>,<5>,<6>,<7>,<8>,<9>,M,<11>,<12>,<13>,$GPVTG,<14>,T,<15>,M,<16>,N,<17>,K,<18>,<19>,<20>,<21>,<22>,<23>

$GPGGA: NMEA-0183 Output Message: Global Positioning System Fix Data (GGA)

1) UTC time of position fix, hhmmss.sss format
2) Latitude, ddmm.mmmm format.
3) Latitude hemisphere, N or S.
4) Longitude, dddmm.mmmm format.
5) Longitude hemisphere, E or W.
6) Position Fix Indicator,
   0 = fix not available, or invalid.
   1 = GPS SPS Mode, fix valid.
   2 = Differential GPS, SPS Mode, fix valid.
   3 = GPS PPS Mode, fix valid.
7) Number of sate1lites in use, 00 to 12.
8) Horizontal Dilution of Precision, 0.5 to 99.9.
9) MSL Altitude, -9999.9 to 99999.9 meters.
10) Geoidal height, -999.9 to 9999.9 meters.
11) Differential GPS (RTCM SC-104) data age, number of seconds since last valid RTCM transmission (nu11 if non-DGPS).
12) Differential Reference Station ID, 0000 to 1023. (null if non-DGPS)
13) Checksum.

$GPVTG: NMEA-0183 Output Message: Course Over Ground and Ground Speed

14) True course over ground, 000 to 359 degrees.

15) Magnetic course over ground, 000 to 359 degrees.

16) Speed over ground, 00.0 to 999.9 knots.

17) Speed over ground, 00.0 to 1851.8 ko/hr.

18) Checksum.

Yield Monitor Sensor Readings:

Example: 197.88,4167.55,10617.49, 1.64, 0.00, 1

19) Real time yield calculation using rough calibration on chopper sensor reading, t/ha.

20) Elevator pressure sensor reading, kPa .

21) Chopper pressure sensor reading, kPa.

22) Ground Speed sensor reading, m/s.

23) Spare sensor reading, not recorded.

Appendix G: Soil Analysis Results

		Soil sample results (0-25cm)																
Point	Yield	pH	Organic C	Nitrate N	Sulfur	Phosphoru	Phosphoru	Potassium	Calcium	Magnesiun	Sodium	Chloride	Electrical C	Copper	Zinc	Manganese	Iron
po No.	t/ha	(1:5 Water)	%C	mg/kg	mg/kg	mg/kg	mg/kg	meq/100g	meq/100g	meq/100g	meq/100g	mg/kg	dS/m	mg/kg	mg/kg	mg/kg	mg/kg
1	130	7	1	6	5	18	9	0.35	12.04	8.76	0.7	15	0.05	1.8	0.3	15	33
2	110	7.9	1	0.7	3	24	4	0.32	14.02	9.83	1.12	15	0.06	1.4	0.1	9	17
3	150	8.3	1	35.9	2	31	6	0.28	12.04	6.59	0.73	15	0.06	1.2	0.3	9	13
4	90	7.5	0.9	0.7	4	17	6	0.45	18.17	11.52	1.19	35	0.06	1.7	0.3	14	30
5	110	7.5	0.8	0.9	5	21	13	0.41	14.77	9.98	1.39	40	0.07	1.9	0.4	13	32
6	130	7.2	1.5	0.6	5	20	12	0.37	11.33	6.9	0.88	30	0.05	1.8	0.6	28	29
7	70	7.4	1.1	0.4	8	10	4	0.2	5.95	6.65	2.23	75	0.08	1.4	0.3	23	21
8	70	7.6	1.1	0.5	5	9	3	0.17	4.97	6.43	2.48	90	0.1	1.2	0.4	19	20
9	90	7.7	1.4	0.7	6	14	4	0.32	8.98	8.81	1.63	40	0.06	1.1	0.7	18	14
10	200	7.4	0.9	0.4	3	16	8	0.21	6.49	3.53	0.72	20	0.04	0.9	0.7	22	22
11	170	8.2	1.5	0.4	3	64	11	0.38	9.72	6.22	0.81	20	0.05	1	0.7	21	14
12	150	6.9	1.5	0.3	7	11	7	0.26	6.59	4.73	0.76	25	0.05	1.2	1	40	21

Continued

					Soil sample results (25-50cm)											
Boron	CEC	ESP	Ca/Mg Rat	se	pH	Sulfur	Phosphoru	Potassium	Calcium	Magnesiun	Sodium	Electrical C	Potassium	CEC	Ca/Mg Rat	ESP	se
mg/kg	meq/100g			dS/m	(1:5 Water	mg/kg	mg/kg	meq/100g	meq/100g	meq/100g	meq/100g	dS/m	meq/100g	meq/100g			dS/m
0.69	21.86	3.2	1.37	0.2	6.8	4	11	0.38	12.99	11.03	1.54	0.05	2.43	25.95	1.18	5.93	0.2
0.77	25.3	4.43	1.43	0.3	8.1	3	13	0.26	9.28	9.73	2.63	0.09	2.32	21.91	0.95	12	0.4
0.73	19.65	3.71	1.83	0.3	7.9	5	11	0.19	7.3	5.79	1.67	0.06	2.45	14.96	1.26	11.16	0.4
0.77	31.34	3.8	1.58	0.3	7.5	4	13	0.46	17.84	12.27	1.85	0.13	2.91	32.43	1.45	5.7	0.6
0.94	26.56	5.23	1.48	0.3	7.3	2	13	0.39	14.18	11.06	2.51	0.12	2.72	28.15	1.28	8.92	0.5
0.77	19.49	4.51	1.64	0.2	6.9	4	11	0.38	12.36	8.61	1.19	0.08	3.2	22.55	1.44	5.28	0.4
1.45	15.04	14.83	0.89	0.4	8.7	6	14	0.29	7.62	11.07	7.26	0.37	3.11	26.25	0.69	27.66	1.7
0.03	14.06	17.64	0.77	0.4	9	4	14	0.26	10.16	11.07	7.58	0.52	3.09	29.08	0.92	26.07	2.3
1.48	19.75	8.25	1.02	0.3	8.8	3	16	0.3	11.47	11.96	3.99	0.25	3.85	27.73	0.96	14.39	1.1
0.57	10.96	6.57	1.84	0.2	6.8	10	9	0.31	8.54	5.98	0.92	0.05	3.75	15.76	1.43	5.84	0.2
1.45	17.14	4.73	1.56	0.2	7	6	11	0.28	7.28	5.34	1.09	0.04	3.14	14	1.36	7.79	0.2
0.64	12.35	6.15	1.39	0.2	6.3	10	8	0.3	8.3	6.76	0.85	0.05	3.12	16.22	1.23	5.24	0.2